Environment of Deposition and Paleogeography of the Late Cretaceous Glenburn Formation, Eastern North Island, New Zealand

By

James Daniel Begg McClintock

A thesis submitted to Victoria University of Wellington in partial fulfilment of requirements for the degree of

Master of Science (MSc) in Geology

School of Geography, Environment and Earth Sciences

Victoria University of Wellington

2018

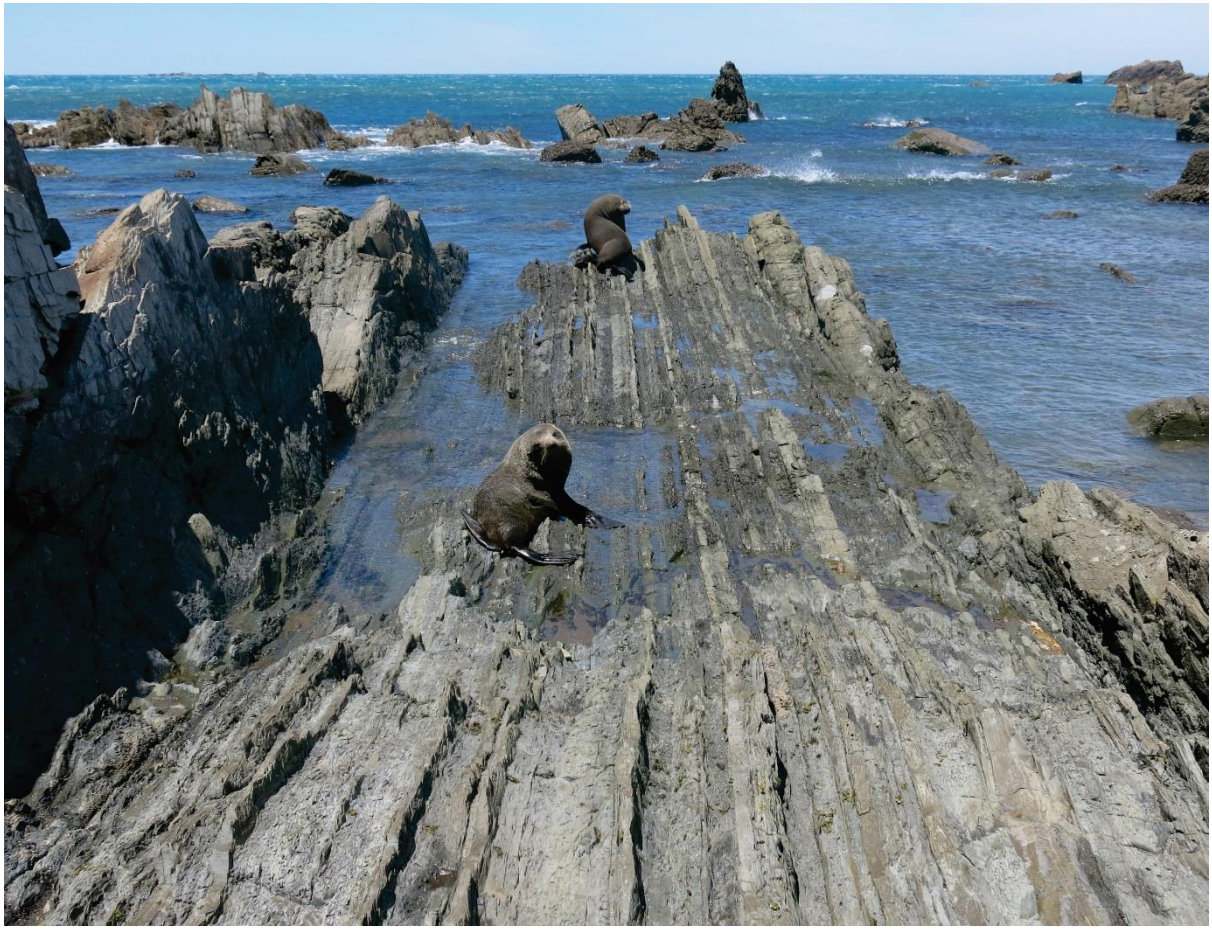

Frontispiece: “A potential reservoir and its seal”

Abstract:

The Glenburn Formation of the East Coast of New Zealand is a Late Cretaceous sedimentary formation consisting of alternating layers of sandstone, mudstone and conglomerate. The Glenburn Formation spans a depositional timeframe of over 10 Ma, is over 1000 m thick, is regionally extensive and is possibly present over large areas offshore. For these reasons, it is important to constrain the paleoenvironment of this unit.

Late Cretaceous paleogeographic reconstructions of the East Coast Basin are, however, hampered by a number of factors, including the pervasive Neogene to modern tectonic deformation of the region, the poorly understood nature of the plate tectonic regime during the Cretaceous, and a lack of detailed sedimentological studies of most of the region's Cretaceous units. Through detailed mapping of the Glenburn Formation, this study aims to improve inferences of regional Cretaceous depositional environments and paleogeography.

Detailed facies based analysis was undertaken on several measured sections in eastern Wairarapa and southern Hawke's Bay. Information such as bed thickness, grain size and sedimentary structures were recorded in order to identify distinct facies. Although outcrop is locally extensive, separate outcrop localities generally lie in different thrust blocks, which complicates comparisons of individual field areas and prevents construction of the large-scale, three-dimensional geometry of the Glenburn Formation.

Glenburn Formation consists of facies deposited by sediment gravity flows that were primarily turbidity currents and debris flows. Facies observed are consistent with deposition on a prograding submarine fan system. There is significant variation in facies both within and between sections. Several distinct submarine fan architectural components are recognised, such as fan fringes, fan lobes, submarine channels and overbank deposits. Provenance and paleocurrent indicators are consistent with deposition having occurred on several separate submarine fans, and an integrated regional paleogeographic reconstruction suggests that deposition most likely occurred in a fossil trench following the mid-Cretaceous cessation of subduction along the Pacific-facing margin of Gondwana.

Table of Contents

Frontispiece i

Abstract: ii

Acknowledgements xi

Chapter 1: Introduction 1

1.1: General Introduction 1

1.2: Aim of Thesis 7

1.3: Conventions Used Herein 7

1.3.1: New Zealand Geological Timescale 7

1.3.2: Palaeontology and Age Correlation 8

1.3.3: The Fossil Record Electronic Database: "FRED" 10

1.3.4: Grid References 10

1.4: Glenburn Formation: Background and Previous Work 10

1.4.1: General Description of the Glenburn Formation 10

1.4.2: Previous Work on the Glenburn Formation 12

1.5.3: Importance of the Glenburn Formation 15

Chapter 2: East Coast Basin Regional Stratigraphy 16

2.1: Southern Hawke's Bay/Wairarapa Cretaceous Stratigraphy 16

2.1.1: Basement 16

2.1.2: Karamea (Red Island) and Hinemahanga Rocks 18

2.1.3: Western Sub-belt Cretaceous Cover Stratigraphy 19

2.1.4: Whangai Formation 21

2.2: Late Cretaceous Sediments Elsewhere in the East Coast Basin 22

2.3: ECB Late Cretaceous to Modern Tectonic History 25
Chapter 3: Fieldwork methodology and section locations 26
3.1: Fieldwork Procedure 26
3.2: Selection of Field Sites 26
3.3: Field site descriptions: 29
3.3.1: Glenburn Coast 29
3.3.2: Totara Stream 31
3.3.3: Motuwaireka Stream 32
3.4.4: Mataikona River 34
3.4.5: Waimata River 35
3.4.6: Mangakuri Beach 37
3.4.7: Waimarama Beach 39
3.5: Conglomerate clast count methodology 42
Chapter 4: Facies analysis methodology 45
4.1: Introduction 45
4.2: Submarine Gravity Flow Transport Processes 45
4.3: Background of Facies Models 47
4.4: Facies Scheme Description 50
4.4.1: Introduction 50
4.4.2: Facies Class A: >5% Granule to Boulder Grade Clastics 53
4.4.3: Facies Class B: Sand-dominated Beds 61
4.4.4: Facies Class C: Sandstone-mudstone Couplets and Muddy Sandstone 64
4.4.5: Facies Class D: Siltstone and Silt-mudstone Couplets 68
4.4.6: Facies Class E: Clay Dominated Mudstone 73
4.5: Chapter summary 74
Chapter 5: Field Results and Interpretations 75

5.1: Measured Section Summaries 75
5.1.1: Honeycomb Light – Appendix D 75
5.1.2: Horewai Point – Appendix E 81
5.1.3: Totara Stream – Appendix F 84
5.1.4: Motuwaireka Stream - Appendix G 89
5.1.5: Mataikona River - Appendix H 91
5.1.6: Waimata River – Appendix I 96
5.1.7: Mangakuri Beach - Appendices J and K 96
5.1.8: Waimarama Beach – Appendix L 104
5.1.9: Section Summary 108
5.2: Conglomerate Clast Counts 108
5.2.1: Introduction 108
5.2.2: Totara Stream Clast Count 108
5.2.3: Glenburn Coast Clast Count 113
5.2.4: Mangakuri Conglomerate Clast Counts 117
5.2.5: Comparison Between Clast Counts 120
5.2.7: Discussion of Clast Counts 121
5.2.8: Section Summary 125
5.3: Additional Observations 125
5.3.1: Thickness of the Glenburn Formation 125
5.3.2: Summary of Paleocurrent Data: 128
5.3.3: Gross Upsection Trend in Facies 130
5.3.4: Possible Subdivisions of the Glenburn Formation 132
Chapter 6: Depositional Environment Interpretation 133
6.1: Depositional Environments of Submarine Gravity Flow Dominated Successions 133
6.2: General Depositional Setting of the Glenburn Formation 133

6.2.1 : Paleodepth 133
6.2.2: Submarine fan or sheet system? 136
6.3: Submarine Fan Generalised Facies Model 137
6.4: Depositional Sub-environments of Field Sites 142
6.4.1: Glenburn Coast Interpretation 142
6.4.2: Totara Stream / Motuwaireka Stream 144
6.4.3: Mataikona River 145
6.4.4: Waimata River 146
6.4.5: Mangakuri/Waimarama Beaches 146
6.5: One Fan System or Multiple? 147
6.6: Summary 148
Chapter 7: Cretaceous East Coast Basin Paleogeographic Reconstruction 149
7.1: Introduction 149
7.2: Paleogeography of the Cretaceous ECB 150
7.3: Proposed Cretaceous ECB History 156
Chapter 8: Conclusions and summary 158
8.1: Key Findings 158
8.2: Implications for Offshore Correlatives 159
8.3 Suggestions for Future Work 159
8.3.1: Further Investigation into WSB Formations 159
8.3.2: Correlative Strata on the Raukumara Peninsula 159
8.3.3: Mapping the Lateral Continuity of the “Totara Stream Lithofacies” 160
8.3.4: Offshore Understanding 160
8.3.5 More Detailed Petrography of Sandstones and Conglomerates 160
References 161
Appendices 172

Appendix B: Index of fossils..... 177
Appendix C: Key for measured sections..... 180
Appendix D: Honeycomb Light Measured Section..... 181
Appendix E: Horewai Point Measured Section..... 183
Appendix F: Totara Stream Measured Section..... 186
Appendix G: Motuwaireka Stream Measured Section..... 195
Appendix H: Mataikona River Measured Section..... 208
Appendix I: Waimata River Composite Measured Section..... 213
Appendix J: Mangakuri Beach Composite Measured Section..... 214
Appendix H: Crampton (1997) North Mangakuri Beach Measured Section..... 216
Appendix L: Waimarama Beach Composite Measured Section..... 218

List of Figures

Figure 1.1: Late Cretaceous reconstructions of Zealandia. 3
Figure 1.2: Late Cretaceous reconstructions of Zealandia. 4
Figure 1.3: NZ sedimentary basins 5
Figure 1.4: Structural divisions of the East Coast Basin 6
Figure 1.5: New Zealand Geological Timescale. 8
Figure 1.6: Comparison of previous names of the Glenburn Formation. 13
Figure 1.7: Summary map of previous studies that mapped Glenburn Formation 14
Figure 2.1: New Zealand basement terranes 17
Figure 2.2: Seismic cross-section of Hawke's Bay 18
Figure 2.3: Cretaceous stratigraphy of Eastern and Western Sub-Belts 21
Figure 2.4: Stratigraphic correlation of Eastern Sub-belt strata 23
Figure 3.1: Map of field site localities. 28
Figure 3.2: Glenburn coast field map 30
Figure 3.3: Totara Stream field map. 32
Figure 3.4: Motuwaireka Stream field map. 33
Figure 3.5: Mataikona River field map. 35
Figure 3.6: Waimata River field map. 36
Figure 3.7: Southern Mangakuri Beach field map 38
Figure 3.8: Northern Mangakuri Beach field map 39

Figure 3.9: Waimarama Beach field map. 41
Figure 4.1: Representative sketches of SGFs 46
Figure 4.2: Bouma sequence diagram 47
Figure 4.3: Lowe Sequence diagram. 48
Figure 4.4: Walker (1978) facies model 49
Figure 4.5: Schematic representation of facies scheme 51
Figure 4.6: Facies A1.1 54
Figure 4.7: Facies A1.2 55
Figure 4.8: Facies A1.3 57
Figure 4.9: Facies A2.1 59
Figure 4.10: Facies A2.2 60
Figure 4.11: Facies B1 62
Figure 4.12: Facies B2 64
Figure 4.13: Facies C1. 65
Figure 4.14: Facies C2.1-C2.3 67
Figure 4.15: Facies C2.4 68
Figure 4.16: Facies D1.1 70
Figure 4.17: Facies D1.2 71
Figure 4.18: Facies D2 72
Figure 4.19: Facies E 73
Figure 5.1: Generalised stratigraphy of different field sections by age 76
Figure 5.2: Honeycomb Light mudstone and conglomerate lens 78
Figure 5.3: Honeycomb Light turbidites 79
Figure 5.4: Honeycomb Light conglomerate and overlying facies. 80
Figure 5.5: Horewai Point conglomerate and parallel stratified sandstone. 82
Figure 5.6: Horewai Point turbidites 83
Figure 5.7: Totara Stream turbidites 86
Figure 5.8: Totara Stream conglomerates. 87
Figure 5.9: Totara Stream thin-bedded turbidites 88
Figure 5.10: Motuwaireka Stream turbidites 91
Figure 5.11: Motuwaireka Stream conglomerate 90
Figure 5.12: Mataikona River mudstone and turbidites 94
Figure 5.13: Mataikona River thick bedded sandstones 95
Figure 5.14: Waimata River turbidites. 98
Figure 5.15: Mangakuri Beach assorted internal sedimentary features 99

Figure 5.16: Mangakuri Beach B, C, E class facies. 100
Figure 5.17: Mangakuri Beach conglomerate facies 101
Figure 5.18: Mangakuri Beach cross bedded gravel and rip-up clasts. 102
Figure 5.19: Mangakuri Beach pebbly sandstone and conglomerate 103
Figure 5.20: Waimarama siltstone, sandstone, thin turbidites 105
Figure 5.21: Waimarama conglomerates and shell-hash lens 106
Figure 5.22: Waimarama turbidites 107
Figure 5.23: Teratan aged conglomerate, Totara Stream. 1109
Figure 5.24: Totara Stream clast count localities 109
Figure 5.25: Comparison of clast counts between Teratan and Mangaotanean sections at Totara Stream 112
Figure 5.26: Locally derived material comparison, Totara Stream 113
Figure 5.27: Upper Honeycomb Light bed 114
Figure 5.28: Lower Honeycomb Light bed 114
Figure 5.29: Comparison of main clast composition of Glenburn Coast 116
Figure 5.30: Comparison between conglomerates at Mangakuri Beach. 119
Figure 5.31: Comparison of clast counts for each locality 122
Figure 5.32: Proportion of indurated material that is sandstone by locality 123
Figure 5.33: Comparison of Teratan aged conglomerates 123
Figure 5.34: Synthesis of paleocurrent directions 129
Figure 5.35: Composite measured section of coarsening trends 131
Figure 6.1: Stacked channel model 140
Figure 6.2: Generalised fan facies model 141
Figure 7.1: Inferred Ngaterian to Arowhanan Stage (99.5 – 93.7 Ma) paleogeography. 154
Figure 7.2: Inferred Mangaotanean to Teratan (93.7 – c. 88 Ma) paleogeography. 154
Figure 7.3: Inferred late Teratan to Piripauan (c. 88 Ma to 83.6 Ma) paleogeography. 155
Figure 7.4: Inferred mid-Haumurian (c. 70 Ma) paleogeography. 155

List of tables

Table 1.1 – NZGT stages 9
Table 4.1 – Facies and their associated transport processes. 52
Table 5.1 – Summary of clast counts, Totara Stream. 110
Table 5.2 – Summary of clast counts, Glenburn 115
Table 5.3 – Summary of clast counts, Mangakuri Beach clast 118
Table 5.4 – Comparison of thicknesses of individual stages by location. 127
Table 5.5 – Summary of paleocurrent directions 128

List of equations

Eq 1 – Confidence interval T-test 43
Eq 2 – Confidence interval comparison test 43

Acknowledgements

First and foremost, I would like to thank my supervisor, James Crampton, for his support and guidance throughout this thesis. Thank you for sharing some of your immense wisdom and enthusiasm, and for always making the time for interesting and informative chats despite your hectic schedule. I am grateful to have been provided with the opportunity to investigate such a fascinating topic.

A huge thanks must go to my field assistants, Andrew and Morgan, for your help and company in the field. Without you guys, I'd still be stuck in the quicksand in Ngahape. Additional thanks must go to Andrew and his family for letting us stay on the family farm in Hastings. Thank you also to Geoff for stepping in at the last minute to help with the long drive to Mangakuri.

I am grateful to the friendly farmers throughout the Wairarapa who allowed me conduct fieldwork on their land: thanks to the proprietors of Glenburn Station, Mataikona Station and Akitio Station, and to George Moore of Riversdale. Additional thanks must go to Forestry Enterprises, IFS Growth and Juken New Zealand, who allowed me to conduct fieldwork in forests they manage. Also, thanks the Cheryl and Barry Eldridge for kindly allowing us to stay in their cottage in Kaiwahata. Without the generosity of the people of the Wairarapa, this project would not have been possible.

Last but not least, thanks to my family for all your support. A huge thanks to Mum and Dad, for all the support and advice throughout the years, and for bravely letting me borrow mum's car for the rough roads of rural New Zealand. Thanks to Lisa, too, for your helpful advice and guidance early on about writing my thesis. Finally, thank you to Grandma, for your support, for the always-interesting geological chats and for the steady stream of fascinating geology articles. You will be pleased to see your rock hammer is still being put to good use!

Dedicated to the memory of my grandfather,

Lindsay Leigh McClintock

1923 - 2017

Chapter 1: Introduction

1.1: General Introduction

The Glenburn Formation of eastern Hawkes Bay and Wairarapa in the North Island of New Zealand is a Late Cretaceous sedimentary formation comprised of interbedded sandstone, mudstone and conglomerate. The formation is thick, well in excess of 1000 m in parts, and is regionally extensive, extending over a distance of at least 200 km. Understanding the depositional environment of the Glenburn Formation is an important step towards reconstructing the paleogeography of Cretaceous New Zealand. Despite its significant regional extent, the depositional environment of the Glenburn Formation is currently poorly constrained.

The Cretaceous Period was a time of major change for the Zealandia subcontinent, the largely submerged continental crust upon which New Zealand lies (Mortimer et al., 2017). It was during this period that Zealandia split from Gondwana, first by separating from Antarctica and then through the initiation of rifting in the Tasman Sea. Although the exact timing is disputed, the current consensus is that subduction along the northern margin of Zealandia ceased either during or shortly before the Late Cretaceous, due to the collision of the Hikurangi Plateau with the Pacific-facing Gondwana plate margin c. 105 Ma (Laird and Bradshaw, 2004; Davy et al., 2008; Davy, 2014; Adams et al., 2016). The Hikurangi Plateau is part of a large igneous province that was erupted c. 120 Ma in the central Pacific Ocean, before colliding with the Gondwana plate margin c. 105 Ma (Davy, 2014). Over a period of c. 5 Ma, the Hikurangi Plateau jammed the Gondwana subduction margin to the point where subduction halted. With the cessation of subduction, the long-term accretion of New Zealand's metasedimentary "basement" halted and a transition from deposition of basement to "cover" rocks occurred (Adams et al., 2013; terms "basement" and "cover" sensu Mortimer et al., 2014). Figures 1.1 and 1.2 show two different interpretations of the Cretaceous paleogeography of Zealandia in published literature. The Glenburn Formation

was deposited from the beginning of the Late Cretaceous onwards (Schiøler and Crampton, 2014), shortly after the inferred cessation of subduction.

The Glenburn Formation lies within the East Coast Basin (ECB). The ECB lies east of the axial ranges of the North Island of New Zealand, extending from the Raukumara Peninsula to the Marlborough Region of the South Island (Figure 1.3). The ECB contains Cretaceous to Quaternary sediments resting unconformably atop metasedimentary basement (Field et al., 1997). Rocks mainly of Triassic to Early Cretaceous age are composed of accretionary wedge material, which form the "Torlesse Composite Terrane" basement of the ECB (Mortimer et al, 2014).

Moore (1988a) subdivided the ECB into two distinct belts: the Western Sub-belt (WSB) and the Eastern Sub-belt (ESB), each with their own unique Cretaceous sedimentary record. Figure 1.4 shows the block divisions and the locations of the ESB and WSB in the North Island, as designated by Moore (1988a). These sub-belts are separated by the Adams-Tinui Fault system in much of the Wairarapa. Division of sub-belts in the Akitio region is complicated somewhat by the presence of an allochthonous nappe of Pahaoa Group sediment (Deltail et al., 1996). The Glenburn Formation lies on the ESB.

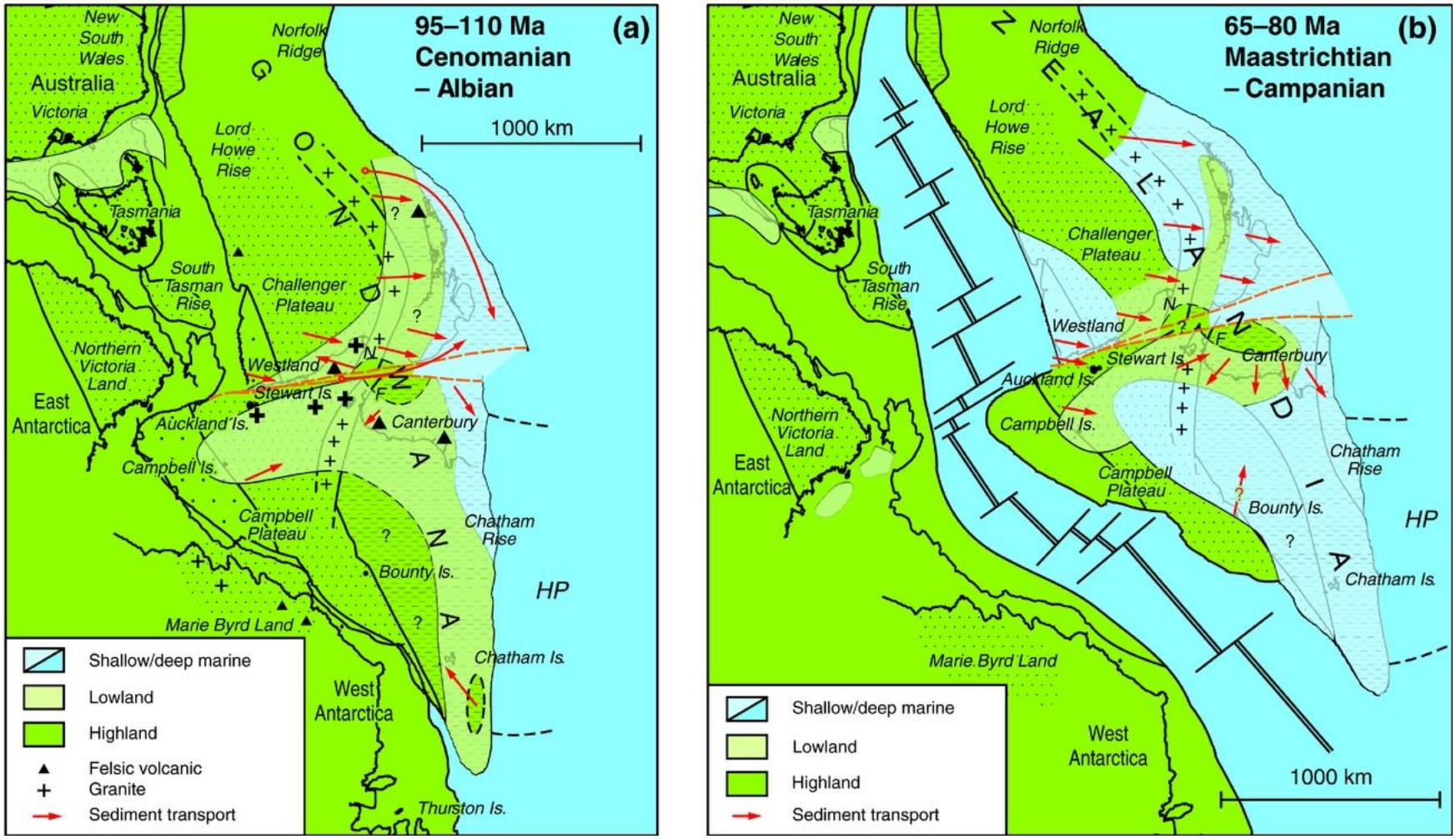

Figure 1.1: Late Cretaceous reconstructions of Zealandia. Initiation of Glenburn Formation deposition occurred somewhere in the latter part of (a) during the Ngaterian (99.5 – 95.2 Ma), whereas the uppermost Glenburn Formation was deposited during or just before (b), in the early Haumurian (c. 80 Ma). From Adams et al., 2016, their Figure 6.

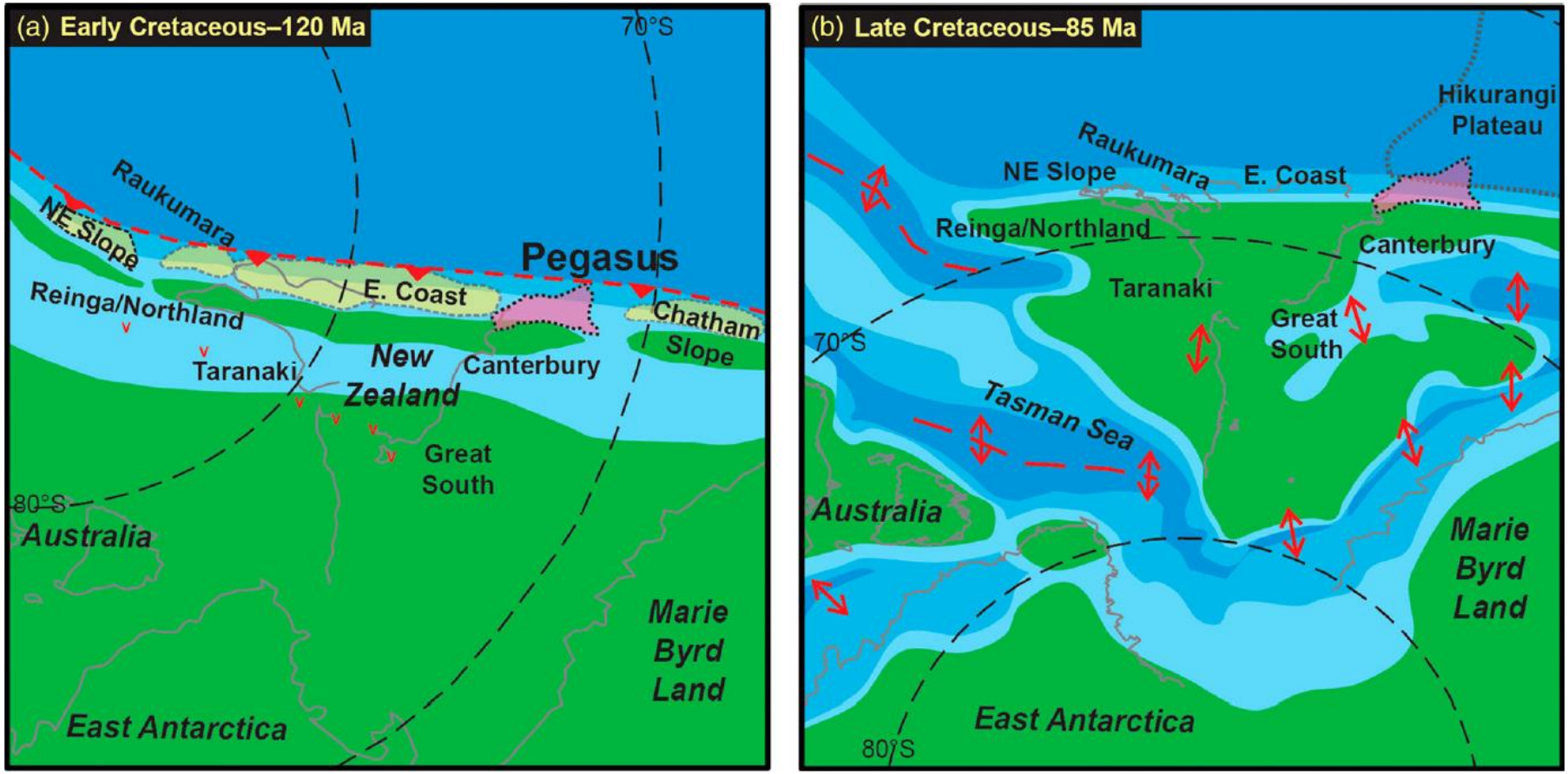

Figure 1.2: One interpretation of Cretaceous paleogeography showing position of the East Coast Basin relative to land, other basins, and the Gondwana subduction margin. From Bland et al., 2015, their Figure 2. Pink polygon represents Pegasus Basin, the topic of their investigation.

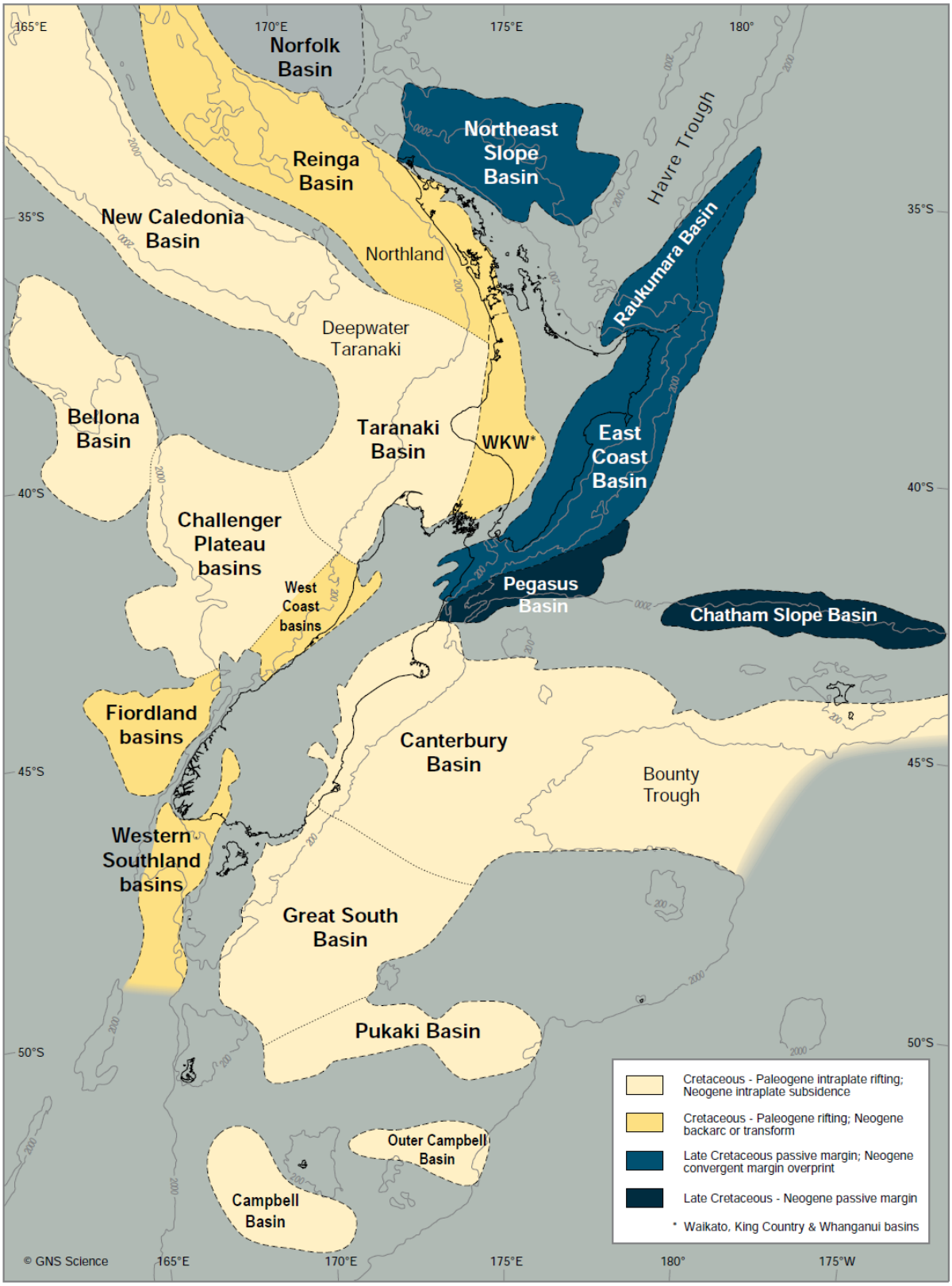

Figure 1.3: Map showing sedimentary basins of New Zealand, demonstrating the extent of the East Coast Basin. From New Zealand Petroleum & Minerals, (2014), p. 14.

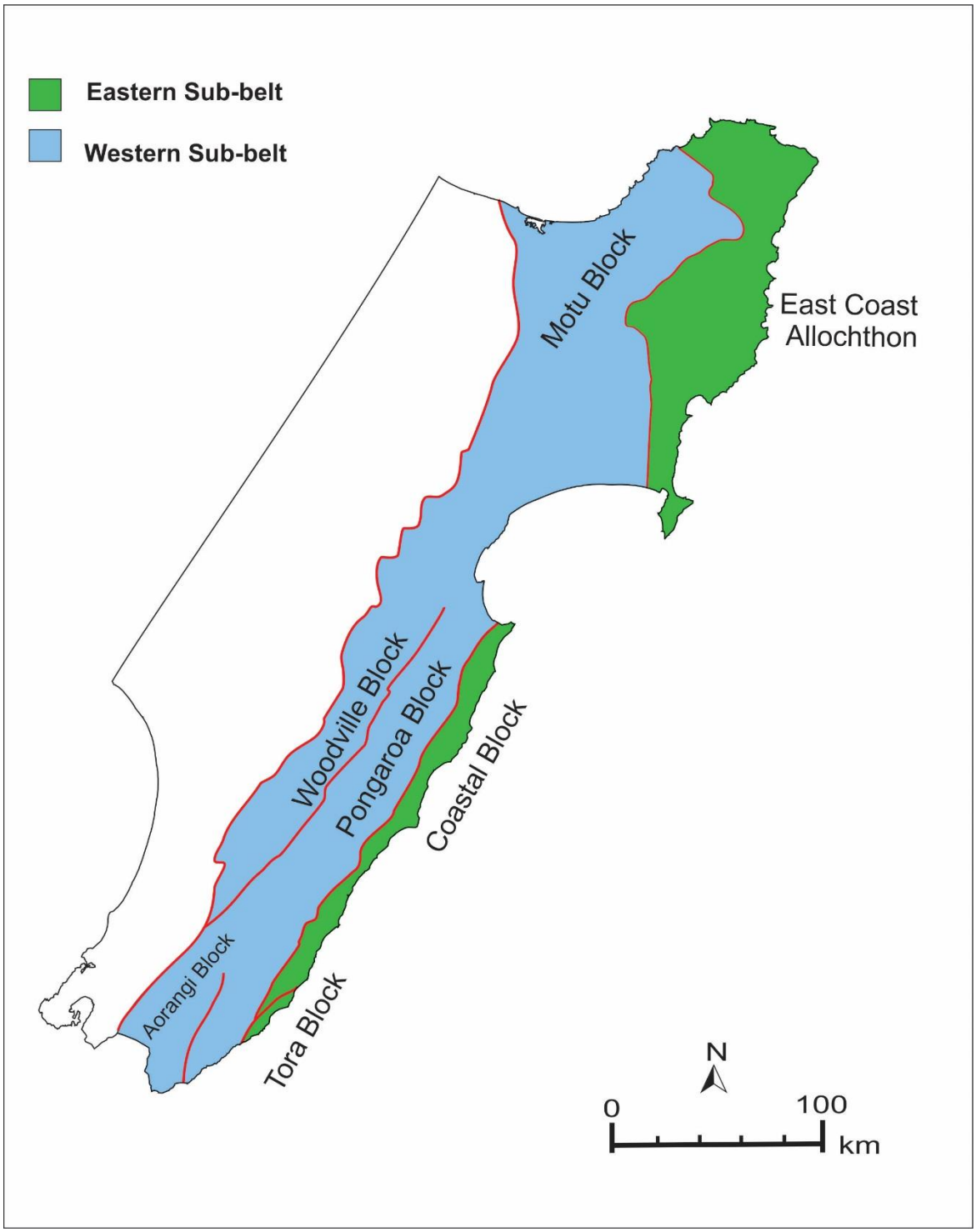

Figure 1.4: Structural divisions of the East Coast Basin, as per Moore (1988a). Base map modified from LINZ NZ coastline 1:250k map

1.2: Aim of Thesis

The depositional environment and paleogeography of the Glenburn Formation have not previously been described in any detail. Studies investigating the Glenburn Formation have historically been either generalised reconnaissance level investigations of the formation in its regional context (e.g., Crampton, 1997; Field et al, 1997) or more detailed but highly localised studies (e.g., Moore, 1980).

In published paleogeographic maps of Cretaceous Zealandia, the ECB is usually simply represented as "marine" without any differentiation between the many different marine depositional environments (e.g., Figures 1 - 2). Detailed sedimentological investigation is required to further constrain the paleogeography of the Late Cretaceous ECB.

This thesis aims to:

- Log representative sections of the Glenburn Formation in detail, with a particular focus on noting the variations in facies both temporally and spatially.
- Determine the overall depositional environment of the Glenburn Formation, including mechanisms of sediment transport, geometry of the system and depth of deposition.
- Recognise variations in sub-environments between sections.
- Produce a depositional model for the ECB during the Late Cretaceous by integrating the results from this study with previous literature.

1.3: Conventions Used Herein

1.3.1: New Zealand Geological Timescale

This study uses New Zealand geological series and stages from the "The New Zealand Geological Timescale" or "NZGT 2015/1" of Raine et al. (2015). Papers cited herein may have used older versions of the NZGT, but because paleontological stage definitions have

remained constant, the assigned ages of rocks do not change. The relevant Cretaceous portion of the New Zealand geological timescale, correlations to the international timescale, and age calibrations are shown in Figure 1.5 (Raine et al., 2015).

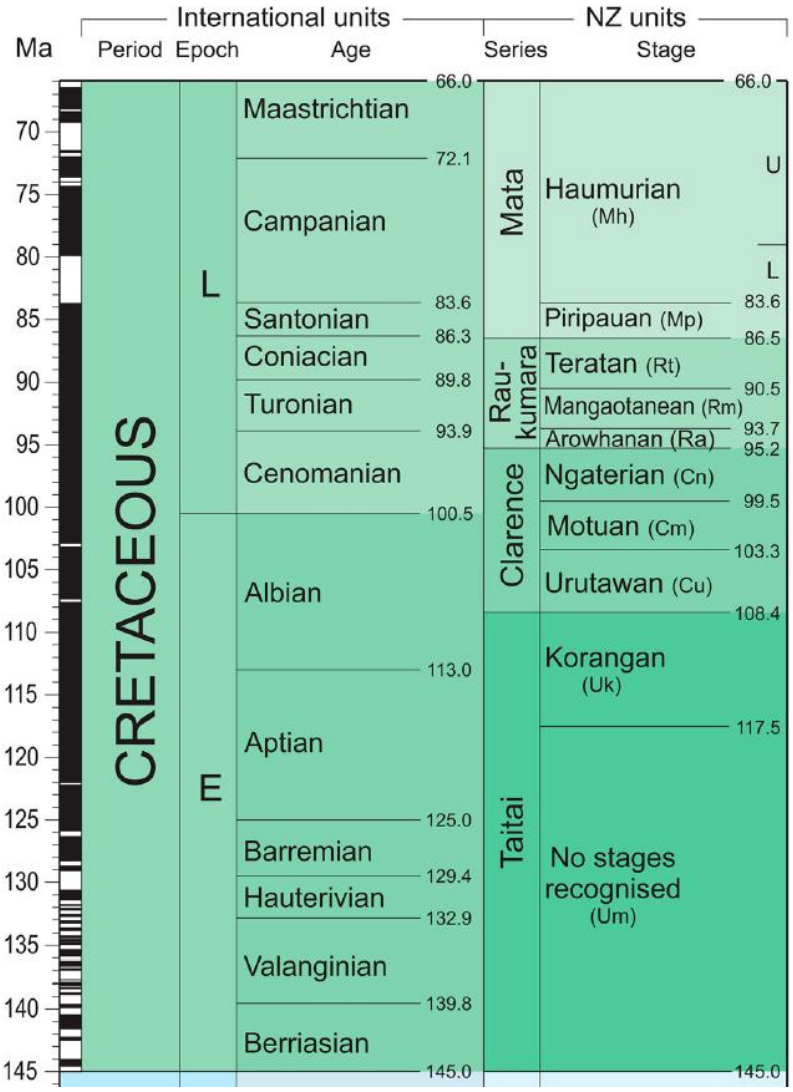

Figure 1.5: New Zealand Geological Timescale, Cretaceous section. Modified from Raine et al. (2015), their Figure 1.

1.3.2: Palaeontology and Age Correlation

Late Cretaceous stages in the New Zealand Geological Timescale are defined primarily using index species of Inoceramidae bivalves. Specimens from three different genera of Inoceramidae have been found in the Glenburn Formation: *Inoceramus, Cremnoceramus* and *Magadiceramus*. The Glenburn Formation includes sediment from Ngaterian to early

Haumurian stages and most localities contains sufficient fossils to constrain strata to specific stages. All stages represented except the Haumurian contain index *Inoceramus* fossils as shown in Table 1.1. Identification of these fossils was based on descriptions by Crampton (1996).

Table 1.1 - NZGT stages and their correlative index fossils, as per Crampton (1996) and Cooper (2004).

Series	**Stage**	**Index fossils**
Mata	Piripauan	*I. pacificus (lower), I. australis (mid-upper)*
Raukumara	Teratan	*I. opetius, I. madagascariensis*
	Mangaotanean	*Cremnoceramus bicorrugatus* (subspecies *bicorrugatus* and *matamuus*)
	Arowhanan	*Magadiceramus rangatira (*subspecies *rangatira* and *haroldi)*
Clarence	Ngaterian	*I. tawhanus, I. fyfei*

Due to the sporadic nature of the fossil record within the Glenburn Formation, stage boundaries are often poorly constrained. Supplementary fossil information is collected from GNS Science's "Fossil Record Electronic Database" (Section 1.3.3) to help determine stages as accurately as possible.

Inoceramid species occupied a wide range of marine habitats and so cannot be used to infer any particular paleoenvironment (Crampton, 1996).

1.3.3: The Fossil Record Electronic Database: "FRED"

Several citations within this study refer to the Fossil Record Electronic Database or "FRED", run by GNS Science (https://fred.org.nz/). This database contains over 100,000 fossil locality records, with a particular focus on recording the locations of fossils found in the field. Additional useful information is often included, such as sedimentological and structural information. Because much of the information recorded within the database is unpublished, it is a valuable resource for finding additional information from field sites, especially in dating strata where this study identified no fossils. Additionally, FRED entries can give useful information about field sites not visited in this study as well as information about currently obscured outcrops. Citations within this study refer to FRED entries by their designated unique "FR number" (e.g., "V23/f0003").

1.3.4: Grid References

The location of features in this study are given in grid reference form (e.g., BL39 414 813), which is based on LINZ's "NZ Topo50" referencing system (https://www.linz.govt.nz/land/maps/topographic-maps/topo50-maps). Conversion between this and several other co-ordinate systems is possible with LINZ's online conversion app (http://apps.linz.govt.nz/coordinate-conversion/).

1.4: Glenburn Formation: Background and Previous Work

1.4.1: General Description of the Glenburn Formation

The Glenburn Formation (Eade, 1966, emended Johnston, 1975, emended Crampton, 1997) comprises alternating mudstones, sandstones and conglomerates. Although exposed thicknesses vary by location, the Glenburn Formation is at least 1100 m thick in places. The

formation displays significant and often rapid changes in facies both horizontally and vertically (Crampton, 1997).

A wide variety of facies are found in the Glenburn Formation. Beds are often normally graded and occasionally inversely graded. Internal sedimentary features such as parallel-, convolute- and cross-lamination are common. Partial “Bouma sequences” (Bouma, 1962) are present throughout the formation (see Figure 4.2). Some beds are channelised and sharp erosive bases are also common. Thickness of individual beds varies immensely, with some parts bedded on a 1-5 cm scale and other parts massive or metre-bedded. Sections vary from richly fossiliferous to almost entirely non-fossiliferous. Carbonaceous material is abundant throughout most of the formation, often concentrated in laminae (Crampton, 1997).

Conglomerate beds vary from <1 m thick up to >13 m thick and display a wide variety of textures, varying from clast to matrix supported, with clasts that may be well to very poorly sorted, angular to well rounded, and granule grade through to boulder grade. These beds may be massive, normally graded, inversely graded or inverse-normal graded. Matrix within these conglomerates consists of either mudstone or sandstone (Crampton, 1997).

Sandstone facies vary significantly, although the majority of sandstone beds are bedded on a 10-30 cm scale, medium- to fine-grained and are normally graded to form a “sandstone-mudstone couplet”. These beds are often parallel- and cross-laminated, and sometimes show convolute-lamination (Bouma divisions T_{bcd}). Other sandstone facies include massive sandstones and thick units that are parallel- or cross-laminated but lack other Bouma divisions (Crampton, 1997).

Mudstone facies are generally silty but sometimes clayey. Mudstones may be well-bedded, weakly bedded or massive (Crampton, 1997). As described above, many mudstone beds form a couplet with a graded sandstone.

The general descriptions of these facies are most consistent with the bulk of the Glenburn Formation having been deposited by a variety of “submarine gravity flows” (SGFs), such as turbidity currents or debris flows (Pickering and Hiscott, 2015). These processes are discussed in further detail in Chapter 4.

1.4.2: Previous Work on the Glenburn Formation

Eade (1966) introduced the name Glenburn Formation to describe Ngaterian to Arowhanan sedimentary rocks on the Tora Block (Figure 1.4). He designated overlying Mangaotanean to Teratan and Piripauan to Haumurian sediment as the Longbush and Tutu formations respectively. Subsequently, Johnston (1971, 1975, 1980) and Moore (1980) expanded the use of the name to the Tinui (NZ topo50 sheet BP36) and Ngahape (northern NZ topo50 sheet BQ35) areas respectively.

Crampton (1997) redefined the Glenburn Formation to incorporate the entirety of Ngaterian to Haumurian "flysch" facies within the Eastern Sub-belt of the East Coast regions of Wairarapa and Southern Hawkes Bay. This expanded the definition of the Glenburn Formation to include several other formations mapped within the ECB. Previous mapped formations now synonymised with Glenburn Formation (Figure 1.6), as defined by Crampton (1997), include:

- Te Mai Formation (Moore, 1980; Johnston, 1971, 1975, 1980; Neef 1992, 1995; Moore and Speden, 1979*)
- Raukumara Formation (Walpole and Burr, 1939; Ridd, 1964)
- Longbush/Tutu Formation (Eade, 1966)
- Kipihana Formation, Wig Sub-group (Neef, 1992, 1995)
- Waimarama Formation (Pettinga, 1980; 1982; Frances, 1993A)

* Moore and Speden (1979) also used Te Mai Formation to describe rock overlying the Springhill Formation, which are now designated as Tangaruhe Formation (Crampton, 1997). "Te Mai Formation" in fault contact with Springhill Formation in the Tinui area noted by Moore and Speden (1979) may be Glenburn Formation, which outcrops around BP36 627 733 (Lee and Begg, 2002).

Outcrops now considered Glenburn Formation have also been mapped in some places under formation names still in use for other strata, such as:

- Tapuwaeroa Formation (Walpole and Burr, 1939; Ridd, 1964**;** Lillie, 1953; Pettinga 1980, 1982)
- Springhill Formation (Neef, 1992)

- Tikihore Formation[+] (V23/f0004)
- Mangaotane Mudstone (V23/f0003)

[+] Tikihore is an age-equivalent facies of the Glenburn Formation on the Raukumara Peninsula, as discussed in Section 2.2.

These examples are all from localities now mapped as Glenburn Formation as emended by Crampton (1997) and have been subsequently mapped as such by Lee and Begg (2002) and Lee et al. (2011).

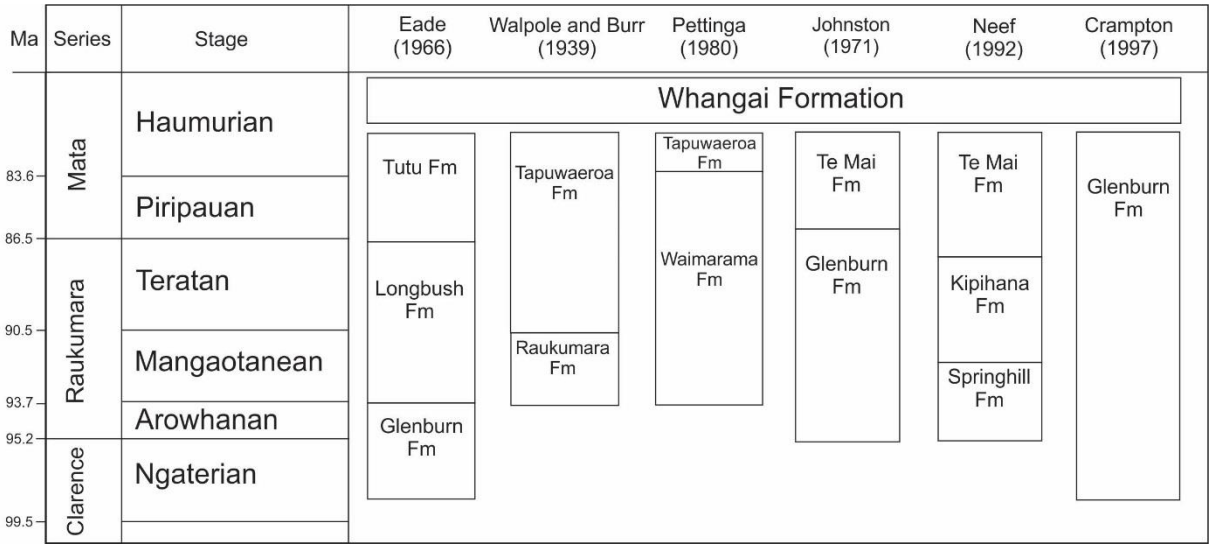

Figure 1.6: Comparison of published names designated for strata now comprising the Glenburn Formation.

Many other studies on the Glenburn Formation simply refer to it by its geological stage or series, such as that of Brown (1943), Wellman (1970) and Kingma (1971). This also includes many unpublished petroleum reports in the Waimarama/Mangakuri area such as Walpole (1940), Haw (1960), Eyssautier and Faber (1966), Rumeau (1966) and De Caen and Darley (1968).

The Hukarere-1 well (Westech Energy Ltd., 2001), drilled in Napier, claimed to have encountered Glenburn Formation underlying Whangai Formation (see Section 2.1.4). This is problematic, because the well was drilled in a location within the WSB (Figure 1.4). It is therefore very unlikely this was Glenburn Formation and was probably the coeval Tangaruhe Formation instead (see Chapter 2).

Although numerous studies in the ECB have incorporated mapping of the Glenburn Formation (Figure 1.7), for the most part this mapping has either been at a reconnaissance level of detail or highly localised. Because outcrop quality naturally varies over time, these earlier studies provide useful information for the present study.

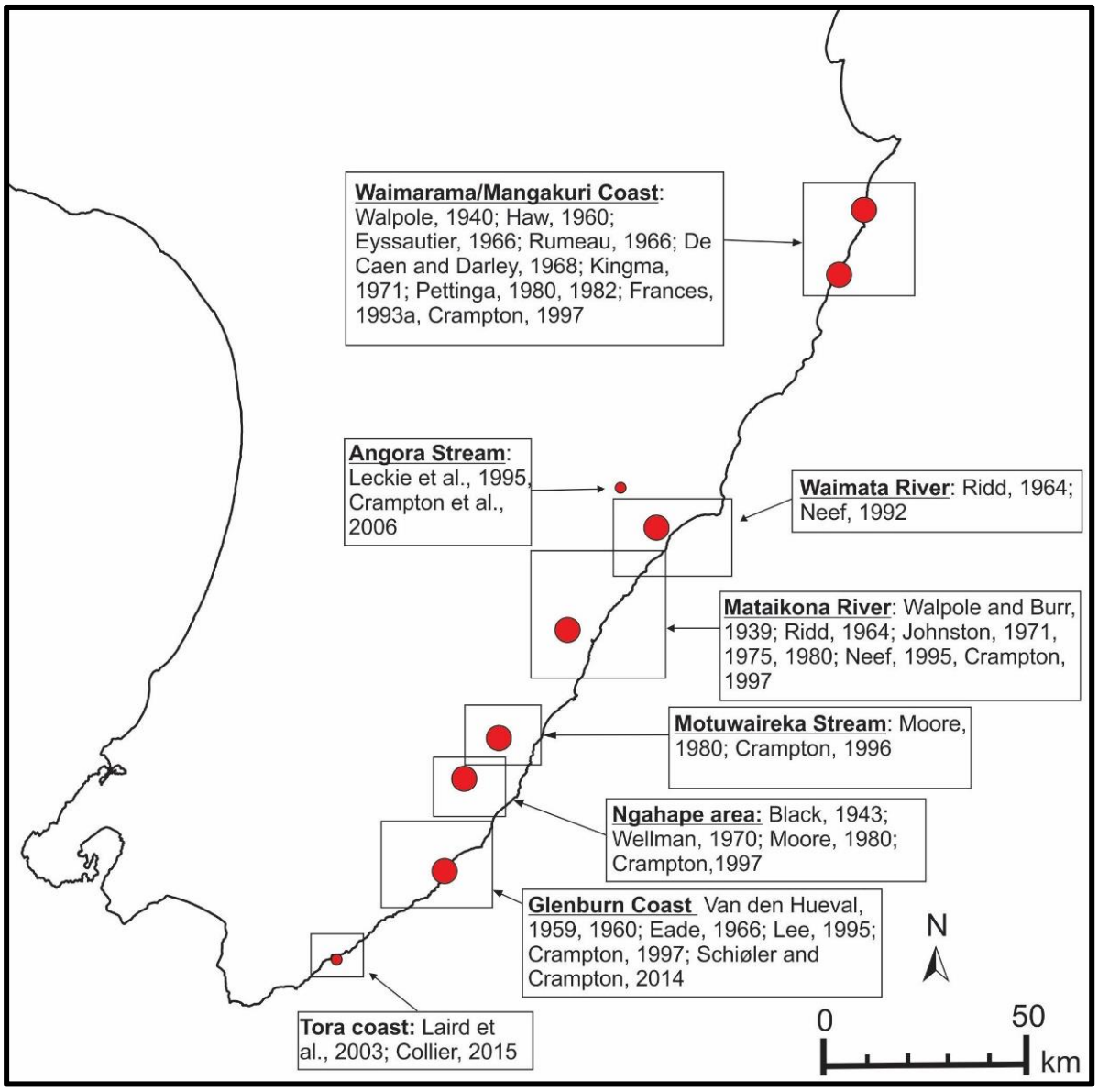

Figure 1.7: Summary map of previous studies that mapped Glenburn Formation, often under different names. Large red circles indicate field sites visited in this study, small red circles indicate localities mentioned but not visited. Outline map of NZ created using LINZ's topo250 coastline map.

1.4.3: Importance of the Glenburn Formation

The Glenburn Formation's importance stems from the fact that it is thick, laterally extensive and spans a period well in excess of 10 Ma. Seismic studies outlined in Chapter 2 suggest it probably extends a significant distance offshore. Because of this spatial and temporal extent, understanding the depositional environment of the Glenburn Formation is a vital part of understanding the Cretaceous paleogeography of the East Coast Basin as well as New Zealand as a whole.

In addition to its paleogeographic implications, Glenburn Formation may prove to be a comparatively non-deformed analogue for much of the Torlesse Composite Terrane. Whereas the Torlesse Composite Terrane is highly deformed due to accretion deformation during subduction along the Gondwana plate margin, Glenburn Formation is inferred to have been deposited shortly after the cessation of subduction and therefore is much less deformed (Adams et al., 2013).

Deep-marine submarine gravity flow successions have become of significant interest to the petroleum industry since the late 20th century (Weimer and Link, 1991). Many significant petroleum systems are found in submarine fan systems. Examples from New Zealand include the Mount Messenger and Moki Formations in the Taranaki Basin, each reservoirs for significant oil fields (King et al., 2007; Grain, 2008).

The Glenburn Formation has been studied briefly for its petrochemical properties and found to be a poor reservoir (Katz, 1988; Frances, 1993a; Tucker, 1992), but the formation contains a significant quantity of organic material, which may suggest source rock potential. Hollis et al. (2005) found high organic total organic carbon but a low hydrogen index, suggesting that, based on their samples, Glenburn Formation had poor potential to generate hydrocarbons. Hollis et al. (2005) acknowledge that more detailed geochemistry is required to assess further the formation's hydrocarbon generating potential. Although no further investigation into source potential is conducted in this study, understanding the geometry and depositional environment of the Glenburn Formation may have important implications for basin modelling.

Chapter 2: East Coast Basin Regional Stratigraphy

2.1: Southern Hawke's Bay/Wairarapa Cretaceous Stratigraphy

2.1.1: Basement

The Glenburn Formation lies within the Eastern Sub-belt of the East Coast Basin (ECB). The extent of the ECB is outlined in Figure 1.3. The following section summarises the rest of the relevant Cretaceous stratigraphy of the basin.

Basement underlying the East Coast Basin is only known in the WSB. Where exposed, basement consists largely of sedimentary rocks including indurated sandstone, argillite and conglomerate (Field et al., 1997; Barnes 1988). In most localities, basement is easily distinguished from cover rocks by the highly indurated and deformed nature of basement strata. This basement is included in the Torlesse Composite Terrane, which can be divided into several distinct terranes based upon age and locality (Figure 2.1; terrane nomenclature after Mortimer et al., 2014). The Hawke's Bay and Wairarapa regions contain rocks of the Rakaia, Kaweka and Pahau terranes, the latter of which includes the Pahaoa Group, which contains the Mangapokia and Taipo Formations (Mortimer et al., 2014, Adams et al., 2013). Pahaoa Group rocks are the oldest exposed basement in the Wairarapa-Hawke's Bay section of the ECB.

Basement underlying the Glenburn Formation is not exposed and remains unknown. Seismic transects by Burgreen-Chan et al. (2016; Figure 2.2) in Hawke's Bay suggest Cretaceous cover rocks lying atop inferred Torlesse basement through to the current Hikurangi Trough. Bland et al. (2015) inferred similar geometry in the Pegasus Basin, which is to the south of the ECB (Figure 1.3). A lack of well control means it is not possible to determine whether the cover sediments offshore are correlative to the Glenburn Formation. Likewise, it is not possible to deduce whether the offshore basement correlates to any onshore terranes. Regardless, these seismic transects indicate Torlesse-type basement is likely to extend a significant

distance offshore of New Zealand, which suggests Glenburn Formation probably overlies similar rocks.

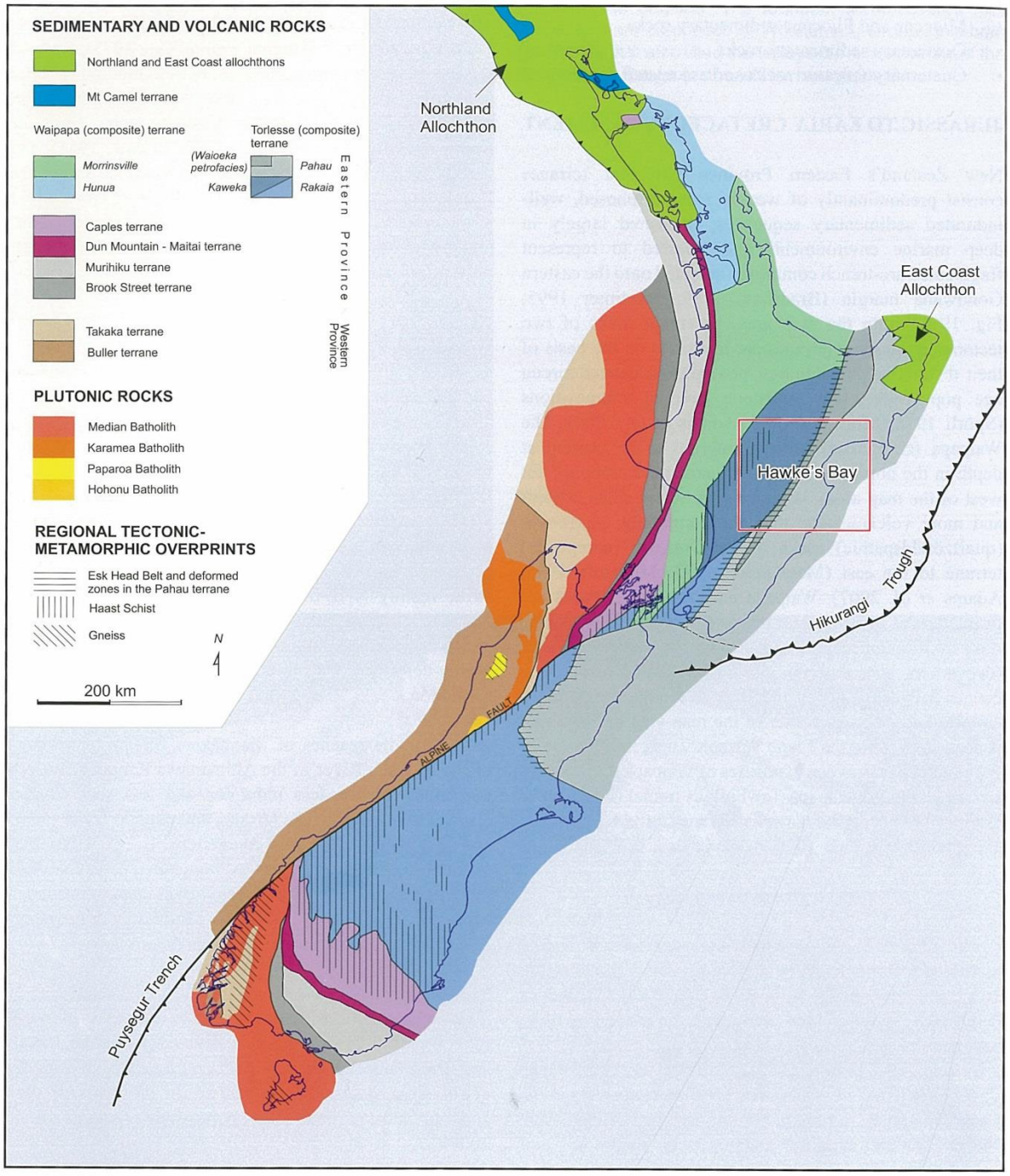

Figure 2.1: New Zealand basement terranes. Pahaoa Group included in Pahau Terrane. From Lee et al. (2011), their Figure 19.

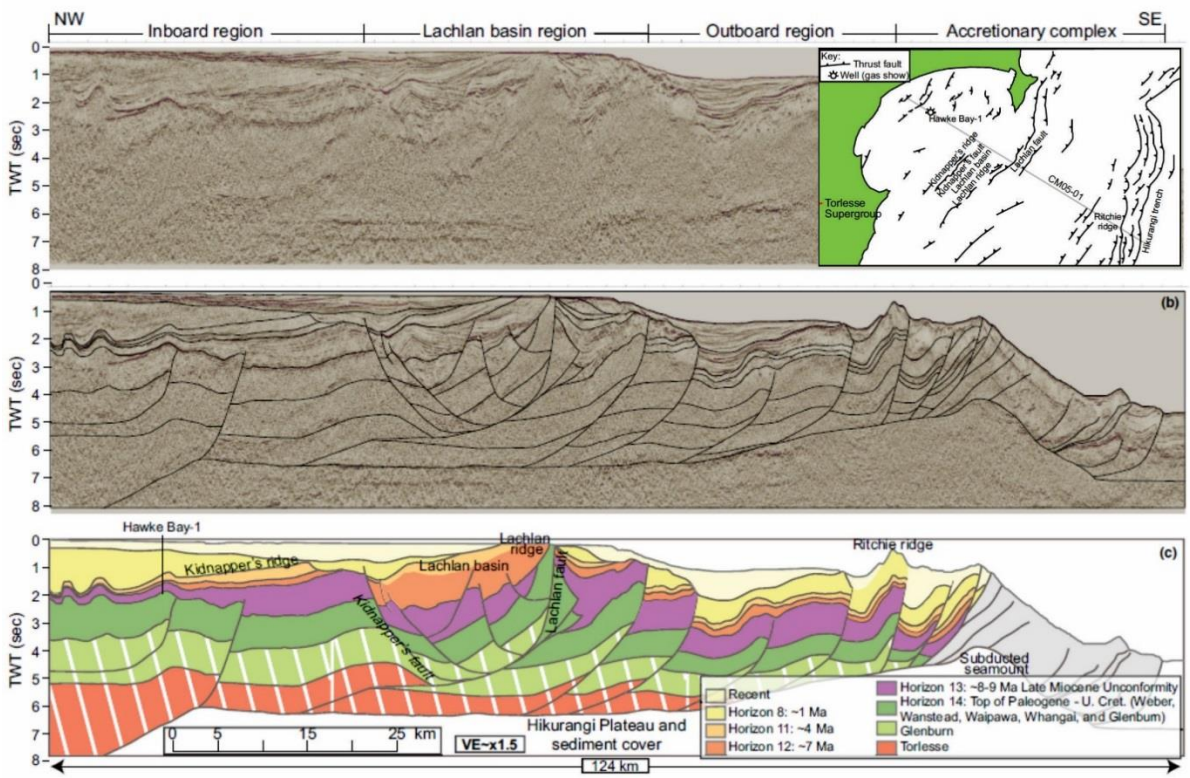

Figure 2.2: Seismic cross-section hypothesising that Glenburn Formation may overlie Torlesse and extend offshore. White cross-hatching indicates uncertainty regarding the boundary between units. Authors acknowledge lack of ties/drilling data to confirm this. Additionally, westernmost sediment are probably within the WSB and therefore would not be Glenburn Formation (Figure 1.4). Inset is location of cross-section, modified from Burgreen-Chan et al. (2016), their Figure 7 (inset from Figure 2).

2.1.2: Karamea (Red Island) and Hinemahanga Rocks

The oldest exposed rocks in the ESB in the Wairarapa/Hawke's Bay region are those associated with the tombolo of Karamea, also known as Red Island, south of Waimarama in southern Hawkes Bay (BL39 412 804). The "Red Island Volcanic Group" (Moore et al., 1987) is comprised of basaltic lava and distinct red volcanically altered limestone, and is of Motuan or older age (Marwick, 1966; Kobe and Pettinga, 1984). Rocks exposed at Karamea are interpreted to be correlative to the Hinemahanga Rocks (BL39 367 711) offshore of Mangakuri Beach (Black et al., 1984; Moore et al., 1987) and possibly volcanic rocks found on the Mahia Peninsula (Francis, 1993b). The Red Island Volcanic Group also shares some

similarities to descriptions of the Matakaoa Volcanics on the Raukumara Peninsula (Francis, 1993b).

How Red Island came to be exposed in a fault sliver adjacent to the Late Cretaceous rocks of the Glenburn Formation may be one of the key pieces in the puzzle of reconstructing the tectonic regime of the Late Cretaceous. If Red Island was emplaced by Cretaceous tectonics (Kobe and Pettinga, 1984), this places a constraint on how long accretion must have continued into the Cretaceous. If a Motuan age is confirmed, this would imply that accretion must have continued into at least the Motuan and possibly longer. Alternately, the Neogene to current tectonic regime may have emplaced the Red Island Volcanic Group into its current position (Kobe and Pettinga, 1984).

2.1.3: Western Sub-belt Cretaceous Cover Stratigraphy

Three formations comprise the Cretaceous cover sequence in the Western Sub-belt of the Wairarapa/Southern Hawke's Bay region: the Gentle Annie, Springhill and Tangaruhe formations. Relative ages of these formations and correlative ESB facies are shown in Figure 2.3.

The Gentle Annie Formation is comprised largely of massive melange, with minor components of interbedded sandstone and mudstone, and massive mudstone, whereas the Springhill Formation is a mudstone-dominated sequence with minor interbedded sandstone and rare conglomerate beds (Crampton, 1997). Together these formations comprise the Mangapurupuru Group. The Mangapurupuru Group is unconformably overlain by the Tangaruhe Formation, which comprises mostly glauconitic interbedded sandstones and mudstones, massive mudstones, and massive sandstones. This formation includes the Mangawarawara Member, a localised, basal, granular to pebbly sandstone and mudstone unit (Crampton, 1997). Tangaruhe Formation is less deformed than the underlying Mangapurupuru Group rocks, suggesting ongoing tectonic deformation in the Late Cretaceous (Crampton, 1989, 1997).

Although none of these formations were examined in this study, due to their similar age and proximity to the Glenburn Formation, their depositional environments are a vital part of

reconstructing the paleogeography of the Cretaceous ECB. Depositional environments for these three formations are poorly constrained.

Moore and Speden (1979, 1984) considered a shelf as the most likely depositional environment for the Gentle Annie Formation, whereas other authors such as Barnes (1988) inferred deposition occurred in a trench slope basin. Crampton (1997) concluded the formation most likely represented the initial rapid infilling of a basin formed by abrupt subsidence or uplift of the hinterland.

Moore and Speden (1979, 1984) and Johnston (1980) inferred a mid- or inner-shelf depositional environment for the Springhill Formation. Conversely, Adams (1985) suggested a fan-margin slope environment for the lower part of the formation, and an upper- to mid-shelf environment for the upper part of the formation. Barnes (1988) postulated, as with the Gentle Annie Formation, that the Springhill Formation was deposited on a trench slope. Crampton (1997) concluded that it was most likely deposited in a restricted basin at neritic or bathyal depths.

The Tangaruhe Formation was deposited contemporaneously with a significant portion of the Glenburn Formation, between the Teratan and Haumurian stages. Crampton (1997) inferred that the Tangaruhe Formation was probably deposited in at least bathyal depths in an anoxic basin, based largely on the absence of any shallow-water indicators, although the paleodepth is very poorly constrained.

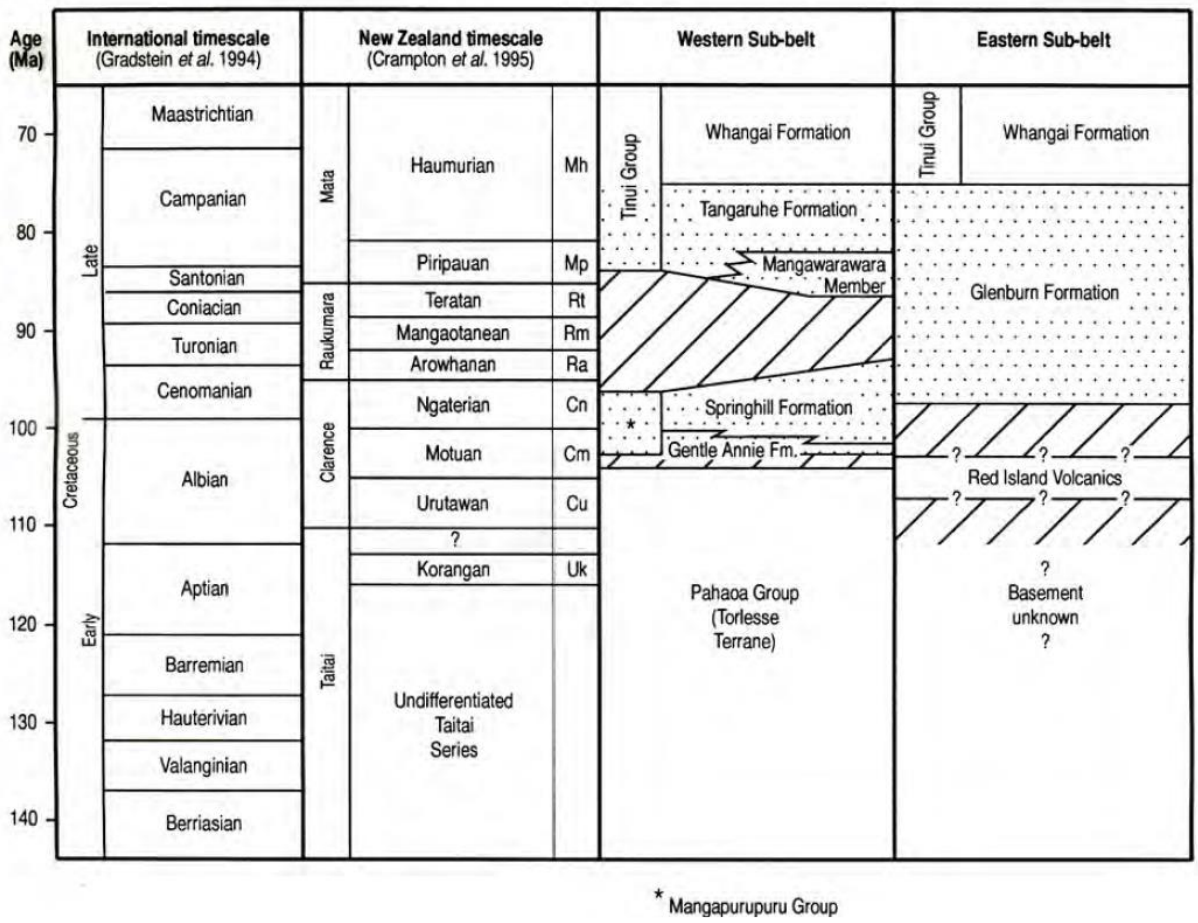

Figure 2.3: Cretaceous stratigraphy of Eastern and Western Sub-Belts, from Crampton (1997), his Figure 3.

2.1.4: Whangai Formation

The Haumurian to Teurian Whangai Formation overlies both the Tangaruhe and Glenburn formations (Moore, 1988b). Previous studies have observed the contact with the Glenburn Formation in several localities, such as in the Ngahape area, Mataikona River and Angora Stream, to be gradational (Moore, 1980; Crampton, 1997; Crampton et al., 2006), although localised disconformities occur (Moore 1980, 1988b). Conversely, on the WSB, the contact between the Tangaruhe and Whangai formations is unconformable and represents several million years of missing time (Crampton et al., 2006). Moore (1988b) noted a difference in facies between eastern and western outcrops of Whangai Formation, but this variation did

not appear to correlate to the Eastern and Western sub-belt boundaries. Hence, the Eastern and Western sub-belt division only applies to formations older than the Whangai Formation.

Despite its regional extent, the depositional environment of the Whangai Formation is poorly constrained. The paleoenvironment of the lowermost Whangai Formation is relevant because the contact between Glenburn and Whangai formations is in parts conformable and gradational. This suggests that the uppermost Glenburn was deposited in a similar depth as the lowermost Whangai Formation.

Moore (1988b) contains an extensive discussion on the depositional environment of the Whangai Formation, and tentatively suggests a mid- to lower neritic or possibly upper bathyal paleodepth. Laird et al. (2003) inferred a neritic depth of deposition for the uppermost Whangai Formation based on the presence of hummocky cross-stratification. Simpson and Jarvis (1993) inferred “generally shelfal” conditions. Leckie et al. (1995) suggested lower neritic to upper bathyal depths for the lower part of the Whangai Formation. Killops et al. (2000) also inferred a lower neritic to upper bathyal depositional environment for the Whangai Formation. Based on an extensive study, including 200 microfossil assemblages derived from FRED, stratigraphic context, and sedimentological data, Hines (2018) inferred that lower parts of the Whangai Formation overlying the Glenburn Formation were most likely deposited in depths of between 600 - 800 m. Because the Glenburn Formation grades conformably into Whangai Formation, uppermost Glenburn Formation was probably deposited at similar depths.

2.2: Late Cretaceous Sediments Elsewhere in the East Coast Basin

Although the Glenburn Formation encompasses a significant part of the ECB’s Late Cretaceous sediment, it is only recognised in the Wairarapa and southern Hawke’s Bay regions of the North Island. Late Cretaceous strata of the Raukumara Peninsula and Marlborough region are similar and likely related to Wairarapa and Hawke’s Bay strata, despite significant outcrop free areas between them (Crampton, 1997).

Based on geological similarities, the Eastern and Western Sub-belt divisions extend into the Raukumara Peninsula. Figure 2.4 shows the correlative Raukumara Peninsula ESB formations. The ESB of the Raukumara Peninsula is allochthonous, and total displacement may be many tens to hundreds of kilometres (Field et al., 1997).

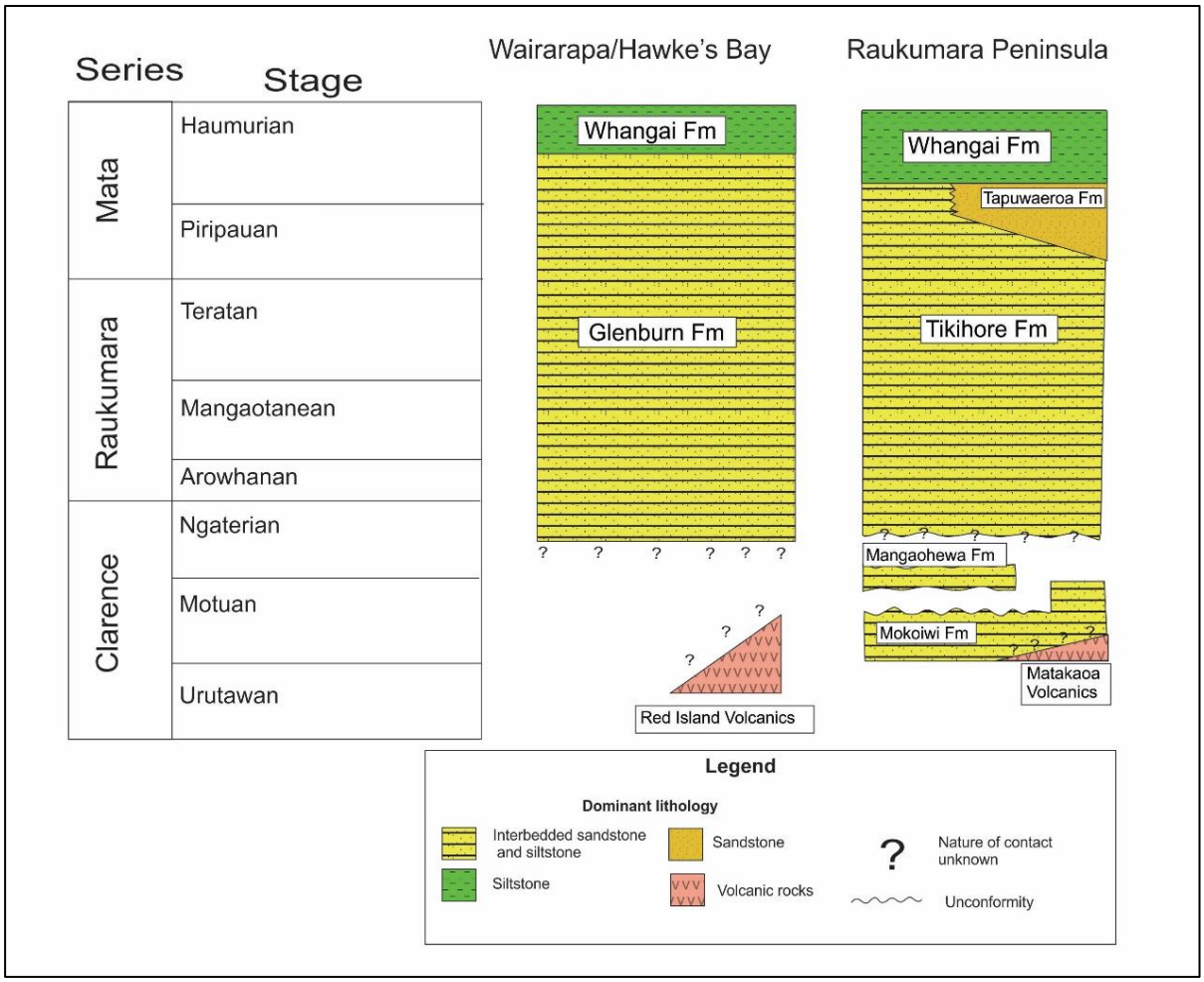

Figure 2.4: Stratigraphic correlation of Eastern Sub-belt strata in the East Coast Basin as described in Field et al. 1997.

The oldest strata exposed on the ESB occur on the Raukumara Peninsula and comprise the Mokoiwi and Mangaohewa formations. The Motuan Mokoiwi Formation is dominantly siltstone with a minor sandstone component and lenses of conglomerate up to 30 m thick. The Mokoiwi Formation contains the Taitai Sandstone Member, a localised thick-bedded, lenticular sandstone unit with minor conglomerate and breccia. The Mangaohewa Formation has a basal breccia unit that grades into sandstone and sandstone-mudstone couplets. It is probably of Motuan or Ngaterian age (Field et al., 1997). Speden (1976) argued for a shelf-

edge depositional environment for these two formations, whereas Kenny (1986) suggested a slope or base of slope environment. Field et al. (1997) concluded these formations were probably deposited in neritic or upper bathyal depths, with the Taitai Sandstone and Mangaohewa Formation the result of infilling of channels or canyons in the shelf-slope break.

The Tikihore Formation is a dominantly centimetre- to metre-bedded alternating sandstone and mudstone sequence of Ngaterian to Piripauan age (Field et al., 1997). Internal sedimentary structures are consistent with deposition primarily from turbidity currents. There have been no detailed studies on the formation, but there appears to be an absence of significant portions of conglomerate facies, in contrast to the Glenburn Formation. In most respects, however, Tikihore Formation shows similar facies to the coeval Glenburn Formation, and so the two units are probably laterally equivalent. A submarine fan depositional environment appears the most likely, though it may require further research to prove this (Field et al., 1997).

The Tapuwaeroa Formation conformably and gradationally overlies the Tikihore Formation. The formations are locally laterally equivalent. The Tapuwaeroa Formation consists of sandstone, mudstone and conglomerate beds (Field et al., 1997). A variety of possible depositional environments have been postulated for the Tapuwaeroa Formation, ranging from prodeltaic bench sheets through to proximal slope deposits (Field et al., 1997). Further research is needed to definitively determine its paleoenvironment. Paleocurrent directions for both the Tikihore and Tapuwaeroa Formations trend generally northwest, a significant contrast to the generally eastward flow of the Glenburn Formation (see section 5.3.2).

Due to the complex tectonic nature of the Marlborough region, is it not certain whether ESB extends this far south (Crampton, 1997). The Mangaotanean to Teratan Burnt Creek Formation shares some apparent similarities with the Glenburn and Tikihore formations, however, Crampton and Laird (1997) noted strong similarities between it and the Moanui Formation of the Western Sub-belt on the Raukumara Peninsula suggesting it is more likely to be part of the WSB.

2.3: ECB Late Cretaceous to Modern Tectonic History

Following the cessation of subduction along the Gondwana plate margin (Section 1.1), the tectonic regime of the ECB transitioned to a passive margin. By the time the uppermost part of the Glenburn Formation was being deposited, Tasman seafloor spreading had begun to dominate the tectonic regime of Zealandia (King et al., 1999). Earliest rifting in the Tasman Sea occurred c. 84 Ma (Giana et al., 1998), in the latest Piripauan to early Haumurian. Subsidence associated with rifting resulted in a widespread marine transgression, followed by a long period of passive margin subsidence. The transition of the relatively coarse facies of the Glenburn Formation into the fine-grained facies of the Whangai Formation is inferred to reflect this transgression.

It was not until the earliest Neogene that convergent plate tectonics were initiated, which has continued to the modern day (King et al., 1999). The convergence between the Pacific and Indo-Australian plate has caused significant tectonic shortening in the ECB. Miocene shortening in the ECB is likely greater than 20-30 km but less than 150 km (Nicol et al., 2007). A series of thrust faults are present in the Wairarapa and southern Hawkes Bay regions, the orientations of which indicate they have brought WSB and ESB rocks closer than their original depositional positions (Lee and Begg, 2002). These thrust faults form a series of wedges. Outcrops of Glenburn Formation may lie on several separate wedges, which adds some uncertainty in correlating different sections because relative motions between wedges are poorly constrained.

Chapter 3: Fieldwork methodology and section locations

3.1: Fieldwork Procedure

This investigation into the Glenburn Formation was fieldwork based, and involved visiting several field sites throughout the Wairarapa/Hawke's Bay regions in order to compare and contrast outcrops of Glenburn Formation between localities.

Fieldwork was undertaken as part of this study using standard techniques. Location was determined using a handheld GPS device, and key characteristics of strata were noted for each locality. Information recorded at each outcrop included grain size, sorting, colour, grading, nature of clasts, and any internal sedimentary features such as lamination. At three different field sites, clasts were counted in conglomerate beds to determine whether clast composition changed over space or time. Bed thicknesses were measured using a tape, and strikes and dips determined using a standard field compass. Where individual beds were recorded, thicknesses were rounded to the nearest centimetre, whereas entire outcrops of similar facies were generally rounded to the nearest decimetre. Where outcrops were separated by significant sections of missing outcrop, distances were calculated using GPS. Stratigraphic thicknesses were calculated using strike and dips of beds, the bearing of tape or bearing to next GPS co-ordinate, and topographic inclination estimated by using GPS co-ordinates and Google Earth. Once stratigraphic thickness of intervals was calculated, this information used to create a series of measured sections using the program CorelDRAW.

3.2: Selection of Field Sites

Mapping localities were selected based on previous work and reconnaissance mapping, using the GNS "QMAP 250k series" (Lee and Begg, 2002; Lee et al., 2011)**,** as well as more detailed work such as that of Crampton (1997) and Moore (1980). Suitability of field sites

was determined using aerial photography such as LINZ's Wellington 0.3 m Rural Area Photos (accessed from https://data.linz.govt.nz/set/4702-nz-aerial-imagery/) and Google Earth. The selection of field sites was decided primarily with the goal of capturing as much of the Glenburn Formation's spatial and temporal extent as possible within an attainable amount of fieldwork.

The sections studied in this thesis are, from south to north (Figure 3.1):

1) Glenburn coast, Wairarapa, which includes the Horewai Point and Honeycomb Light sections
2) Totara Stream ("Kaiwhata Stream" of Crampton (1997) and Moore (1980)), Ngahape.
3) Motuwaireka Stream, Riversdale.
4) Mataikona River, including outcrops in Smoky Gully Stream
5) Waimata Stream
6) Kairakau/Mangakuri Beach
7) Waimarama Beach

Crampton (1997) noted both Totara Stream and Mataikona River as possible reference sections, due to the thickness of the sections exposed and the relatively good stratigraphic continuity. However, both these sections have recently been subject to forestry harvesting, which appears to have degraded much of the outcrop mapped by Crampton (1997) and Moore (1980). At present, the Motuwaireka Stream section (Appendix G) appears to be the most complete section, speculatively due to the presence of regenerating bush rather than farmland or forestry in the section logged. It is, however, very difficult to access and the rugged and steep nature of the headwaters of the stream make logging it in detail a difficult task. Unfortunately, this leaves very few other potential locations for a more complete type section than the current Glenburn Station type section, which is limited in both age and thickness.

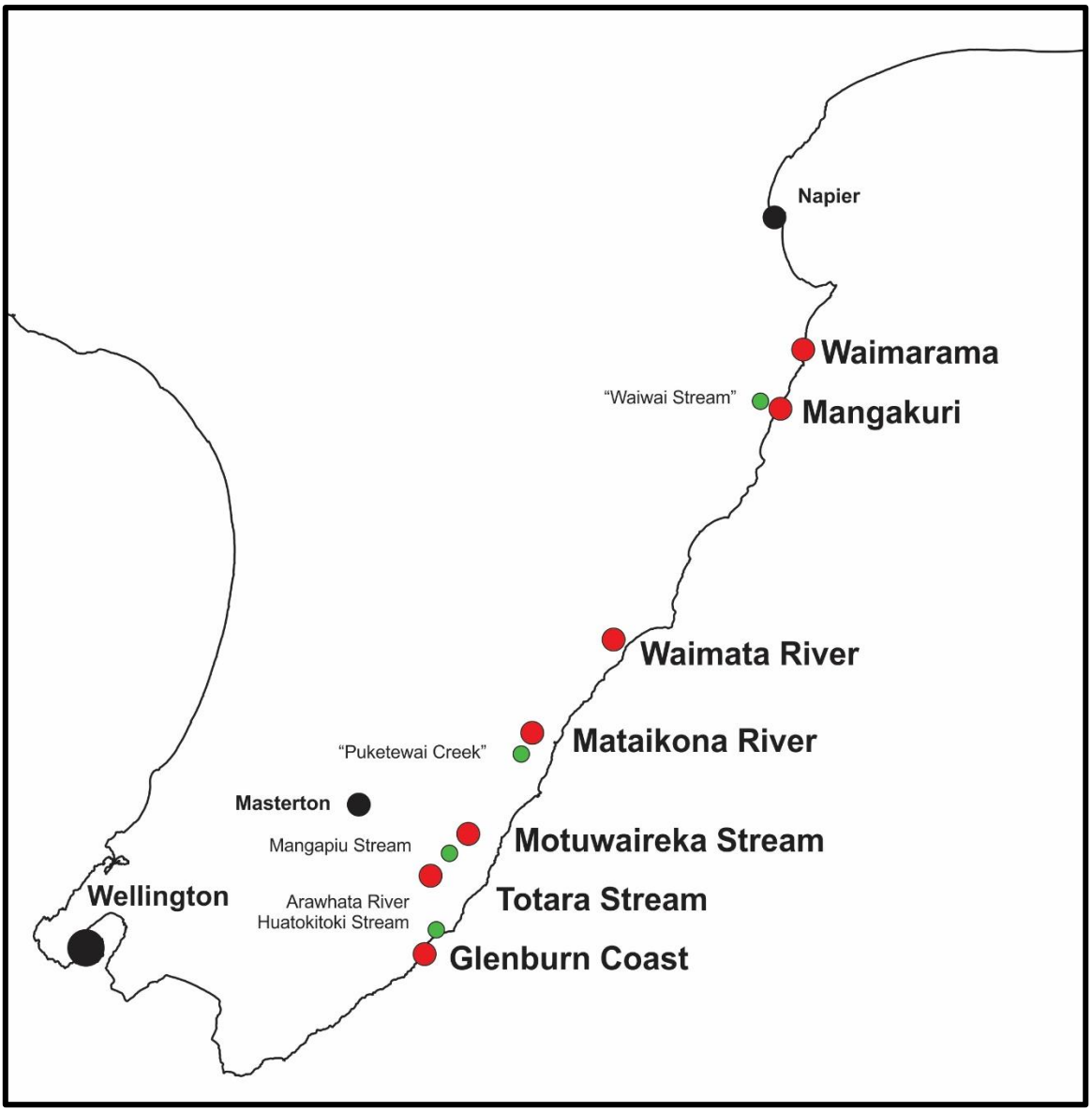

Figure 3.1: Map of field site localities (red circles) and localities considered as potential future field sites (green circles). New Zealand outline map created from LINZ topo250 coast map.

A number of other potential field sites exist in the Wairarapa and Hawke's Bay regions. These include several mapped by previous studies such as the Huatokitoki Stream near Glenburn (Lee, 1995; BQ35 418 278), Puketewai Creek (Johnston, 1980, which he assigned as the type section for the Te Mai Formation; BN36 732 830) and the "Waiwai Stream" in Hawkes Bay (Haw, 1960; BL39 325 693). However, interpretations based on existing geological maps and satellite photographs suggest that the sections listed above are either not particularly thick or currently have poor outcrop and hence were not included in this study.

3.3: Field site descriptions:

3.3.1: Glenburn Coast

Glenburn Station is a remote coastal farm station in southeastern Wairarapa that lends its name to the Glenburn Formation. The tectonic regime in the area is very complex and several distinct tectonic thrust wedges of Glenburn Formation have been mapped (Lee and Begg, 2002). The field sites visited in this section are those exposed on the shore platform at Horewai Point, between BQ35 380 208 and BQ35 382 209, and the shore platform ~2 km south of Horewai Point between BQ35 370 190 and BQ35 368 188 (Figure 3.2), assigned as "Honeycomb Light" by Crampton (1997). These were chosen as they are the best preserved outcrops of Ngaterian to Arowhanan Glenburn Formation known. Minor faults cut both sections, and the complex tectonic regime in the region does mean the two sections might be separated by significant faults.

The boundary between Ngaterian and Arowhanan sediments is marked by a thick conglomerate, up to 13 m at Horewai Point and a thinner but still significant 3 m at Honeycomb Light. Schiøler and Crampton (2014) suggest there is an unconformity representing and entire dinoflagellate zone either below or above this horizon at Horewai Point. This may represent over 400,000 years of missing time. Beds at Honeycomb Light generally strike NNW-SSE, and dip and young steeply to the south-west. At Horewai Point, beds strike approximately N-S and dip either very steeply to the east or are vertical, younging to the east.

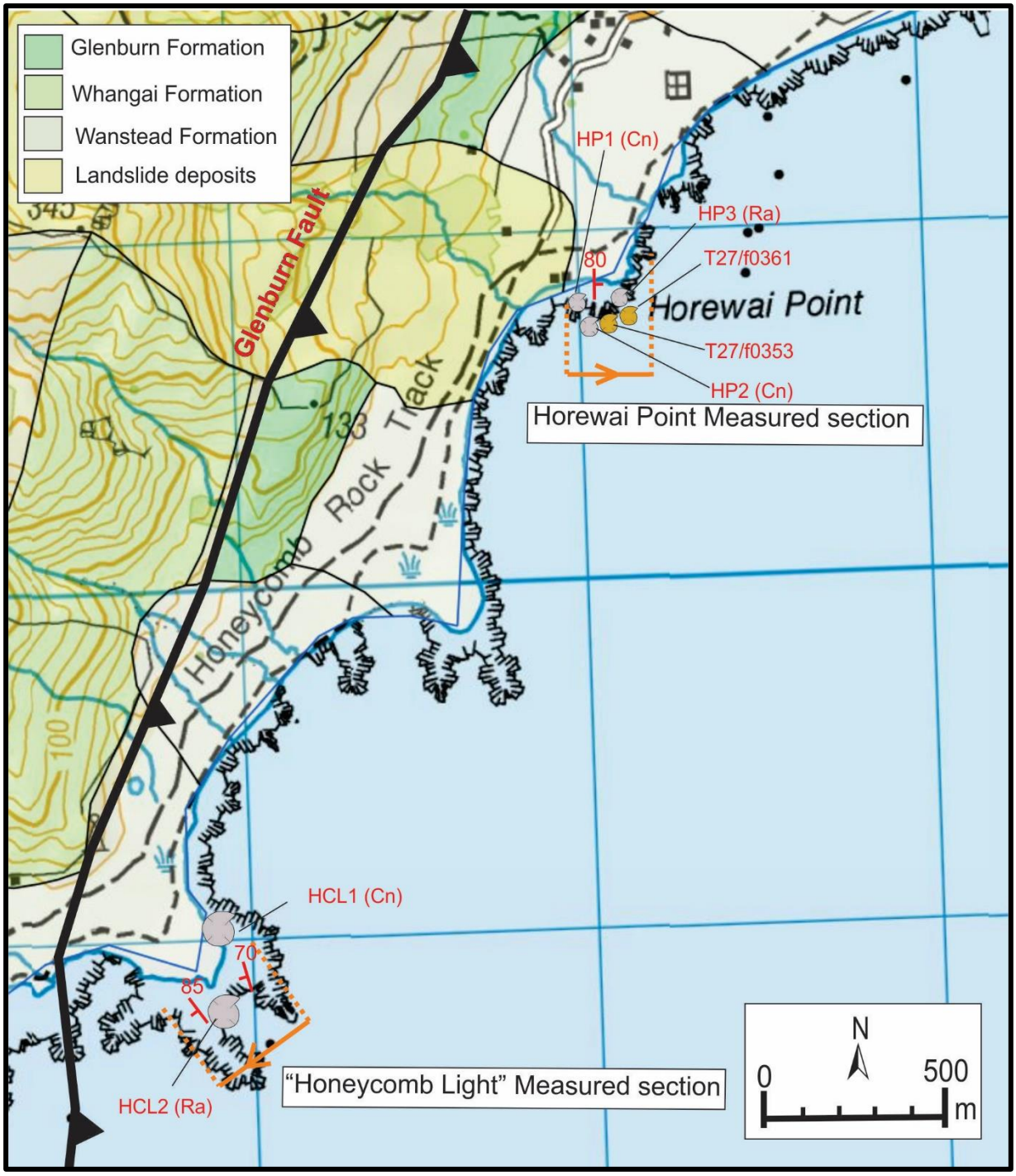

Figure 3.2: Glenburn coast field map, showing labelled fossil localities, with grey representing fossils from this study and orange representing FRED samples used (see appendix B) and generalised strikes and dips directions. Base map LINZ topo50 map (sheet BQ35), with grid lines numbered for reference, overlain by GNS's New Zealand Geology Web Map, accessed from http://data.gns.cri.nz/geology. In this map, coastal outcrops of Glenburn Formation are mapped as "Holocene shoreline deposits".

3.3.2: Totara Stream

Totara Stream is a large tributary of the Kaiwhata River, near Ngahape, Wairarapa. Crampton (1997) and Moore (1980) referred to the lower parts of the stream as "Kaiwhata Stream". The official LINZ Topo50 map lists the name as Totara Stream and so this name is preferred here. The stream has a significant catchment area, and Moore (1980) used the name Totara Stream for the upper reaches of the northern branch of the stream. Previous studies of the area include those of Brown (1943), Wellman (1970), Moore (1980) and Crampton (1997). The section is accessible from the settlement of Ngahape.

The entirety of the stream lies within the Ngāumu State Forest, a large commercial pine forest plantation covering much of the hill country of the eastern Wairarapa. Ongoing forestry work in the upper parts of the section has severely restricted access to this area for the duration of this study. Because of this, only one day of fieldwork was possible, so analysis of this section is supplemented by work carried out here by both Crampton (1997) and Moore (1980). Additionally, heavy flooding in the weeks prior to this excursion, combined with recent pine harvesting, appears to have negatively affected outcrop exposure due to multiple slumps and high sedimentation. Forestry Enterprises (upper part of the section) and IFS Growth (lower part of the section) currently manage the forestry blocks.

The section examined concerns the lowermost part of the stream, between its confluence with the Kopi Stream and the Pukeroro Fault (BP35 460 423 to BP35 448 428; Figure 3.3). The upstream limit (BP35 460 423) was because of a large debris dam blocking the stream. Strike of beds generally trended NE/SW with dips typically between 40-60 degrees, younging downstream to the northwest. This study did not observe the fault bounded stratigraphic lower contact with the Paleocene to Eocene aged Huatokitoki Formation (Wanstead Group) mapped by Crampton (1997). Whangai Formation conformably overlies Glenburn Formation here and, although the contact is currently obscured, it was observed to be gradational here by Crampton (1997). This section contains rocks from the late Mangaotanean to the early Haumurian.

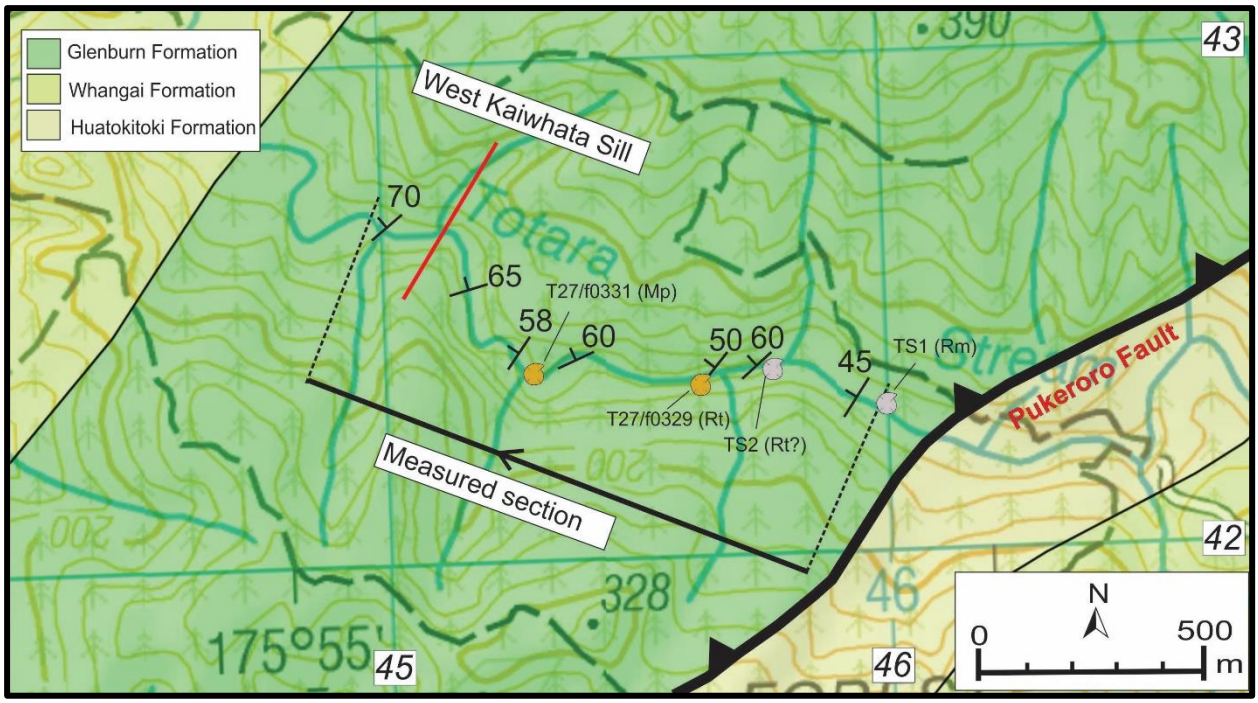

Figure 3.3: Totara Stream field map. Base map LINZ topo50 map (sheet BP35), overlain by GNS's New Zealand Geology Web Map.

3.3.3: Motuwaireka Stream

Motuwaireka Stream is a small stream with headwaters in the hills of the Ngāumu Forest, flowing through the Rewa Bush Conservation Area before flowing out into the Pacific Ocean through the coastal town of Riversdale. The section relevant to this study is contained entirely within the Rewa Bush Conservation Area and a small amount of farmland to the immediate south (BP36 522 499 to BP35 513 515; Figure 3.4). Reconnaissance mapping (Lee and Begg, 2002) suggests Glenburn Formation continues further north, until the forestry road identified on LINZ's Topo50 as Rewa Road, and further south until the river bends eastwards. There are two main branches of the Motuwaireka Stream in this area Figure 3.4) although only the northern branch was examined here. Outcrops downstream of the confluence of the main two branches were poorly exposed, and mapping by Moore (1980) and Crampton (1996) demonstrates there is an anticline at ~BP36 526 498, which would suggest there may be a repeat of the section upstream.

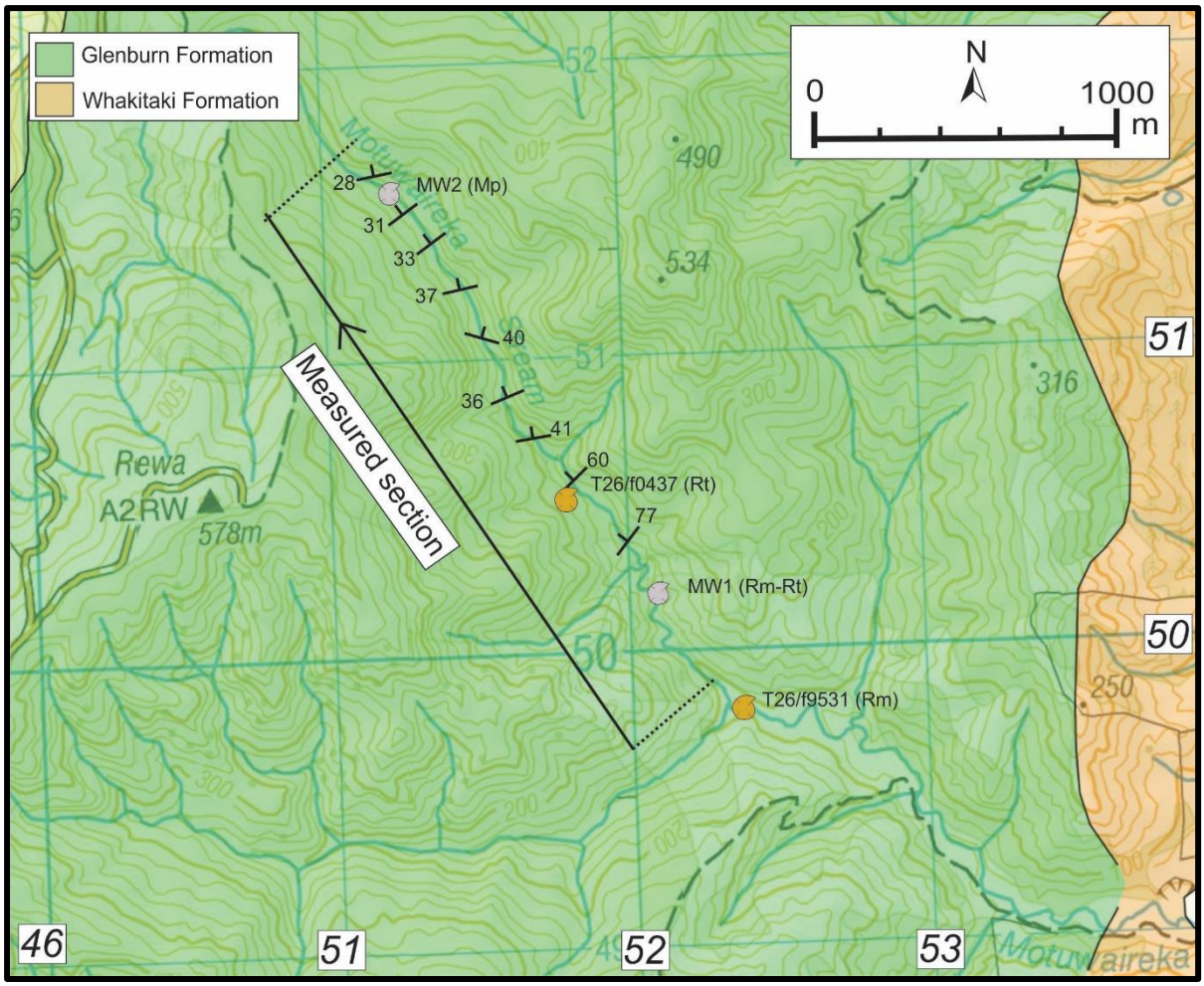

Figure 3.4: Motuwaireka Stream field map. Base map LINZ topo50 map (sheets BP35 (west) and BP36 (east), division along "52" easting), overlain by GNS's New Zealand Geology Web Map.

Fieldwork in this study was conducted via access through farmland from the south. The steep, rugged nature of the stream meant the upper reaches were difficult to access. Further fieldwork could potentially access the stream from the north depending on forestry activity, via Kintail Road, a paper road maintained by local forestry (currently Juken New Zealand), although the flattening of topography near the headwaters may suggest poor outcropping. Despite the fact that the legal paper road extends along Motuwaireka Stream quite some way, there is no actual formed road or track there.

This section does not encounter either a lower or an upper contact of Glenburn Formation, but it spans at least Mangaotanean through to Piripauan-aged strata based on the sparse fossils observed. Moore (1980) mapped the lower contact of the Glenburn Formation here to be a fault contact with Whangai Formation, though Lee and Begg instead mapped the

contact with the Miocene Whakataki Formation. Lee and Begg (2002) mapped the upper contact exposed near Rewa Road with the Whangai Formation as a conformable contact. Strikes of beds generally trended NE-SW with dips to the NW that tended to decrease upstream from ~80° to ~30°.

3.4.4: Mataikona River

The Mataikona River is a river located north of Castle Point. The section of the river mapped begins roughly 6 km from the mouth of the river, at the southern end of the forestry block north of Mataikona Station (BN36 742 861 to BN36 736 867; Figure 3.5). The type section of the Te Mai Formation of Johnston (1971, 1975, 1980) was located along a tributary on the true right of the Mataikona River ("Puketewai Creek"; BN36 732 830). However, currently obscured outcrop means no section was measured there. Another tributary further north, Smokey Gulley Stream, has also been previously mapped. In this study, only a small section of the lower part was accessible due to logging operations in the headwaters. The river was accessed via the south through Mataikona Station.

There are several other outcrops of Glenburn Formation in the immediate vicinity (Lee and Begg, 2002; Neef, 1995), such as along Waipaua Stream (BN37 778 864). However, outcropping is generally poor and discontinuous or does not represent enough stratigraphic thickness to warrant a measured section.

The lower contact of the Glenburn Formation here is with the Whangai Formation, against an unnamed thrust fault (Figure 3.5; Lee and Begg, 2002). Glenburn Formation grades conformably to Whangai Formation in the northern part of this area (Crampton, 1997), which was not observed in this study due to obscured outcrop. Strata from the Mangaotanean to Haumurian stages are present. Outcropping was generally discontinuous, and large portions of the section are obscured. Strikes of beds trended NNE/SSW, generally dipping moderately steeply and younging to the NW.

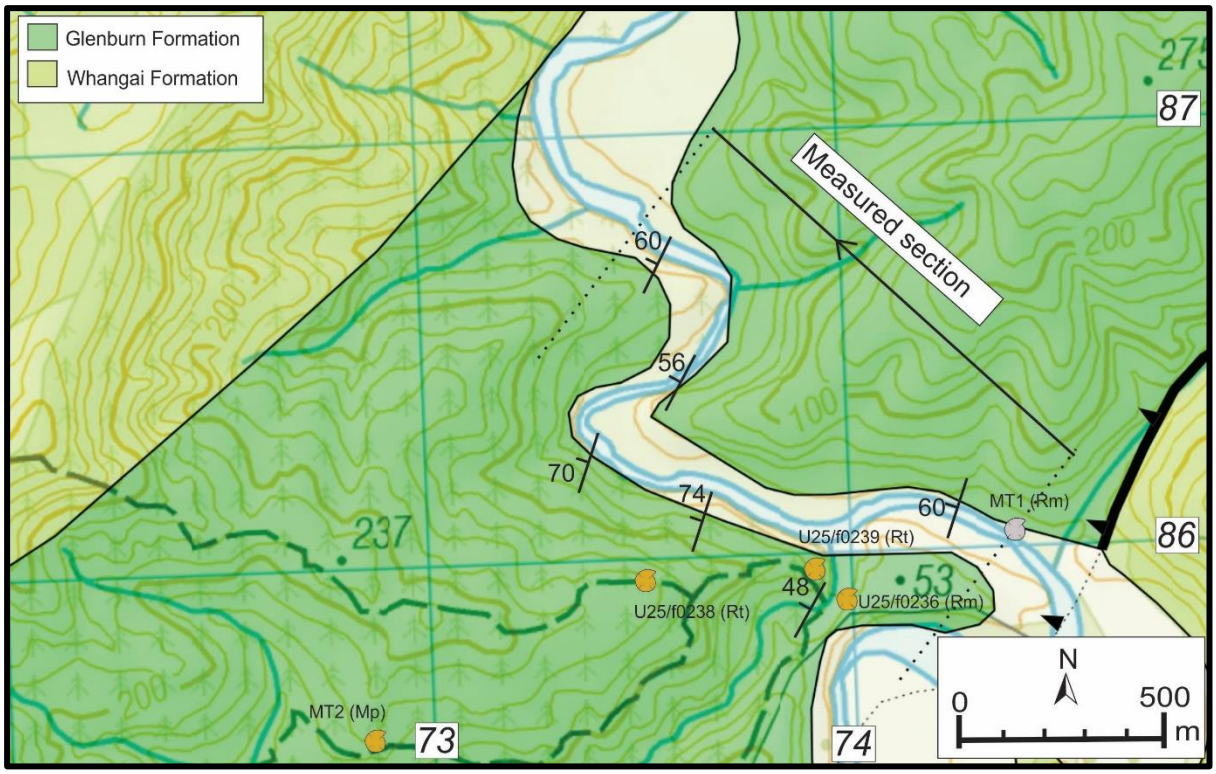

Figure 3.5: Mataikona River field map. Base map LINZ topo50 map (sheet BN36), overlain by GNS's New Zealand Geology Web Map.

3.4.5: Waimata River

The Waimata River is a small river located approximately 9 km northeast of the larger Akitio River. The region is highly complex structurally, with several large faults passing through the river including the Whakataki Fault (Lee and Begg, 2002). The river runs mainly through forestry and bush. The river was accessed from the west, via Akitio Station. Outcrop in the Waimata River is currently poor and discontinuous, with much of the river running along strike, and hence the region is not conducive to a measured section. Instead a small composite section is shown in Appendix I, spanning outcrop from approximately BN37 952 091 to BN37 942 104 (Figure 3.6).

The only macrofossils identified in this section were of Teratan Age (*Inoceramus opetius).* Neef (1992) mapped the Akitio area in detail and noted Mangaotanean-Teratan thin-bedded sandstones, which he designated as the "Kipihana Formation". Thicker bedded strata were assigned to the "Te Mai Formation". These formations are now considered as part of the

Glenburn Formation (Crampton, 1997). Neef (1992) also mapped some of the Cretaceous ESB strata as Springhill Formation; however, this is now considered Glenburn Formation as well due to its stratigraphy and position within the ESB (Crampton, 1997). There is no record of conglomerate within the Glenburn Formation in the immediate vicinity of Waimata River by this study or previous work. Beds tended to strike NE/SW and dip steeply to near-vertically, younging to the northwest.

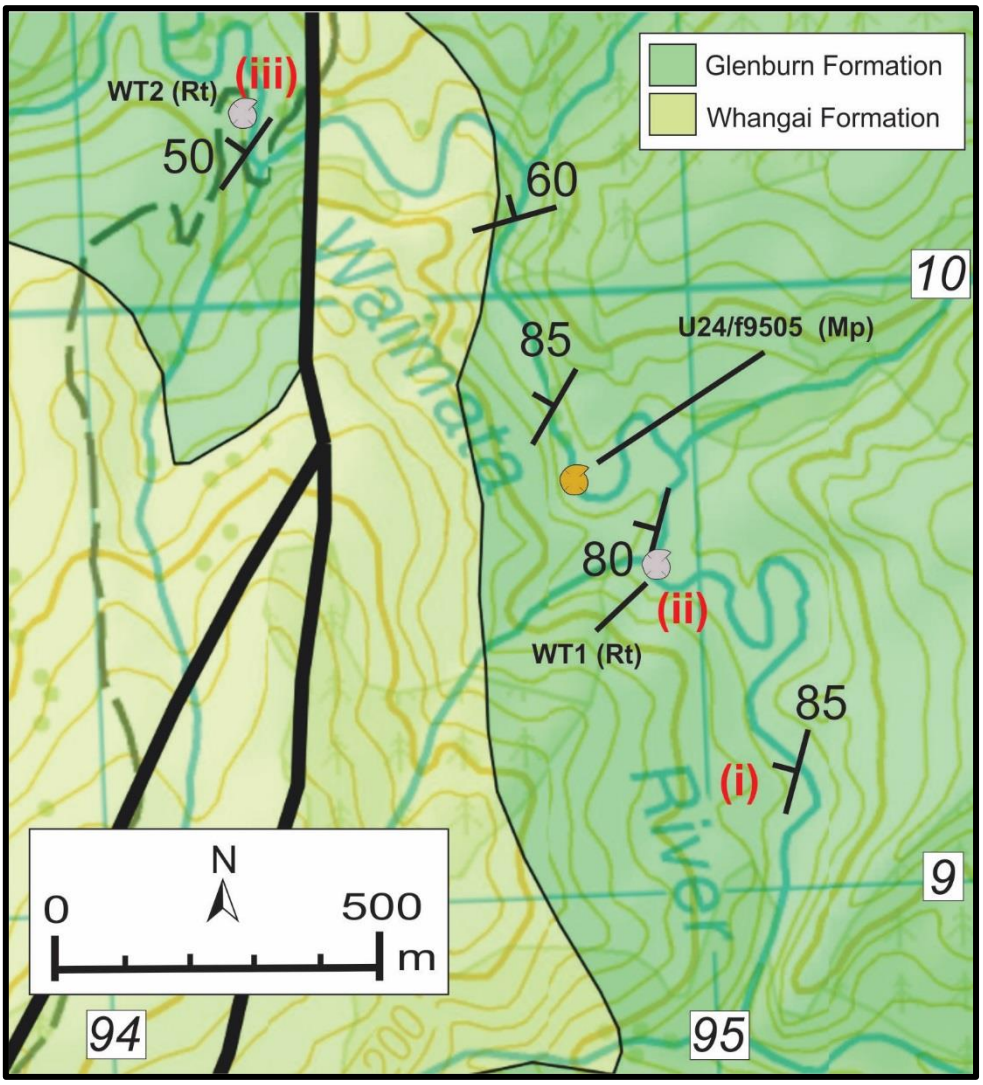

Figure 3.6: Waimata River field map. Base map LINZ topo50 map (sheet BN37), overlain by GNS's New Zealand Geology Web Map. Composite section numbers indicated in red.

3.4.6: Mangakuri Beach

Glenburn Formation outcrops in a thin band along the coast of southern Hawkes Bay, south of Kairakau, for approximately 10 km south along the beach (BL39 356 699 to BL39 327 637, Figure 3.7, Figure 3.8). This section is accessible from the settlement of Mangakuri. The area is highly faulted meaning stratigraphic thickness is difficult to determine. Outcrops are exposed on the shore platform as well as small coastal cliffs. Much of this outcrop is only visible at low tide. Only Glenburn Formation and a Late-Cretaceous to Neogene melange are present on this part of the coast (Lee et al., 2011). Fossil records suggest a Piripauan to Teratan age, and a Teratan age for outcrops north of Mangakuri (Appendix B). Beds tended to strike NE/SW, younging and dipping to the NW, although some beds were inferred to be overturned based off order of Bouma divisions (Figure 3.7).

Also of note is the presence of offshore early Cretaceous volcanic facies at Hinemahanga Rocks, which are probably related to Red Island at Waimarama. A brief discussion of these rocks is found in Section 2.1.2: Karamea (Red Island) and Hinemahanga Rocks.

An additional point of interest is that a fossil hunter recovered a reptile vertebra from the mouth of the Mangakuri River, from within the Glenburn Formation (FRED V22/f0474). This is likely a plesiosaur fossil and represents the only vertebrate fossil recovered thus far from the Glenburn Formation.

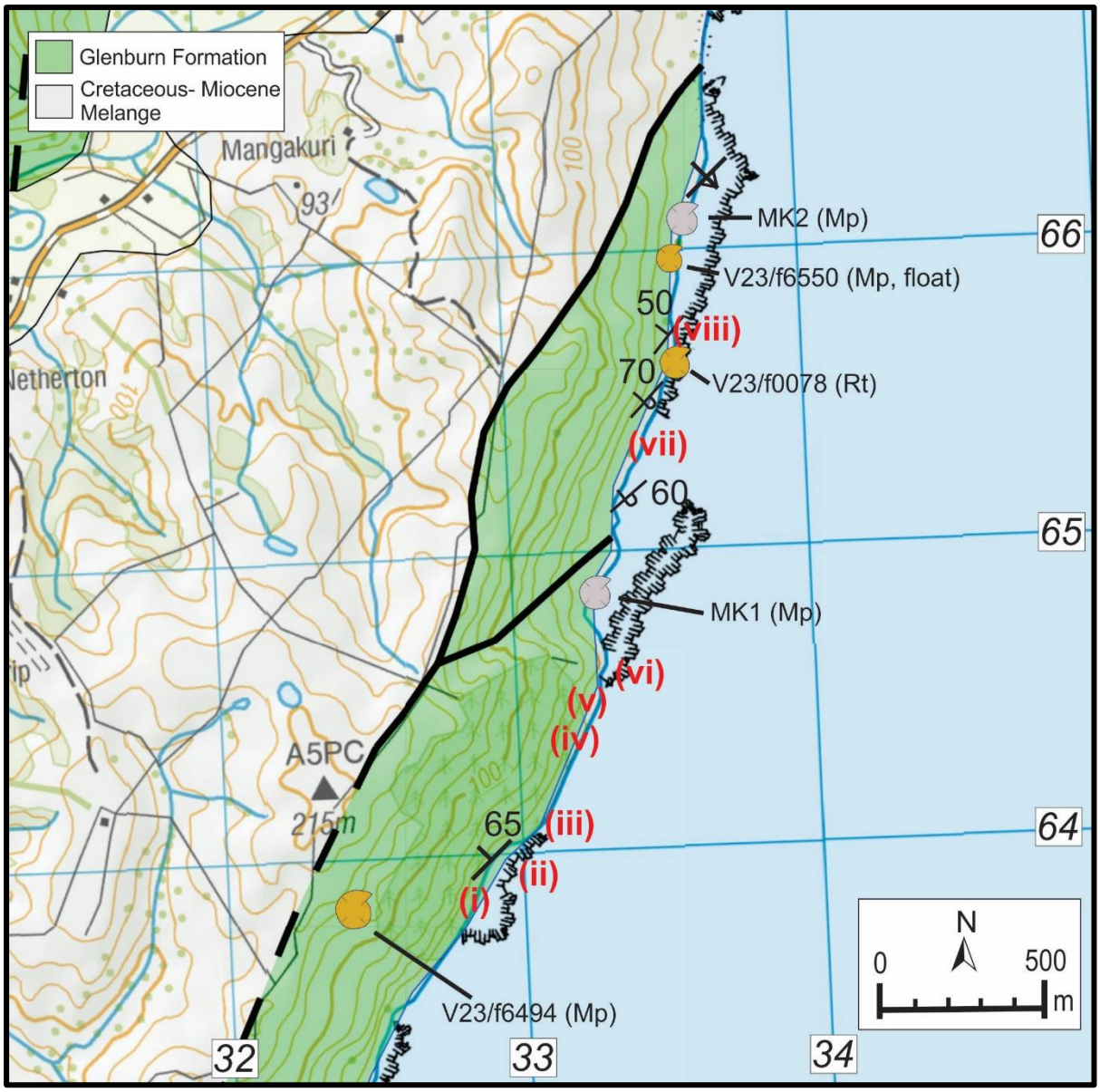

Figure 3.7: Southern Mangakuri Beach field map. Base map LINZ topo50 map (sheet BL39), overlain by GNS's New Zealand Geology Web Map. Composite section numbers indicated in red.

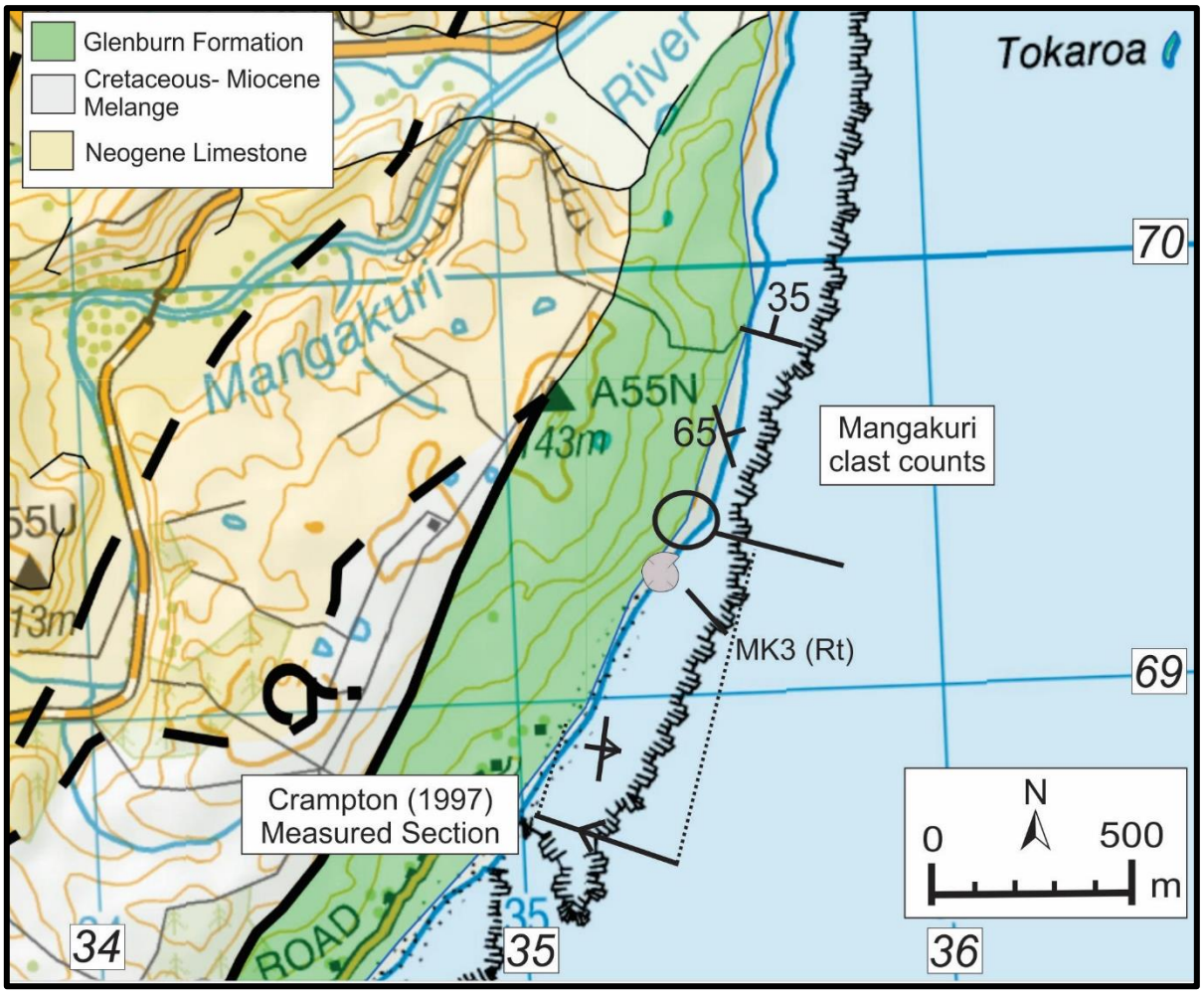

Figure 3.8: Northern Mangakuri Beach field map. Base map LINZ topo50 map (sheet BL39), overlain by GNS's New Zealand Geology Web Map. "Tokaroa" in top right is one of the Hinemahanga Rocks.

3.4.7: Waimarama Beach

Waimarama is the northernmost location where the Glenburn Formation is exposed. Glenburn Formation outcrops to the south of the settlement of Waimarama, in a series of faulted blocks. Glenburn Formation is found both on shore platforms and on steep sea-cliffs. The entire section is very heavily faulted. A composite section was taken between approximately BL39 402 791 and BL39 426 826

The northernmost part of the section contained abundant macrofossils including *Inoceramus opetius* and *Inoceramus madagascariensis,* which indicate a Teratan age. Southernmost outcrops also contained *Inoceramus opetius*, although possible *Cremnoceramus bicorrugatus*

fossils have been recovered from the area around Red Island, which might suggest some Mangaotanean aged strata (Figure 3.9; Appendix B). Due to the complex tectonics, strikes and dips of beds varied significantly, but generally strikes trended NE/SW and dipped moderately steeply to near-vertically.

One of the local points of interest is the Early Cretaceous volcanics of Karamea, also known as Red Island, discussed briefly in Section 2.1.2 (Kobe, 1976; Kobe and Pettinga 1984; Black et al., 1984; Moore et al., 1987). Karamea is an approximately 40 m high hill joined at low tide to the mainland by a tombolo. How this sequence ended up where it is remains unresolved. Two main explanations have been proposed; either Red Island was accreted during the later stages of subduction along the Gondwana margin, or it was emplaced in its current location by Neogene tectonic deformation (Kobe and Petting, 1984).

Moderately common small, dark red clasts in conglomerates at Mangakuri Beach possibly originate from either Red Island or similar deep marine volcanic deposits. Positive identification of origin is not possible without geochemical analysis.

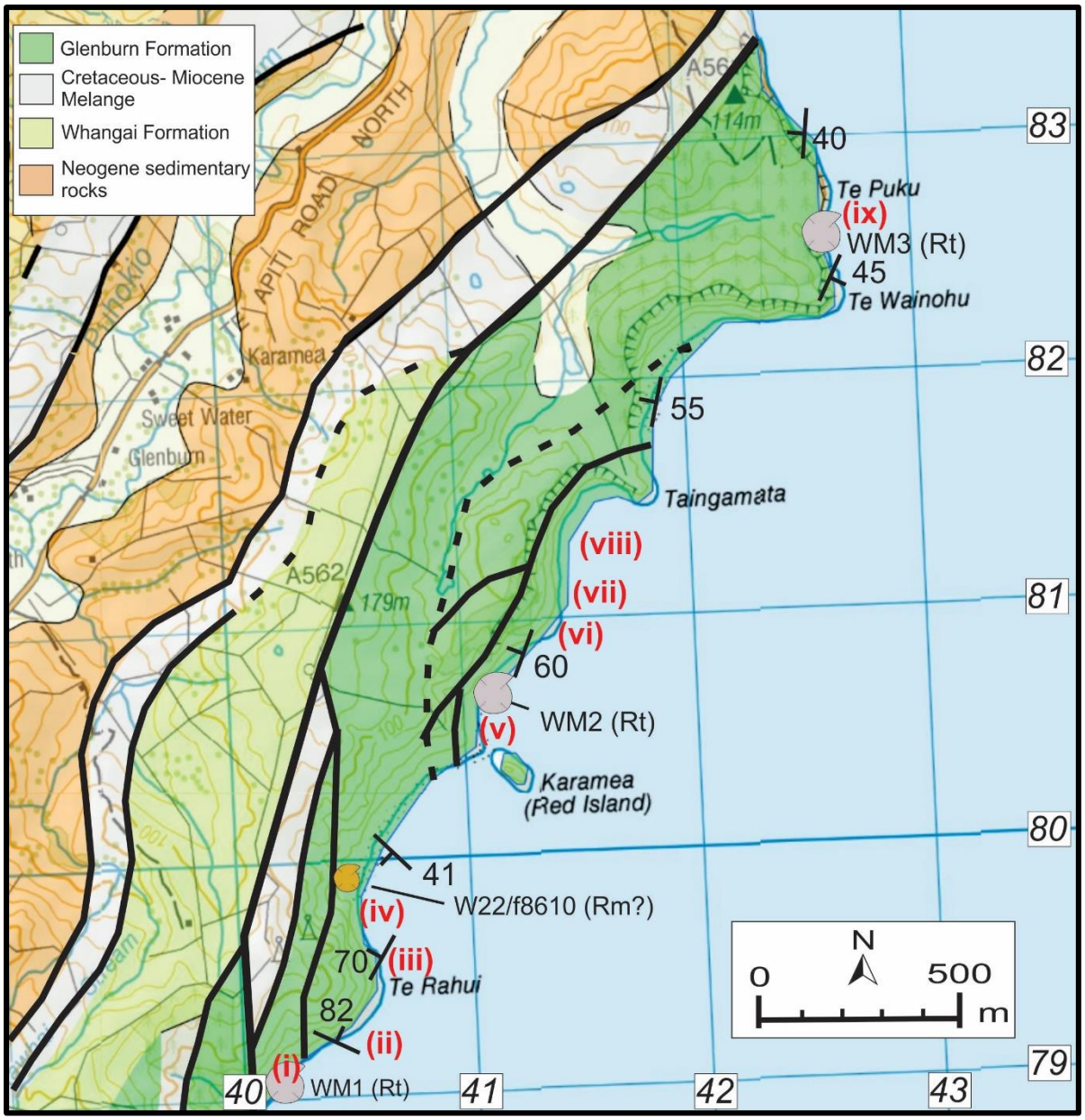

Figure 3.9: Waimarama Beach field map. Base map LINZ topo50 map (sheet BL39), overlain by GNS's New Zealand Geology Web Map.

3.4: Conglomerate clast count methodology

Clasts were counted in conglomerates at three different localities to deduce whether clast composition proportions changed significantly over time and space. The conglomerates chosen were from the Glenburn coast area (latest Ngaterian to Arowhanan), Totara Stream (Mangaotanean and Teratan) and Mangakuri Beach (Teratan). Crampton (1997) and Johnston (1980) also noted conglomerates in the Mataikona River and in the nearby vicinity; however these conglomerates are currently either obscured or inaccessible. Motuwaireka Stream and Waimarama Beach also contain conglomeratic beds. This study did not take clast counts at these localities as they are spatially and temporally largely correlative with the strata in Totara Stream and Mangakuri Beach respectively.

This study uses the clast counting method from Howard (1993). This paper suggests a clast count of 400 is an ideal balance between precision and labour. The method aims to achieve as random and representative a sample as possible. True random selection of which section of a conglomerate outcrop to survey is not usually possible because outcrops in the Glenburn Formation are often partially obscured or are tilted such that only small areas of outcrop are visible.

In order to randomise as best as possible, outcrops were divided into 1 m wide blocks and selected using a pseudorandom number generator. This helps to minimise statistical errors introduced by conscious or subconscious bias towards more “interesting” looking sections of outcrop. Howard (1993) suggests sample width should be at least 2.5x the dimensions of the long axis of the largest clasts, so if clasts are >40 cm in length a larger sample division may be necessary, e.g., 1.5 m or 2 m. Once a conglomerate bed was selected, the section exposed was measured along strike with a tape measure to find the total width exposed. A pseudo-random number generation function on a graphics calculator then produces a number between one and the width of the total exposure to determine an interval by which to survey. Once a metre-wide interval has been established, the clasts are counted systematically using the “area or ribbon method” described in Howard (1993), using a marker pen to mark every clast as it is counted off. This process was repeated until the desired sample size was achieved.

It is acknowledged that this does not produce a truly random sample as there is no way for accounting for any bias in what strata are preserved and exposed. There is also possibly preferential erosion of softer clasts such as mudstones. It is likely that highly indurated clasts such as Torlesse style greywackes and argillite are preserved preferentially.

At least one sample for each clast type identified was collected for laboratory examination to help rectify some in-field identification errors. Because some different clast lithologies may bear close resemblance to one another, there is a potential for error here.

Significance testing

Proportional confidence interval testing can be used to test whether differences in clast composition are statistically significant. Confidence intervals (CI) for each proportion are calculated with the equation:

Eq 1: $$\hat{p} \pm t * \sqrt{\frac{\hat{p}(1-\hat{p})}{n}}$$

Where $\hat{p}$ is the sample proportion, t is the calculated value of student's T-distribution based on n-1 degrees freedom for a given confidence interval and n is the total clast count (Howard, 1993). For n = 400, as in all individual counts for this study, t for 95% confidence is 1.97 and t for 99% confidence is 2.59 (3 s.f.).

To test for a significant difference in proportions between proportions $\hat{p}_1$ and $\hat{p}_2$, equation 2 is used:

Eq. 2: $$\hat{p}_1 - \hat{p}_2 \pm t * \sqrt{\frac{\hat{p}_1(1-\hat{p}_1)}{n_1} + \frac{\hat{p}_2(1-\hat{p}_2)}{n_2}}$$

Where t is the tabulated t-distribution value for $n_1 + n_2 - 2$ degrees of freedom. Because in this study all values of n = 400, any comparison between two individual beds will have 798 d.f. The null hypothesis in this equation is that there is no significant difference between the two populations.

Eq. 2 gives an interval between two numbers. If 0 lies between these, e.g., -1.24 $< \hat{p}_1 - \hat{p}_2 <$1.5, the null hypothesis is not rejected and there is no statistically significant difference between populations. If 0 does not lie between these two numbers, e.g., -1.24 $< \hat{p}_1 - \hat{p}_2 <$-

0.12, the null hypothesis is rejected and there is a statistically significant difference between the two populations.

Although 95% confidence is standard procedure, the potential for field identification errors and counting errors mean a more stringent confidence interval may be appropriate. As such, comparisons in this study uses a 99% CI, and therefore a t value of 2.58 is used in the equations above.

A note on error bars

The graphs presented herein are for comparative purposes and therefore do not use 99% confidence interval error bars. This is because comparing two separately derived confidence intervals introduces a significant type I error (Payton et al., 2000) and statistically significant population differences cannot be discounted by overlapping confidence. MacGregor-Fors and Payton (2013) suggest that using 94% CI error bars best represents a 99% confidence test in graphical form. Because the aim of the graphs is to demonstrate in graphical form whether there are statistically significant differences, this 94% CI is used for the error bars on graphs.

Differentiation of common clasts

Sedimentary clasts make up the majority of clasts in all conglomerates studied. However, there is usually a distinction in the degree of induration, which is likely a representation of exotic material versus “locally derived” material. As such, the following sections use “indurated sandstone” and “argillite” to refer to sandstone and mudstone clasts that are inferred to be from indurated material (likely Torlesse sourced). The results use mudstone and sandstone as terms to refer to material clearly less indurated that is likely to have been derived intra-basinally. The siderite cement commonly found in mudstone clasts in Totara Stream is probably due to post depositional processes, but are listed as separate classes due to the clear distinction between them and non-sideritic mudstone clasts.

Chapter 4: Facies analysis methodology

4.1: Introduction

Determining the depositional environment of interbedded sedimentary successions such as the Glenburn Formation requires the use of detailed facies analysis. The following chapter presents the facies scheme used in this study, as well as a brief introduction to the processes that transport and deposit sediment gravity flows.

4.2: Submarine Gravity Flow Transport Processes

Sediment gravity flows (SGFs) are responsible for delivering vast amounts of sediment in to the deep ocean (Pickering and Hiscott, 2015; Shanmugam, 2016). A comprehensive discussion on the mechanics and physics of the different types of SGFs is found in Pickering and Hiscott (2015).

Pickering and Hiscott (2015) describe four main types of SGF:

- Cohesive debris flows and mudflows
- Inflated sandflows
- Concentrated density flows (also commonly referred to as “high-density turbidity currents”)
- Turbidity currents

The various other names used by other authors for these processes are discussed in Pickering and Hiscott (2015). These mechanisms can transport sediment hundreds to thousands of kilometres on slope gradients of less than 5°.

The characteristic deposits of these different SGFs are summarised in Figure 4.1 and Table 4.1. Some facies are diagnostic of a certain SGF process. For example, graded “Bouma sequences” (Figure 4.2) are the result of turbidity currents, whereas graded conglomerates are the result of concentrated density flows (“Lowe sequence”; Figure 4.3). Other facies, such as disorganised conglomerates, can be transported and deposited by several different processes (Pickering and Hiscott, 2015).

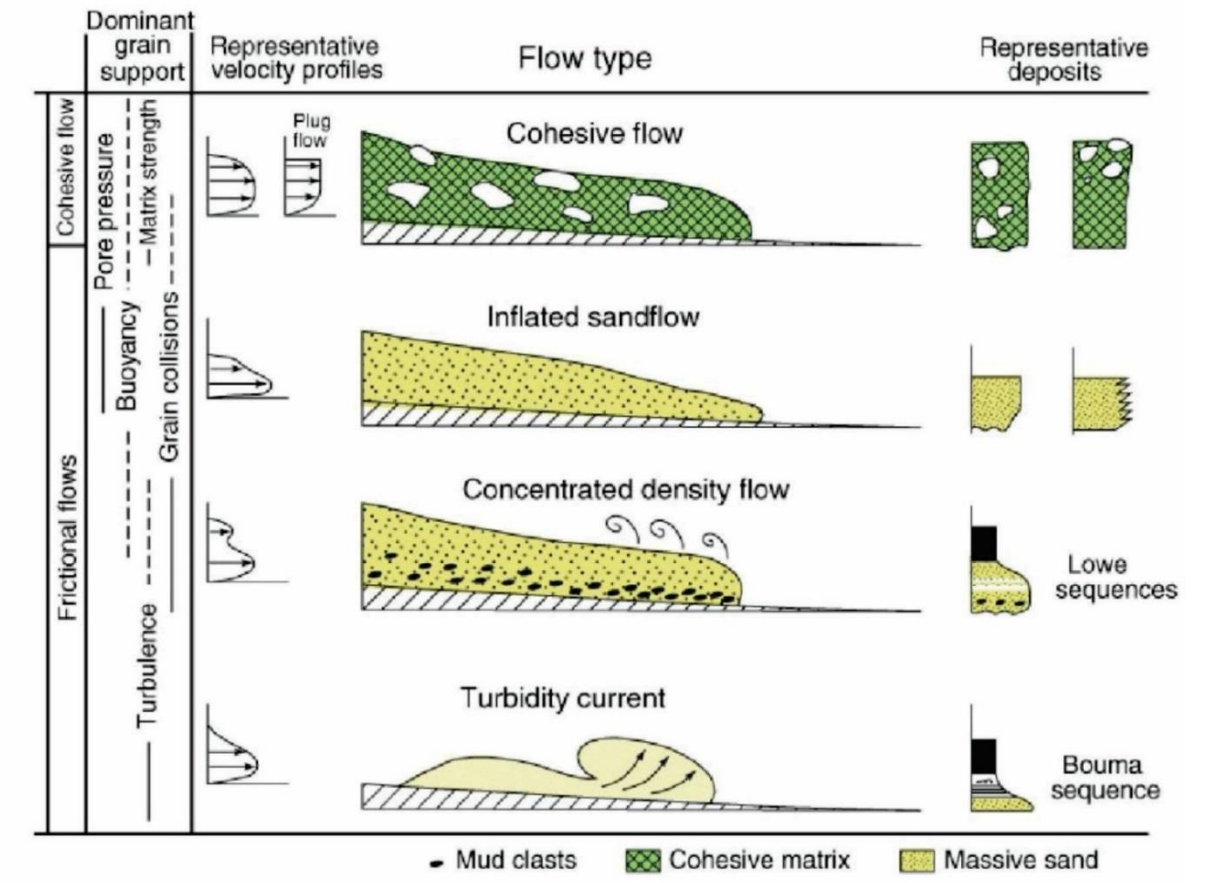

Figure 4.1: Representative sketches of SGF types, their dominant method of grain support, velocity profiles and resulting deposits. From Pickering and Hiscott (2015), their Figure 1.22, based off the classification scheme of Mulder and Alexander (2001). “Representative deposits” are not exhaustive, see Table 4.1. Bouma and Lowe sequences shown in more detail in figures 4.2 and 4.3.

4.3: Background of Facies Models

SGFs have been an area of significant interest among sedimentologists, particularly in the past 50 or so years. Mutti et al. (2009) contains a comprehensive discussion of the history of research into turbidites and other SGF deposits. To summarise, although the term "flysch" had been used to describe what are now recognised as turbidites since the early 19th century, it was not until the mid-20th century that the connection was made between turbidity currents, themselves a relatively recent concept, and the graded sandstone beds commonly associated with flysch deposits. Kuenen and Migliorini (1950) was the first widely read publication to state this finding.

This paper paved the way for the likes of the classic "Bouma sequence" of Bouma (1962; Figure 4.2), which revolutionised deep marine sedimentology and gave field geologists an easy to remember and effective tool for classifying graded sedimentary beds in the field. However, Bouma's facies descriptions are increasingly regarded as a significant oversimplification of the very complex topic (Shanmugam, 1997, 2000).

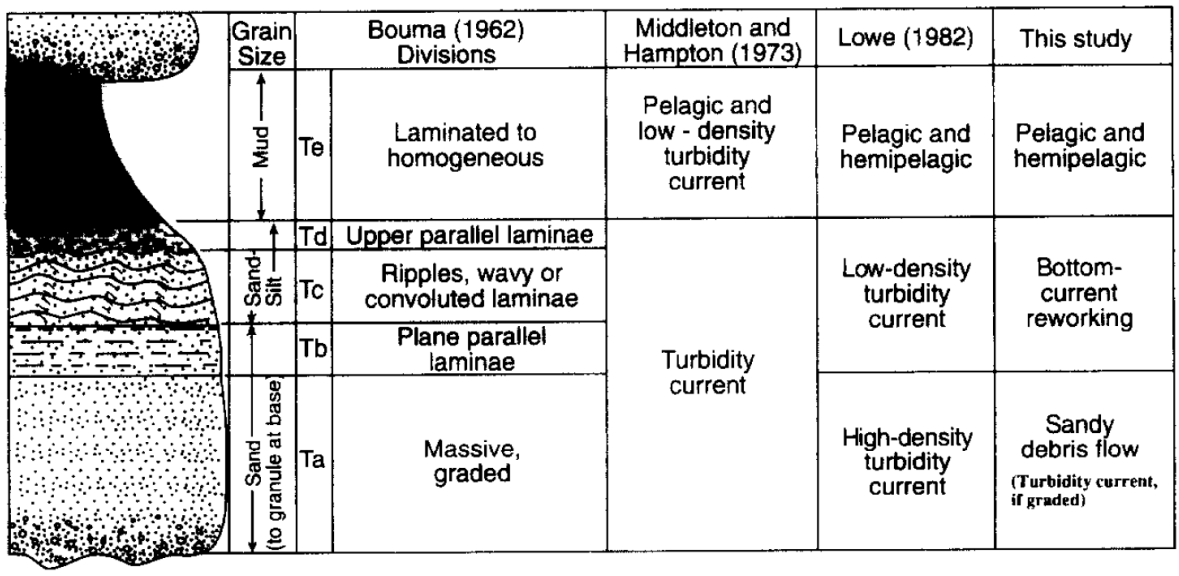

Figure 4.2: Bouma sequence and various interpretation of mechanisms. From Shanmugam, 1997, his Figure 1.

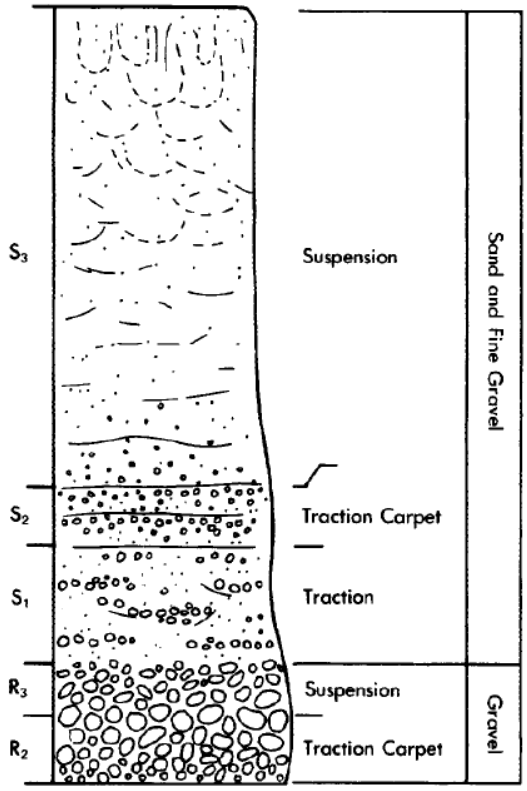

Figure 4.3: "Lowe Sequence", showing typical facies of a concentrated density flow. From Lowe (1982), his Figure 8.

Many studies over the past 50 or so years have attempted to create depositional environment based facies models, such as the widely cited fan models of Bouma (1962), Mutti and Ricci Lucchi (1978) or Walker (1978, Figure 4.4) but these models are generally now regarded as too simplistic (Shanmugam, 2016; Pickering and Hiscott, 2015). Pickering and Hiscott (2015), in concluding their chapter on submarine fan systems, state:

> "…frustrating as it may be to readers searching for simple and general models, we do not conclude with a set of distinct depositional models for submarine fans."
> (Pickering and Hiscott, 2015, p. 882)

Issues surrounding the use of simplistic models are compounded by the fact that deep water submarine fan systems may have very similar facies to shallow delta-front deposits (Mutti et al., 2003, 2007) and non-fan "sheet" systems (Pickering and Hiscott, 2015). Because of these

issues, assigning individual facies to a particular depositional environment is untenable and no individual facies is considered diagnostic of any part of a submarine fan. Because of this, other aspects such as stacking patterns and horizontal facies variability are necessary to determine depositional environments of individual outcrops (Pickering and Hiscott, 2015). As such, a descriptive facies scheme is presented in the following section, and interpretations of these facies made in Chapter 6 using broad-scale trends and facies associations.

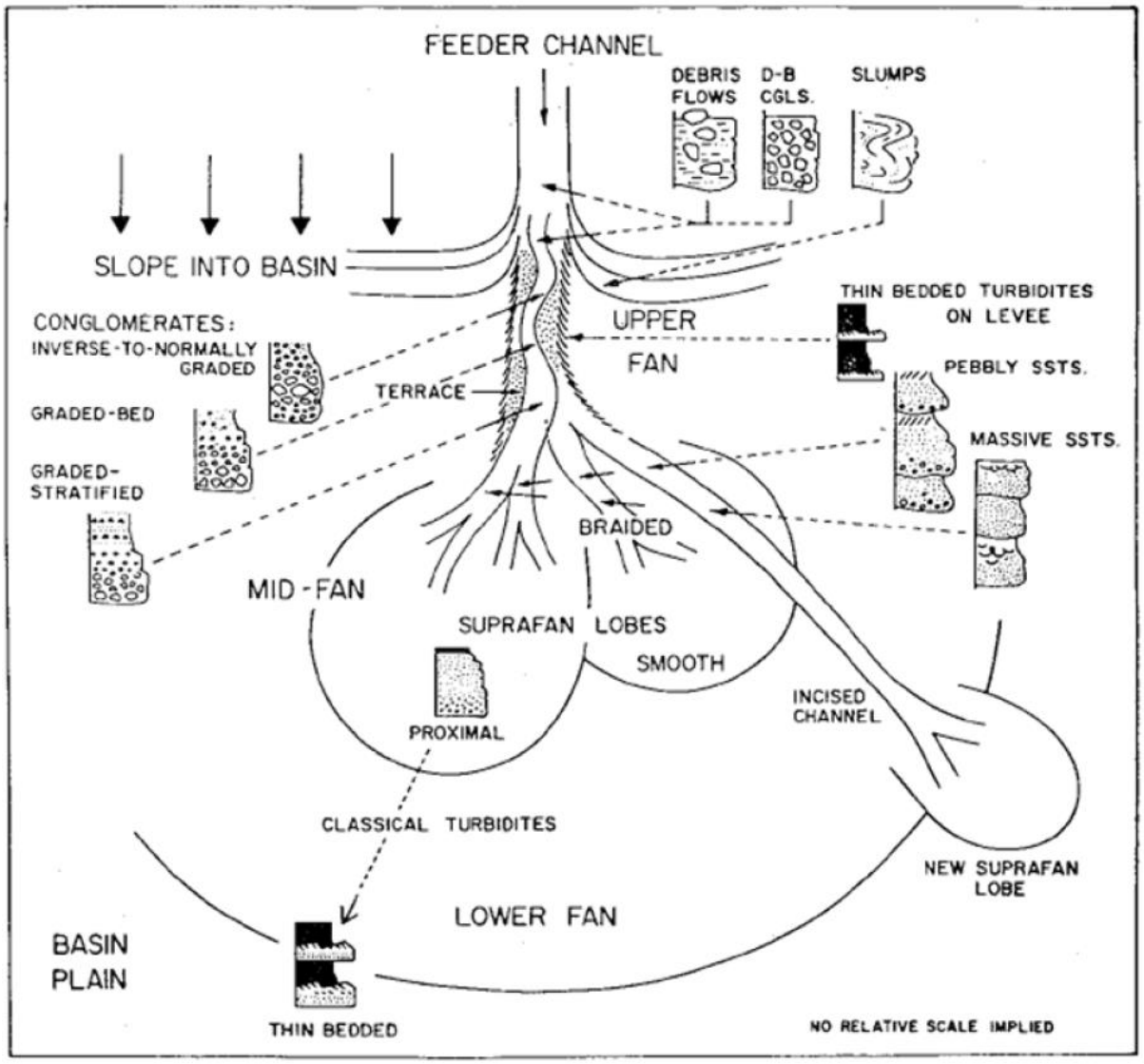

Figure 4.4: Walker (1978) facies model. Now widely considered oversimplified, but commonly cited as a broad approximation of the distribution of facies within a submarine fan. His Figure 18.

4.4: Facies Scheme Description

4.4.1: Introduction

The sedimentary facies classification scheme used in this study is based upon that of Pickering and Hiscott (2015), a recent update of the widely cited scheme of Pickering et al. (1989). This is a hierarchical scheme whereby facies are sorted first by grain size and then subdivided based on other key features such as sorting and grading. The scheme of consists of seven facies groups: A, B, C, D, E, F and G. No depositional environment is implied for individual facies; instead, these are simply descriptive of the sedimentary features of individual beds. The facies scheme used herein is adapted from Pickering and Hiscott (2015) to exclude several facies that have not been observed in the Glenburn Formation.

Both F and G (chaotic and ooze deposits respectively) are excluded as they were not observed. As such, five facies classes are represented here: A, B, C, D and E. These broadly represent a progressive fining of sediments. Each facies class is divided into two groups: disorganised and organised, and these groups further divided into individual facies (Figure 4.5). The facies scheme of Pickering and Hiscott (2015) lists the potential transport and depositional processes for each of the individual facies. These are replicated in the descriptions below. All facies descriptions are a modification of those in Pickering and Hiscott (2015), and all information regarding transport and depositional processes are taken directly from their scheme.

In the descriptions that follow, standard terms for bed thicknesses classes follow Ingram (1954):

- laminae, <1 cm;
- very thin beds, 1 – 3 cm;
- thin beds, 3 – 10 cm;
- medium beds, 10 – 30 cm;
- thick beds, 30 – 100 cm;
- very thick beds, >100 cm thick.

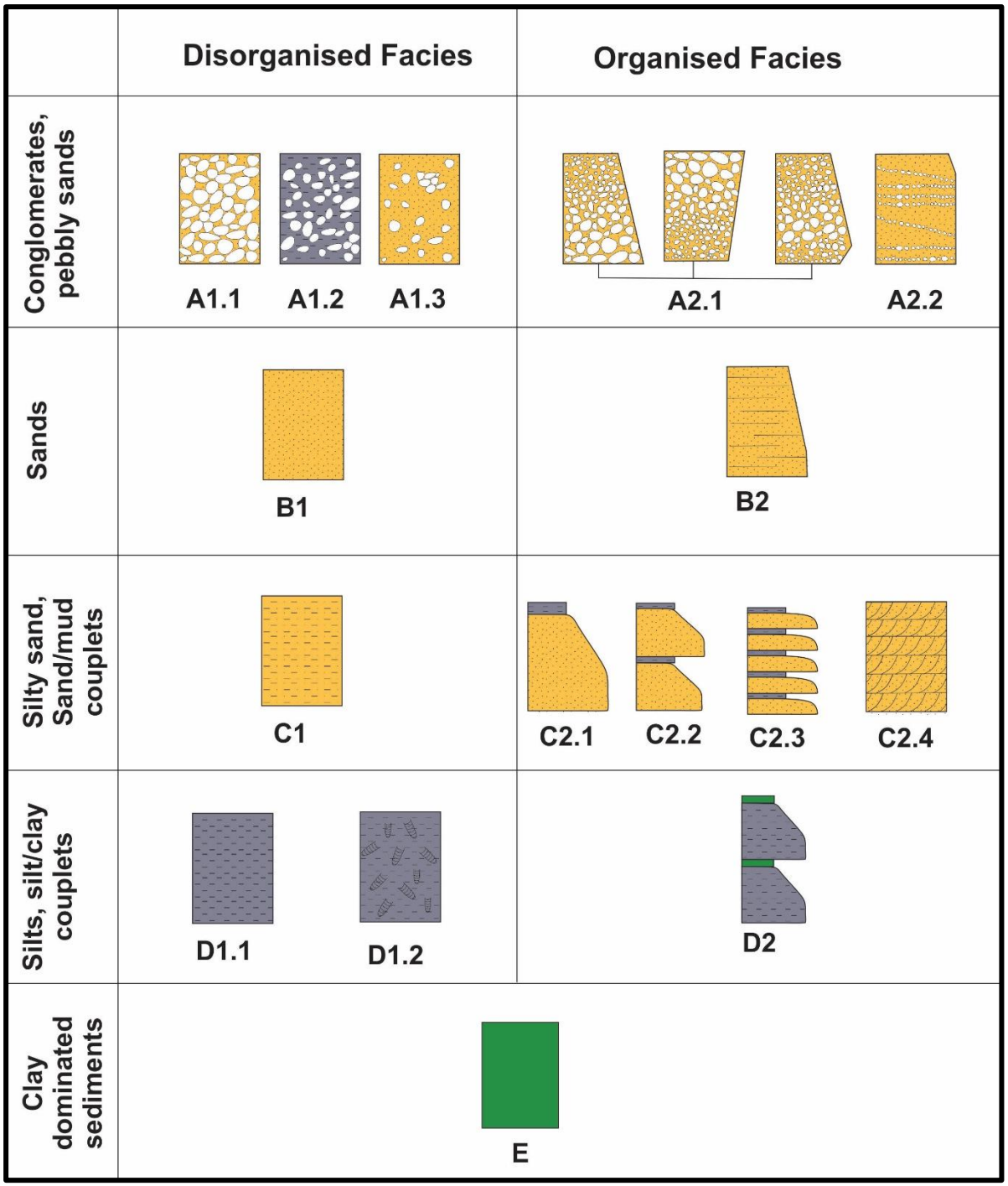

Figure 4.5: Schematic representation of facies scheme used herein, which was adapted from Pickering and Hiscott (2015; their Figure 2.4). Yellow represents sand dominated beds/matrix, grey represents siltstone and green represents clay. In Facies C1 dashes are used to denote the presence of silt in a sand dominated bed. Facies A2.1 represents graded conglomerates, which may be normally, inversely or normal-inversely graded. Given the similar transport mechanisms and the lack of any clear pattern of spatial distribution of these different types of grading in fan systems (Surlyk, 1984), subdivision of this into three separate facies was deemed unnecessary.

Table 4.1 - Facies and their associated transport processes, described by Pickering and Hiscott (2015) or most likely processes for facies not included in their scheme (denoted by question marks). Facies E may have a variety of different processes including turbidity currents and pelagic sedimentation, but without the ability to confidently identify features such as grading in such fine sediment, there is no way of discerning which process is responsible. [1]Thick beds of Facies C2.1 represent sediment deposited by flows transitional between concentrated density flows and turbidity currents. [2] If similar to B2.2 of Pickering and Hiscott - only in confined channels where bottom currents are particularly strong.

Transport Process	Associated Facies
Debris flow, including cohesive debris flows	A1.1, A1.2 D1.1 C1
Concentrated density flows	A1.1, A1.3, A2.1, A2.2 B1, ?B2 C2.1[1] D1.1
Inflated sand/gravel flows	A1.1, A1.3 B1
Turbidity currents	B2 C2.4 C2.1[1], C2.2, C2.3, C2.4 D2
Bottom/contour currents	?C2.4[2] D1.2

4.4.2: Facies Class A: >5% Granule to Boulder Grade Clastics

This facies class includes all conglomerates and pebbly or gravelly mudstone and sandstone. In the Glenburn Formation, the majority of beds of this class consists of matrix-supported pebble to cobble conglomerate. Notable exceptions occur in the Hawke's Bay region where pebbly sandstone and granule conglomerates are common.

A1: Disorganised conglomerates

Unsorted and ungraded conglomerates make up the first facies group. Further subdivision of this facies group is based on the clast frequency and the composition of the matrix. Pickering and Hiscott (2015) divide this in to four different facies, which includes "gravelly mud" and "pebbly sand". These facies are dominantly fine-grained with a secondary component of coarse clastic material. For the sake of simplicity Pickering and Hiscott (2015)'s Facies A1.2 ("disorganised muddy gravel") and A1.3 ("disorganised gravelly mud") are combined here as they each have very similar transport/depositional processes, and gravelly mudstone was very rare in this study.

A1.1: Disorganised conglomerate (Figure 4.6)

Disorganised conglomerates are the most widespread of the Class A1 facies in the Glenburn Formation. Individual beds may be gravel dominated and relatively well sorted or very poorly sorted with gravel to boulder-sized material. This facies may be either clast supported or matrix supported. A sandy matrix may comprise up to 50% of the rock volume. Where the matrix is mudstone rather than sand and comprises >5% of the total rock volume, it is instead classed as Facies A1.2. Where clasts are dispersed in a sandy matrix (>50% matrix) it is instead Facies 1.3. Large sandstone "rafts" of intraformational material up to boulder sized may occasionally be present.

Transport processes: debris flows, concentrated density flows and inflated gravel/sand flows.

Depositional processes: cohesive freezing on decreasing slope grade.

Figure 4.6: Disorganised conglomerate. New Zealand fur seals (*Arctocephalus forsteri*) for scale (male, top left; others females). Honeycomb Light section (Appendix D, 80-84 m), Glenburn coast. BQ35 369 189.

A1.2: Disorganised muddy conglomerate (Figure 4.7)

Facies A1.2 comprise conglomerates that contain between 5% and 95% muddy matrix. This facies is usually bedded on a <1 metre-scale. The majority of beds of this facies were found in the upper Mangaotanean section at Motuwaireka Stream. One interval of gravelly mudstone was found in Totara Stream (Figure 4.7a). This facies incorporates Facies A1.2 and A1.3 of Pickering and Hiscott (2015).

Transport processes: Cohesive debris flows.

Depositional processes: cohesive freezing.

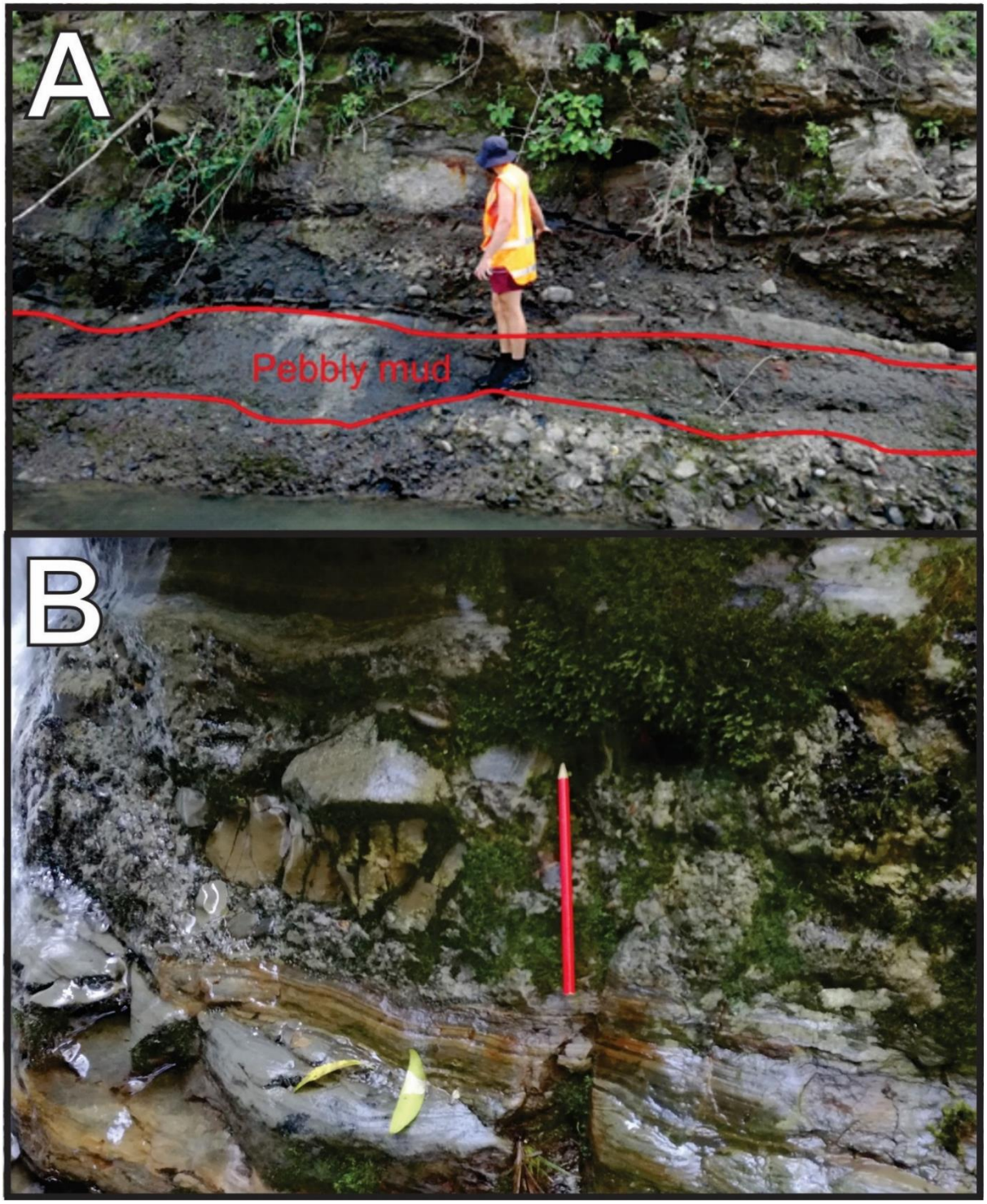

Figure 4.7: A) Poorly sorted muddy conglomerate and gravelly mudstone with pebbly mudstone interval highlighted. Totara Stream section (Appendix F, 95-100 m). BP35 458 424. B) Very poorly sorted muddy conglomerate, Motuwaireka Stream section (Appendix G, 696 m). Pencil ~18 cm long. Note large cobble sized clast. BP35 515 511.

A1.3: Disorganised pebbly sandstone (Figure 4.8)

Pebbly sandstone are beds predominantly composed of sand (>50%) but with a significant component of gravel or coarser material (>5% total rock volume). Although classed as "disorganised", coarse material is commonly concentrated in patches or stringers. Grading and stratification are absent. Mudstone rip-up clasts may also be a significant component of beds. Facies A1.1 commonly grades into A1.3. These beds are common in the Mangakuri/Waimarama area.

Transport processes: concentrated density flows and inflated sand flows.

Depositional processes: collective grain deposition owing to increased intergranular friction as flow decelerates.

A2: Organised conglomerates

A significant portion of conglomeratic facies observed in the Glenburn Formation show some form of grading. How pronounced this is varies significantly, with some beds grading through to sandstone whereas some show only subtle variations in clast size. Grading may also be pronounced in clast frequency, whereby concentration of clasts increases or decreases but clast size remains the same.

Beds may be normally graded (fining upwards), inversely graded (coarsening upwards), or inverse-normal graded (coarsening rapidly at the base before fining upwards). An earlier hypothesis by Walker (1978) that these variations in grading represent proximity to the depositional source appear to have no empirical basis (Surlyk, 1984). Instead, the nature of grading appears to depend on the depositional processes. Inversely graded beds result from coarser clasts lagging behind finer clasts in a concentrated density flow or by intense grain interaction, whereas normally graded beds are deposited grain by grain in a similar manner to turbidites. Inverse-normal graded beds are generally assumed to have resulted from a combination of these processes. Stratified conglomerates were not observed in the Glenburn Formation and hence are not included in this scheme.

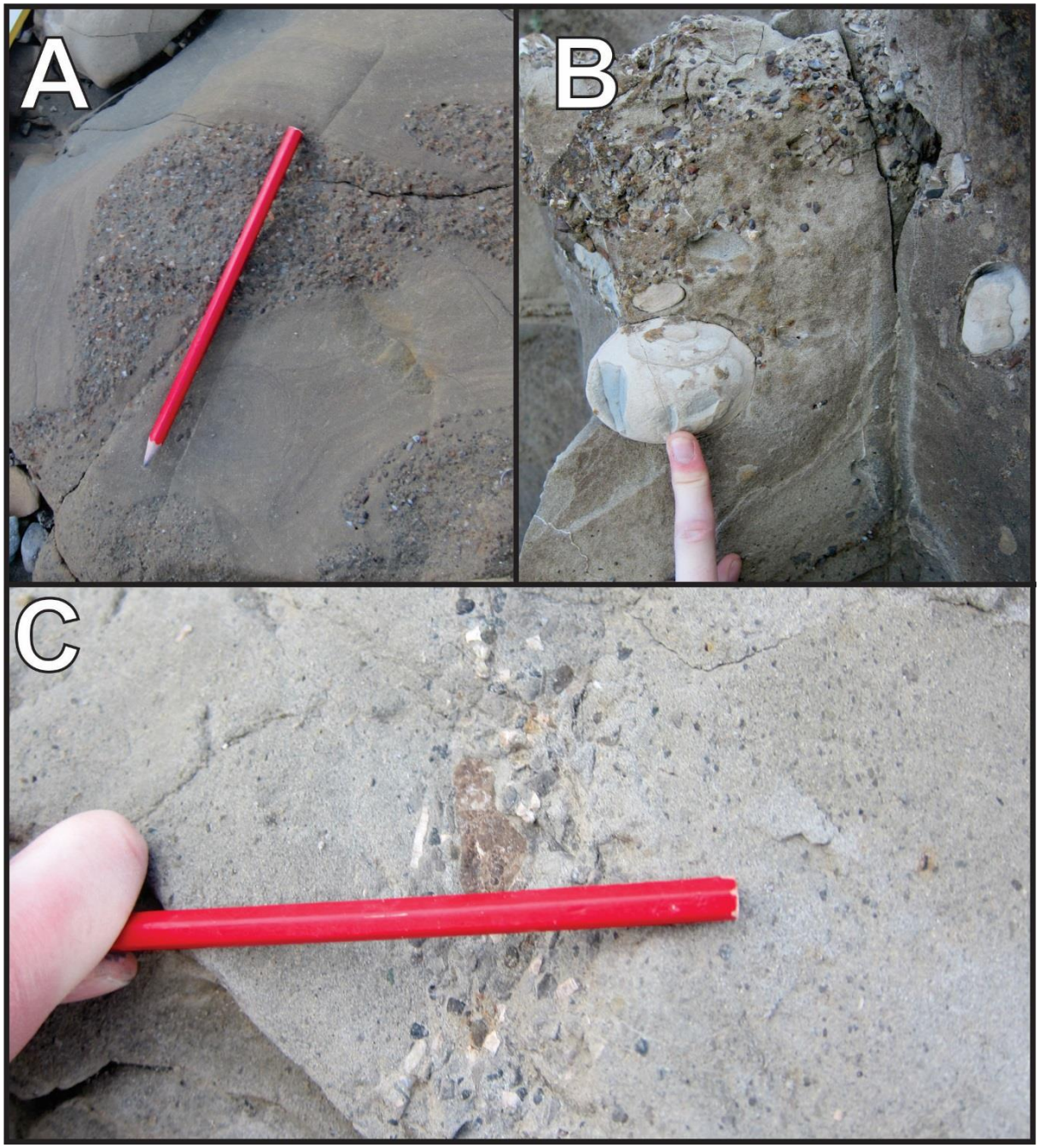

Figure 4.8: A) "Pockets" of pebbles within sandstone beds, representing soft sediment deformation. Northern Mangakuri area (Appendix K, ~220 m–250 m). Beds steeply dipping into page, younging upwards. BL39 351 689. B) Disorganised pebbly sandstone. Contains large mudstone concretion, most clasts pebble sized. Northern Mangakuri area (Appendix K, ~220 m–250 m). Bed upright, dipping ~60 degrees out of page. BL39 351 689. C) Close-up of pebble clasts in sandstone, southern Waimarama (Appendix L-ii). Note abundance of white *Inoceramus* fragments. Bedding vertical, younging to the right. BL39 404 792.

A2.1: Graded conglomerates (Figure 4.9)

Graded conglomerates were abundant in the Glenburn Formation. This includes the three types of graded conglomerates listed above. Schematic representations of these facies are shown in Figure 4.1. The scheme of Pickering and Hiscott (2015) recognises two different facies in this group; normally graded conglomerates and inversely graded conglomerates (which included inverse-normal graded conglomerates). This study did not encounter enough different conglomerates to justify these divisions, so instead a simplified version is used. Sandstone rafts of intraformational material may be present within beds.

Transport processes: concentrated density flows

Depositional processes: inverse grading due to rapid deposition due to increased intergranular friction or by coarser population lagging within density flow. Normal grading by grain-by-grain deposition.

A2.2: Organised pebbly sandstone (Figure 4.10)

This facies consists of sand dominated beds (>50% total volume) with a significant (>5%) component of granule or larger sized clasts. Broadly speaking this facies is very similar to A1.3, except there is either grading (normal or inverse) or stratification present. Clasts may be indurated material or locally derived mud “flakes” of intraformational material. Fragmented fossil material may also be present.

Transport process: Concentrated debris flows.

Depositional process: grain-by-grain deposition from suspension.

Figure 4.9: Normal grading in steeply dipping conglomerate bed, younging towards river. Motuwaireka Stream section (Appendix G, 689 m). BP35 517 507.

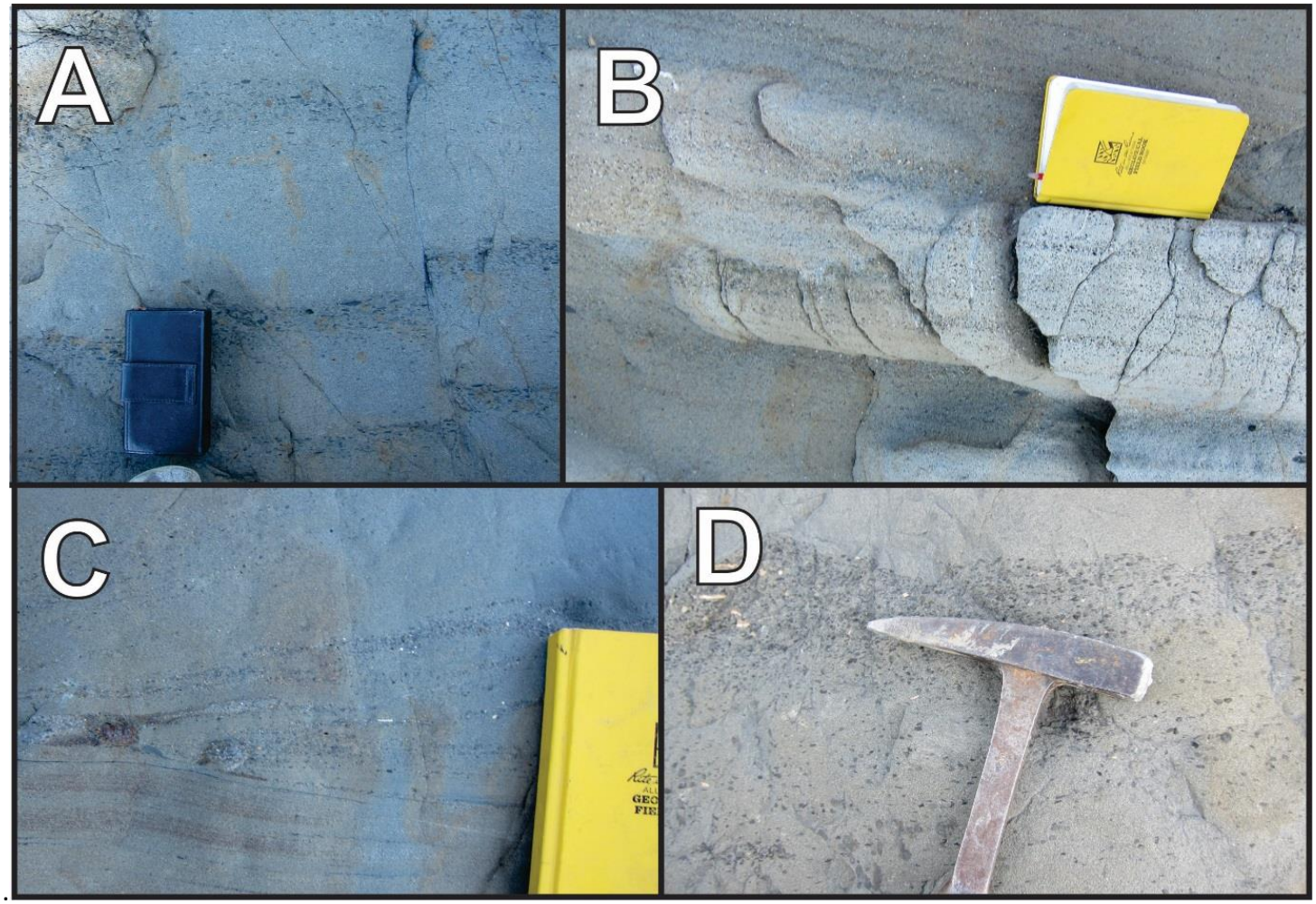

Figure 4.10: A) Stratified pebbly sandstone from southern Mangakuri (Appendix J-iii), with granule- to pebble-sized mudstone rip-up clasts in bands. Camera case (~12 cm) for scale. BL39 330 641 B) Stratified granular "pebbly" sand, southern Mangakuri Beach. Notebook 19 cm long (Appendix J-vii). BL39 335 655. C) Cross-beds of granule to pebble grade material, southern Mangakuri Beach (Appendix J-ii). BL39 335 656. D) Normally graded overturned beds of granule grade pebbly sandstone, Waimarama Beach (Appendix L-iii). BL39 404 792.

4.4.3: Facies Class B: Sand-dominated Beds

This facies class includes all sand dominated facies that are not obviously a part of the classic "turbidite" model of Bouma (1962). According to Pickering and Hiscott's (2015) classification this includes sand beds that are >80% sand, and <20% mud and <5% pebble grade. As with Facies Class A, this is divided into those beds that are organised and those that are not. This class was particularly prevalent at Mataikona and the Mangakuri/Waimarama area.

B1: Disorganised sandstone (Figure 4.11)

This facies is generally thick- to medium-bedded massive sandstone beds, and generally displays little or no grading. Dish structures may be present in some beds, but otherwise internal sedimentary features are uncommon. Pickering and Hiscott (2015) subdivide this facies into B1.1 and B1.2, based off bed thickness, but no Facies B1.2 (coarse, thin-bedded sandstone) beds were observed in the Glenburn Formation and so only Facies B1.1 of Pickering and Hiscott (2015) is included here.

Transport processes: concentrated density flows, inflated sand flows.

Depositional process: rapid deposition either from rapid deceleration of flow or by intense intergranular friction.

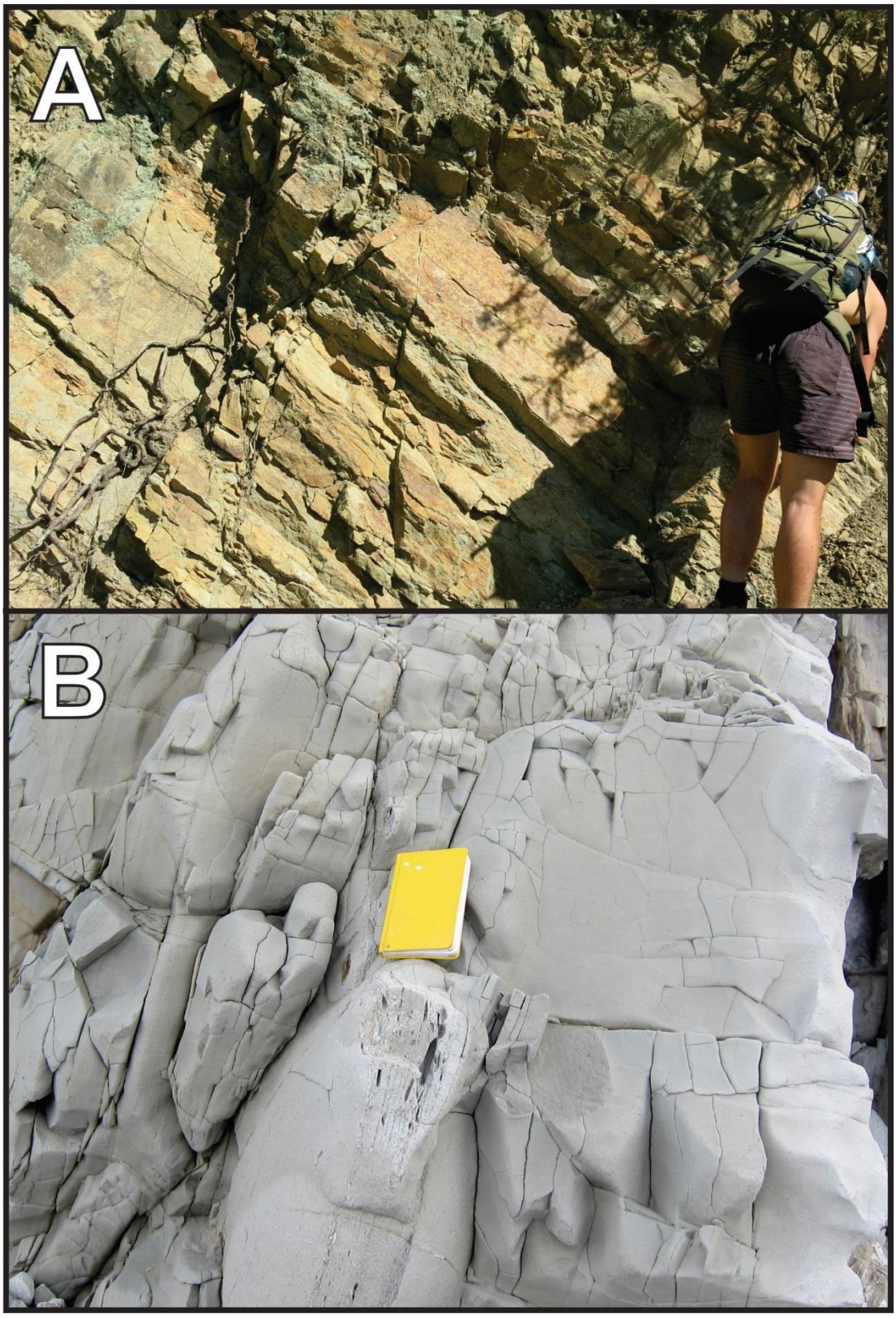

Figure 4.11: A) Highly weathered massive sandstone beds, Mataikona River section (Appendix H, 655-660 m). Dipping and younging towards top right of photo. BN36 734 863. B) Structureless, thick sandstone. Interval of parallel-laminated gravelly material below notebook. Beds steeply dipping, younging to the left. Waimarama Beach (Appendix L-iv). BL39 405 798.

B2: Parallel-stratified sandstone (Figure 4.12)

Parallel-stratified sandstone are the only organised sandstone dominated facies noted in this study. This facies consists of thick sandstone beds with internal layering up to 10 cm thick. The description of facies here differs somewhat from Pickering and Hiscott (2015). This study assigns parallel laminated or stratified sandstone beds without any other obvious Bouma divisions as Facies B2. These beds may therefore actually be deposits of turbidity currents where the rest of the Bouma sequence is missing. However, because of their common occurrence and distinction from sandstone-mudstone couplets, they are designated their own facies.

Because this facies is different from Facies B2.1 in Pickering and Hiscott, the depositional mechanism for this facies not certain. It is probably the result of amalgamated beds (stacked beds of a similar description) of the lower parallel laminated (Bouma T_b) division of turbidity currents.

It is proposed that these are the result of successive SGFs eroding any overlying deposits, leaving just the T_b division. Parallel-laminated or stratified divisions are common in concentrated density flows, but the absence of obvious inverse grading between laminae contradicts the typical profile of a concentrated density flow described in Pickering and Hiscott (2015).

Figure 4.12: Parallel-stratified thick sandstone beds (prominent raised beds), with sandstone-mudstone couplets of Facies C2.3 (centre). Horewai Point (not on measured section due to faulting). Beds overturned; younging to the left of photo. White fronted tern ~30 cm in length circled for scale BQ35 381 208.

4.4.4: Facies Class C: Sandstone-mudstone Couplets and Muddy Sandstone

Facies Class C consists of beds with a significant component of both sandstone and mudstone, manifesting either as a poorly sorted mixture of mud and sand or as a graded sandstone-mudstone couplet, the latter of which largely represent the “classic” turbidite of Bouma (1962).

C1: Muddy sandstone (Figure 4.13)

This facies consists of sandstone with a high concentration (20-80%) of silt or clay. Generally, these beds lack internal sedimentary features, although minor parallel-lamination and convolute bedding may be present. Mudstone clasts and sandstone rafts may occur within beds.

Transport processes: sand/mud load cohesive flows.

Depositional processes: rapid deposition due to intergranular friction or cohesion.

Figure 4.13: Muddy sandstone beds. Waimarama (Appendix L-v). Younging upwards in photo. BL39 404 792.

C2: Sandstone-mudstone couplets

Sandstone-mudstone couplets have a plethora of variations. The thickness both overall and of the relative components vary, as do the grain size and internal sedimentary features. The entire classic "Bouma sequence" of T_{abcde} (Figure 4.2) is rarely observed in outcrop, but partial sequences (e.g., T_{bcd}) are commonly observed. Figure 4.14 shows Facies C2.1 to C2.3.

C2.1: Thick-bedded sandstone-mudstone couplets

C2.2: Medium-bedded sandstone-mudstone couplets

C2.3: Thin-bedded sandstone-mudstone couplets

Transport processes: Facies C2.1 is transported by flows transitional between concentrated density flows and turbidity currents, whereas Facies C2.2 and C2.3 are transported by turbidity currents with thickness generally inversely proportional to concentration and velocity of the current.

Depositional processes: Generally grain by grain settling but may also be by burial or tractional transport as bed load.

C2.4: Cross-bedded fine sandstone and silty sandstone (Figure 4.15)

This is a new facies not described by Pickering and Hiscott (2015). This constitutes thick beds of fine sandstone or silty sandstone that contain abundant cross-lamination on a 5-10 cm scale but no mud-couplet element. This may constitute amalgamated beds of the cross-bedded part of a Bouma sequence. Because these beds are often thick (1 m+) and are not sandstone-mudstone couplets, they are assigned their own facies. These beds may contain some parallel-lamination, but are mostly cross-laminated. Laminations frequently contain concentrated silt-grade organic material.

This differs from Facies B2.2, “cross-stratified sands”, in Pickering and Hiscott (2015) because the facies described here is generally fine-grained rather than coarse-grained, and the silty component of the laminations suggest they are more accurately included in Facies Class C.

Because this facies is not described in Pickering and Hiscott (2015), the transport and depositional processes are not certain. These beds resemble the T_c division of turbidity currents, so may represent turbidites where the overlying T_{de} portions have been eroded. Alternately, several authors have proposed that bottom currents may produce cross-lamination in sandstones (Shanmugam, 2008). Either of these explanations is plausible, although the nature of bottom current deposits (contourites) are still the subject of significant debate (Pickering and Hiscott, 2015).

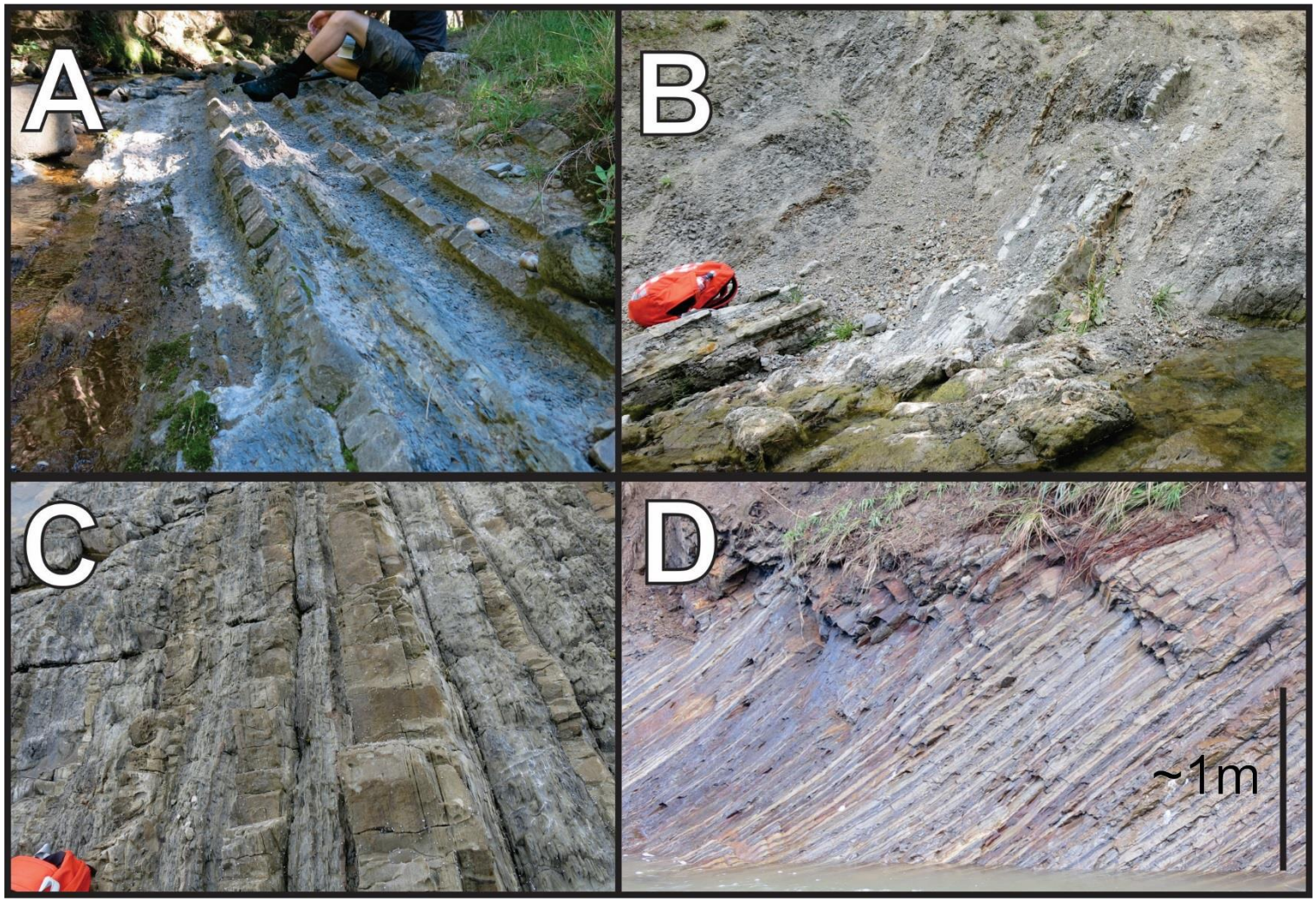

Figure 4.14: A) Sandstone-mudstone couplets of Facies C2.2 (centre/right) and C2.3 (left) Smokey Gulley Stream, Mataikona River section (Appendix H, 100-102 m). Beds younging to the right. BN36 740 859. B) Sandstone-mudstone couplets of Facies C2.2 and minor C2.3 with a thick mudstone component. Waimata River, (Appendix I-i). BN37 950 097. C) Facies C2.1, C2.2 and C2.3 beds, Horewai Point section (Appendix E, ~77-80 m). Backpack for scale in bottom left. BQ35 382 209. D) Facies C2.3 and C2.2 beds, Totara Stream (Appendix F, 943 m). BP35 448 428.

Figure 4.15: Cross-lamination in sandstone, including possible antidunes. Totara Stream (Appendix F, 12 m). BP35 459 422.

4.4.5: Facies Class D: Siltstone and Silt-mudstone Couplets

Facies Class D represents beds with a significant silt and mud component and a relatively small component of sands (>80% total mud, >40% silt, <20% sand). This class includes "massive" siltstone as well as silty mudstone and siltstone-claystone couplets.

D1: Disorganised siltstone

Although disorganised mudstone can seem similar to one another, a key distinction is in the degree of biotubation. Structureless siltstone and silty mudstone are distinct from those that have been mottled by bioturbation. The former, although fine-grained, are likely evidence of rapid deposition by density flows or sliding, whereas the latter are likely to represent slow deposition due to grain by grain settling from suspension.

D1.1: Structureless siltstone (Figure 4.16)

This facies consists of medium to thick-bedded, essentially structureless silts. In this context structureless implies a lack of internal sedimentary features such as grading. Weak bedding may be noticeable, due to these beds having been deposited by SGFs. Siltstone may have a sandy component, and may show poorly defined grading. Floating mudstone clasts may be present.

Transport processes: concentrated density flows or highly fluidised silty cohesive flows.

Depositional processes: rapid deposition due to increased cohesion and intergranular friction.

D1.2: Mottled siltstone, sandy siltstone and mudstone (Figure 4.17)

This facies is characterised by mottling due to extensive mottling and bioturbation, and is Facies D1.3 of Pickering and Hiscott (2015). Bed shape is irregular and the base and tops of beds may be sharp or gradational. Grading may be present on a mm-scale or up to tens of cm thick. While bioturbation can be present in many facies, distinct mottling is considered indicative of slow rates of deposition and thus is not typical of SGFs such as turbidites.

Transport processes: Bottom currents such as contour currents.

Depositional processes: Grain by grain deposition with subsequent bioturbation.

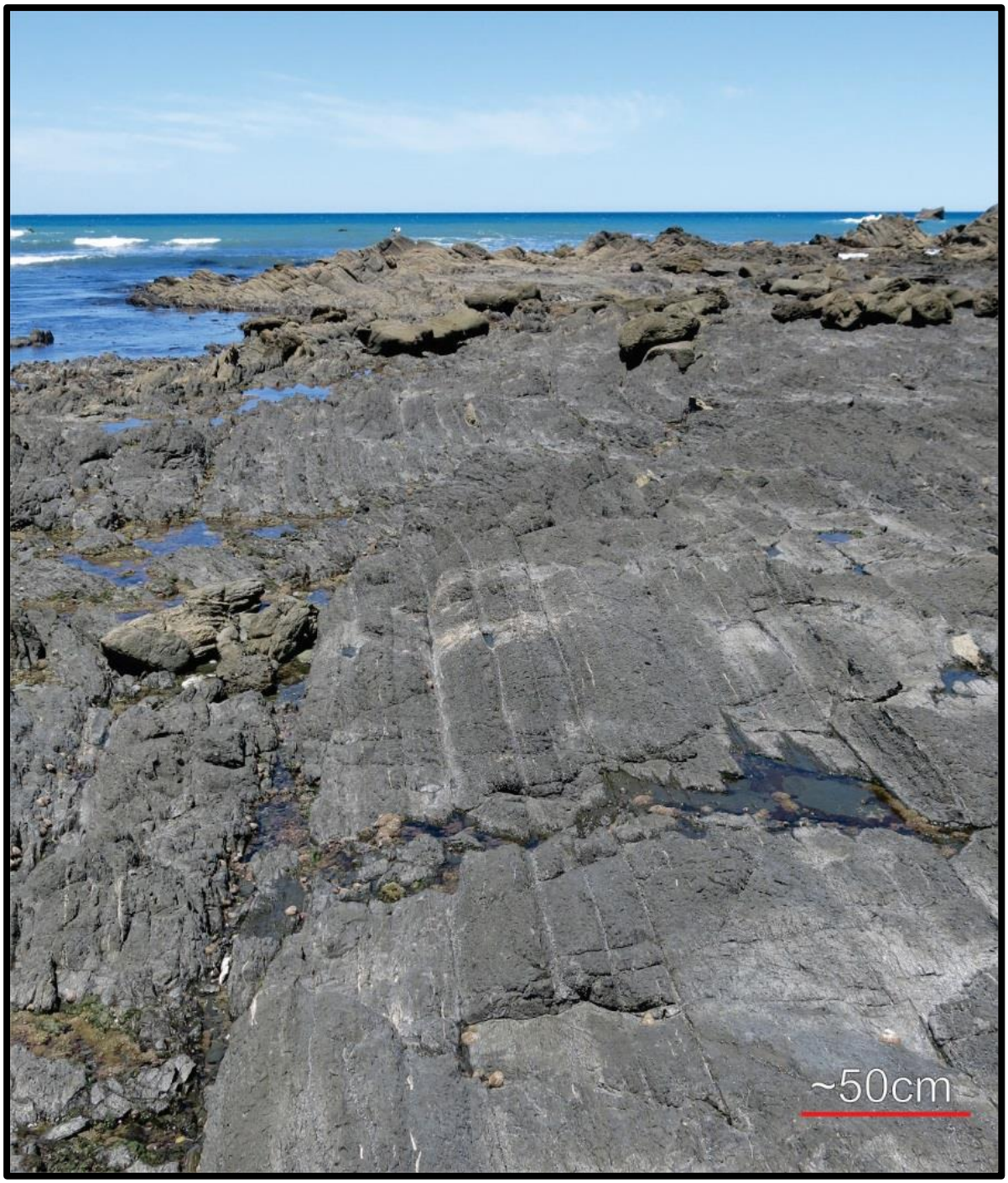

Figure 4.16: Weakly bedded internally structureless siltstone, Honeycomb Light section (Appendix D, 15-20 m). BQ35 369 189.

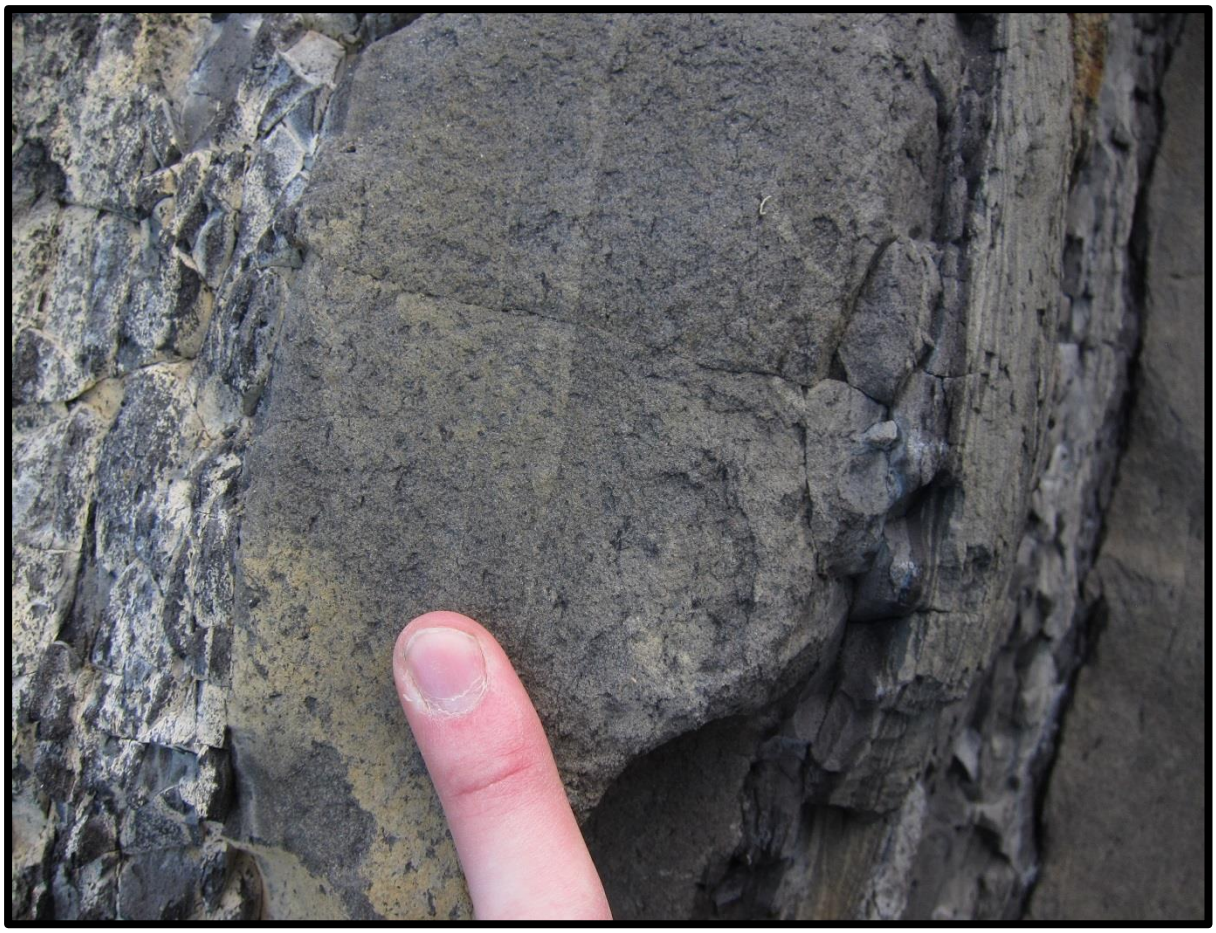

Figure 4.17: Mottled sandy siltstone (centre) and clay (right), Waimarama Beach (Appendix L, vii). Beds dipping into page, younging to top right. BL39 414 810.

D2: Organised siltstone (Figure 4.18)

Facies Class D also includes fine graded beds that may be the product of turbidity currents. Pickering and Hiscott (2015) divide their Facies Group D2 into three different facies: graded-stratified silt, thick and irregular laminae of silt and mud, and thin and regular silt and mud. Only "graded silt" beds were present within the Glenburn Formation, and hence there is no subdivision.

This facies is generally thin to medium-bedded, representing the T_{de} interval of the classic Bouma Sequence (Figure 4.2). They are generally sharp-based and normally graded.

Transport processes: Turbidity currents

Depositional processes: grain-by-grain deposition from suspension.

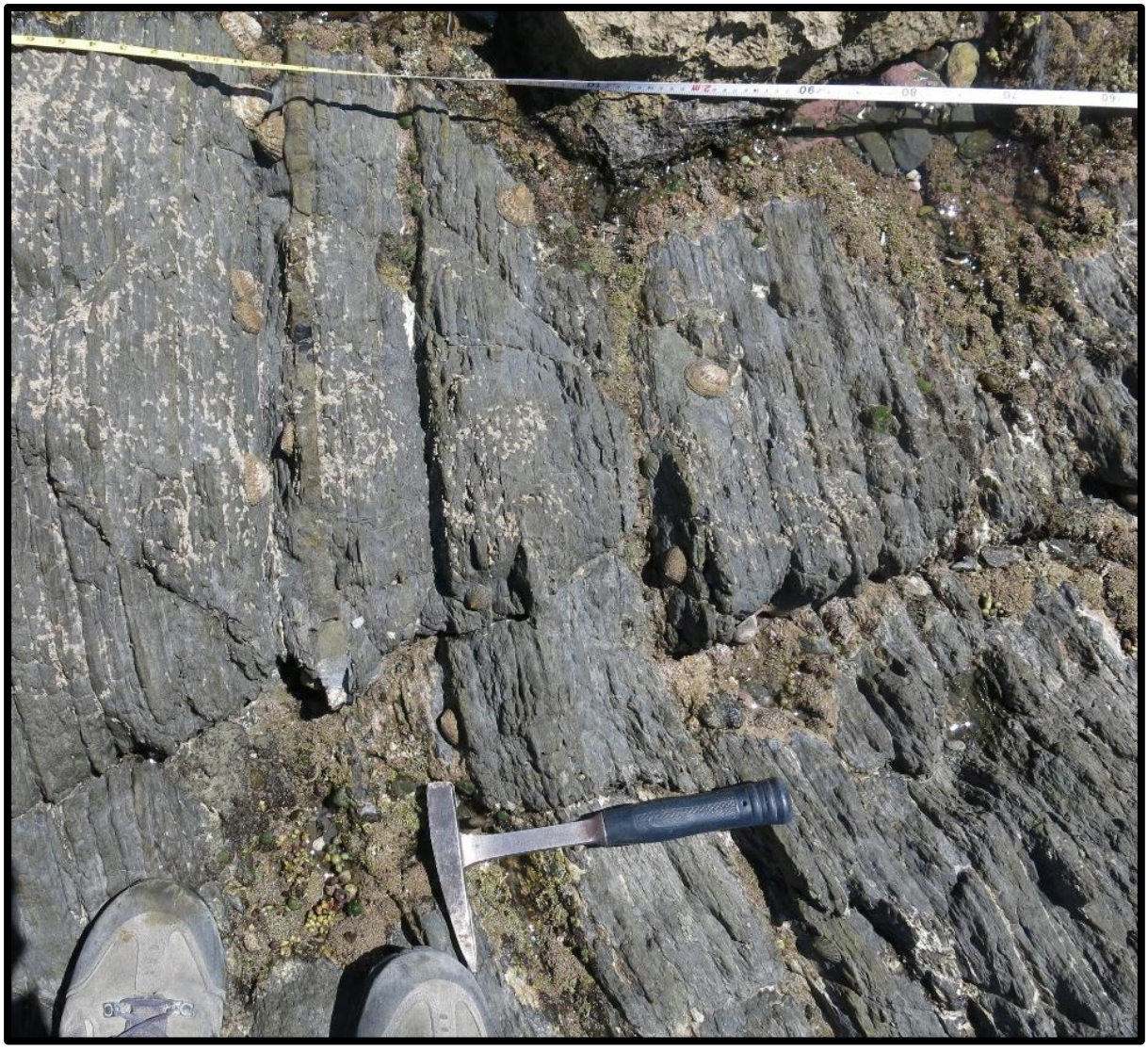

Figure 4.18: Thin-bedded, fine siltstone-mudstone couplets, Honeycomb Light (Appendix D, ~23 m). Beds vertical, younging to the right. BQ35 369 189.

4.4.6: Facies Class E: Clay Dominated Mudstone

Facies E: clayey mudstone (Figure 4.19)

This class is comprised of the finest mudstone facies, where <40% of the sediment is silt, regardless of other features. As Pickering and Hiscott (2015) note in describing this facies class, the difference between the subclasses in this class are best studied with advanced methods such as scanning electron microscopy or X-radiographs, which is beyond the scope of this study and thus no subdivisions of this facies class are recognised.

Transport processes: Pelagic sedimentation due to currents/aeolian processes, bottom currents, distal turbidity currents, biogenic processes.

Depositional processes: generally settling of fine particles, may be deposited rapidly by flocs.

Figure 4.19: Silty clay with large concretion, Horewai Point (Appendix E, ~5 m). BQ35 375 199.

4.5: Chapter summary

This chapter describes an adaption of the Pickering and Hiscott (2015) facies scheme that is used throughout the rest of this thesis, as well as a brief introduction to facies schemes and why one is appropriate for SGF dominated successions such as the Glenburn Formation. Because of the correlation with this facies scheme and that of Pickering and Hiscott (2015), the depositional and transport processes of facies observed in the field can be interpreted. A few deviations are made from the Pickering and Hiscott (2015) scheme, such as the introduction of Facies C2.4, but for the most part facies are either directly from their scheme or from an amalgamation of facies from their scheme (e.g., Facies A2.1). This scheme allows for succinct description of common facies between different localities and hence an efficient way to compare and contrast the differences between the sections examined in this study.

Chapter 5: Field Results and Interpretation

5.1: Measured Section Summaries

This section provides a summary description of facies observed at each section. Measured sections and their key are found in the appendices D to L. Figure 5.1 shows generalised lithologies of these sections by age, as determined using biostratigraphy.

5.1.1: Honeycomb Light – Appendix D

Lowermost strata in the Honeycomb Light section are silt-dominated rocks of Facies Class D with occasional thin sandy beds (Figure 5.2a). The lack of pervasive mottling within siltstone, combined with the concentration of Inoceramus fossils in layers, indicates weak bedding and suggests these are SGF deposits. Facies D1.1 is assigned. Occasional silt-clay couplets are Facies D2 (Figure 4.18), whereas thin, graded and parallel-laminated sandstones are Facies C2.3 turbidites. Ages are moderately well constrained by fossils; *Inoceramus fyfei* indicates an upper Ngaterian age for these strata (Crampton, 1996; T27/f0364). At least 25 m of Facies D1.1 dominated sediment is preserved. Some Facies D2 beds are preserved and are inferred to be distal sandy turbidite deposits (Table 4.1).

Sandstone-mudstone couplets increasingly dominate the succession above 25 m from the base (Figure 5.3a). Beds are generally each 10-20 cm thick for both the sandstone and siltstone components. These are Facies Class C; Facies C2.3 at the base with Facies C2.2 becoming increasingly common upsection. Above 37 - m upsection, Facies C2.2 is the most common facies. Between 61 m and 66 m, beds are Facies C2.1. These beds show clear grading, as well as T_{bc} Bouma Divisions (Figure 4.2; Figure 5.3b), and are therefore interpreted as turbidite deposits.

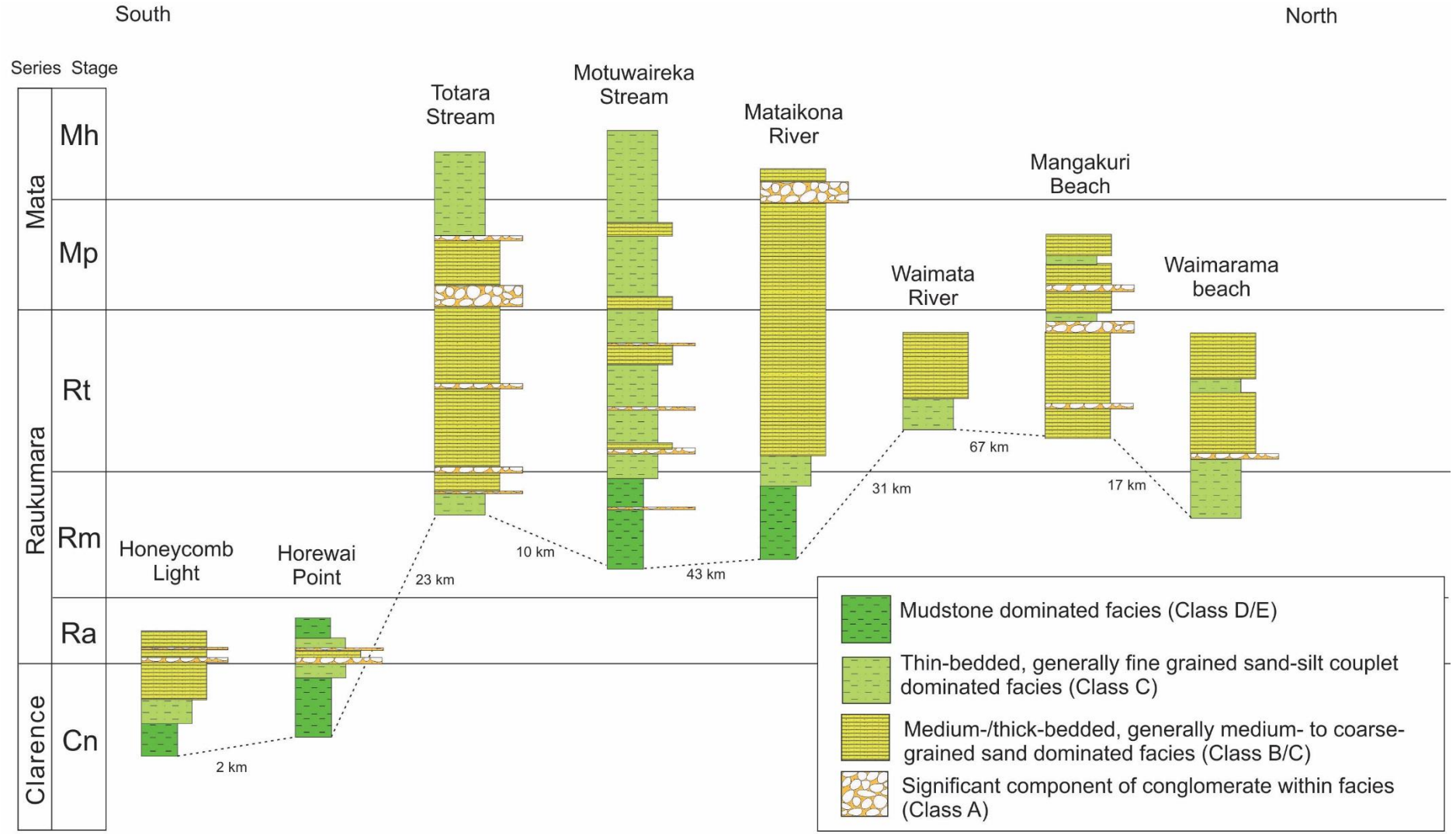

Figure 5.1: Generalised stratigraphy of different field sections by age, from south (left) to north (right). No vertical scale implied. Approximate distance between bases of sections noted. Stage abbreviations as per Figure 1.5.

Approximately 81 m above the base of the measured section, the oldest conglomerate bed is exposed. It is ~3 m thick, and represents a single SGF event as evidenced by the lack of internal bedding. Because it is clast supported and lacks internal grading, it is designated Facies A1.1. Crampton (1997) places the base of the Arowhanan Stage just below this conglomerate, though this is not well constrained.

Directly above this conglomerate, ~3 m of Facies C2.2 sandstone-mudstone couplets are preserved, which are overlain by decimetre to metre-bedded parallel-laminated Facies B2 sandstone (Figure 5.4). These are interpreted as turbidite deposits. An up to 60 cm thick graded, channelised, conglomerate of Facies A1.1 is present within the sandstone beds, pinching out over ~ 4 m (Figure 5.2b). This is interpreted as a channelised debrite (debris flow deposit).

More disorganised conglomerate (Facies A1.1) is present at ~90 m, which represents another debris flow, above which Facies C2.2 and C2.1 sandstone-rich turbidites dominate the succession. Siltstone components in beds are 5-15 cm thick but sometimes not present, probably due to erosion between beds. One more Facies A1.1 conglomerate debrite was present at ~ 98 m. Above this are more Facies C2.2 sandstone turbidite dominated beds. Although not observed in this study, Crampton (1997) mapped ~30 m more sediment above the top of this section, which suggests similar facies with conglomerate becoming less common to absent upsection. Conglomerates are interpreted as debris flow deposits, whereas class C facies are interpreted as turbidites.

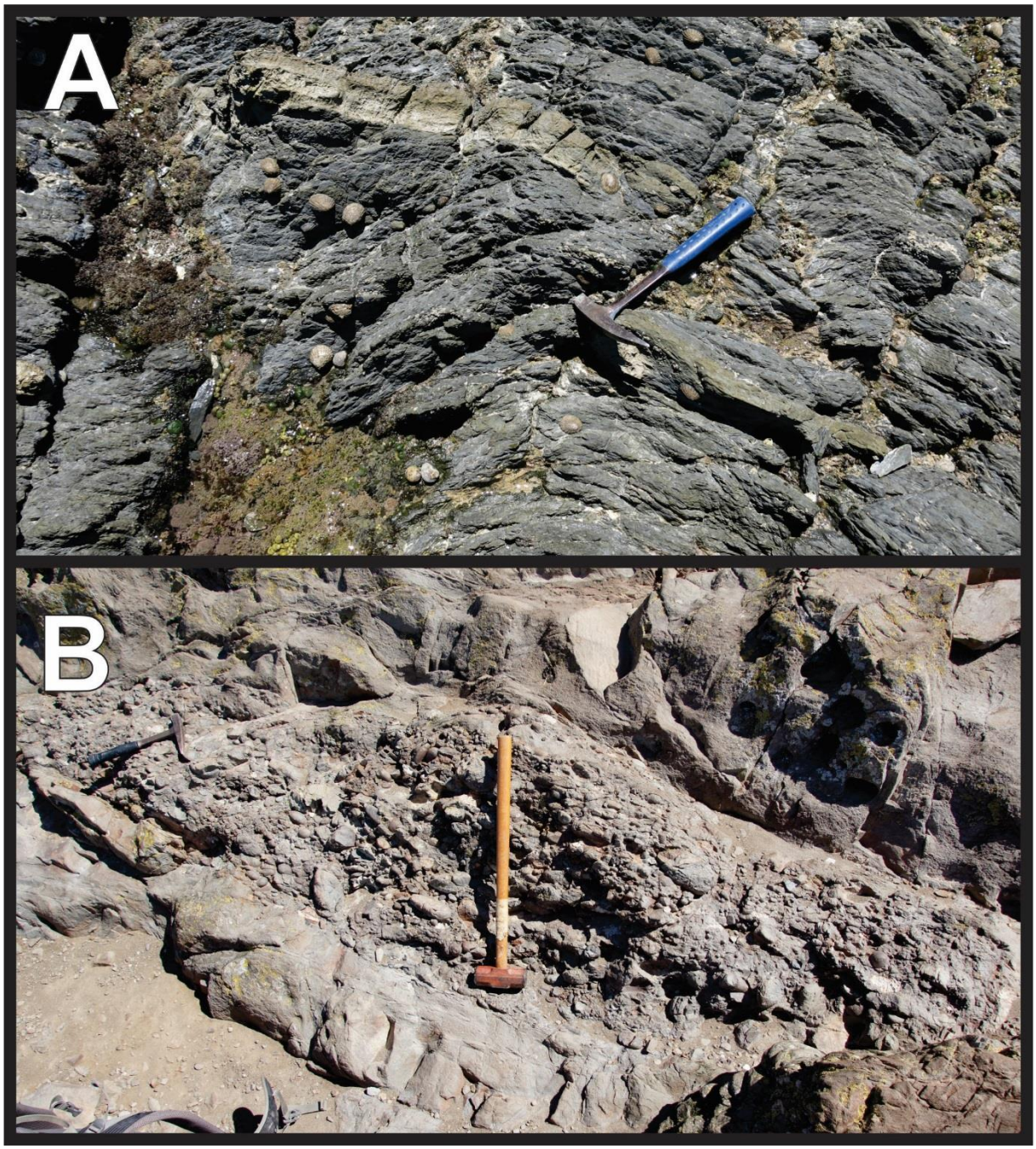

Figure 5.2: A) Honeycomb Light. Massive mudstone (Facies D1.1) with elongate concretion. ~10 m upsection, BQ35 369 189). B) Honeycomb Light. Channelised conglomerate of Facies A1.1. Sledgehammer (~60 cm long) and rock hammer for scale. Younging upwards. ~89 m upsection, BQ35 369 189.

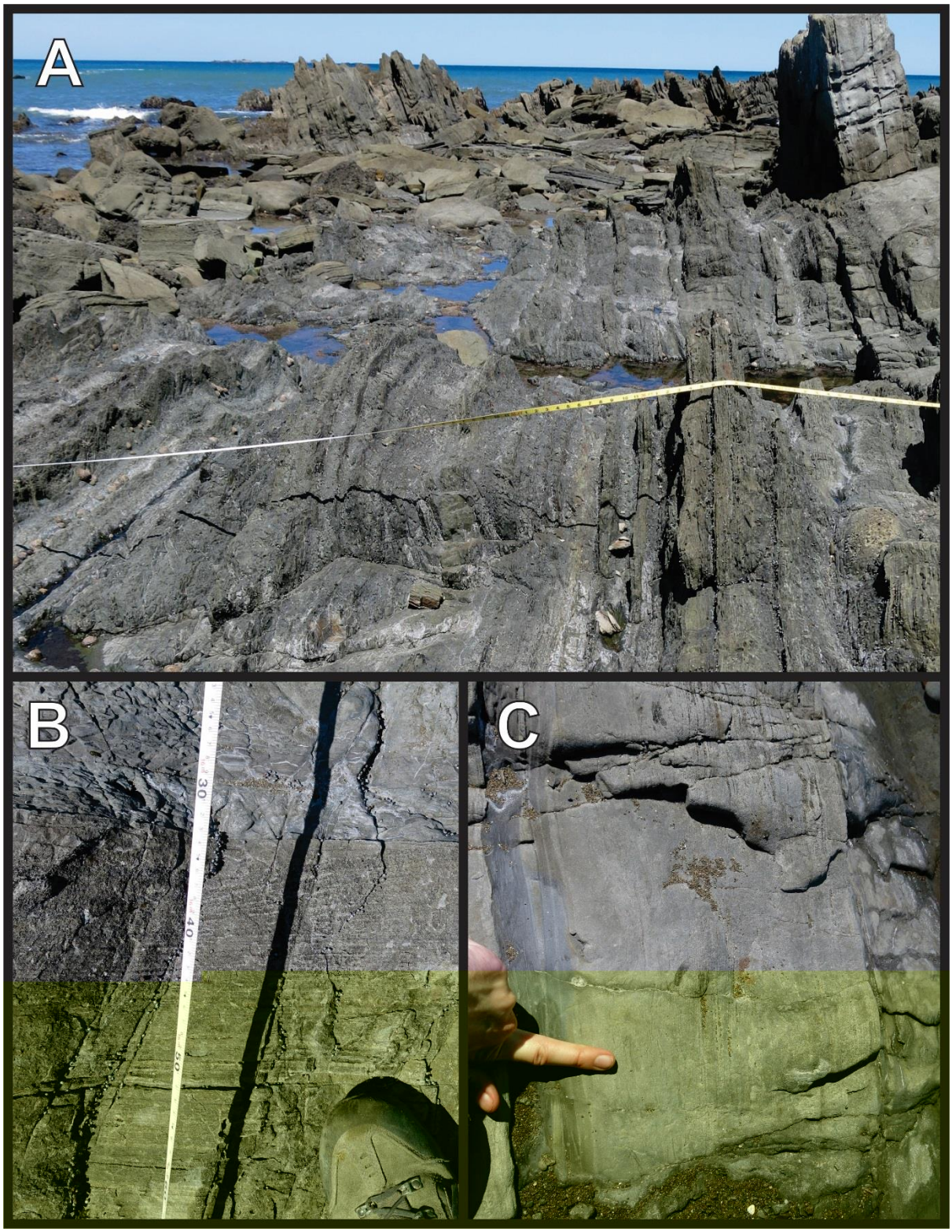

Figure 5.3: A) Honeycomb Light. Thin-bedded turbidites mostly of Facies C2.3, thick C2.1 bed present on extreme right. Beds younging to right. Divisions on tape measure feet/inches. ~55-62 m upsection, BQ35 369 189. B) Parallel and cross-lamination in graded sandstone bed of Facies C2.2. Younging upwards. ~75 m upsection, BQ35 369 189. C) Graded sandstone bed of Facies C2.2, younging to the left. ~78 m upsection, BQ35 369 189.

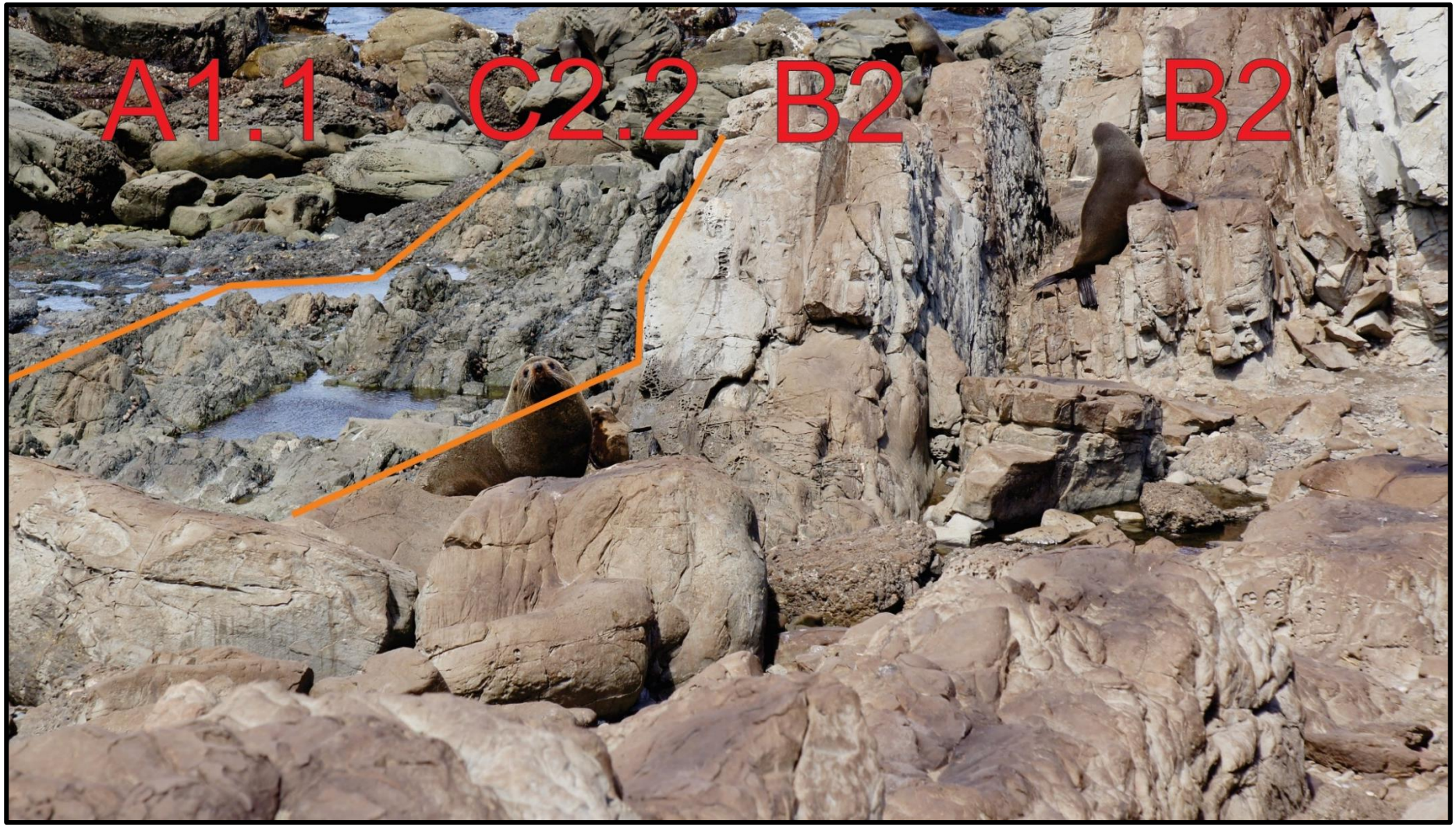

Figure 5.4: Honeycomb Light. Oldest conglomerate and overlying facies, orange lines showing divisions Honeycomb Light. Younging to right. Male NZ fur seal (left/front) and female (right/back) for scale. ~80-88 m upsection BQ35 369 189.

5.1.2: Horewai Point – Appendix E

Lowermost strata exposed at Horewai Point comprise silty claystone and represent the only Class E-dominated strata mapped in the Glenburn Formation (Figure 4.19). Mottling and burrowing is most common in the base, which is generally massive. Upsection, bedding becomes increasingly prominent. Thin sandy beds of Facies C1 or C2.3 (sandy debrites or turbidites) up to 10 cm thick and concretions <50 cm in diameter that are commonly concentrated in layers occur throughout, becoming more frequent upsection. Silt-grade sediment is also more common upsection, and the strata gradually transition upsection into a Facies D1.1 dominated succession. Bedding and only minor bioturbation suggest deposition by SGFs rather than bottom currents. Abundant fossils indicate that the lower part of the succession is Ngaterian aged (*Inoceramus fyfei*).

Approximately 37 m from the base of the section, there is an up to 13 m thick conglomerate (Figure 5.5a, c). This bed has a sharp, erosive lower contact and is assigned Facies A1.1 due to a lack of grading and high clast density. The lack of any internal bedding suggests this conglomerate was the product of a single debris flow event.

Above this conglomerate are sandstone-mudstone couplets of Facies C2.2 that represent turbidite deposits, as evidenced by abundant grading and T_{bcde} Bouma divisions (Figure 5.6). Schiøler and Crampton (2014) mapped the Ngaterian-Arowhanan boundary at ~52m on this section. From 55 m onwards, there are a mixture of Facies C2.2 and C2.1 turbidites, with the mudstone component often missing or much thinner than the sandstone component. Another Facies A1.1 conglomerate debrite is present around 70 m from the base of the sequence, overlain Facies C2.2 turbidites. A small fault occurs at around 76 m. Overlying this fault is an inversely graded ~70 cm thick Facies A2.1 conglomerate debrite. Above this, the prevalence of sandstone beds slowly decreases, and mudstone dominated Facies C2.3 and D2 turbidites make up the bulk of the remaining visible section. Schiøler and Crampton (2014)'s measured section shows siltstone dominates the succession further upsection too. Figure 5.5b shows B2 sandstone in the vicinity, which not included in measured section, because of a minor fault separating the measured section from this outcrop.

Figure 5.5: Horewai Point A) Large sandstone raft in Facies A1.1 conglomerate. ~40 m upsection, BQ 35 381 208 B) Facies B2 stratified sandstone (raised) with Facies C2.3 sandstone-mudstone couplets between them. Younging to the left. Circled is a white-fronted tern for scale, ~30 cm in length. BQ35 381 207. C) Mudstone packet within thick Facies A1.1 conglomerate. ~42 m upsection, BQ 35 381 208.

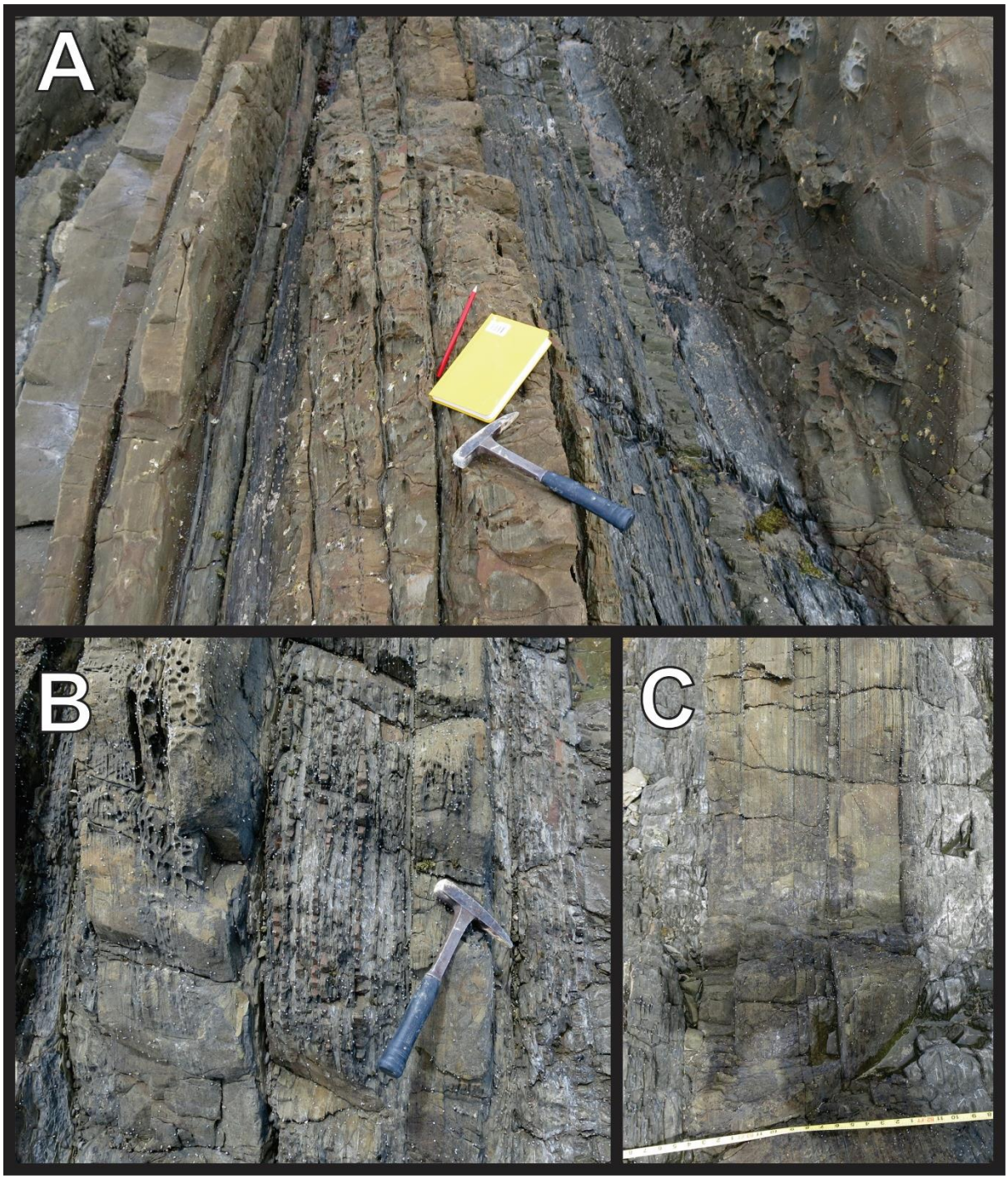

Figure 5.6: Horewai Point. A) Sand dominated turbidites of Facies C2.2 (below and to the left of hammer) and C2.3 (to the right of hammer). Younging to the left. Note discontinuity of beds above hammer. Bed to far right is Facies C2.1. ~140-142 m upsection, BQ35 382 209. B) Turbidites of Facies C2.2 interbedded with thinner C2.3 turbidites. Younging to left. ~73 m upsection, BQ35 382 209. C) Organic-rich parallel-laminations in Facies C2.2 bed. Younging to the left. ~77.5 m upsection, BQ35 382 209.

5.1.3: Totara Stream – Appendix F

The outcrop at Totara Stream was relatively discontinuous, although the well documented fossil record and lack of any mapped significant faults suggest the section is most likely one single section. Lowermost strata (0-18 m) are dated as Mangaotanean by the presence of *Cremnoceramus bicorrugatus* and are generally fine-grained beds of Facies C2.1 (Figure 5.7a) and C2.4 (Figure 5.7b, d, e). These are inferred to be deposits of turbidity currents, based on normal grading and Bouma T_{bc} divisions. One laterally discontinuous band of conglomerate is present at ~12 m upsection (Figure 5.8a). A lack of internal grading suggests this is Facies A1.1 and hence a debrite. Outcrop is generally discontinuous. At around 72 m, outcrop becomes dominantly sandy siltstone to well sorted, massive sandstone of Facies B1, with one inverse-normal graded conglomerate of Facies A2.1, both of which are interpreted to represent concentrated density flow deposits. Sandstone-mudstone couplets of Facies C2.2 to C2.3 and occasional Facies A2.1 or A1.2 conglomerate beds (e.g., Figure 5.8b), which are inferred to represent turbidites and concentrated debris flows respectively (Table 4.1), comprise the strata present at 95 m to 105 m. Around 200 m of section is missing before the next outcrops, which show similar facies to those at 95 m. *Inoceramus opetius* indicates a Teratan age for these strata. Graded Facies C2.2 sandstones are often amalgamated, and Facies A2.1 conglomerate beds display a variety of styles of grading. A ~4 m thick interval of Facies B2 parallel-stratified sandstone occurs between 332-336 m, possibly reflecting erosion within stacked turbidites. Between 354 m and 361 m, five separate conglomerate beds are present, separated by siltstone or sandstone beds. Sandstones overlying these conglomerates may be part of the same depositional event as the underlying conglomerate, forming a Lowe Sequence (Figure 4.3). *Inoceramus pacificus* indicates a Piripauan age for these strata.

Between 440 m and 445 m, there are thick Facies C2.1 turbidites, overlain by a Facies A2.1 conglomerate that pinches out horizontally and a Facies B2 sandstone, again likely reflecting concentrated debris flow deposits. Around 130 m of section is missing after this. The next outcrops observed, at ~595 m, are more Facies B2 sandstones, A2.1 normal-graded conglomerates, and intervals of Facies C2.3 or D2 graded turbidites.

The next exposed outcrops in this section are those of the intruding Haumurian to Teurian (Moore 1980) West Kaiwhata Sill (743 - 749 m). Crampton (1997) mapped a possible fault near this, but no evidence of this is currently exposed.

Strata stratigraphically above the sill, ~815 m from the base and above, are all thin-bedded, Facies C2.2 to C2.3 turbidites with very abundant, distinct organic laminae (Figure 5.9). Sandstone beds are jarositic (Figure 5.7c, Crampton, 1997) and very fine, with granule sized coaly fragments abundant throughout. Some beds may be classed as Facies D2. No conglomerates were noted above the West Kaiwhata Sill. A Piripauan age is inferred for these strata.

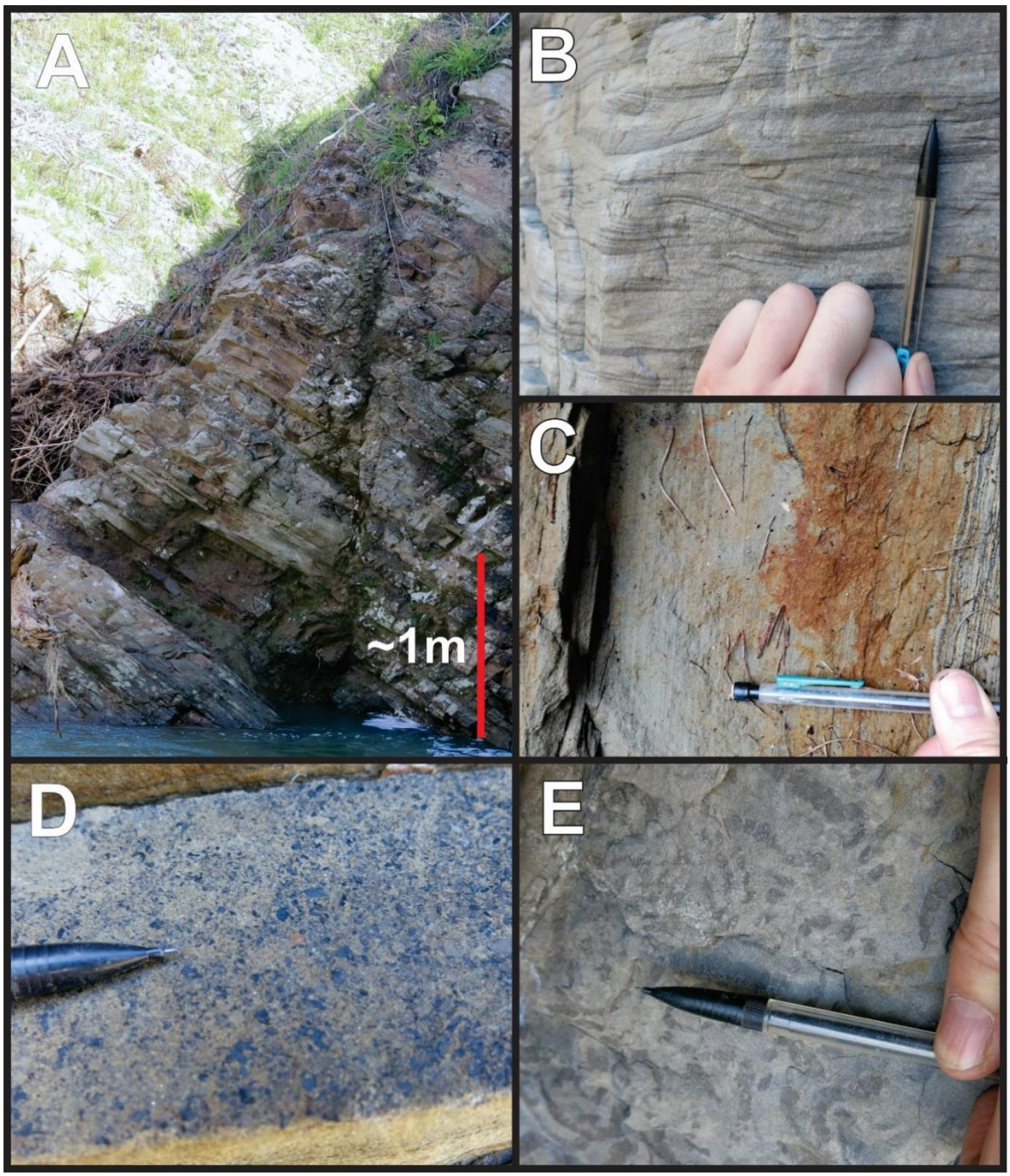

Figure 5.7: Totara Stream. A) Graded sandstone beds of Facies C2.2 to C2.1. Beds below base of measured section. BP35 463 422. B) Organic-rich cross-lamination in thick sandstone beds of Facies C2.4. ~12 m upsection, BP35 463 422. C) Carbonaceous granules in Facies C2.2 bed, younging to the left. ~835 m upsection, BP35 450 427. D) Carbonaceous material up to granule size. Cross-section of Facies C2.4 bed, younging out of page. ~16 m upsection, BP35 463 422. E) Bioturbated sandstone, facies C2.4. ~12 m upsection, BP35 463 422.

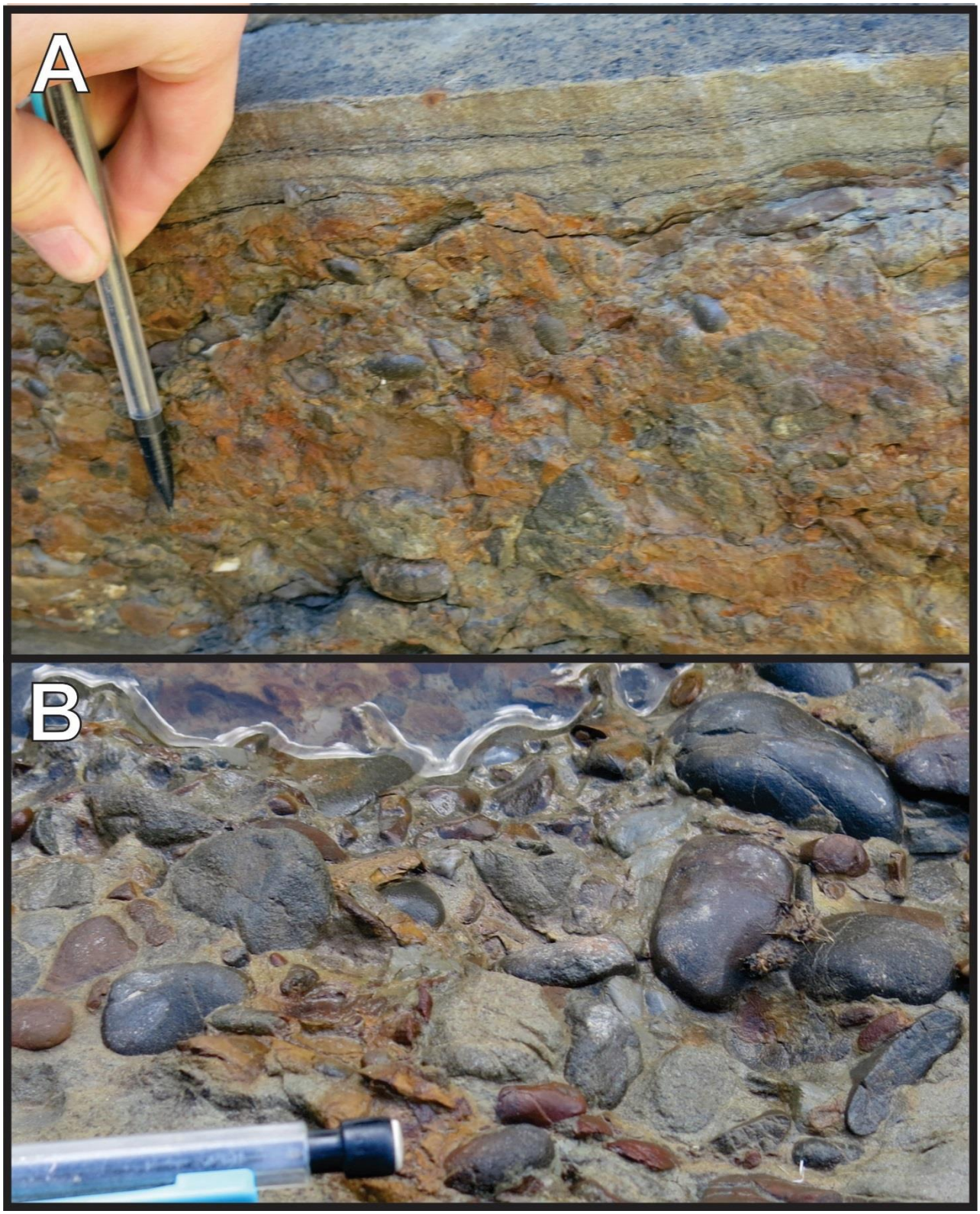

Figure 5.8: Totara Stream. A) Conglomeratic band of Facies A1.1 conglomerate. ~15 m upsection, BP35 462 422. B) Close-up of typical Totara Stream conglomerate clasts showing size, sorting, rounding and lithological variations (Facies A2.1). ~319 m upsection, BP35 463 422.

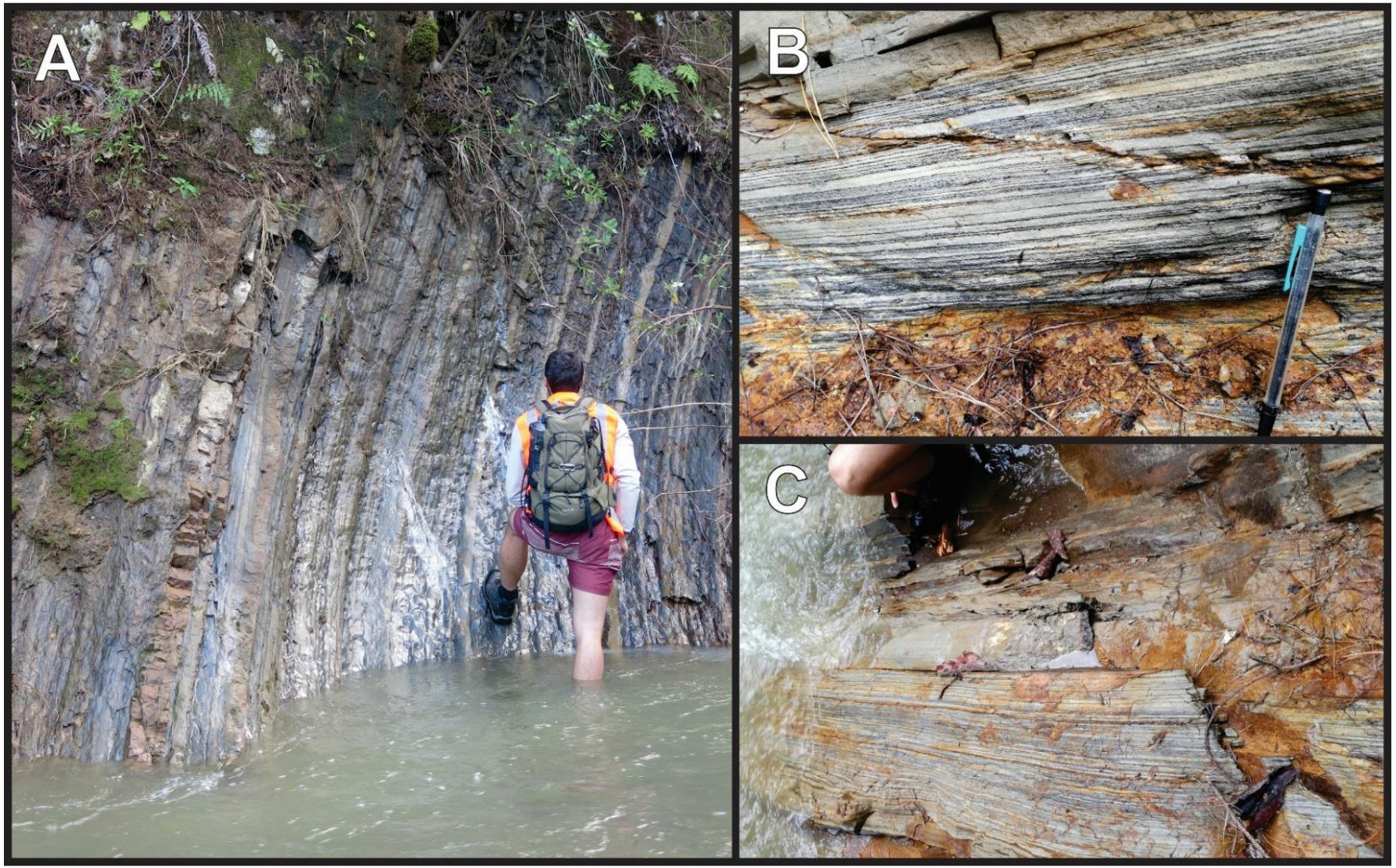

Figure 5.9: Totara Stream. A) thin-bedded Facies C2.2 to C2.3 turbidites. Younging to left. ~940 m upsection, BP35 448 428. B) Close-up of organic-rich laminae in Facies C2.2 bed. Younging upwards. ~833 m upsection, BP35 450 427. C) Laminae-rich sandstones overlain by non-laminated sandstones. Younging upwards. ~830-835 m upsection, BP35 448 427.

5.1.4: Motuwaireka Stream - Appendix G

Lowermost strata mapped in Motuwaireka Stream, between 0 and 138 m upsection, are of Mangaotanean age, as deduced by the presence of *Cremnoceramus bicorrugatus* (T26/f9531). These strata consists of heavily weathered, weakly bedded siltstone of Facies D1.1 and occasional thin-bedded (<15 cm) graded sandstone beds of Facies C2.3. As described in Table 4.1, Facies D1.1 are the deposits of either muddy debris flows or concentrated density flows whereas Facies C2.3 are turbidites. Around 500 m of stratigraphic section is omitted from the measured section between these lowest outcrops and the next, though some occasional poorly exposed, heavily weathered outcrops of siltstone were observed between the two sites. This suggests similar facies dominate the succession in this interval. There may be some repetition of strata within this interval, although no significant faults have been recorded in this interval (Lee and Begg, 2002).

The next well-exposed strata, at 601 m, are of questionable age, with fossil *Inoceramus spedeni* indicating a Mangaotanean to Teratan age (Crampton, 1996). These rocks were dominantly more Facies D1.1 and rarely Facies C2.3, but included occasional muddy conglomeratic Facies A1.2 debrites. From 660 m onwards, Facies C2.2 and C2.3 sandstone-mudstone couplets dominate the succession (such as Figure 5.10a), which are interpreted to be turbidites. *Inoceramus opetius* indicates a Teratan age. Occasional 1-2 m thick graded (Facies A2.1) and ungraded muddy (Facies A1.2) conglomerates are present, deposited by concentrated density flows (Figure 4.7b, Figure 4.9, Figure 5.11). From 830 m onwards, Facies C2.2 turbidites are present along with a few Facies B2 beds. Sections alternate from being dominantly Facies C2.2, and dominantly Facies C2.3. Carbonaceous material is often concentrated in cross-lamination (Figure 5.10b). Occasional channelised Facies A1.2 debrites and B2 sandstone beds occur, which are probably turbidites. *Inoceramus australis* was found near in-situ around 1000 m up the section, suggesting a Piripauan age. One short interval of Facies C2.1 beds is found around 1065-1075 which may be the deposit of a concentrated density flow or a turbidity current (Table 4.1). Sandstone-mudstone couplets similar to Totara stream of Facies C2.3 represent the highest strata observed (Figure 5.10c).

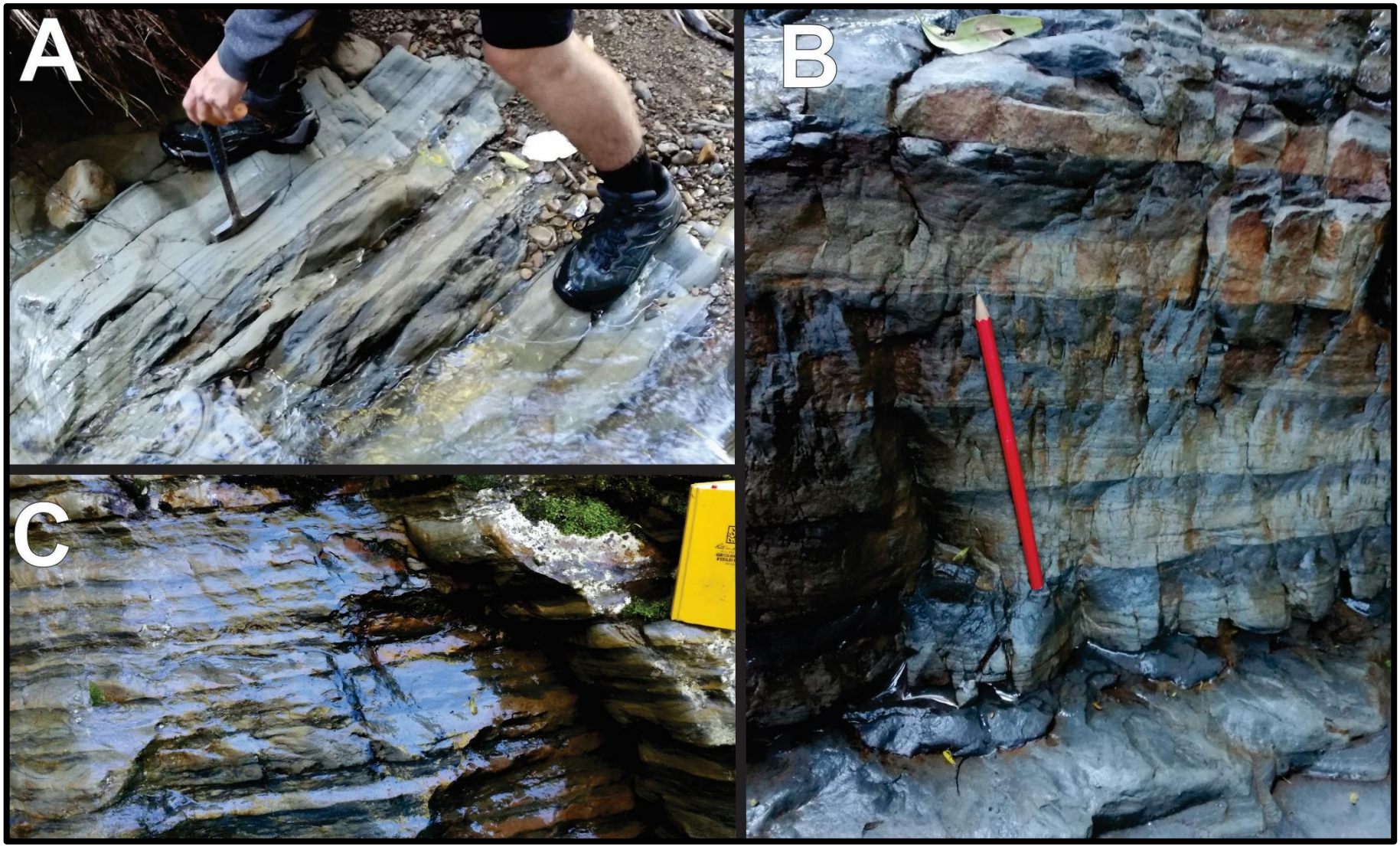

Figure 5.10: Motuwaireka Stream. A) Sand-dominated turbidites (Facies C2.2), with sands sometimes amalgamated, e.g., by hammer. Younging to the left. ~950 m upsection, BP35 514 514. B) Carbonaceous cross-laminae in Facies C2.3 turbidites. Younging upwards. ~970 m upsection, BP35 514 514. . C) Thin-bedded, organic-rich graded sandstone-mudstone couplets of Facies C2.3. Younging upwards in photo, pencil ~18 cm long. ~1140 m, BP35 513 515

Figure 5.11: Motuwaireka Stream. Non-graded muddy conglomerate (Facies A1.2) overlying sandstone-mudstone couplets (Facies C2.2/C2.3). 650 m upsection, BP36 521 503.

5.1.5: Mataikona River - Appendix H

The Mataikona River section is stratigraphically very different to the Totara Stream and Motuwaireka Stream sections. Although outcrop is discontinuous, no large faults have been mapped in the section and the fossil record suggests the section is most likely continuous. Lowermost strata are fine-grained siltstone (Figure 5.12a; Facies D1.1, rare D1.2) with occasional sandstone (Facies B2 and C2.3) turbidites. Siltstone are generally weakly burrowed and highly weathered, but some zones are mottled and therefore assigned Facies D1.2. Facies D1.1 likely represent concentrated density flows and D1.2 is possibly bottom current deposits. These lowermost strata are Mangaotanean in age as inferred from *Cremnoceramus bicorrugatus.* Facies C2.2 turbidites occur over a 2 m thick interval at between 8 and 10 m upsection (Figure 5.12b, c).

A significant amount of outcrop is missing above this section. The next exposed outcrops, at 98 m, are in Smokey Gulley Stream and are Facies C2.2 to C2.3 turbidites (Figure 4.14a). Crampton (1997) maps these beds as oldest Teratan in age; no fossils were found in the present study.

At 376 m, after another large gap in outcrop, there is a slumped zone of sandstone beds up to 150 cm thick (Figure 4.11). Some are graded and coupled with thin siltstones (Facies C2.1) and others appear massive (Facies B1). Facies B1 are produced from either inflated sand flows or concentrated density flows, whereas C2.1 are generally due to flows transitional between concentrated density flows and turbidity currents. Similar outcrop appears further upsection at 655 m but is generally thinner-bedded on a 10-20 cm scale (Figure 5.13a, b, c).

After another gap in outcrop of ~100 m, at 770 m, rocks of facies C2.1, C2.2 and B1 outcrop, with all outcrops observed above this following similar patterns. These are interpreted as a mixture of turbidites and concentrated density flows or inflated sand flows. These are probably Piripauan aged sediments based on Crampton (1997).

Although not observed here due to obscured outcrop, Crampton (1997) noted a 50 m-thick section of conglomerate bedded on a 1-5 m scale in the lower Haumurian. This conglomerate was described as clast supported, well sorted, pebble to sparse cobble dominated and subangular to subrounded, and would likely be a debrite. No other conglomerates were noted in the immediate vicinity of this section, and no other Haumurian conglomerates were mapped in any part of this study. Walpole and Burr (1939) mapped “fine conglomerate” midway up Smokey Gully Stream (“Pukueamuku Stream” in their publication). This appears to be roughly along strike from late Mangaotanean to early Teratan sediments. Crampton (1997) also mapped Smokey Gully Stream but did not note any conglomerate, though what he described as “very coarse” sandstone may be the equivalent facies.

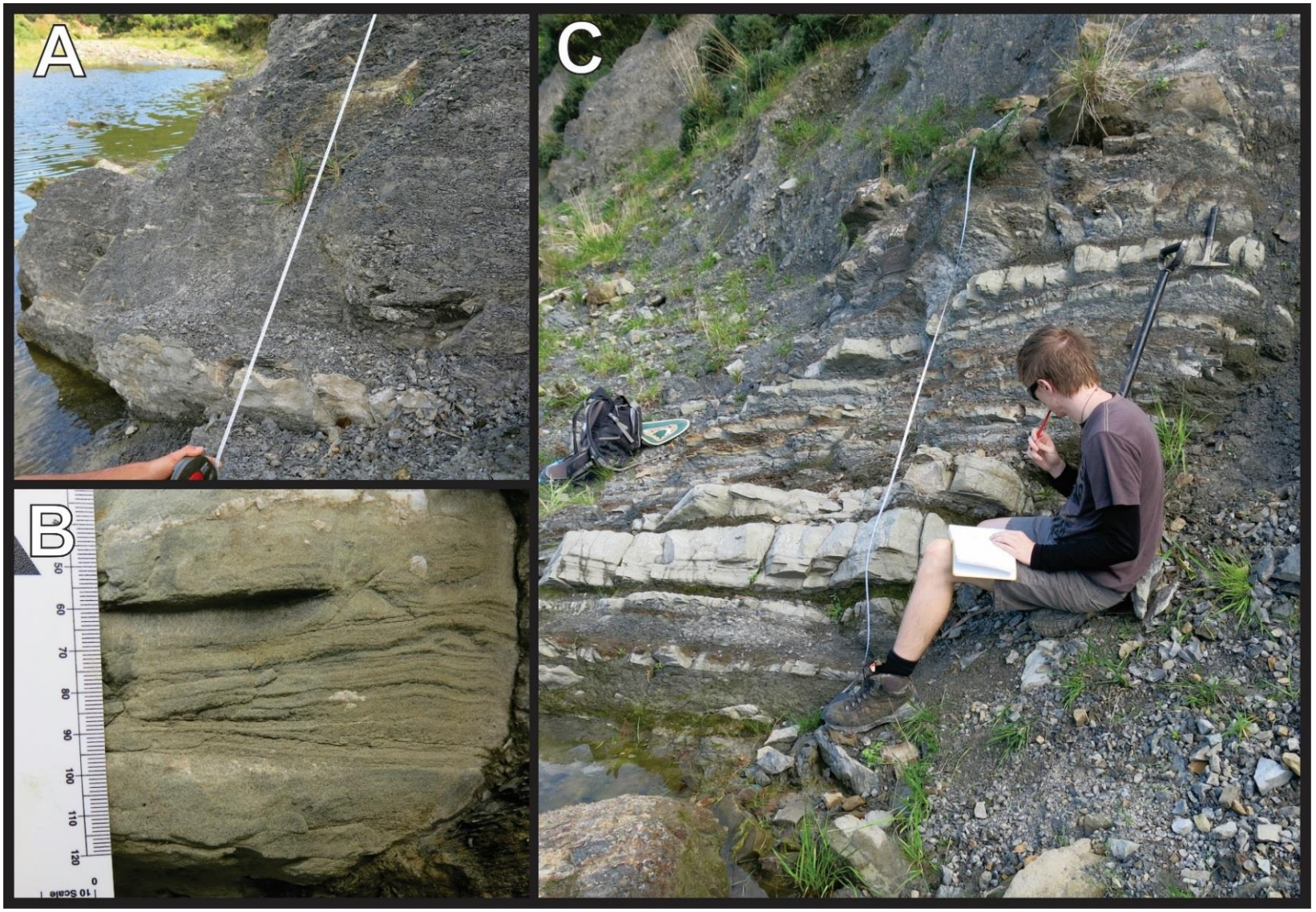

Figure 5.12: Mataikona River. A) Thick siltstone (Facies B1.1) intervals with occasional sandstones (Facies B2 or C2.3). ~2 m upsection, BN36 745 859. B) Cross-lamination in graded sandstone bed (Facies C2.2). ~9 m upsection, BN36 745 859. C) Sandstone-mudstone couplets of Facies C2.2 and C2.3. 8 – 10m upsection, BN36 743 861.

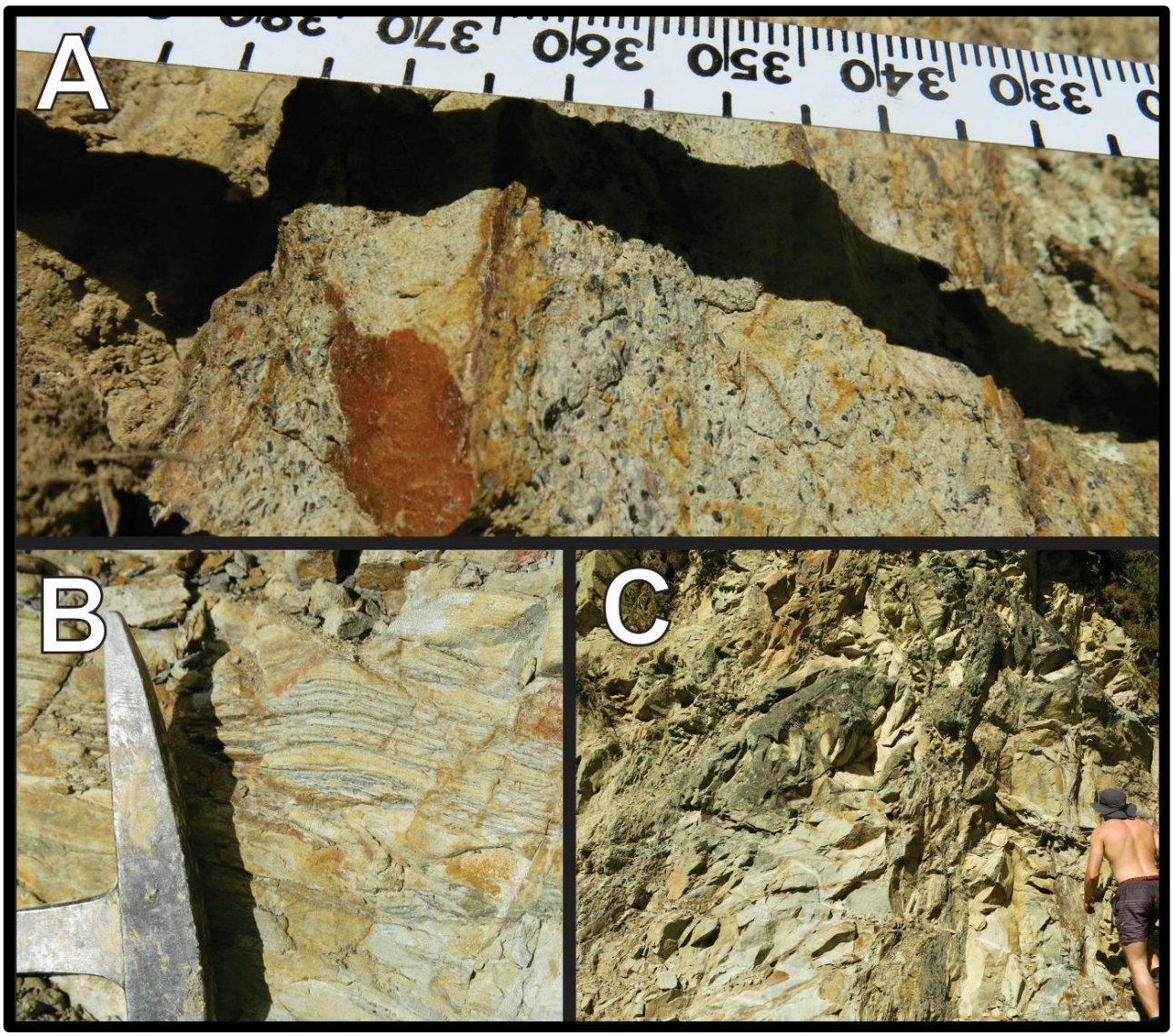

Figure 5.13: Mataikona River. A) Carbonaceous granules within sandstone beds (Facies B1.1), younging to left. ~380 m upsection, BN36 736 862. B) Organic lamination in thick sandstone of Facies C2.1. Younging upward. ~947 m upsection, BN36 736 867. C) Thick, massive, coarse sandstone of Facies B1.1. Youngs to right. ~375-380 m upsection, BN36 736 862

5.1.6: Waimata River – Appendix I

The Waimata River showed generally very poor continuity of outcropping and therefore no measured section was possible. A composite section is instead presented in Appendix I. Regardless, a few well preserved outcrops were present. All facies exposed were either Facies C2.1, C2.2 or C2.3 sandstone-mudstone couplets (Figure 5.14) and therefore interpreted as turbidite deposits. The only fossils noted in this study were *Inoceramus opetius,* which dates these strata as Teratan aged. Bed thickness was highly variable with sandstone beds up to 1 m thick. Sandstone contained common convolute- and parallel-lamination and occasional cross-lamination. Mudstone interbeds were commonly very highly weathered so no internal sedimentary features could be recognised.

5.1.7: Mangakuri Beach - Appendices J and K

Mangakuri Beach displayed a number of distinct facies associations in a tectonically complex area. Because the tectonic regime was not mapped, the stratigraphic relationship between individual outcrop sites is unknown. Because of this, a composite section is presented instead. Although some observations were made north of Mangakuri Beach settlement, Crampton (1997) contains a significantly thicker and detailed log than was possible at present, owing to obscured outcrop and unfavourable tides during present fieldwork. Because of this, the log in Crampton (1997) is included in the appendix and his observations are used as part of the interpretations discussed in chapter 6. Strata observed are summarised below.

Southernmost outcrops (Appendix J-I to I-iii) showed a variety of facies. Sandstone dominated facies included graded parallel-, convolute- and cross-laminated sandstones (Facies C2.2, C2.3; Figure 5.15a, c, d), cross-laminated sandstone (Facies C2.4; Figure 5.15b), and massive sandstone with occasional organic rich interbeds (Facies B1 or C1; Figure 5.16c, d). These are mostly interpreted as turbidites, except for Facies B1, which may have been deposited by concentrated density flows or inflated sand flows, and C1, which is interpreted as a sandy debrite. Clasts in Facies Class A conglomerates were mostly mudstone rip-up clasts, and were either graded (Facies A2.1; Figure 5.17a), non-graded (Facies A1.1; Figure 5.17c, d; Figure 5.18a), or dispersed in a sandy

matrix (Facies A1.3 and A2.2 Figure 5.18b). These are interpreted as either concentrated density flows or debrites. Inoceramus pacificus (V23/f6494) date these strata as Piripauan.

Strata between the southernmost outcrops and Mangakuri village are mostly consistent with these descriptions, although a few other facies were noted. At BL39 332 643, a >20 m wide channelised massive sandstone (Facies B1; Appendix J-iv) incises parallel-stratified sandstones (Figure 5.16b), which is a channelised concentrated density or inflated sand flow deposit. At BL39 332 644 (Appendix J-v), a pebbly conglomerate consisting mainly of indurated material and fossil fragments underlies fine, graded Facies C2.3 beds (Figure 5.19b). Above this bed are parallel-laminated sandstone beds of Facies B2, massive sandstone beds of Facies B1 and parallel-stratified pebbly sandstone beds of Facies A2.2 (Figure 4.10b; Figure 5.17b), a mixture of concentrated density flow deposits and turbidites. Nearby, thick cross-beds of gravel in an otherwise medium-grained, massive sandstone overlie sandstone beds displaying distinct convolute- and parallel-lamination which are interpreted as turbidites, and included occasional outsized clasts (Figure 5.15e; Figure 5.16a, Appendix J-viii). Some packages of sandy siltstone did not show internal grading or bedding and are therefore classified as Facies C1, and are possibly sandy debrites (Figure 5.16d).

North of Mangakuri village beds are dominantly graded sandstones with a minor siltstone component. Parallel, cross- and convolute-lamination mean these beds are generally classified as Facies C2.1-C2.3 turbidites depending on bed thickness (Crampton, 1997). Occasional graded, granule to pebble conglomerate beds are also present (Facies A2.1), deposited by concentrated density flows (Figure 5.19b, c). Crampton (1997) mapped one ~12m thick conglomerate, the thickest part of which was not observed in this study. Grading indicates this is also a Facies A2.1 bed. Pebbly, non-stratified sandstone (Facies A1.3) also occur on small cliffs (Figure 4.8a, b; Figure 5.19a).

The fossil record in the southern part of Mangakuri Beach is sparse. Although Inoceramid fragments are abundant, no intact fossils were collected in this study. Fragments of *Inoceramus pacificus* and *Inoceramus australis* were tentatively identified in the field. FRED samples suggest *Inoceramus australis, Inoceramus pacificus and Inoceramus opetius* may be present in the vicinity (see Appendix B). A Teratan to Piripauan age is assumed for south Mangakuri Beach strata. *Inoceramus madagascariensis* was collected from northern Mangakuri Beach which suggests a Teratan age.

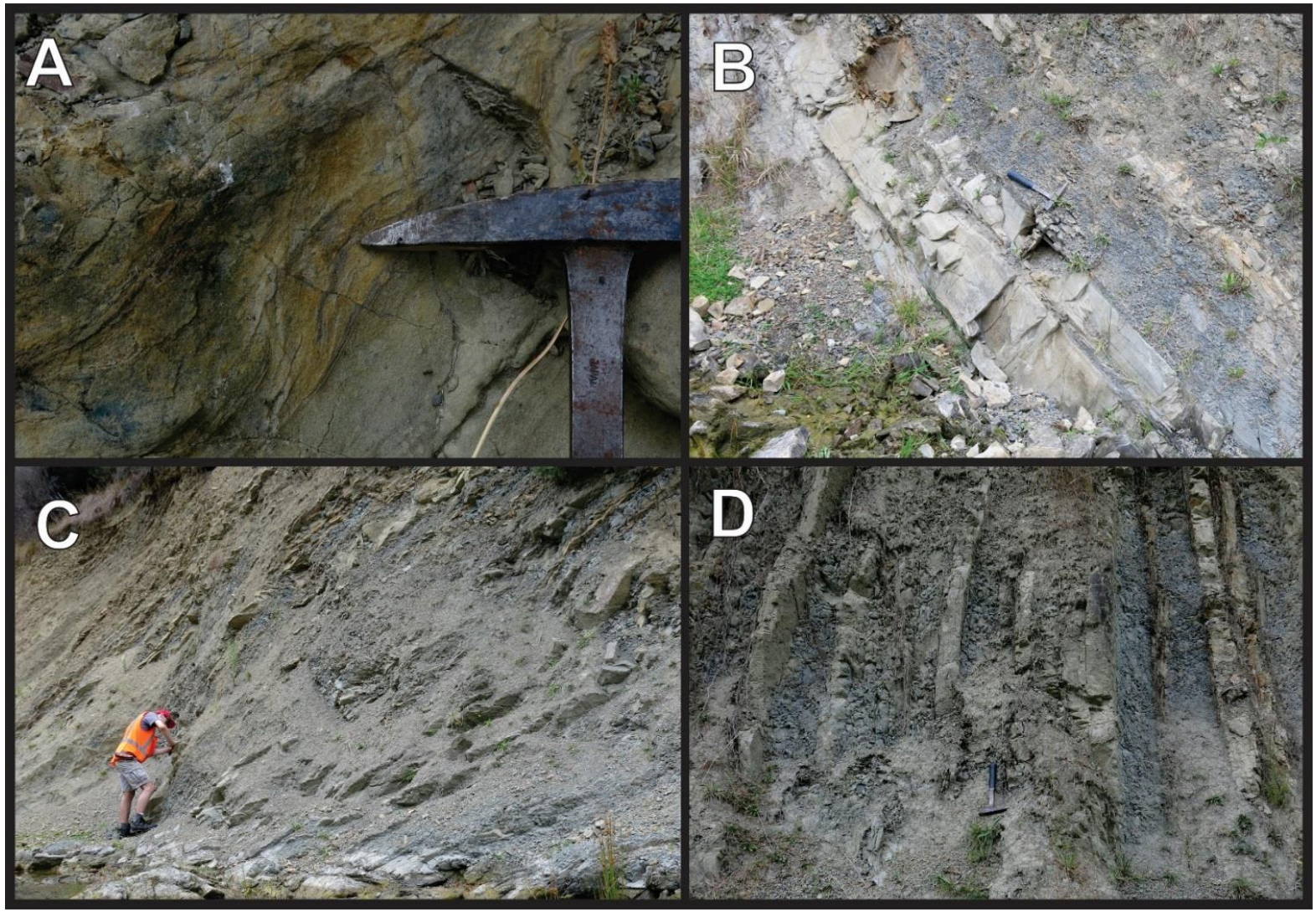

Figure 5.14: Waimata River. A) Silty convolute-laminae in Facies C2.1 sandstone bed. Younging towards top left. Appendix I-iii, BN37 947 101. B) Thick- to medium-bedded turbidites (Facies C2.1, C.2). Younging towards top right. Appendix I-iii, BN37 9516 0914. C) Thin turbidites dominated by mudstone, younging towards top left (Facies C2.2, C2.3). Appendix I-i, BN37 948 098. D) Medium-bedded, fine-grained turbidites, younging to the right (Facies C2.2). Appendix I-ii, BN37 947 010.

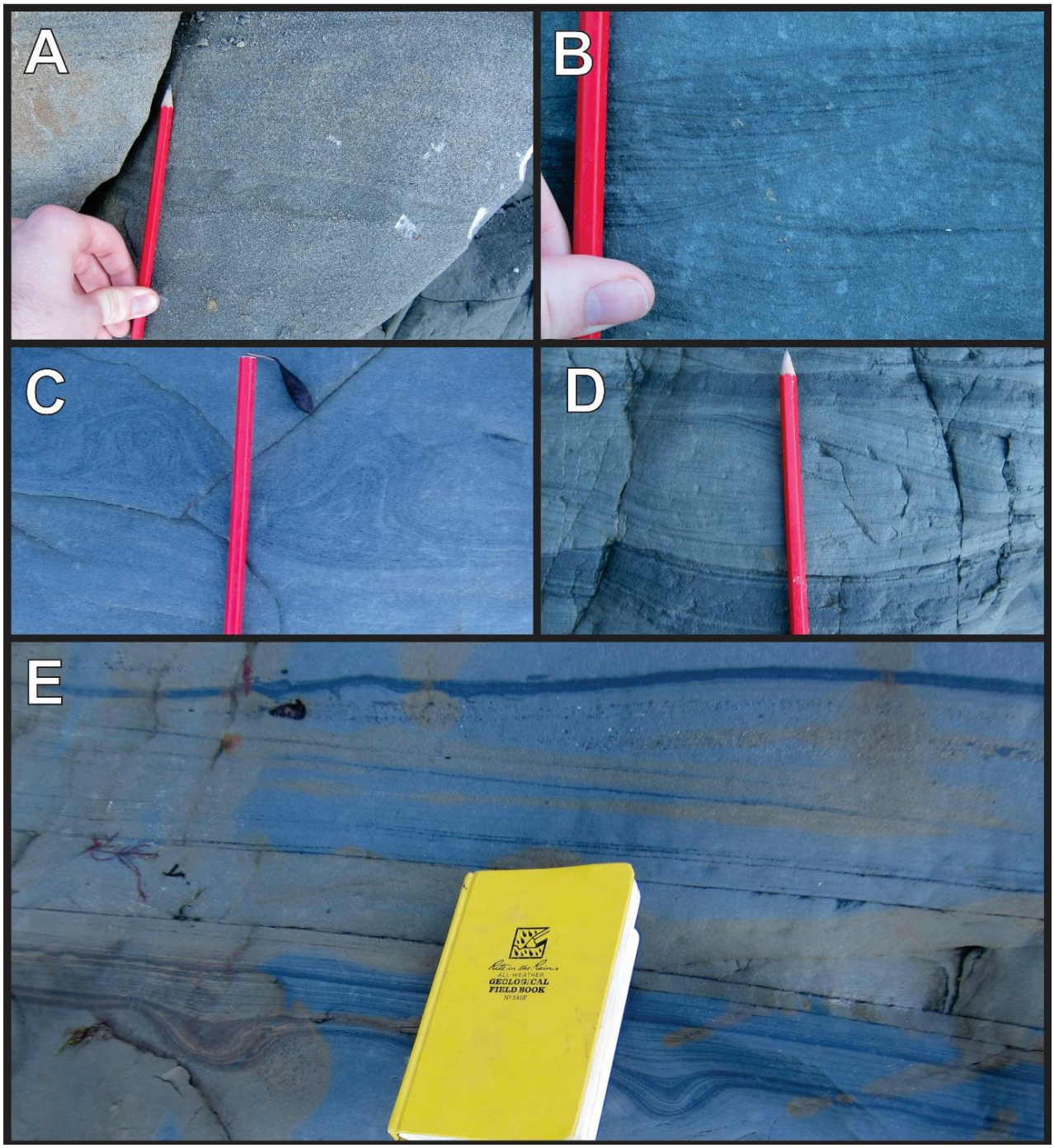

Figure 5.15: Mangakuri Beach. A) Flame structures in a thick, graded sandstone (Facies C2.1), younging upwards. Appendix J-i, BL39 329 639. B) Cross-bedding in silty sandstone, younging upwards. Appendix J-i BL39 329 639. C) Convolute-lamination in graded silty sandstone (Facies C2.1). Appendix J-iii, BL39 330 640. D) Prominent cross-bedding in graded Facies C2.2 sandstone-mudstone couplet. Appendix J-i BL39 329 639. E) Convolute-lamination in thick laminated sandy units (Facies C2.2). Cross-bed/dune structure notable at top of photo with pebbly sandstone (Facies A1.2) and a thick silty later draping it. Appendix J-viii, BL39 337 663.

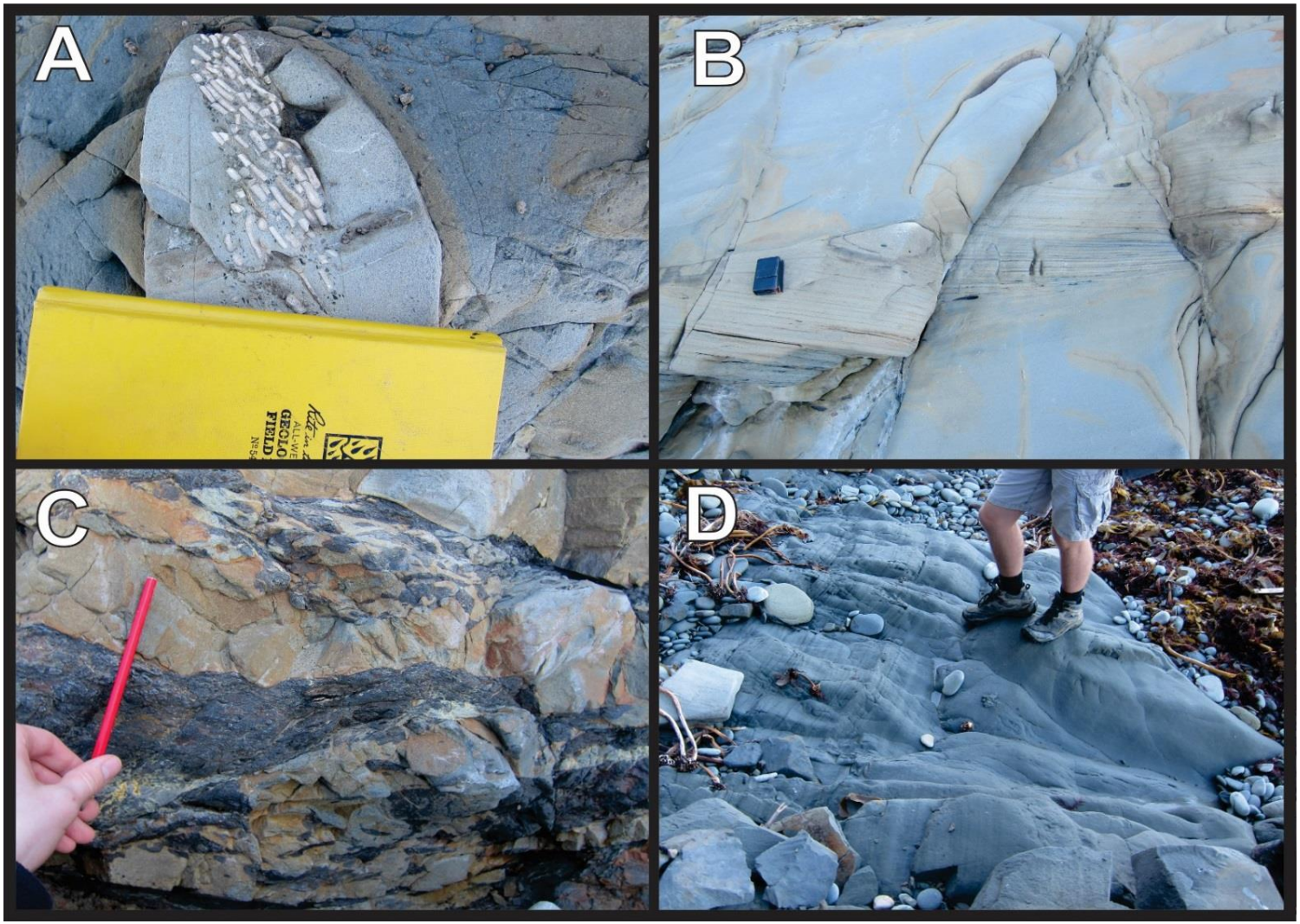

Figure 5.16: Mangakuri Beach. A) Outsized sandstone clast in mud-flake-rich sandstone, containing abundant unidentified inoceramid fragments. Bed dipping steeply into page, younging towards top right. Appendix J-viii, BL39 337 663. B) Channelised B1 sandstone, incising parallel-stratified B2 sandstone. Dipping shallowly into page, younging upwards. Appendix J-iv, BL39 332 643. C) Organic-rich mudstone (Class E) draping sandstone (Facies B1). Shallow dipping into page, younging upwards. Appendix J-iii, BL39 332 643. D) "Featureless" sandy siltstone (Facies C1) (right) overlain by graded Facies C2.3 sandstone. Beds near vertical, dipping to the right. Appendix J-i, BL39 330 641.

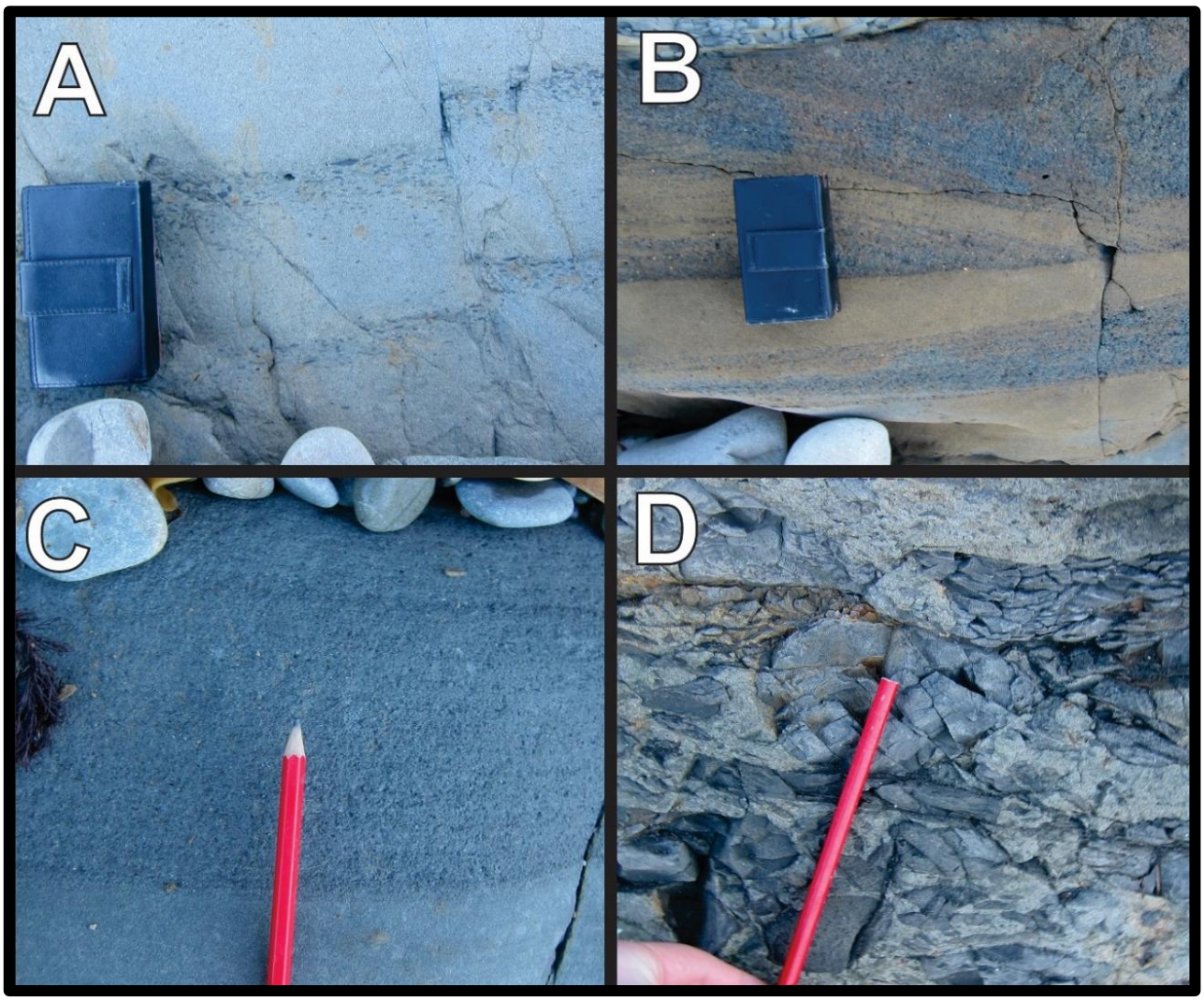

Figure 5.17: Mangakuri Beach. A) Normally graded overturned pebbly sandstone. Younging towards bottom of photo. Granule-sized clasts mostly comprised of mudstone rip-up clasts. Mangakuri composite Appendix J-iii, BL39 330 641. B) Cross-beds in pebbly sandstone/granular conglomerate (Facies A1.1/A1.2, top half of photo) overlying a granular conglomerate that is in turn overlain by featureless sandstone (Facies B1). Younging upwards. Appendix J-viii, BL39 337 661. C) Very coarse sandstone (Facies B2) overlying a bioturbated silty sandstone (Facies C1), younging upwards. Appendix J-i, BL39 329 639. D) Cobble grade mudstone rip-up clast dominated conglomerate (Facies A2.1), younging upwards. Appendix J-i, BL39 330 641.

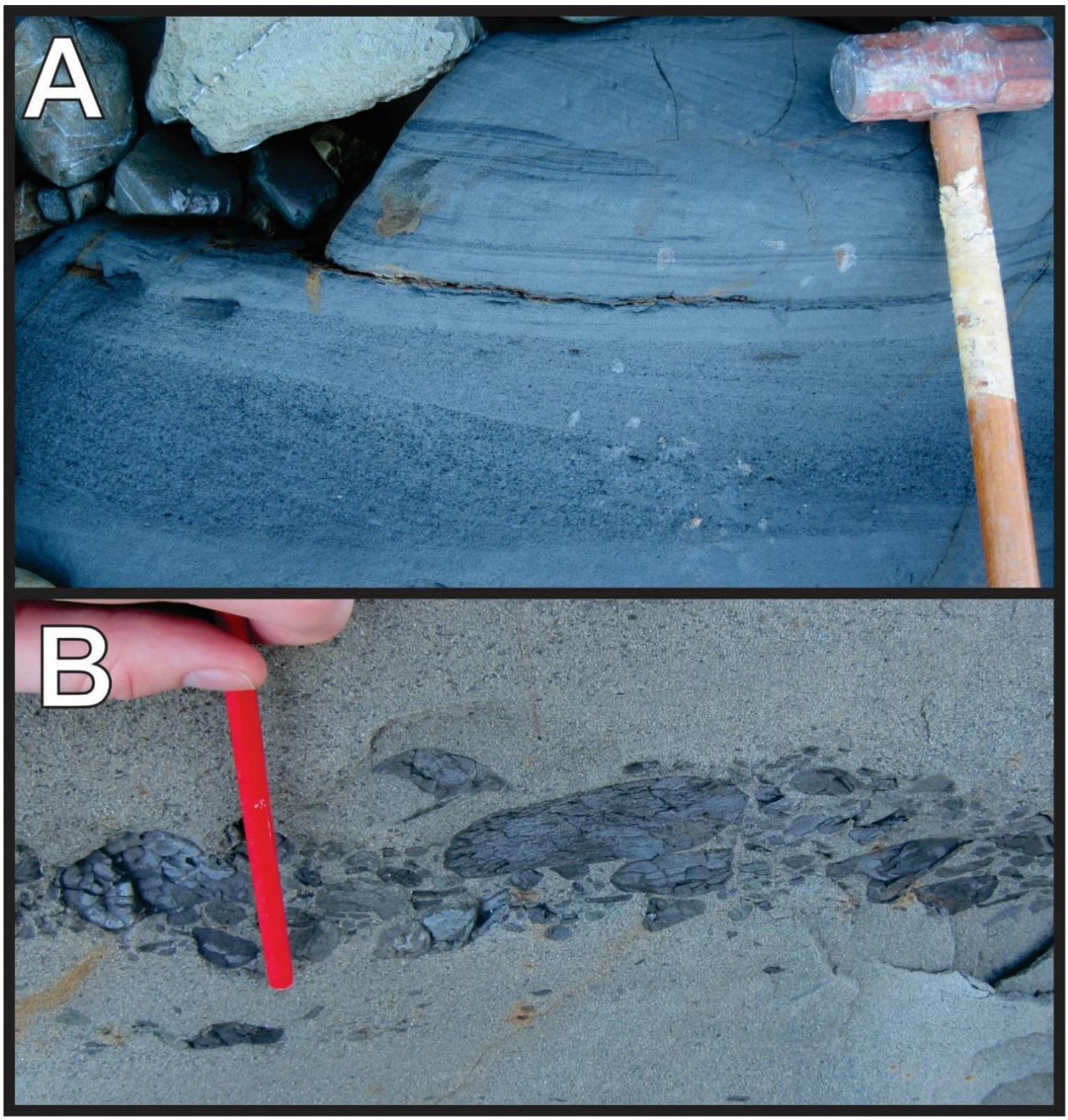

Figure 5.18: Mangakuri Beach. Trough cross-bedding in graded granular conglomerate (Facies A2.1) overlain by similar features in laminated sandy siltstone (Facies B2). Youngs upwards. Appendix J-ii, BL39 330 641. B) Dense layer of rip-up clasts in a pebbly sandstone (Facies A2.2). Youngs upwards. Appendix J-i, BL39 330 641.

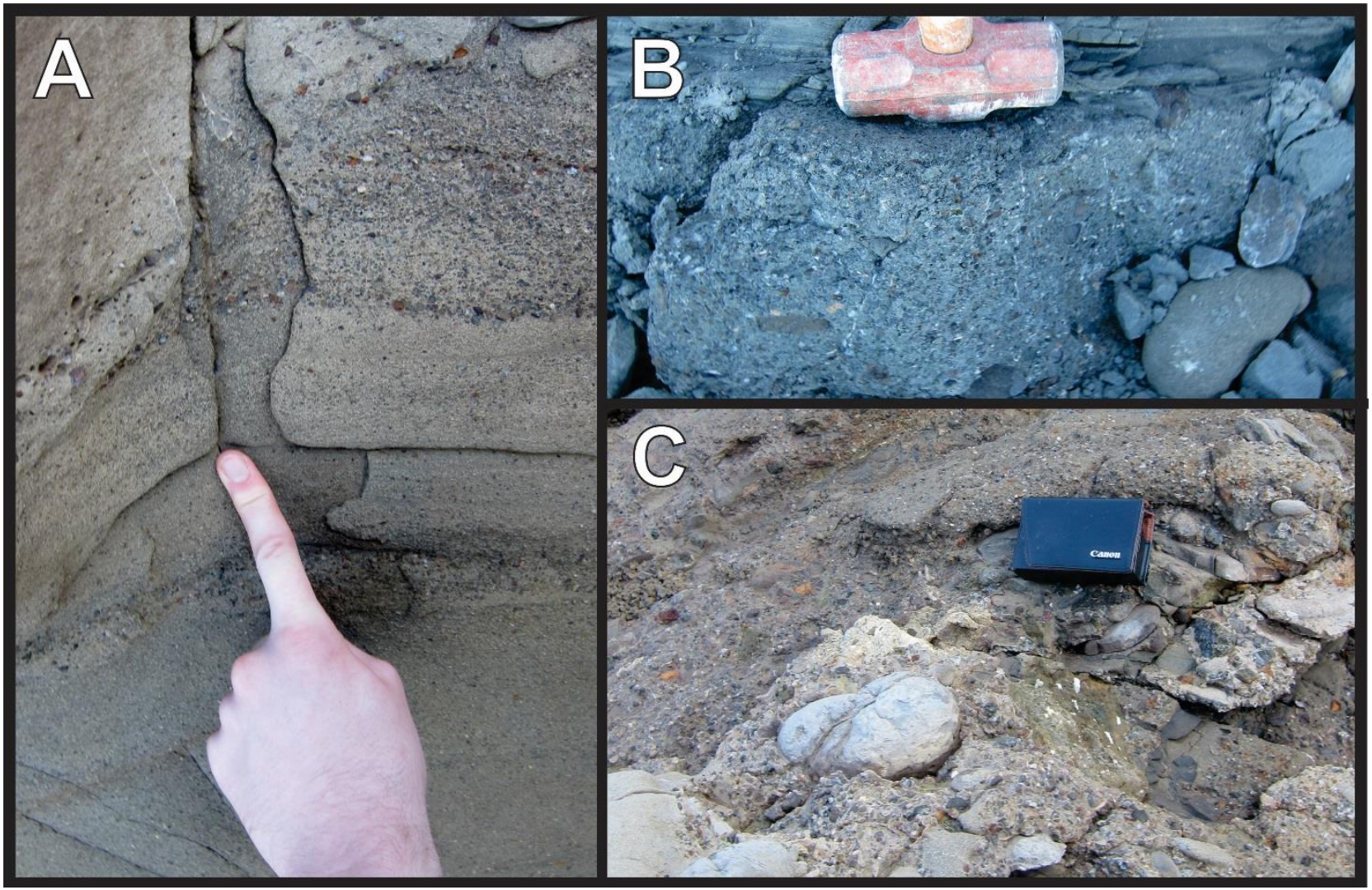

Figure 5.19: Mangakuri Beach. A) Pebbly sandstone of Facies A2.2. Pebble concentration varies, but generally stratified. Bed younging direction inferred to be upwards. At ~ 200-225 m Appendix K, BL39 355 695 B) Facies A2.1 graded pebbly conglomerate, younging upwards. Appendix J-v, BL39 333 645. C) Poorly sorted conglomerate with camera case for scale. Bed youngs towards bottom left. At ~184 m, Appendix K, BL39 355 695.

5.1.8: Waimarama Beach – Appendix L

The complex nature of the tectonic regime also makes spatial relationships of facies observed at Waimarama Beach suspect, and so as with Mangakuri, a composite section is presented. Stratigraphy observed is summarised below.

Southernmost outcrops consisted of highly weathered, sometimes graded siltstone of Facies D2 (locally D1.2), overlain by graded Facies C2.3 interbeds of fine sandstone and siltstone (Figure 5.20a, d). These sandstone beds show abundant carbonaceous parallel-stratification as well as cross-beds and are therefore interpreted as turbidites. Intact *Inoceramus opetius s*uggest a Teratan age for these sediments.

At BL39 405 793, a pebbly, fossil rich conglomerate of Facies A1.3 (Figure 4.8c; Figure 5.21a) is overlain by mudstone beds (Facies D2/D1.2) similar to those described above and thick, medium- to coarse-grained massive sandstone beds of Facies B1 (Figure 5.20c). Facies A1.3 and B1 are either the deposits of concentrated density flows or inflated sand/gravel flows. Sandstone beds contain abundant granule- to pebble-sized rip-up clasts of mudstone (Figure 5.20b). Peculiar shell beds are also present, occurring often in lenses as well as in hashes ("Bicorrugatus hash" of De Caen and Darley, 1968), which is best classed as a Facies A1.1 conglomerate (Figure 5.21c).

Facies at BL39 411 808 were dominantly Facies C1 massive silty sandstone debrites and Facies B2 parallel-laminated sandstones which are probably turbidites. At BL39 414 810, a ~15 m thick succession of medium- to thick-bedded graded Facies C2.1 and C2.2 turbidites occurs, with sandstones separated by thin (<10 cm) mudstones (Figure 5.22). Mudstone interbeds are commonly very organic-rich and black (Figure 5.22a). One normally graded cobble conglomerate (Facies A2.1) is found at BL39 415 814 (Figure 5.21b), but otherwise Class A beds are restricted to granule and rare pebble sized beds <30 cm thick. Northernmost outcrops are parallel-stratified and graded sandstones (Facies B2 or C2 but missing mudstone couplet), massive silty sandstone (Facies C1) and very fine conglomerates (Facies A1.3, A2.1, A2.2). These are interpreted as turbidites, sandy debrites and concentrated density flow deposits respectively.

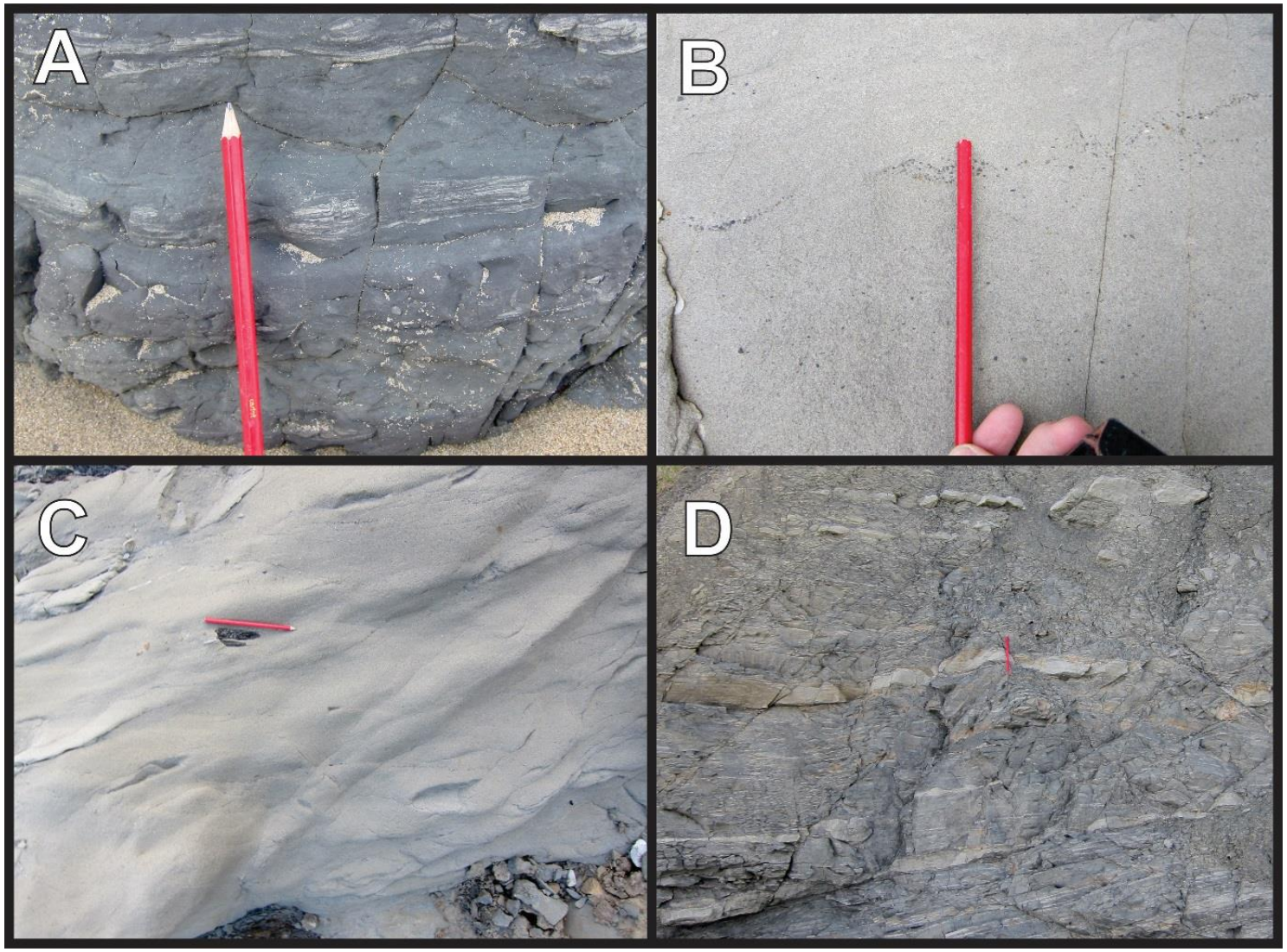

Figure 5.20 - Waimarama. A) Massive siltstone of Facies D1.1 to D1.2 (sparse bioturbation). Appendix L-i, BL39 402 792. B) Stringer of pebbles in a massive Facies B1 sandstone. Appendix L-ii, BL39 406 794. C) Massive disorganised sandstone (Facies B1), with mudstone rip-up clast near pencil. Appendix L-ii, BL39 404 792. D) Thin-bedded, siltstone dominated Facies C2.3 sandstone-mudstone couplets. Appendix L-i, BL39 402 792.

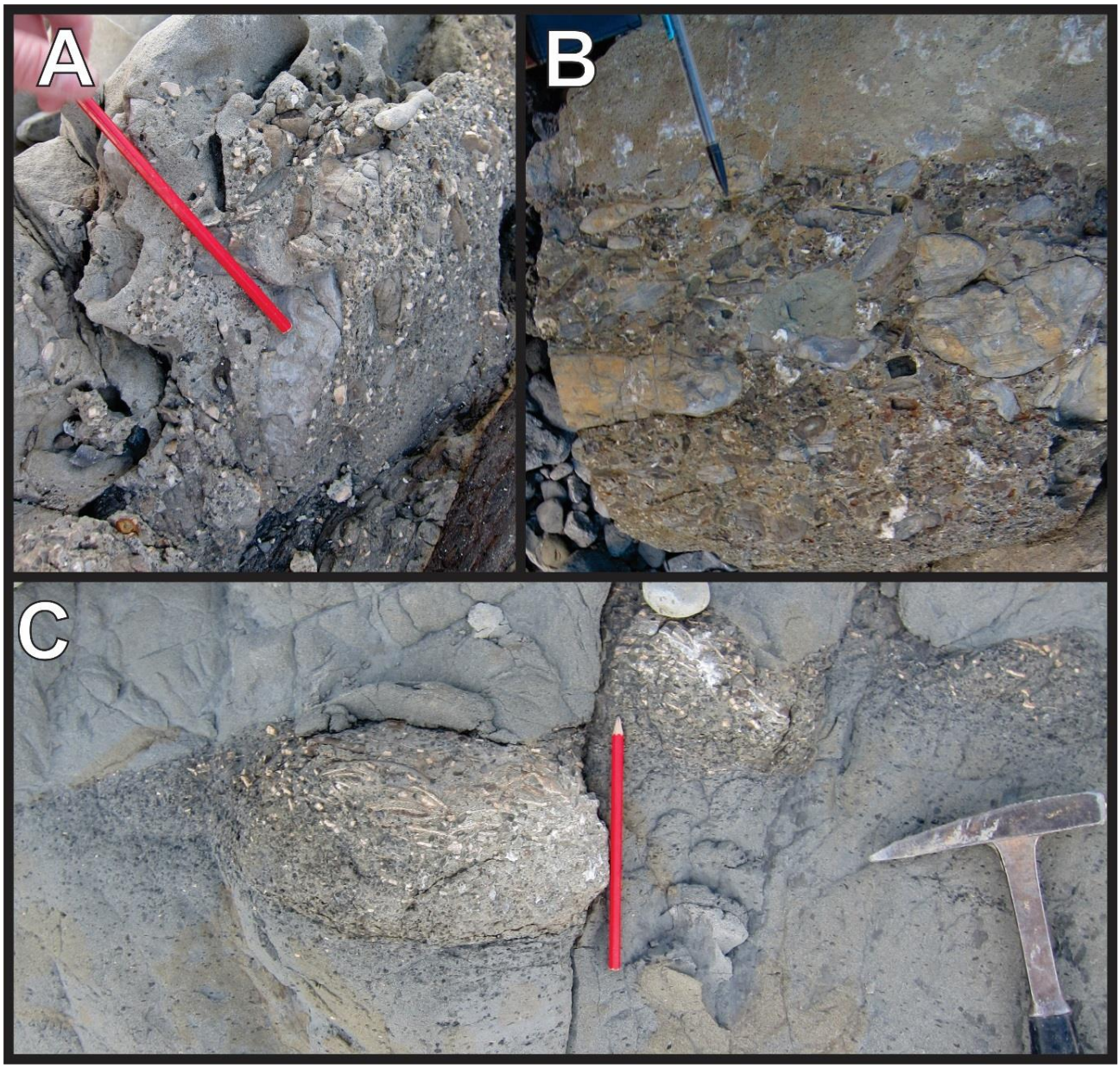

Figure 5.21: Waimarama. A) Disorganised pebbly conglomerate with abundant inoceramid fragments. Younging direction unknown. Appendix L-ii, BL39 406 793. B) Graded conglomerate of Facies A2.1; probably inverse graded and upright. Appendix L-viii, BL39 415 814. C) Large lens of pebbly grade material, mostly inoceramid fragments and rip-up clasts. Inferred to be overturned and younging downwards. Overlies Facies C1 silty sandstone (top of photo), channelised. Appendix L-iii, BL39 406 794.

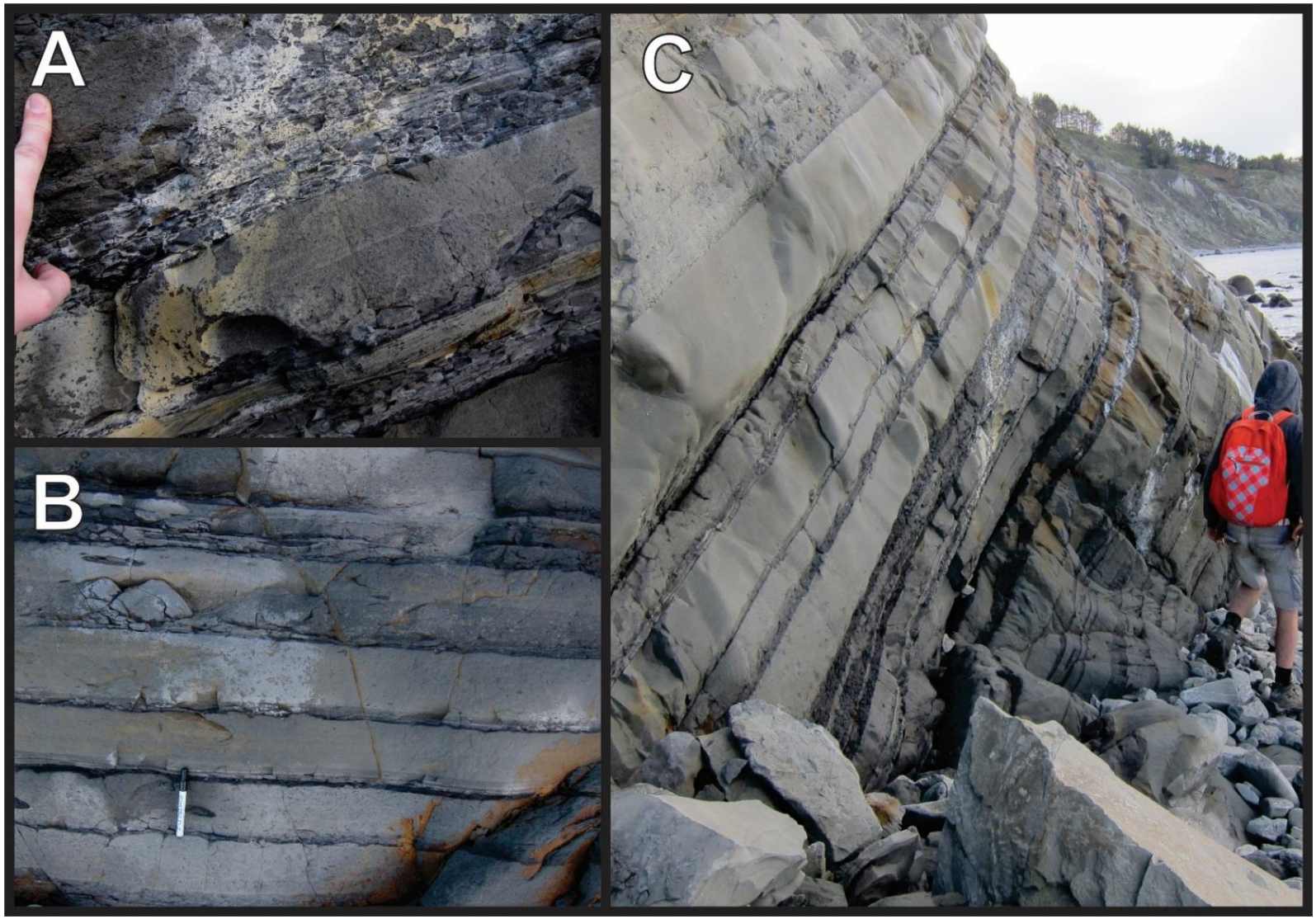

Figure 5.22: Waimarama. A) Sandstone-mudstone couplet of Facies C2.2 with a thick carbon-rich mudstone component, younging upwards. Appendix L-vi, BL39 414 810. B) Facies C2.2 graded sandstone with a thin siltstone component. Rip-up clasts such as those near pen occur sporadically. Younging towards top of photo. Appendix L-vii, BL39 414 811. C) Sandstone-mudstone couplets of Facies C2.1 and C2.2. Youngs to top left. Appendix L-vi, BL39 414 810.

5.1.9: Section Summary

Although there are significant variations in facies between different sections of the Glenburn Formation, throughout the sections studied the vast majority of sediment is inferred to have been deposited by SGFs. Turbidity currents and debris flows are the most common inferred transport mechanism for sediment for the Glenburn Formation. Fossils either collected in this study or from previous FRED entries tend to constrain the age of strata fairly well, but in places there are significant gaps in outcrop which might introduce some uncertainty to the continuity of outcrop. Regardless, a large volume of Glenburn Formation was able to be examined and interpreted over a significant extent both spatially and temporally.

5.2: Conglomerate Clast Counts

5.2.1: Introduction

This section presents the results of clast counts at three different localities (Glenburn coast, Totara Stream and Mangakuri Beach), as outlined in section 3.5. The purpose of this investigation was to attempt to discern whether the provenance of Glenburn Formation conglomerates changed over time and space, which may indicate differences in provenance between locations and therefore be relevant to paleogeographic reconstructions of the ECB.

5.2.2: Totara Stream Clast Count

Two separate conglomerate beds were studied in Totara Stream; one from the upper Mangaotanean (or possibly lower Teratan; BP35 482 444) and one from the Teratan (or possibly lower Piripauan; BP35 479 446), as deduced from nearby fossil localities. These beds are both well-sorted and dominantly consist of sub-rounded to sub-angular pebble to cobble clasts. The conglomerates are locally clast supported, but otherwise supported by a sandy matrix (Figure 5.23). The Teratan conglomerate shows minor normal grading, which is not present in the

Mangaotanean conglomerate. In each instance, visible outcrop was poor making random sampling somewhat difficult to do while maintaining a clast count of 400.

Figure 5.23: ~Teratan aged conglomerate, Totara Stream (BP35 479 446)

Due to difficulties in access and scheduling around forestry work, conglomerate clasts were counted further upstream than where the section was measured (Figure 5.24). Due to the river's course, these conglomerates were approximately along strike from the measured section (Section 5.3.1) and the outcrops observed were consistent in nature to the outcrops downstream.

Table 5.1 summarises counts of different clasts for the two conglomerate beds in Totara Stream. Only clasts comprising >1% of total count are included, with the rest included in "other". Minor clast types include basalt, red chert, rhyolite, inoceramid fragments and reworked conglomerate clasts.

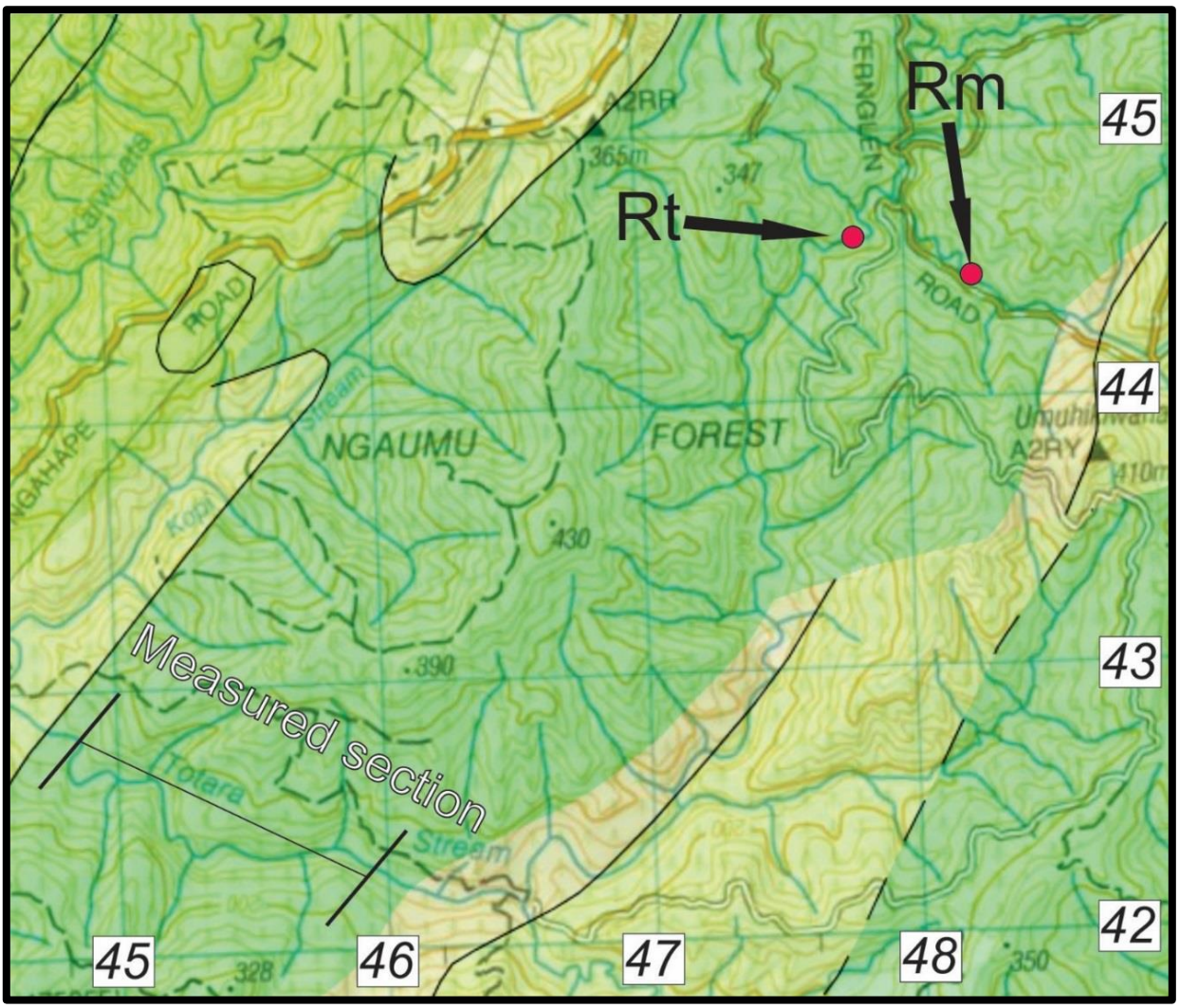

Figure 5.24: Location of Teratan (Rt) and Mangaotanean (Rm) conglomerates relative to measured section described in Section 5.3.1.

Table 5.1 – Summary of clast counts, Totara Stream.

Lithology	Count – Mangaotanean (proportion)	Count – Teratan (proportion)
Indurated sandstone	155 (39%)	192 (48%)
Argillite	64 (16%)	59 (15%)
Sandstone (non-indurated)	46 (12%)	72 (18%)
Siderite cemented mudstone	113 (28%)	14 (4%)
Mudstone	10 (3%)	44 (11%)
Quartz	4 (1%)	6 (2%)
Other	8 (2%)	13 (3 %)
TOTAL	400	400

Distinction between indurated “basement” type sandstone and cover sandstone was often difficult to make due to the high degree of weathering of outcrop, and thus it may not be entirely appropriate to present these as two separate categories. Regardless, there are some clear differences in the two populations, most notably in the siderite count of the older conglomerate versus the siderite count in the younger conglomerate (Figure 5.25).

In the instance of Totara Stream, it appears that “siderite” clasts (as per Moore 1980) may represent locally derived mudstone clasts that have been weathered significantly post-deposition. If combined with non-indurated sandstone and mudstone, this gives an approximate estimation of “locally” derived material to indurated material. In this instance, the Mangaotanean conglomerate is 42.3% locally derived whereas the Piripauan conglomerate is 32.5% locally derived. Even at the 99% confidence interval, the null hypothesis of eq. 2 is rejected indicating the older conglomerate has a higher portion of locally derived material (Figure 5.26).

There is a higher ratio of mudstone/siderite to sandstone among locally derived sediments within the older conglomerate. In the older conglomerate, 73% of locally derived clasts are mudstones, compared to 45% in the younger conglomerate.

The ratio of argillite to indurated sandstone observed between beds does not change at a statistically significant ($p > 0.05$) level.

Comparison of clasts with proportions of <5-10% of the total count have little interpretive value (Howard, 1993). Red chert, similar to that found at Red Island in Waimarama, was found in the Piripauan bed. The Mangaotanean bed contained one large clast of what appeared to be mafic rock, possibly spillite as described by Moore (1980). A few clasts of felsic volcanic rock that are probably rhyolite were found in each bed, which concurs with the findings of Moore (1980).

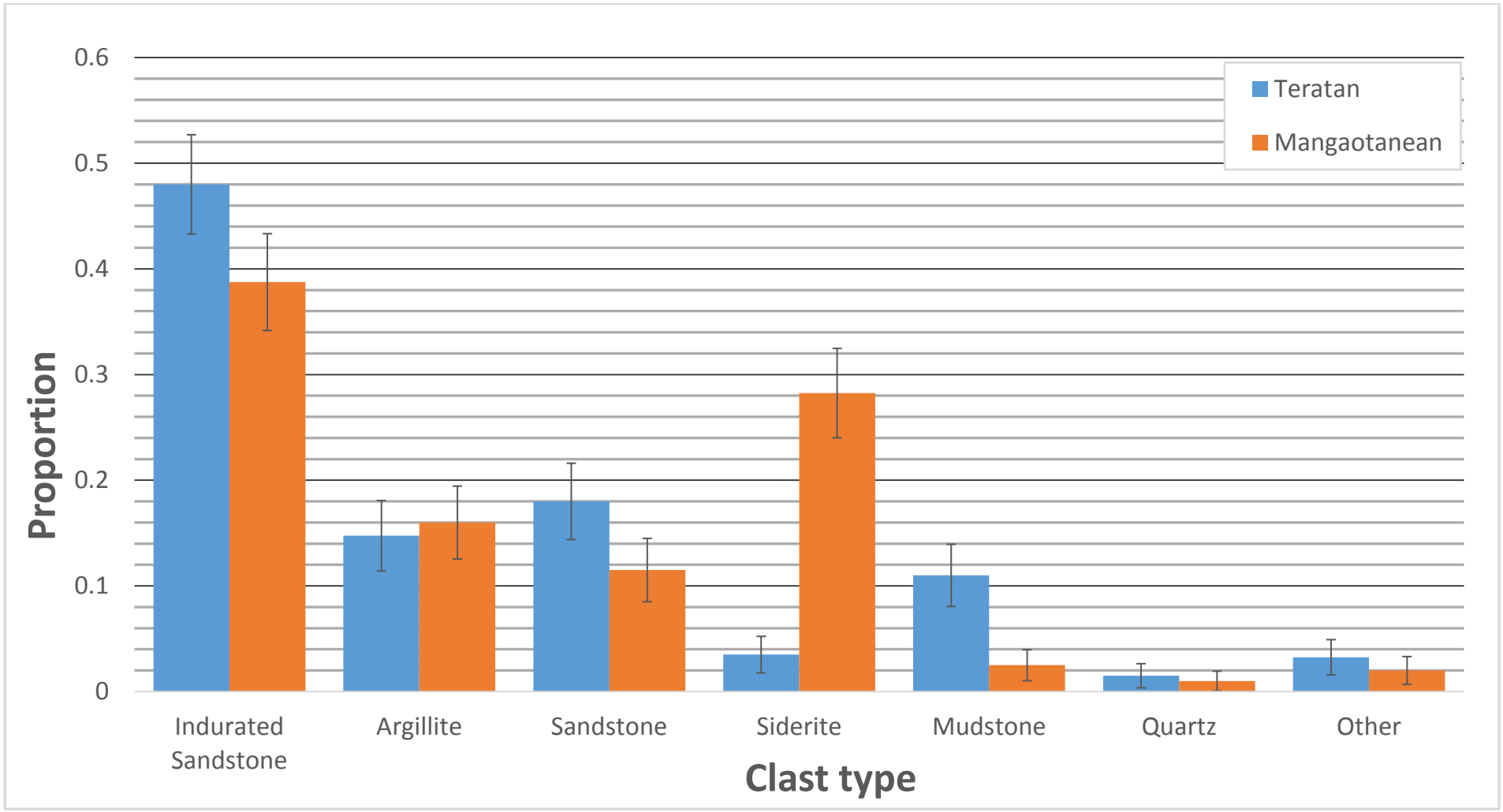

Figure 5.25: Comparison of clast counts between Teratan and Mangaotanean sections at Totara Stream, with 94% CI error bars (indicating approximate 99% confidence of difference between sample counts)

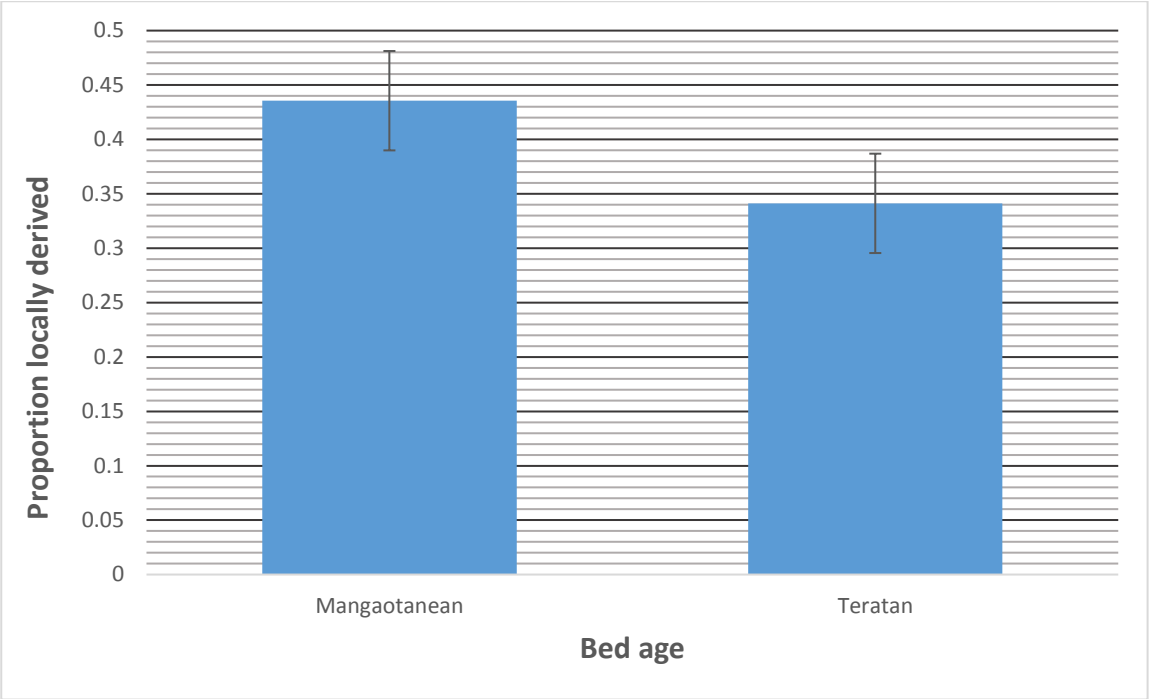

Figure 5.26: Proportion of locally derived material for two beds in Totara Stream. Error bars are 94% CI's, see section above for explanation

5.2.3: Glenburn Coast Clast Count

Clast counts were taken from three conglomerate beds on the Glenburn coast in Wairarapa; one at Horewai Point (Appendix E) and two at Honeycomb Light (Appendix D). The Horewai Point conglomerate and the older of the two Honeycomb Light conglomerates are found just above the inferred Ngaterian-Arowhanan boundary and are thus approximately coeval. The second conglomerate at Honeycomb Light was deposited around 10 m upsection from the first.

The Horewai Point conglomerate (BQ35 381 208) is ~11-13 m thick. It is moderately well sorted, clast-supported, and dominated by sub-rounded to well-rounded cobble clasts. Occasional boulder sized rafted sandstone clasts are present (Figure 5.5a, c). At Honeycomb Light (BQ35 369 189) two separate but very similar conglomerates were studied. The first is a ~3 m thick well sorted, clast supported, well-rounded pebble to cobble conglomerate. Sandstone rafts are also present (Figure 4.6, Figure 5.28). The second conglomerate is similar, but only ~1 m thick (Figure 5.27). The table below (Table 5.2) summarises the clast counts and proportions:

Figure 5.27: Upper Honeycomb Light bed, BQ35 369 189

Figure 5.28: Lower Honeycomb Light bed close-up. BQ35 369 189

Table 5.2 - Summary of clast counts, Glenburn Coast

Lithology	Horewai Point	Lower Honeycomb Light	Lower Honeycomb Light
Indurated sandstone	276 (69%)	267 (67%)	239 (60%)
Argillite	31 (8%)	40 (10%)	44 (11%)
Sandstone	49 (12%)	36 (9%)	55 (14%)
Mudstone	2 (<1%)	18 (5%)	26 (7%)
Quartz	2 (<1%)	10 (3%)	7 (2%)
Reworked concretion	26 (7%)	21 (5%)	15 (4%)
Other	14 (4%)	8 (2%)	8 (2%)
TOTAL	400	400	400

In Table 5.2 and Figure 5.29, “other” clasts include red chert, mafic volcanic rock, inoceramid fragments and reworked granular conglomerate. These reworked conglomerate clasts were only found in the younger Honeycomb Light bed. Reworked concretions were generally orange-brown or pink, probably reflecting different degrees of weathering, or possibly siderite cementation, rather than different lithologies.

The Horewai Point and older Honeycomb Light conglomerate have a very similar percentage of total indurated clasts (77%). Because of their current proximity and concurrent time of deposition, it is possible they are both deposits from the same event. The ratio of indurated sandstone to argillite is also not statistically significantly different.

There is a statistically significant difference between the proportions of non-indurated mudstones between the two beds (Figure 5.29). The Honeycomb Light section has significantly more mudstone than Horewai Point. In each instance, mudstone represents less than 10% of the total volume of the bed and so it is difficult to make any statistically valid conclusions from this (Howard, 1993).

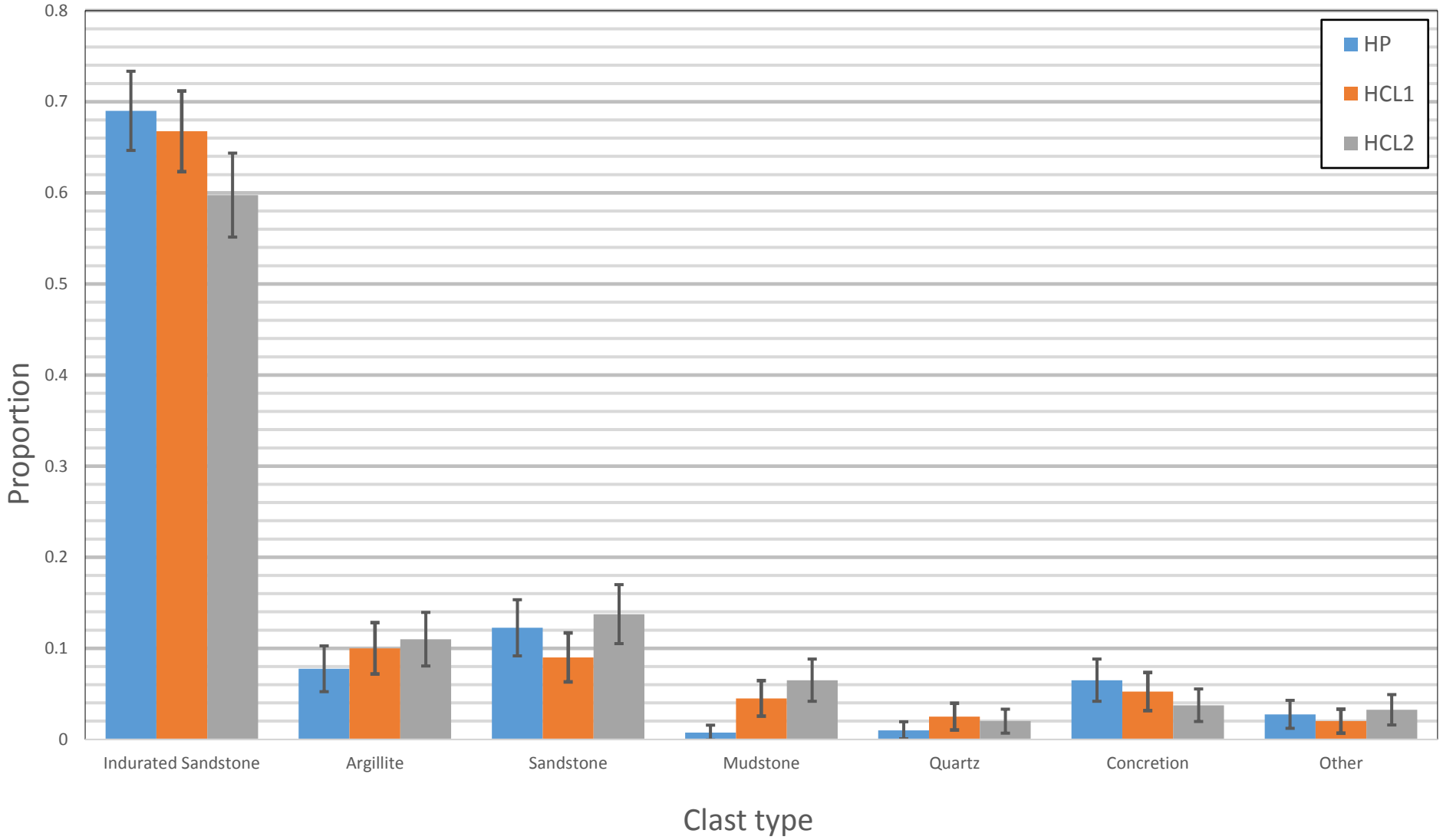

Figure 5.29: Comparison of main clast composition of Horewai Point (HP), and two Honeycomb Light (HCL1 and HCL2) conglomerates.

Comparison between Honeycomb Light conglomerates

There is no statistically significant difference in the proportion of total indurated material between the two Honeycomb Light sections at 99% confidence. There may be a statistically significant difference in the proportion of indurated sandstone between the two localities, though differentiation between indurated sandstone, argillite and less indurated sandstone is sometimes difficult and thus this has little interpretive value. This same reasoning applies to the difference between the ratios of non-indurated sandstone of the two beds, where it is statistically significant at the 95% level but not the 99% level. The presence of rare fine granular conglomeratic clasts in the younger Honeycomb Light bed and absence in the older bed is notable despite being too rare to prove there is a significant difference.

5.2.4: Mangakuri Conglomerate Clast Counts

Clasts were counted in two separate conglomerate beds in the coastal section between the Mangakuri and Kairakau settlements (BL39 355 694). These beds are relatively close stratigraphically (~20 m vertical separation) and are most likely Teratan in age based on nearby fossils. Both beds are poorly sorted pebbly sandstones, with most clasts being granules to small pebbles with occasional sandstone rafts 30 cm+ diameter (Figure 5.19c). Due to difficulty in identifying smaller clasts, only clasts larger than 1 cm in diameter were counted. Clasts vary in roundness, with smaller clasts being well-rounded to sub-rounded whereas larger clasts are angular. The smaller clasts tend to be dominantly indurated material such as argillite and indurated sandstone whereas the larger clasts are dominantly non-indurated sandstone that likely represent rafts and reworked Glenburn age equivalent sediment.

Table 5.3 summarises clast counts for Mangakuri Beach. “Other” includes reworked glaucony and basalt clasts that each represented <1% of total clasts.

Table 5.3 – Summary of clast counts, Mangakuri Beach

Clast lithology	Bed 1	Bed 2
Indurated Sandstone	130 (33%)	104 (26%)
Argillite	165 (41%)	181 (45%)
Sandstone	57 (14%)	43 (11%)
Mudstone	11 (3%)	1 (<1%)
Concretion	7 (2%)	1 (<1%
Quartz	14 (4%)	25 (6%)
Chert	9 (2%)	17 (4%)
Inoceramus fragment	5 (1%)	15 (4%)
Siderite	1 (<1%)	8 (2%)
Other	1 (<1%)	5 (1%)
Total	400	400

Crampton (1997) recorded ~37% total sandstone, 33-44% total mudstone and siltstone, 8-25% quartz and 6-8% fossil fragments in a Mangakuri Beach conglomerate. This is largely consistent with results from this survey, of 45% mudstone 42% sandstone. However, both quartz and fossil fragments were rarer in this study (5% and 3% respectively).

Argillite was the most common indurated clast type, comprising >40% of total clasts. Chert was a rare but conspicuous component of both beds. Most red chert clasts occurred as well rounded, 1-2 cm pebbles. However one larger (~7-8 cm across) angular clast was recovered from the second bed. This closely resembled several large cobbles and boulders present on the beach between Mangakuri and Kairakau, which were possibly sourced from Hinemahanga rocks.

At least one large, well-indurated clast within the formation contained relatively well-preserved inoceramid shells. However, due to the level of induration, determining the particular species was not possible.

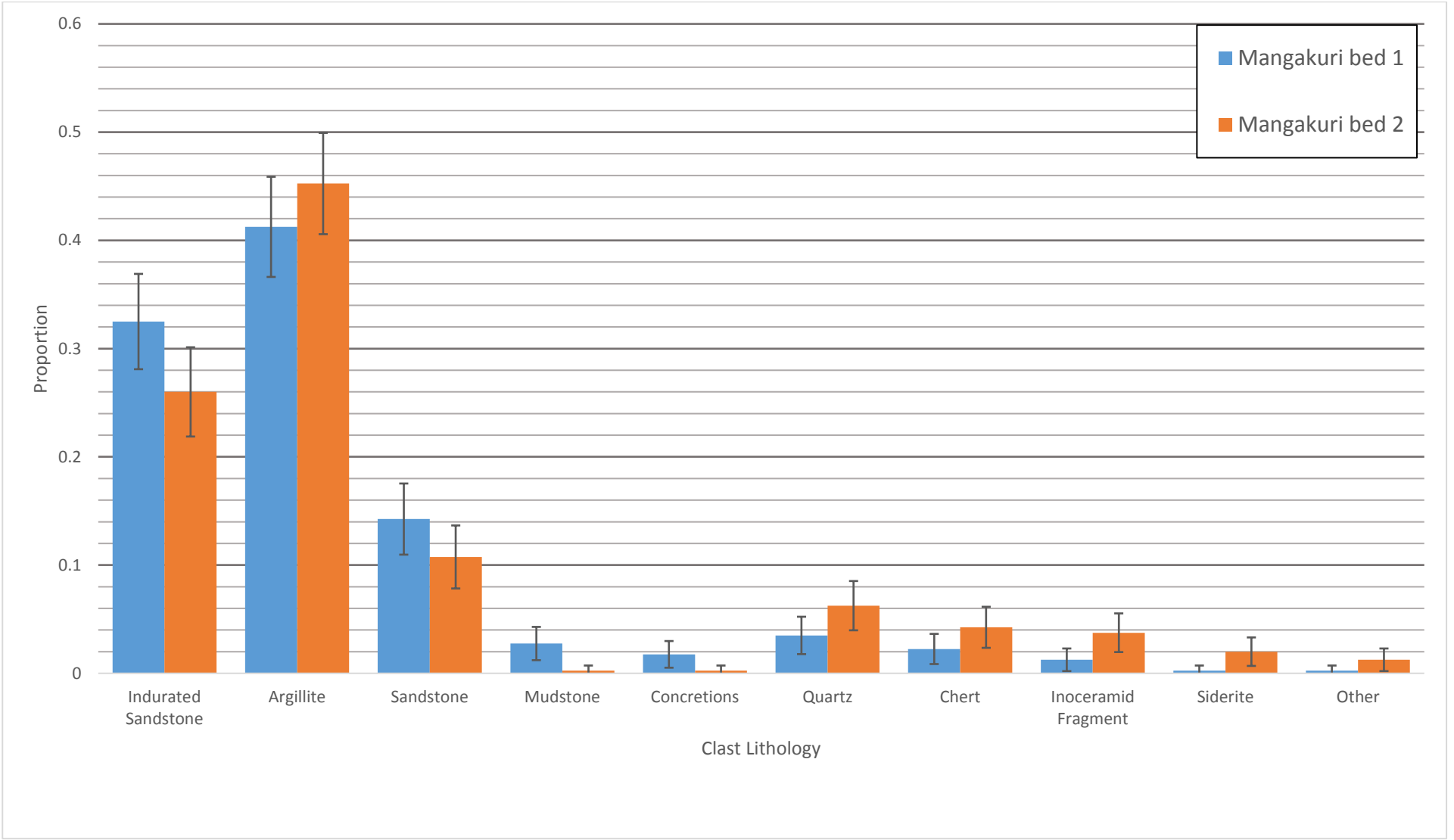

Figure 5.30: Comparison between older (bed 1) and younger (bed 2) conglomerates at Mangakuri Beach.

5.2.5: Comparison Between Clast Counts

When comparing the counts of clasts between field sites, significant differences are immediately noticeable (Figure 5.31). A few statistically significant conclusions can be drawn from this data:

- Glenburn coast conglomerates have a higher proportion of indurated sandstone than Mangakuri Beach or Totara Stream. Conversely, Mangakuri Beach conglomerates contain a much higher proportion of argillite. In the case of Totara Stream, the higher proportion of "locally derived" material (sandstone and mudstone) can explain a significant part of this. However, as illustrated by Figure 5.32, the differences between the ratios of indurated sandstone to argillite varies significantly by locality. This indicates a variation in provenance of the conglomerates.
- The Totara Stream conglomerates both have a significantly higher proportion of locally derived material than other localities. This may be due to inherent variability in rip-up clast concentration within beds, or may be due to variations in transport and depositional processes of the conglomerates. There is most likely an element of both of these factors involved. The abundant siderite cemented mudstone clasts in Totara Stream are also rare elsewhere. It is unclear whether they were siderite cemented prior to redeposition or whether this is a post-depositional feature. However, the absence of siderite in some of the rip-up clasts in Totara Stream may suggest the clasts were cemented prior to redeposition.
- There is little variation in the proportion of less-indurated sandstone between localities. However, these sandstones are often visually different. Glenburn coast less-indurated sandstone generally more closely resembles the more indurated varieties of sandstone whereas Totara Stream sandstone has Glenburn Formation-like lithologies, often with organic material inside that is lacking in clasts on the Glenburn coast.
- There is some variability among minor clast lithologies. Glenburn coast conglomerates have significantly more reworked concretions, whereas Mangakuri Beach conglomerates contain more quartz and inoceramid fragments. Due to the low proportion of the total count for these lithologies, the statistical significance is questionable.
- Although too rare to draw conclusions from, spillite and rhyolite were only found at Totara Stream, and chert is more common at Mangakuri Beach.

Perhaps the most interesting comparison is between Mangakuri Beach and the Teratan Totara Stream conglomerate. Because they were both deposited during the same geological stage, this provides a crude control for the variability in provenance over time. Figure 5.33 is a comparison of clasts that have statistically significant proportions. This figure shows that proportions of indurated sandstone, argillite, non-indurated sandstone and mudstone are all different with 99% confidence. Although the locally derived clasts may be due to variability within the bed, the different ratios of indurated sandstone to argillite suggests different provenance.

5.2.6: Discussion of Clast Counts

The conglomerate clast counts within the Glenburn Formation shows that at each locality studied, there are often significant differences in the bulk composition of clasts. This could be for several reasons:

- Variability in distance from source. Softer clasts, such as less indurated reworked sedimentary rocks, are more likely to be destroyed prior to deposition. The further clasts have to travel, the lower the expected proportion of softer material there should be (Howard, 1993).
- Clast composition may reflect the mass transport process involved. For example, a more energetic debris flow may contain more rip-up clasts and therefore a greater proportion of non-indurated clasts. Variability in locality derived material, such as in the two Totara Stream conglomerates, may simply be due to an uneven distribution of rip-up clasts within beds rather than variability between beds.
- Clast composition may reflect differences in the provenance. If Glenburn Formation was deposited from a single point source, the source material would be expected to be relatively constant between rocks of the same age. Provenance may change over time, so discerning whether there are multiple sources is not possible by comparing beds of different ages.

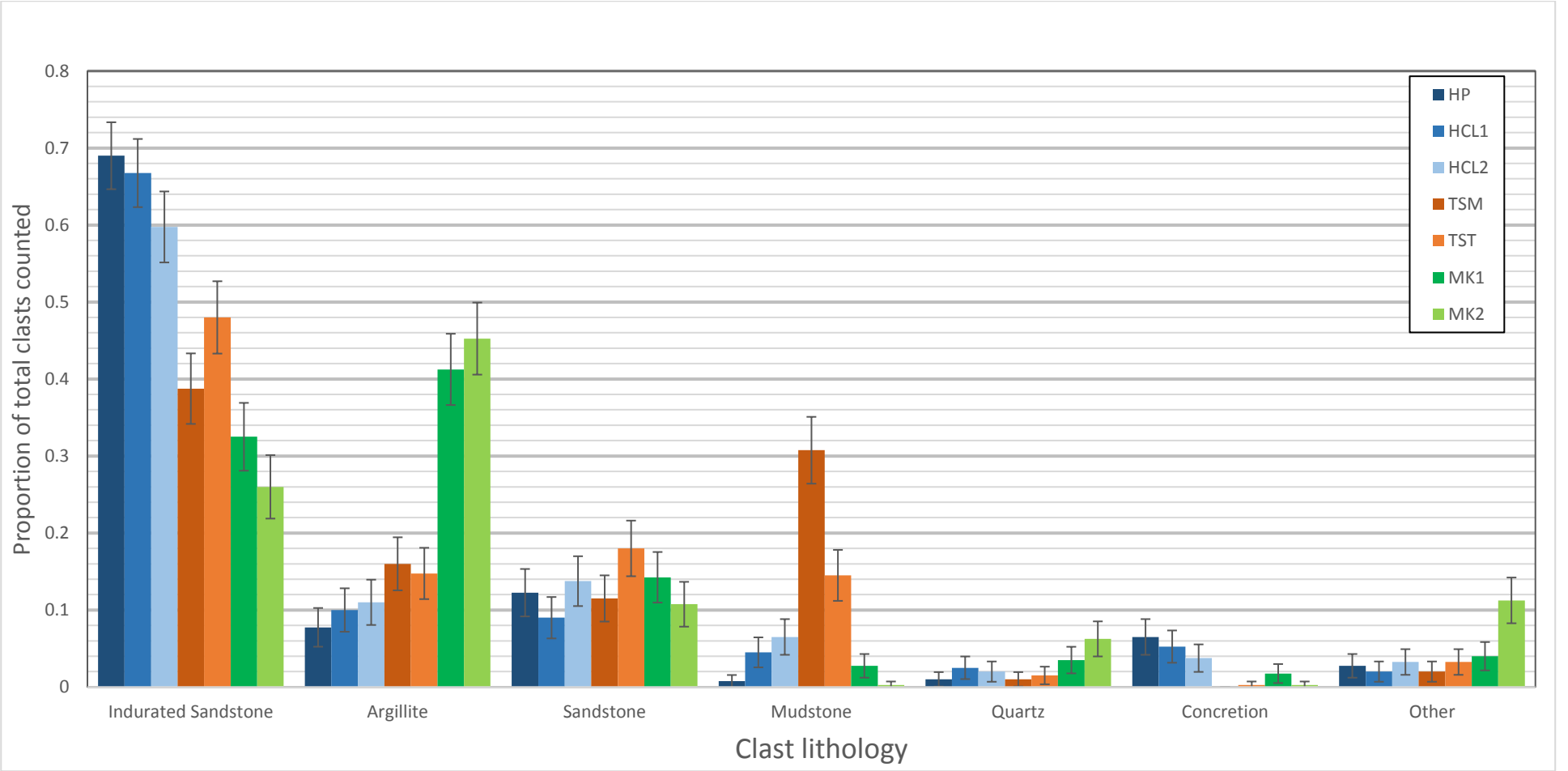

Figure 5.31: Comparison of clast counts for each locality, with error bars representing 99% comparative CIs. Mudstone includes siderite cemented mudstone clasts. Blue shades are Glenburn coast, orange shades are Totara Stream and green shades are Mangakuri Beach. HP = Horewai Point, HCL1 = Honeycomb Light (older) HCL2 = Honeycomb Light (younger), TSM = Totara Stream Mangaotanean, TST Totara Stream Teratan, MK1 = Mangakuri (older), MK2 = Mangakuri (younger).

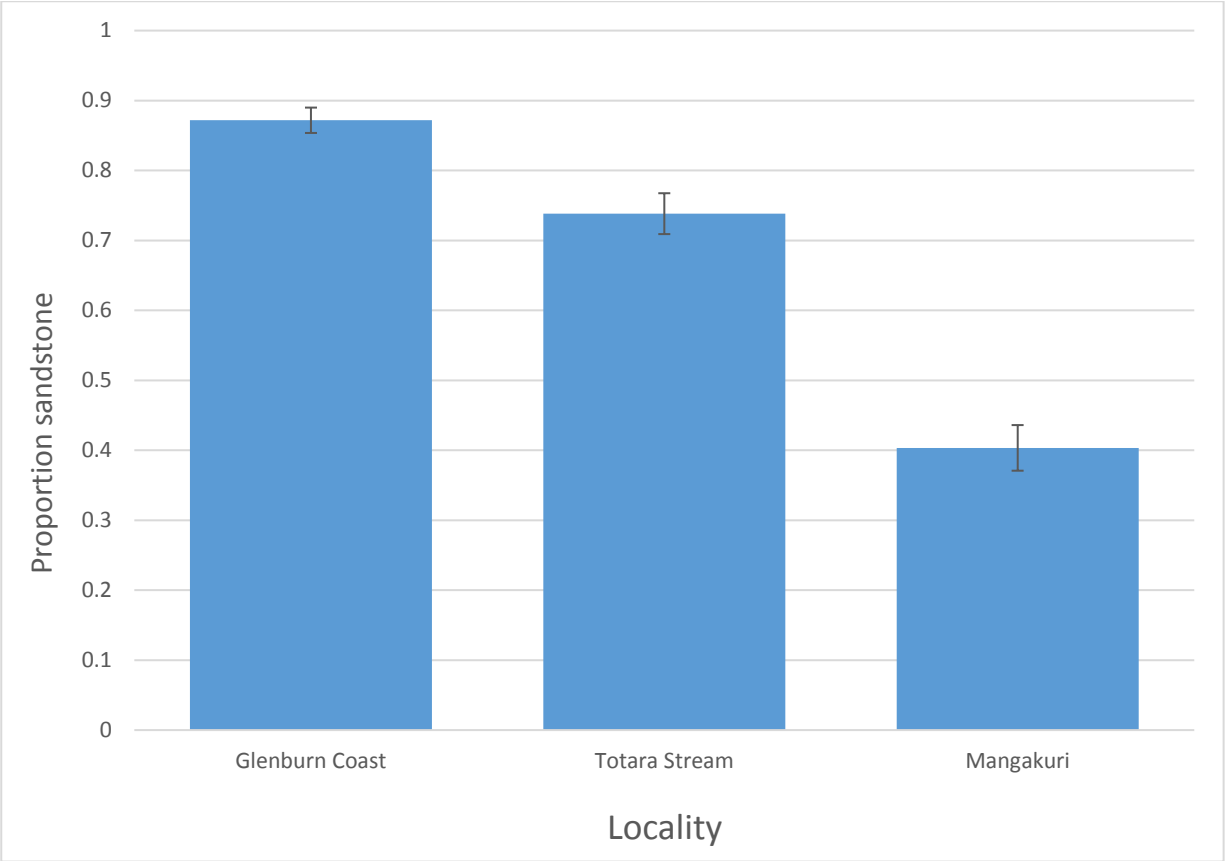

Figure 5.32: Proportion of indurated material that is sandstone by locality, used as a proxy for provenance differences.

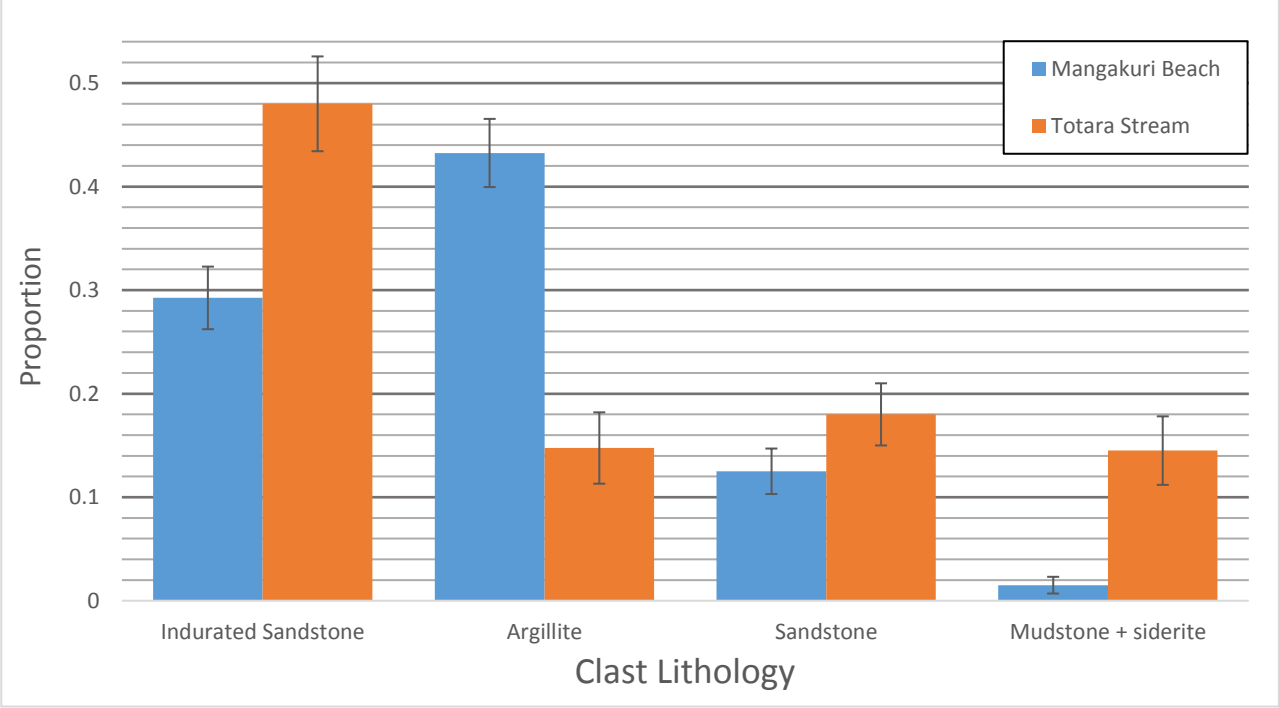

Figure 5.33: Comparison of Teratan aged conglomerates, which allows basic control for variability over time. Mangakuri Beach vs Totara Stream.

The latter explanation is preferred when comparing the ratio of argillite to indurated sandstone (e.g., ~60% argillite in Mangakuri compared to ~26% in Totara Stream). Both lithologies are very hard and thus equally likely to be preserved, and indurated material will not be "ripped up" by the debris flow as non-indurated mud may be. Given the approximately coeval depositional between Mangakuri Beach and Totara Stream conglomerates, the simplest explanation would be that the source rocks for the clasts were different and thus they were separate depositional systems. Although it is of tenuous statistical significance, the absence of rhyolite and spillite everywhere but in Totara Stream supports this.

Glenburn coast indurated sandstone clasts appear somewhat different to those at Totara Stream and especially Mangakuri. Many indurated sandstone clasts at Glenburn are very coarse-grained, whereas those at Mangakuri appear finer grained and more indurated. This also suggests different basement terranes being primary sources of material in these two locations. A more in depth study of conglomerate clasts may provide further information regarding this.

The simplest explanation for the variation in the proportion of mudstone/siderite clasts between locations is either a difference in erosional or depositional process. The majority of mudstone clasts appear to be rip-up clasts, the concentration of which varies significantly within beds in the Glenburn Formation. Mudstone rip-up clasts are extremely common in the Mangakuri area, especially within sandstone beds, yet less common in the two pebbly sandstones surveyed for the purpose of this study. On the other hand, Totara Stream conglomerates have a very high proportion of rip-up clasts compared to the other two sections. Although the concentration varies within beds, the much higher proportion of rip-up clasts in Totara Stream than elsewhere may suggest a greater component of erosion in the SGF responsible for depositing the conglomerate.

Another point of interest is the source of non-indurated sandstone clasts. These may be sourced either from the Glenburn Formation itself via reworking, or by a nearer-shore sandstone exposed to erosion. Large (>30 cm), highly angular rafts present in several beds are likely to have been sourced locally, probably from older Glenburn Formation, Springhill Formation, or an unknown coeval formation that is not currently exposed.

5.2.7: Section Summary

To summarise the findings of this section: significant variability in clast composition over space and time suggests provenance varied significantly for the Glenburn Formation. Temporal variability may suggest progressive erosion of different inland lithologies, whereas spatial variability gives strong evidence of multiple depositional systems feeding the Glenburn Formation. Further investigation into the chert clasts found at Mangakuri Beach may deduce whether these clasts were derived from Red Island/Hinemahanga Rocks or reworked from a different accreted ocean floor assemblage.

5.3: Additional Observations

5.3.1: Thickness of the Glenburn Formation

The total thickness of the Glenburn Formation is difficult to determine due to the complex Neogene deformation that has affected the outcrop distribution of the formation, combined with the lack of a complete, uninterrupted section. However, the section exposed at Motuwaireka Stream indicates a thickness of at least 1150 m, and does not represent the complete section, being restricted to the Mangaotanean to Piripauan stages based on fossils identified in this study. Extrapolating to the observed Whangai Formation contact north of Motuwaireka Stream (Moore, 1980), a thickness of 2 km+ is possible, although caution must be applied in assuming the thickness of stages between localities is constant. Additional uncertainty comes from the lack of constraint on intra-stage structural thickening or thinning.

In addition to the measured thicknesses in this study, a number of other studies have recorded thicknesses by stage for the Glenburn Formation, which are summarised in Table 5.4. Van den Heuvel (1960) mapped a combined total of 4900 ft (~1500 m) of Ngaterian to Piripauan sediment in one thrust wedge in the Flat Point area. Eade (1966) mapped a combined total thickness of Glenburn Formation of approximately 5,500 ft (1,676 m), including his Longbush and Tutu Formations that are now considered part of the Glenburn Formation. This was also measured in

the Glenburn/Flat Point region. In accordance with Van den Heuvel (1960), the post-Arowhanan sections measured are significantly thinner than those exposed in other sections further north.

The variability in sediment accumulation rates both within and between sections is immediately noticeable (Table 5.4). For example, despite the thick-bedded nature of Teratan aged sediment in Totara Stream (Appendix F; Crampton 1997), the total thickness mapped is only on the order of 200-250 m. In contrast, the Piripauan Stage is c. 1.1 Ma shorter than the Teratan Stage (Raine et al., 2015) and yet is represented by over 700 m of sediment. Such discrepancies could be due to large-scale erosion, sediment bypass, periods of non-deposition, or variations in the frequency of SGF events. Conversely, in the Flat Point area, Van den Heuvel (1960) mapped the Teratan Stage as ~450 m thick compared to ~150 m and ~120 m for the Mangaotanean and Piripauan stages respectively. The sharp contrast between field sites in Table 5.4 indicates the rates of accumulation within the depositional system of the Glenburn Formation was highly asymmetric both temporally and spatially.

Seismic transects of the Hawke's Bay region by Burgreen-Chan et al. (2016) suggest Glenburn Formation may be as thick as 6 km (Figure 2.2). This is beyond the highest estimate of thickness based on onshore outcrops. This is possibly due to the difficulty in distinguishing Torlesse from Glenburn Formation. Other potential factors include underestimation of the effect of tectonic shortening, or perhaps thickening of the Glenburn Formation offshore. Regardless, as acknowledged by Burgreen-Chan et al. (2016), little interpretive value can be given to this without a well-tie to corroborate seismic facies to.

Table 5.4 - Comparison of thicknesses of individual stages by location, showing the variability in sediment accumulation/preservation rate spatially and a minimum estimate of thickness.

Stage	Totara Stream (This study, Crampton 1997)	Motuwairekа Stream	Mataikona River (This study, Crampton (1997)	"Mt Adams Area" – Eade (1966)	"Flat Point area" Van den Heuvel (1959, 1960)
Rm	>120 m	>?600 m	>320 m	~450 m	~150 m
Rt	~210 m	~500 m	~375 m		~450 m
Mp	~725 m	>100 m	~225 m	~300 m	~120 m
Mh	?50 m	--	~280 m		--
Min est.	1105 m	1200 m	1200 m	~1650 m (including Cn-Ra)	~1500 m (including Cn-Ra)

5.3.2: Summary of Paleocurrent Data:

Despite the near-ubiquitous presence of unidirectional SGFs, paleocurrent directions for the Glenburn Formation are in many sections difficult to ascertain. Bedding surfaces are often not exposed or too heavily weathered to preserve anything useful. However, paleocurrent indicators, such as flute or groove casts and parting-current lineations are common enough to determine paleocurrents to a first order of accuracy. Due to the rarity of indicators in some sections, the summary diagram below combines this study's paleocurrent measurements with those of previous studies. For a list of individual paleocurrents used, refer to Appendix A. A summary of average paleocurrent directions, determined using circular statistics (Fisher, 1993), by age/locality is tabulated below (Table 5.5) and are represented on Figure 5.34.

Table 5.5 – Summary of paleocurrent directions by age/locality. Uses data from this study, Van den Heuvel (1959), Johnston (1980), Pettinga (1980) and Crampton (1997). ± Values given as one standard deviation, calculated using circular statistics as described in Kraus and Geijer (1987). [1]Described as roughly southeast flowing, no precise figure given. [2]Mangakuri Beach estimate based on channel geometry and cross-lamination but significant uncertainty due to tectonic effects.

Locality	Age	Number of measurements	Paleocurrent Direction
Glenburn area	Ngaterian	4	093° ± 7
Glenburn area	Raukumara Series	10	088° ± 23
Glenburn area	Piripauan	4	068° ± 6
Motuwaireka	Late Teratan – Piripauan	3	097° ± 7
Mataikona River	Mangaotanean-Piripauan	17	080° ± 28
Mataikona River	Haumurian	10	101° ± 17
"Tinui area"	?Raukumara	?	~135° [1]
Waimata River	Teratan	3	071° ± 4
Mangakuri	Piripauan	2	~90° [2]
Waimarama	Raukumara	60	109° ± 44

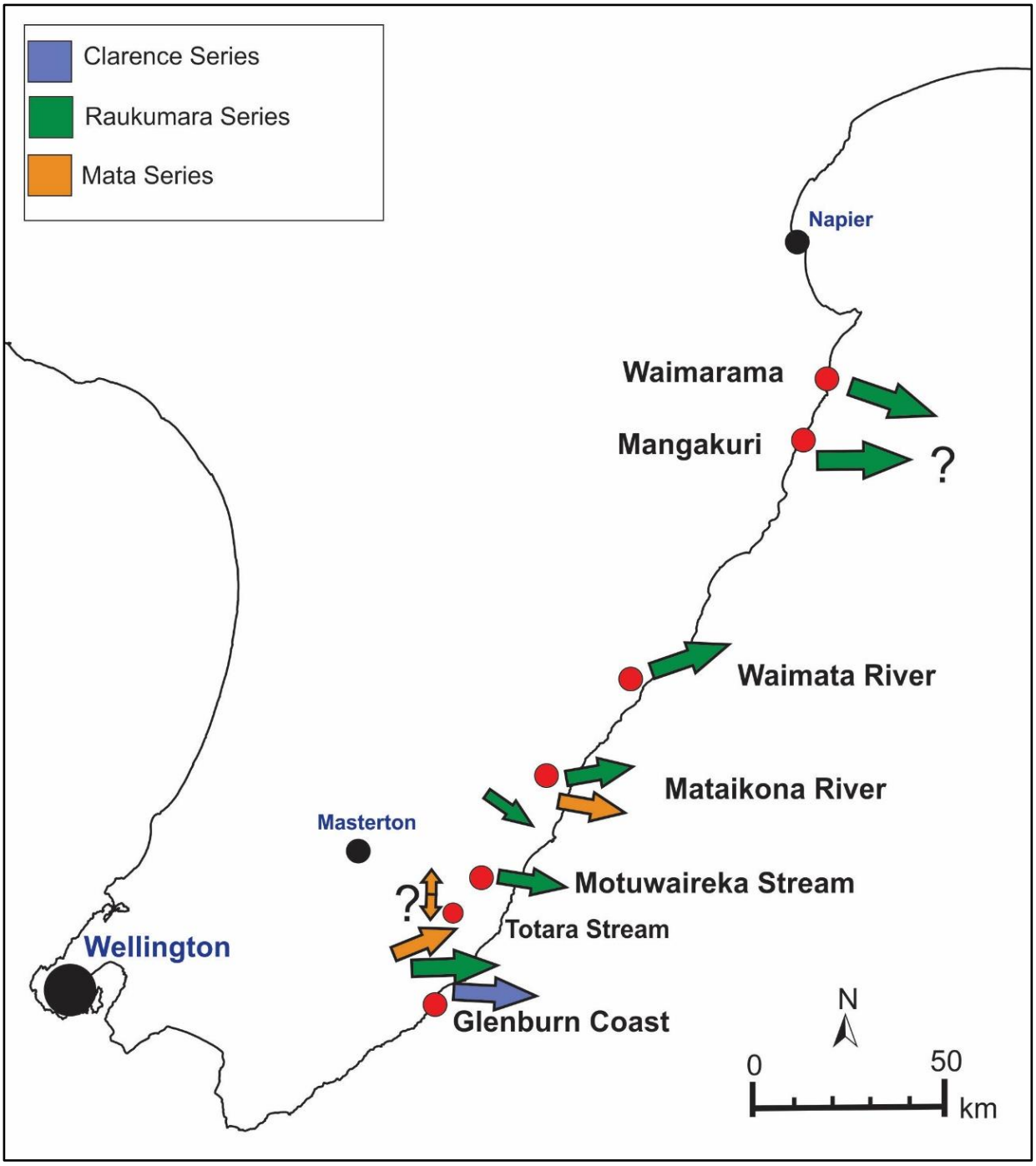

Figure 5.34: Synthesis of paleocurrent directions noted in the Glenburn Formation. Sourced from: This study, Van den Heuvel (1960), Johnston (1980), Pettinga (1980), Moore (1980) and Crampton (1997). Totara Stream paleocurrents from Moore (1980) were an outlier, indicating north-south flow. Waimarama and Mangakuri measurements somewhat suspect due to pervasive tectonics.

Paleocurrents are dominantly east-flowing in all localities, except for measurements in Totara Stream by Moore (1980) which were north-south. One explanation for this deviation would be if the paleocurrents were measured from levee/overbank deposits, where paleocurrent directions can differ significantly from the main channel (Pickering and Hiscott, 2015). There are some trends over time in the Glenburn area and the Mataikona River; however, these changes have questionable significance. The only discernible pattern in paleocurrents appears to be that they are nearly all east-flowing.

5.3.3: Gross Upsection Trend in Facies

Both the Mataikona and Motuwaireka sections show a distinct coarsening of facies from Mangaotanean through to Teratan times (Figure 5.35). In Motuwaireka Stream, this is represented by a change from siltstone (Class D) facies in the Mangaotanean Stage into sandstone-mudstone couplets and conglomerates (Facies Group C2 and Class A) facies in the Teratan Stage. In the Mataikona River, a Facies Class D dominated Mangaotanean succession is overlain by thick-bedded strata of Facies Classes B and C. A similar coarsening/thickening upward trend is seen in the Ngaterian-Arowhanan strata at Honeycomb Light (Appendix D). While there may be what appears to be small-scale (metre to tens of metre) trends in other sections such as Motuwaireka, Chen and Hiscott (1999) trends on such a small scale are generally not statistically significant and cannot be used to determine depositional environment.

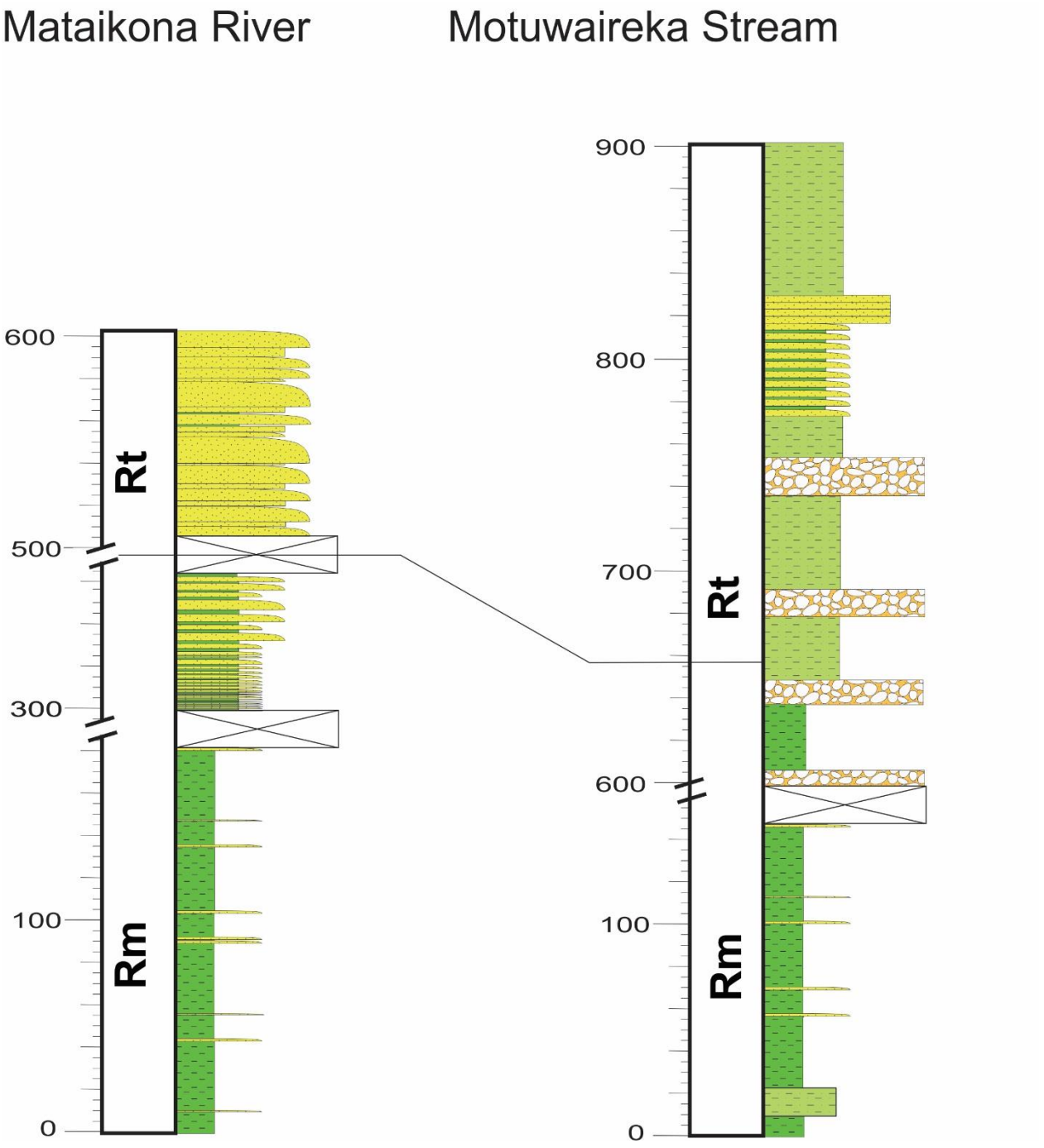

Figure 5.35: Composite measured section for the late Mangaotanean and Teratan in Mataikona River and Motuwaireka Stream, the two sections where a coarsening trend was noted for these stages. Bed thicknesses highly exaggerated. Generalised and some extrapolation used; refer to Appendices G and H for more in depth measured section. Mataikona River section supplemented with information from Crampton (1997), ~200 m of additional Mangaotanean Strata included which was not observed in this study.

5.3.4: Possible Subdivisions of the Glenburn Formation

Moore (1986) suggested Glenburn Formation may someday warrant elevation to group status. The lack of any clear lithostratigraphic divisions in strata makes subdividing the Glenburn Formation into multiple formations impractical. For example, the distinct thin-bedded upper Piripauan to lower Haumurian facies in Totara and Motuwaireka streams do not correlate well with similar aged strata in the Mataikona River. Instead, it is tentatively suggested that the highly jarositic, thin-bedded, organic-rich facies in the Mata Series of Totara and Motuwaireka streams may warrant elevation to member status. Further fieldwork is required to confirm the horizontal continuity of these facies. Similar facies were mapped by Lee (1995) in coeval strata in the Glenburn area, which were deposited on the same thrust wedge as those in Totara Stream (Lee and Begg, 2002). Until lateral continuity can be proven, it is proposed that these thin to medium-bedded, organically laminated, distinctly orange (jarosite/siderite weathered; Moore, 1980; Crampton 1997) weathered beds be assigned as a lithofacies. Because Totara Stream contains the best-exposed outcrops of this, the "Totara Lithofacies" is proposed as a potential name.

Siltstone dominated successions of Mangaotanean age exposed at the Mataikona River and Motuwaireka may also warrant designation as a distinct member. Thick siltstone units were not observed in any strata younger than Mangaotanean, although the Ngaterian section at Glenburn coast was similarly siltstone-dominated. If further mapping finds a similar abundance of fine-grained deposits in the Mangaotanean Glenburn Formation, this could also be designated as a member. A lithofacies designation is again suggested for the time being. The best exposed example of this lithofacies is at Mataikona River, so the "Mataikona Lithofacies" is proposed as a potential name.

Chapter 6: Depositional Environment Interpretation

6.1: Depositional Environments of Submarine Gravity Flow Dominated Successions

SGF deposits, including the turbidites and debris flow deposits that constitute the majority of the Glenburn Formation, can be deposited in several different environments. In the marine realm, they are typically associated with deep marine fan systems, although very similar systems may be found in shallow marine environments (Mutti et al., 2007). SGF deposits also occur in lacustrine environments (e.g., Moernaut et al., 2014), though the abundant occurance of marine fossils such as inoceramids discounts this possibility as a depositional environment for the Glenburn Formation. Distinguishing between deep marine and shallow marine SGF dominated successions can be difficult and requires paleodepth analysis as well as careful geological mapping and facies analysis (Mutti et al., 2007).

This study adopts the definition of "deep marine" used by Pickering et al. (1989), defining it as ocean beyond the continental shelf break. This generally means depths of greater than 100-200 m, and thus is usually below storm wave base. Sediment may be deposited in this environment by a variety of different processes, such as through SGFs, bottom currents, pelagic sedimentation, and biogenic sedimentation.

Facies analysis of measured sections of the Glenburn Formation discussed in Chapter 5 are all consistent with a submarine fan depositional environment, for the reasons discussed in the following sections.

6.2: General Depositional Setting of the Glenburn Formation

6.2.1: Paleodepth

Because this study did not conduct any detailed analysis of paleodepth, determining the paleodepth for the Glenburn Formation requires an examination of wider published literature. Facies patterns observed for the Glenburn Formation could represent either shallow or deep

marine deposits (Mutti et al., 2007). Previous studies have suggested various paleodepths for the Glenburn Formation. Moore (1980) inferred shallow neritic depths for the Glenburn Formation in the Ngahape area. Laird et al. (2003) inferred that upper Glenburn Formation was deposited above wave base. Lee (1995) divided the Glenburn Formation into a lower and upper unit in the Huatokitoki Stream. She concluded that the lower (Ngaterian to Mangaotanean) unit was deposited in a submarine fan, possibly on a basin plain, and that the upper (Teratan to Piripauan) unit was deposited in shallow water. Pettinga (1980), Neef (1992, 1995) and Crampton (1997) inferred deposition in a submarine fan at bathyal depths. Crampton (1997) suggests that there may also be shallowing upsection. The findings in this study support deposition having occurred below wave base. The following paragraphs describe evidence for this conclusion.

Glenburn Formation in parts is overlain conformably by the Whangai Formation, which is most likely at least lower neritic in depth if not deeper (Section 2.1.4). Unless there was a major subsidence event at the transition from Glenburn to Whangai formation, this suggests the upper Glenburn Formation was deposited in similar depths. This provides evidence for deposition in bathyal or greater depths, although the paleodepth of the Whangai Formation is still a matter of some contention.

Moore (1980) inferred a shallow water, shelf or marine delta environment for the deposition of the Glenburn Formation, based on abundance of conglomeratic facies and parallel-laminated carbonaceous sandstone. Lee (1995) used similar reasoning to infer a shallow depth for the upper Glenburn Formation. She cited abundant cross-bedding, plant material and laminated fine sandstone beds as evidence of shallow water. However, none of these characteristics are exclusive to shallow marine environments and cannot be used to infer paleodepth (Pickering and Hiscott, 2015).

Additionally, Moore (1980) inferred that Te Mai Formation (upper Glenburn Formation) was deposited in a tidal setting based on the presence of ripple cross-lamination, flaser-bedding and lenticular beds. These features certainly are typically associated with tidal flats and subtidal environments (Boggs, 2006), but may also be formed by contour currents in a deep marine setting (Rebesco et al., 2014, Martín–Chivelet et al., 2008). Shanmugam et al. (1993) emphasises that what he interpreted as contourites closely resemble tidal and shallow marine environments and that the association of stratigraphically nearby sediments is important for distinguishing between the two. However, the nature of the deposits of contour currents is still a matter of significant contention and some dispute the conclusions of the above authors (Pickering and Hiscott, 2015).

If the Glenburn Formation was deposited in shallow water above storm wave base, wave modified features such as hummocky cross-stratification should be common. Laird et al. (2003) noted, of the Glenburn Formation in the Tora (BR34 080 994) area, one possible horizon of hummocky-cross stratification in a sandstone bed.

Contrary to this, neither this study nor Crampton (1997) identified any hummocky cross-stratification in Glenburn Formation facies. Some authors have suggested sedimentary features similar to hummocky cross-stratification may be produced in deep turbiditic submarine environments (Mulder et al., 2009), which might mean false positive identification. This is however still an issue of contention and other authors suggest hummocky cross-stratification is only possible due to storm waves (Higgs, 2011). This study did not visit Tora, however, so the presence of localised hummocky cross-stratification cannot be completely discounted. Collier (2015) also undertook a measured section of Glenburn Formation at Tora and did not note the presence of any hummocky cross-stratification. If present, this would support suggestions of shallowing upsection. Alternatively, Cretaceous strata exposed at Tora may instead be a nearer-shore equivalent of the Glenburn Formation that is not exposed elsewhere; without stratigraphic continuity, this is difficult to deduce. Regardless, the complete absence of hummocky cross-stratification in any section visited in this study is strong evidence that the majority of the Glenburn Formation was deposited below wave base.

The only other evidence of a shallow water environment for the Glenburn Formation is the preliminary palynofacies in uppermost Glenburn Formation in Totara Stream recorded in Crampton (1997), which “may” suggest upper neritic depth. Further investigation would be needed to verify this suggestion. Conversely, other palynofacies from Totara Stream, Mangakuri and Waimarama consistently suggested lower neritic or greater depths (Crampton 1997). Leckie (1995) suggested bathyal depths or greater for uppermost Glenburn Formation in Angora Stream (BM37 953 171). Considering SGFs redeposit sediment from shallower depths, it is possible the shallow water indicators may have been reworked.

Another issue with the inference that Glenburn Formation was deposited in a shallow environment is that it raises questions as to where the largely coeval Tangaruhe Formation was deposited. Paleocurrent directions dominantly indicate a western origin for sediments within the Glenburn Formation (Section 5.3.2), and the Tangaruhe Formation was deposited a significant distance westward of the Glenburn Formation during the early Mata Series (Crampton, 1997). The Tangaruhe Formation was most likely deposited in bathyal or greater depths (see Section 2.1.3).

Considering the Glenburn Formation was deposited outboard of the Tangaruhe Formation, a slope or greater depth is likely for the Glenburn Formation as well unless there was a corresponding significant topographic rise offshore of the WSB.

Because of the uncertainties highlighted above, there is insufficient evidence to support the suggestion that the uppermost Glenburn Formation was deposited above storm wave base. This suggestion cannot be entirely discounted, however, and it is possible localised sections of Glenburn Formation, such as the section at Tora measured by Laird et al. (2003), were deposited in a shallow environment. Based on the evidence above, a bathyal or greater depth is inferred for the bulk of Glenburn Formation.

6.2.2: Submarine fan or sheet system?

Deep marine SGF successions are generally deposited either in a submarine fan environment or as part of a "sheet-like" system (Pickering and Hiscott, 2015). Differentiation between the two systems may be difficult in some circumstances, but key differences suggest that at least the majority of the Glenburn Formation was deposited in a submarine fan. Evidence for this interpretation is discussed below.

Pickering and Hiscott (2015) list a number of identifying features for basin-floor sheet systems. These systems contain strata of Facies Classes B, C, D and E, but are predominantly fine-grained and thin-bedded. Conglomerate beds (Facies Class A) typically are not present in these systems. Beds are laterally extensive, lack channelised features and tend to contain a relatively high proportion of pelagites and hemipelagites. Differentiation between basin floor sheets and fan lobe fringe deposits is not always possible, and may require consideration of the overall stratigraphic framework of a succession.

Submarine fan systems are recognised by a number of key characteristics. Fans typically consist of distinct sub-environments: channels, levee/overbank deposits and lobes. Canyon-fill successions are also commonly associated with submarine fans. Distinguishing between these sub-environments requires at times detailed analysis of facies associations and bed geometry. The overall thickening/coarsening upward trend, abundance of conglomerates, rapid vertical facies variations and common channelised bed geometry is, however, strong evidence that the Glenburn

Formation was deposited in a submarine fan environment (Pickering and Hiscott, 2015). Hence, the facies based depositional model presented below focusses on the facies associations within a submarine fan to try to discern the fan sub-environments of different sections of Glenburn Formation.

6.3: Submarine Fan Generalised Facies Model

This section outlines the facies associated with different elements of a submarine fan setting. Modern research has shown that "one-size-fits-all" models of facies distributions within deep marine systems are untenable. Regardless, there have been many published facies-based studies on both modern and ancient fan systems. A very well documented example of a submarine fan succession in New Zealand is the Miocene Mount Messenger Formation in Taranaki (King et al., 2007). Pickering and Hiscott (2015) contains an extensive synopsis of many of these case studies, and interpretations herein are based on their generalised summaries of the available literature. Individual facies may be deposited in several different environments, but some general trends for deep marine deposits as summarised by Pickering and Hiscott (2015) are outlined below:

- Conglomerates (Facies Class A) are generally restricted to submarine canyons, channels and valleys. Conglomerates may be deposited by large slope sediment slides, although these usually consist entirely of intraformational clasts (Pickering and Corregidor, 2005).
- Submarine canyon deposits can be difficult to recognise in outcrop and identification requires good lateral and vertical continuity of outcrop. Facies are generally coarse-grained (A and B) but may have significant components of Facies Classes C, D and E. Sand grade beds are usually either structureless or parallel-stratified, and sandstone-mudstone couplets are not usually a significant component. Conglomerate beds may show cross-beds or "dunes" of gravel grade material (Ito and Saito, 2006). Positive identification of a canyon usually requires observation of a distinct canyon wall.
- Submarine channels may occur as part of channel-levee systems in the upper fan, or as channels within a lobe system. Channel-fill successions commonly contain a variety of facies. An erosional base that cuts into finer-grained, non-channelised deposits is diagnostic but may be difficult to recognise in limited exposure outcrops. Channels commonly show a gross thinning and fining upward trend. As well as Facies Class A

conglomerates, channel-fill successions generally contain abundant sandstones usually of Facies Class B as well as sandstone-mudstone couplets of Facies Class C. Channel-fill succession are often associated with levees, outlined below. Channels are often stacked with lateral offset (Figure 6.1). Channel geometry varies immensely; they are typically between 10 to 1000 m deep, 0.1 to 50 km wide, and 10 to 3000 km long (Stow and Mayall, 2000).

- Levee or overbank deposits are typically thin-bedded SGFs. Beds are mostly rhythmic silty turbidites around 1-5 cm thick with occasional thicker medium to fine-grained sandstone beds. Facies class C, D and E may each be present. These successions will generally pinch out of several hundred metres, although this is generally not noticeable in outcrop.
- Submarine lobe systems comprise the majority of the sediment volume of submarine fan systems. They can be broadly divided into three sub-environments: lobes, lobe fringes and fan fringes (Figure 6.2).
    - Beds within the main lobe are typically medium- to very thick-bedded and comprised primarily of very coarse- to medium-grained sandstone. Mudstone generally makes up <20% of all sediment. Shallow, wide channels with conglomeratic fill may also be present. Sandstones beds are often amalgamated, and some beds are graded turbidites with T_{abc} Bouma divisions. Facies Classes B, C and occasionally D are represented.
    - Lobe fringes are typically medium to thin-bedded SGF deposits, comprised of fine-grained sandstone and siltstone. Bouma divisions T_{bcde} may all be present. Bedding is generally quite regular, both vertically and laterally, with only subtle trends vertically if any. Strata are mostly Facies Classes C and D.
    - Fan fringe represents the most distal part of the fan system. Beds are thin to very thin, comprising very fine sandstone to siltstone or claystone. Sandstone makes up <40% of total sediment, and amalgamation of sandstones is entirely absent. T_b to T_e Bouma divisions are common in turbidites. Facies Classes C, D and E may all be present.

As the descriptions above summarise, individual facies associations in isolation may have ambiguous depositional environments. The conclusions drawn herein are therefore based on consideration of vertical and lateral facies associations and the wider context of each measured section. Despite poor three-dimensional understanding of bed geometry and large gaps in

outcrop, analysis shows that several different submarine fan sub-environments are present within the Glenburn Formation. These environments include channel fills, levee/overbank deposits, lobe deposits, lobe fringe deposits and probable fan fringe deposits. A canyon fill may also be present in the Mangakuri area. Despite the limitations of generalised models, in most cases the paleogeographic inferences are thought to be robust and largely in line with those summarised in Pickering and Hiscott (2015). A figure summarising these trends is included below (Figure 6.2).

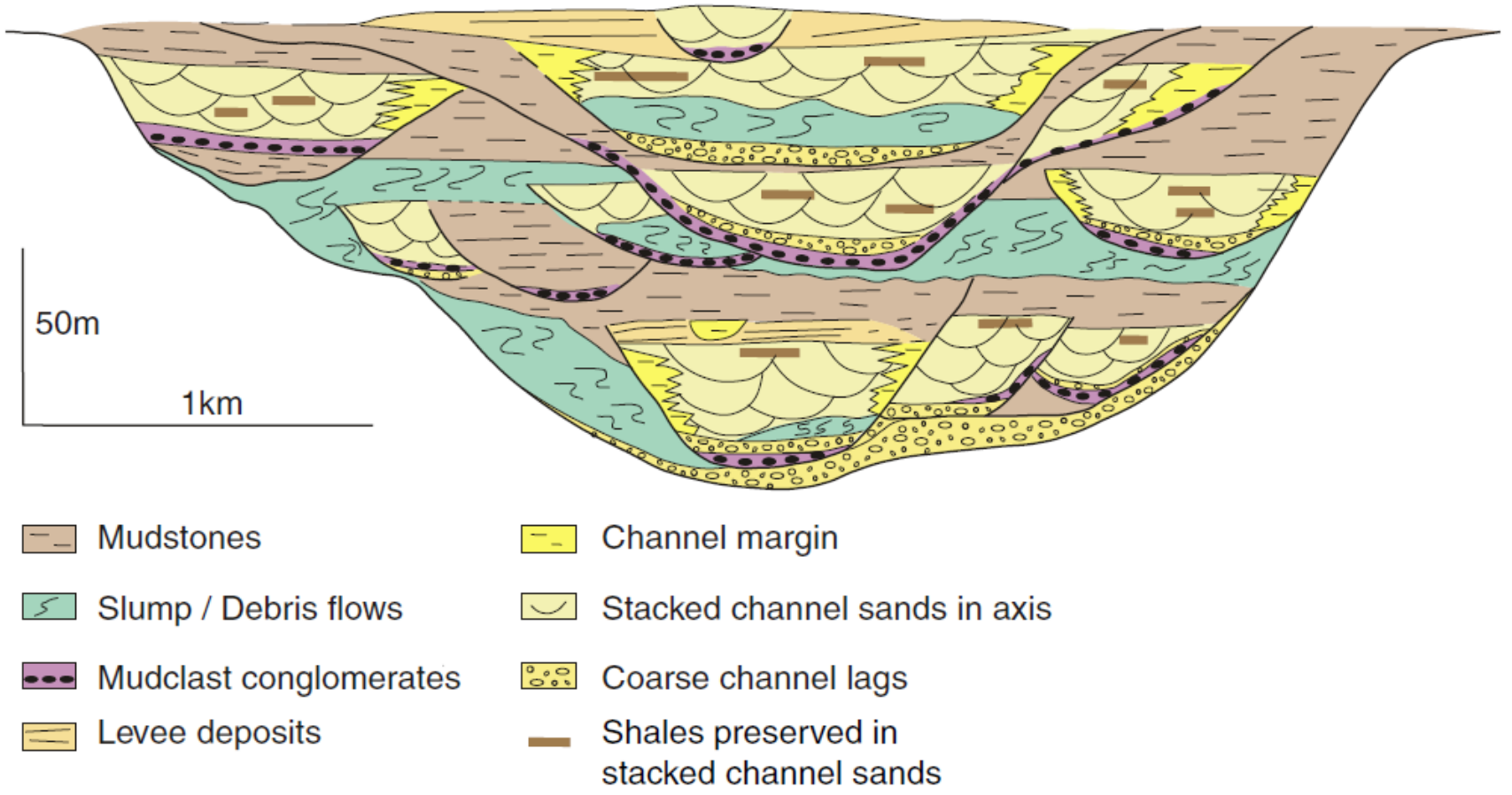

Figure 6.1: One example of a stacked channel model, showing horizontal offset of channels. Based primarily on seismic data from West Africa. From Mayall et al. (2006), their Figure 23.

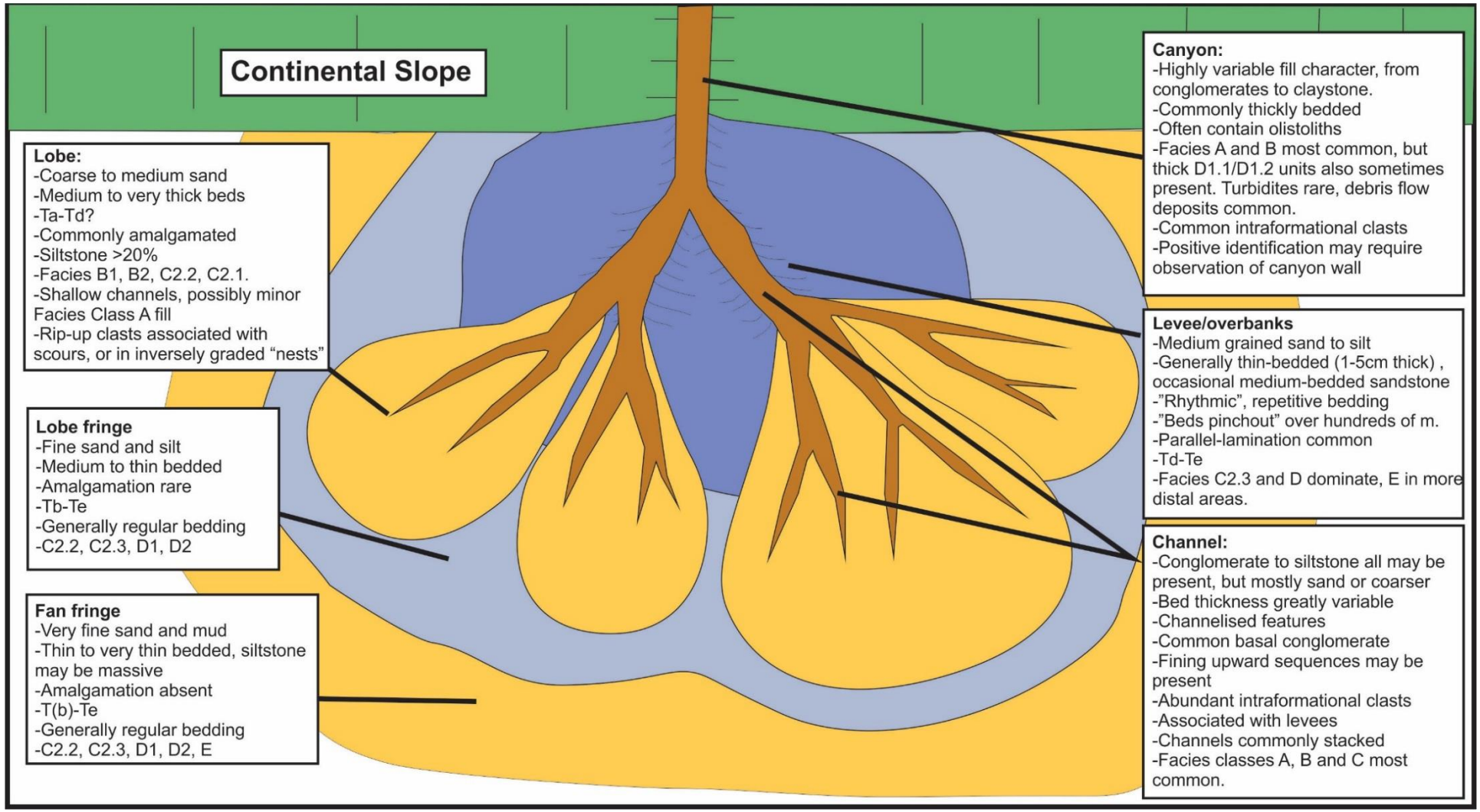

Figure 6.2: Generalised fan facies model, based on descriptions from Pickering and Hiscott (2015) and papers cited within.

6.4: Depositional Sub-environments of Field Sites

The following section considers the facies observed within the Glenburn Formation and compares findings with the descriptions of separate fan elements from Pickering and Hiscott (2015) and the references therein, as summarised in Section 6.3 and in Figure 6.2. Because of temporal and spatial similarities, some separate sections are considered together.

6.4.1: Glenburn Coast Interpretation

Honeycomb Light and Horewai Point (Appendix D and E) are the oldest sections of Glenburn Formation included in the study. The facies described in Chapter 5 are most consistent with the incisions of a channel into distal fan-fringe deposits due to lobe progradation.

Lowermost strata in both sections are primarily Facies Class D, with occasional Facies Class E and Facies C2.3 units. Facies D2 is interpreted as the deposits of distal turbidites (Figure 4.18), whereas the beds of Facies D1.1 (Figure 4.16) were probably deposited by muddy cohesive flows (Table 4.1). The low proportion of mottled siltstone (Facies D1.2) indicates sediment was primarily deposited by SGFs, and pelagic sedimentation was only a minor component. Thin Facies C2.3 beds are the result of larger turbidity currents than Facies D2 turbidites. All of these facies match the description of a fan fringe, but may also be the deposits in a "sheet system" rather than a canyon fed fan (Pickering and Hiscott, 2015).

At Honeycomb Light, a coarsening-up sequence is well preserved through the Ngaterian Stage (Appendix D, ~25 m to 81 m). Upsection, strata become dominantly Facies C2.1, C2.2 and C2.3 sandstone-mudstone couplets (Figure 5.3a). Amalgamation of sandstones is absent, and facies are generally fine-grained sandstone and siltstone. Bouma divisions of T_b to T_d are present. These facies associations match closely the description of a lobe-fringe setting as summarised in Figure 6.2. Therefore, it is inferred that this succession represents the progradation or migration of a submarine lobe, either onto a distal fan fringe or onto sediments deposited as part of a sheet system. At Horewai Point, this coarsening-up is not preserved.

Both of the sections contains a thick conglomerate (Facies A1.1) just below the Ngaterian-Arowhanan boundary (Figure 4.6 and Figure 5.5c; Appendix D, 81–84 m; Appendix E, 36–49 m). The inclusion of sandstone rafts indicate the debris flow was erosive upstream (Figure 5.5c). The well rounded cobbles of extrabasinal indurated material is consistent with a basal channel deposit (Pickering and Hiscott, 2015). Schiøler and Crampton (2014) inferred that there is an unconformity representing at least 400,000 years of missing time associated with this conglomerate at Horewai Point. An erosional channel could explain why this unconformity exists, and an undulating lower contact provides evidence of erosion below the conglomerate bed. The lack of a coarsening-up sequence underlying this conglomerate at Horewai Point may be because this channel eroded those sandstone beds there but not at Honeycomb Light, a hypothesis supported by the greater thickness of conglomerate at Horewai Point that could indicate closer proximity to the channel axis. Because submarine channels commonly have very high width to depth ratios, and may be up to several kilometres in width (Stow and Mayall, 2000), the lack of obvious channel geometry in outcrop does not contradict this hypothesis.

Strata above the conglomerates are inferred to be channel-fill deposits. Common occurrence of Facies B2 parallel laminated sandstone (Figure 5.4, Figure 5.5b) and additional conglomerate beds (Figure 5.2b) are consistent with being channel fill descriptions, as is the general fining upward trend at Horewai Point (72 m and above). Crampton (1997) notes common occurrence of channelised sandstones on the Glenburn coast, which is consistent with this finding.

Uppermost facies at Horewai Point (100-150 m) tend to be thinner-bedded than those immediately above the oldest conglomerate, comprising of interbedded graded siltstones and sandstones (Figure 4.14c). As described in section 6.3, thin-bedded, fine-grained facies such as this are typical of overbank deposits or lobe fringes. Because these thin-bedded facies overlie inferred channel fill, it is inferred that these thin-bedded strata are levee/overbank deposits formed following lateral migration of the channels.

To summarise, Glenburn Formation at the Glenburn coast represents either a fan-fringe or a basin floor sheet system at the base of the section, which was overlain by lobe-fringe and then channel and channel-levee deposits. This succession of settings is inferred to reflect either the migration of a lobe or the progradation of a fan system. A small unconformity at Horewai Point indicates significant amounts of sediment may have been eroded from underneath the thick, channel-fill conglomerate mapped. Erosion and removal of transitional facies by a large channel might help explain the apparently rapid transition from fan-fringe/basin floor deposits into coarse, thick-

bedded facies. A channel-fill sequence is overlain by overbank deposits at Horewai Point, indicating that the channel migrated away from the site of deposition by the top of the section.

6.4.2: Totara Stream / Motuwaireka Stream

The sections at Totara and Motuwaireka streams are contained within the same thrust wedge (Lee and Begg, 2002) and reconnaissance mapping by Moore (1980) found only minor thrust faults between the two sections. Because of their similar location and ages, it is assumed they were in similar proximity to one another when deposited as they are now. Hence, they are interpreted together.

The Motuwaireka Stream section contains a significantly thicker Mangaotanean section than is exposed at Totara Stream. Lowermost facies are dominantly siltstone and sandstone beds that are mostly graded. Peculiar, isolated Facies A1.2 conglomerate beds within dm-bedded mudstone and fine sandstone beds (Figure 5.11, 610 to 665 m) are difficult to explain, but may be evidence of mud filled channels, such as those described by Mayall et al. (2006; Figure 6.1). Regardless, Teratan aged facies above this such as at 689 – 698 m and 832 – 847 m are medium-bedded, fine-grained, occasionally amalgamated sandstones (Facies C2.2 or B2; Figure 5.10b) interbedded with graded conglomerates (Figure 4.9), consistent with channel fill as described by Pickering and Hiscott (2015). Common thin-bedded turbidites (Facies C2.3) throughout the Teratan- to Piripauan-aged section (common from 665 m onwards) of Motuwaireka Stream may be either channel fill or levee/overbank deposits (Figure 5.10c). The abundance of rip-up clasts in conglomerates shows a component of erosion.

Correlative Totara Stream strata (late Mangaotanean to Teratan) contain a variety of facies. Interbedded sandstone and siltstone are common, such as between 0 and 5 m (Facies C2.2; Figure 5.7a), as are cross-laminated silty sandstone such as those between 11 and 18 m (Facies C2.4; Figure 4.15), and graded conglomerate such as those between 354 and 361 m (Facies A2.1, A1.2, Figure 5.8). Minor amounts of massive sandstone (Facies B1) and siltstone (Facies D1) are located throughout. The abundant conglomeratic facies with high proportions of rip-up clasts and amalgamated sandstones (e.g., Appendix F, 100-104 m) are consistent with deposition in a channel or a series of stacked channels. The fact that the Totara Stream Teratan section is significantly thinner than the overlying Piripauan section despite being thicker-bedded (Table 5.4)

may suggest erosion of strata at Totara Stream, which would support the channel-fill interpretation.

Uppermost (Piripauan) strata observed in both Totara Stream (817 m onwards) and Motuwaireka Stream (1100 m onwards) are generally fine-grained, thin-bedded Facies C2.3 deposits with abundant parallel and some cross-lamination (Figure 5.9, Figure 5.10c). Occasional medium-grained and moderately thick sandstone beds are also present (Figure 5.7c). These are a very close match to the facies model description of overbank deposits. This overbank interpretation is supported by the presence of an underlying, thick inferred channel-fill sequence. It is inferred that this transition to overbank deposits is due to the migration of the feeding channel.

Moore (1980), who mapped the Ngahape area more extensively than this study, noted how late-Piripauan and younger strata almost entirely lacked conglomerate. The sections in this study are consistent with this finding. This could mean the migration of the main channel system laterally away from the area, meaning the only sediment being deposited were levee/overbank deposits.

To summarise, sections from Totara and Motuwaireka streams show evidence of a thick channel-fill and levee/overbank sequence. Oldest strata at Motuwaireka Stream have a somewhat ambiguous depositional environment, but the mudstone-dominated facies are consistent with either a fan fringe or a distal mud-rich overbank or interchannel setting (Pickering and Hiscott, 2015). Considering the channel-fill sequence interpreted above, the latter interpretation may be more plausible.

6.4.3: Mataikona River

Lowermost facies at Mataikona River are siltstone dominated strata of Facies D1.1 and D1.2 with occasional sandy turbidite deposits of Facies C2.3 and C2.2 (Figure 5.12a). Graded sandstone beds are thin to medium-bedded, with Bouma divisions T_{bcde}. Mottling is present but not common. Because lowermost strata are comprised of <20%, sandstone these are most consistent with fan-fringe deposits as described in Figure 6.2. Upsection (98 - 120 m), sandstone beds are generally thicker, fine-grained, medium-bedded, Facies C2.2 to C2.1 sandstone-mudstone couplets, which are consistent with being lobe fringe deposits (Figure 4.14a, Figure 5.12c). Above 375 m, facies are dominantly amalgamated Facies B1 and C2.1, very coarse to fine sandstones with only a minor siltstone component (Figure 5.13a, c; Figure 4.11a). These facies strongly match the descriptions of

inner lobe deposits in Figure 6.2. Strata observed above 665 m are all relatively consistent with being lobe deposits. A 50 m thick, 1 m- to 5 m-bedded conglomerate mapped by Crampton (1997) probably represents a channel fill, based on the context of the sediment below and channel fill descriptions in Figure 6.2.

The section in the Mataikona River is interpreted to represent the progradation or migration of a submarine fan lobe. Potential channel deposits in the uppermost part of the section overlying lobe deposits would suggest progradation of the fan system.

6.4.4: Waimata River

Outcrop was poor in Waimata River, but all beds observed were Facies C2.1 to C2.3 sandstone-mudstone couplets. Based on the fan model used, medium to thin-bedded sandstone-mudstone couplets (Facies C2.2 and C2.3; Figure 5.14c, d) were probably deposited on a lobe-fringe, whereas thick sandy Facies C2.1 beds (Figure 5.14b) were possibly deposited as part of a lobe. Without better-constrained stratigraphy, confidence in this interpretation is low.

6.4.5: Mangakuri/Waimarama Beaches

The sections exposed at Mangakuri and Waimarama beaches are in close proximity, although the complex local tectonic regime makes it difficult to infer the original stratigraphic relationships of the outcrops observed. Northern Mangakuri Beach strata are Teratan aged, whereas southern Mangakuri Beach strata are inferred as mostly Piripauan in age (Figure 3.7, Figure 3.8).

Facies observed in southern Mangakuri share some similarities to canyon fill successions. Ito and Saito (2006) observed cross-stratified conglomerates (such as Figure 4.10c, Figure 5.17b), overlain by pebbly sandstone and conglomerate (such as Figure 5.19b) and structureless sandstones in a canyon fill succession (such as Figure 5.16d). Other literature summarised in Pickering and Hiscott (2015) suggests that the abundant mudstone clasts in sandstones are also common in canyon fill. Without an observed canyon-wall boundary it is not possible to prove this. Because of the channelised features (Figure 5.16b), abundant and often large intraformational rip-up clasts

(Figure 5.17d, Figure 5.18b) and occasional conglomerates (Figure 5.16d), strata in southern Mangakuri Beach may also be a channel-fill sequence as described in section 6.3.

In northern Mangakuri, facies are consistent with a channel-fill succession as described in section 6.3, evidenced by the thick channelised conglomerate, abundant intraformational clasts, and channelised/wedge shaped amalgamated sandstones (Appendix K; Crampton, 1997).

Tectonic disruption means it is very difficult to make inferences regarding the depositional environment of facies observed in Waimarama. Facies include thin to thick-bedded sandstone-mudstone couplets of Facies C2.1 to C2.3 (Figure 5.20d, Figure 5.22) , thick beds of structureless siltstone and sandy siltstone of Facies D1, D2 and C1 (Figure 5.20a, b, c), pebbly sandstone of Facies A1.3 with abundant intraformational material (Figure 5.21a), and graded conglomerates of Facies 2.1 (Figure 5.21b)

The distribution of facies at Waimarama does not closely match generalised descriptions of any element of a fan system. It is possible that the tectonic disruption has juxtaposed rocks deposited in significantly different depositional environments. The presence of conglomerate beds suggests at least some strata were deposited in either a channel or a canyon. The lens shaped, fossil-rich bed shown in Figure 5.22c has an erosive base suggesting possibly a “megaflute” or shallow channel (Pickering and Hiscott, 2015). Unfortunately, with the available data, no definitive sub-environment can be determined.

6.5: One Fan System or Multiple?

One question regarding the depositional environment that Crampton (1997) posed was whether the Glenburn Formation was part of a large single fan system or deposited by several separate fans. Although the formation is spatially extensive, some modern day fans such as the Bengal and Amazon fans cover areas well in excess of 100,000 km^2 (Barnes and Normark, 1985). Whether there were multiple fans present is difficult to deduce given the lack of horizontal continuity of outcrops. There is some evidence, however, suggesting that the Glenburn Formation having been deposited as several separate fans:

- Paleocurrents: paleocurrent indicators are somewhat rare in the Glenburn Formation (see Section 5.3.2). However, if the entirety of the Glenburn Formation was deposited by one large fan from a singular source, paleocurrent directions should show a broadly radial pattern, with northernmost outcrops generally sourced from northerly flows and southernmost outcrops generally sourced from southerly flows. This is not the case; there appears to be no discernible special trend in the nature of paleocurrents with trends being generally eastward.
- Clast counts: Ratios of argillite to indurated sandstone between contemporaneous conglomerates of Teratan age in Totara Stream and northern Mangakuri are significantly different. A simple explanation for this difference is that onshore provenance was different between the two locations in the Cretaceous. For this to manifest itself as a difference in the ratio of clasts, sediment would probably have been fed by different canyon systems. Because both indurated sandstones and argillite are very durable clasts, preferential preservation of one clast type within a debris flow is unlikely. Statistically rigorous conclusions cannot be drawn from rare clasts types so no inference is made based on the presence of certain rare clasts in each locality.

6.6: Summary

To summarise, based on the available, albeit sparse data, Glenburn Formation is interpreted to have been deposited on more than one submarine fan below wave base. Several submarine fan sub-environments are represented between sections, including fan-fringe, lobe-fringe, lobe, channel, channel-levee and possibly canyon-fill. Although there is some uncertainty, for the most part facies associations are in accordance with descriptions of submarine fans from previous literature. The coarsening- and thickening-upward trend observed in the Honeycomb Light, Motuwaireka Stream and Mataikona River sections suggests fan progradation.

Chapter 7: Cretaceous East Coast Basin Paleogeographic Reconstruction

7.1: Introduction

This chapter combines the interpretations drawn herein and in other literature on the ECB to propose a reconstruction of the Cretaceous ECB. This model includes both the Eastern and Western sub-belts and the overlying Whangai Formation.

Pickering and Hiscott (2015) state:

> "In the absence of any oceanic basalts associated with deep-marine sediments, it is probably impossible to differentiate a forearc basin, accretionary-prism slope basin and trench fill. Apart from the depositional site, there appear to be no unique sedimentary characteristics of trench-fill siliciclastics." (Pickering and Hiscott, p. 938)

This means the facies observed within the Glenburn Formation could have been deposited in any of the settings listed by Pickering and Hiscott (2015) above. The Early Cretaceous volcanics at Red Island are most likely an ocean floor succession (Kobe and Pettinga, 1978), however their relationship to the Glenburn Formation remains poorly understood (Section 2.1.2), and they may or may not represent basement to the Glenburn Formation.

Because of this ambiguity, paleogeographic reconstructions require a more holistic approach than formation-by-formation determination of paleogeography. Instead, this study considers Cretaceous successions of the Eastern and Western sub-belts together, and the broader stratigraphic context, to attempt to construct a best-fit model for the paleogeography of the ECB.

7.2: Paleogeography of the Cretaceous ECB

Observations from this study are largely consistent with the paleogeographic reconstruction proposed by Crampton (1997). It is emphasised, however, that there are multiple plausible depositional environments for each of the formations listed, as discussed below.

The model developed herein assumes no significant strike-slip movement along the faults separating Eastern and Western sub-belts, such as the Adams-Tinui Fault system or those of the Akitio Fault Zone. Deltail et al. (1996) proposed up to 300 km of lateral displacement along these fault systems during the Neogene. This hypothesis has been questioned and Nicol et al. (2007) instead suggest <10 km of strike slip movement has occurred on faults east of the Axial Ranges. If there is confirmation of large horizontal displacement across Neogene Faults in the ECB, adjustments to the model might be required.

The present study follows the findings of Nicol et al. (2007) and assumes that the only significant fault movement between sub-belts is dip-slip. Therefore, Western Sub-belt strata currently adjacent to Eastern Sub-belt strata are assumed have been shorewards during the Cretaceous Period, based on the dominant east-flowing paleocurrents (Section 5.3.2). Post-depositional tectonic shortening has brought the two sub-belts spatially closer along an approximately east-west axis (Section 2.3). Therefore, the two sub-belts were deposited further apart than they currently lie relative to one another.

The following evidence is considered:

General evidence

- All Cretaceous strata on both sub-belts were most likely deposited at depth of outer shelf or deeper (see Chapter 2 for discussion regarding WSB).
- The sharp contrast in sedimentary facies between Eastern and Western Sub-belt facies suggests a separate depositional environment for each sub-belt.
- Both sub-belts are overlain, in parts conformably, by the Whangai Formation, that was most likely deposited in <800 m water depth (Section 2.1.4).
- Significant Neogene tectonic shortening has brought ESB and WSB closer together than their original positions, probably on the order of ten or more kilometres (Nicol et al., 2007).

Western Sub-belt

- Pahaoa Group sediments underlie WSB facies. The Pahaoa Group was most likely deposited in a slope basin (Barnes, 1988). The angular unconformity separating Pahaoa Group sediment from overlying Mangapurupuru Group sediment is intra-Motuan (Crampton, 1989). This puts some constraint on the distance Pahaoa Group sediment could have been moved tectonically before the Mangapurupuru Group was deposited on top of it.
- The facies of the Gentle Annie Formation are consistent with deposition following rapid tectonic uplift, possibly due to the impact of the Hikurangi Plateau with the Zealandia continental crust (Crampton, 1989). It is likely new accommodation space on the accretionary wedge slope was created due to a significant tectonic event, which was infilled by the Gentle Annie and Springhill formations (Section 2.1.3).
- The high proportion of hemipelagic massive mudstone in the Springhill Formation (Crampton, 1997) is consistent with deposition within a deep but relatively near-shore depositional environment (Section 2.1.3).
- Tangaruhe Formation unconformably overlies Mangapurupuru Group sediment, with significant unconformity (Crampton, 1997). This indicates a period of non-deposition or significant erosion, or some combination of both.
- The thickness of Gentle Annie Formation is on the order of 400-700 m, whereas Springhill Formation is most likely around 750 m (Crampton, 1997), although Johnston (1980) estimated as much as 2200 m may be present in the Tinui area. Pervasive faulting may have caused an overestimation of thickness. Tangaruhe Formation is <300 m thick where measured (Section 2.1.3).
- In the WSB paleocurrents are also probably mostly east-flowing, aside from some possible west-flowing paleocurrents in the Springhill Formation (Crampton, 1997).

Glenburn Formation

- This study concludes that Glenburn Formation was deposited on multiple submarine fans that were probably canyon fed (Section 6.2).
- Paleocurrents in the Glenburn Formation are dominantly east-flowing (Section 5.3.2). If it were deposited in a trench paleoenvironment, along-trench axis paleocurrents would be expected to be roughly north-south, but these are not observed outside of Totara Stream.

This means a confined trench is considered unlikely (as per descriptions in Pickering and Hiscott, 2015).

- There is some evidence of reworking of Springhill Formation into the Glenburn Formation (Crampton, 1997).
- Glenburn Formation is >1000 m thick in places, and may exceed 2000 m assuming Ngaterian to Haumurian continuity in southern regions (Section 5.3.1). Including the effects of compaction the original sedimentary thickness would have been even greater.
- Glenburn Formation outcrops are present in several different thrust wedges (Lee and Begg, 2002). It is plausible that strata deposited on the Glenburn coast was deposited kilometres or even tens of kilometres offshore from those in Totara Stream, having been subsequently brought closer by Neogene tectonic shortening.

If negligible vertical tectonics is assumed (uplift or subsidence), an original pre-compaction thickness of Glenburn Formation of 2-3 km, and an inferred depositional depth of 600 - 800 m for the conformably overlying Whangai Formation (Hines, 2018), an approximate depth of deposition for the basal Glenburn Formation would be approximately 2.5 – 4 km. Although this assumption will be incorrect to some degree, the depth estimate would be consistent with deposition in a shallow trough or a lower trench slope environment. Abnormally thick oceanic lithosphere, such as the Hikurangi Plateau, is associated with shallow trench depths (Abbott et al., 1994). A potential modern analogue for a subduction trough with a similar water depth is the Hikurangi Trough, which is between approximately 2.65 to 3.75 km deep (Lewis et al., 1998). Alternately, the subduction trench may have been completely filled with sediment when subduction ceased. A modern analogue for this would be the Cascadia Subduction Zone, where maximum water depths are ~2.5 km owing to the youth and buoyancy of the subducting oceanic lithosphere, which makes the subduction trench indistinguishable from regular ocean floor (Davis and Hyndman, 1989).

The widespread distribution of outcrop combined with the sedimentary thickness of the Glenburn Formation supports deposition within a canyon fed trough rather than a restricted slope basin. Most slope basis contain sediment fill <1 km thick, although some may be significantly thicker (Underwood and Moore, 1995). However, thicker successions are generally deposited on an active accretionary margin (e.g., Davey et al., 1986). Because the Glenburn Formation was deposited following the cessation of accretion, it is unlikely that a slope basin that existed when subduction ceased would contain enough accommodation space for the Glenburn Formation. The thickness of

the Glenburn Formation makes interpretation as anything other than a trench fill difficult to explain. Additionally, possible extension of Glenburn-type facies significantly offshore, as inferred by others such as Burgreen-Chan et al. (2016), is more plausible if deposition occurred in a trench rather than a slope basin. Offshore Cretaceous sediment may have also been deposited on the Pacific oceanic plate once the paleotrench had been filled.

A cartoon showing the inferred depositional environment for ESB and WSB Cretaceous formations over time is shown in figures 7.1, 7.2, 7.3 and 7.4.

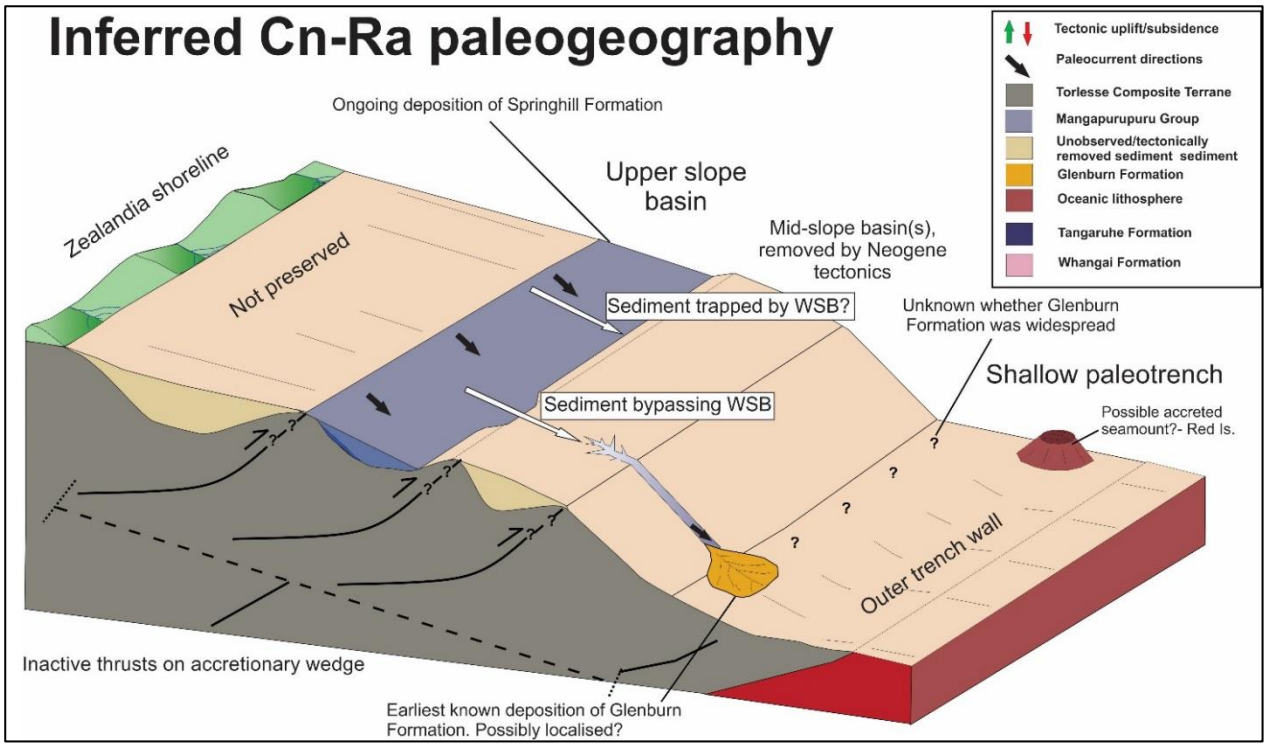

Figure 7.1: Inferred Ngaterian to Arowhanan Stage (99.5 – 93.7 Ma) paleogeography.

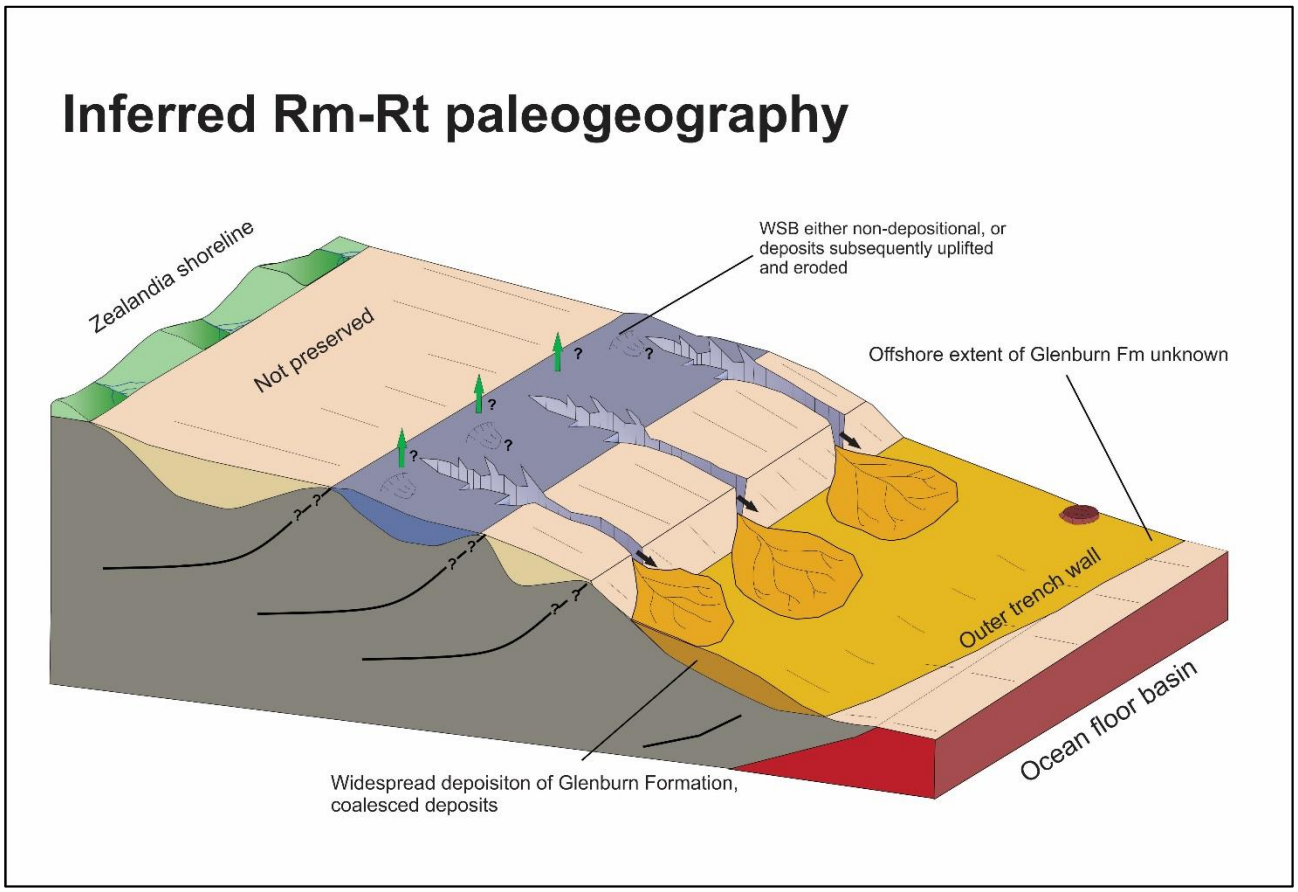

Figure 7.2: Inferred Mangaotanean to Teratan (93.7 – c. 88 Ma) paleogeography.

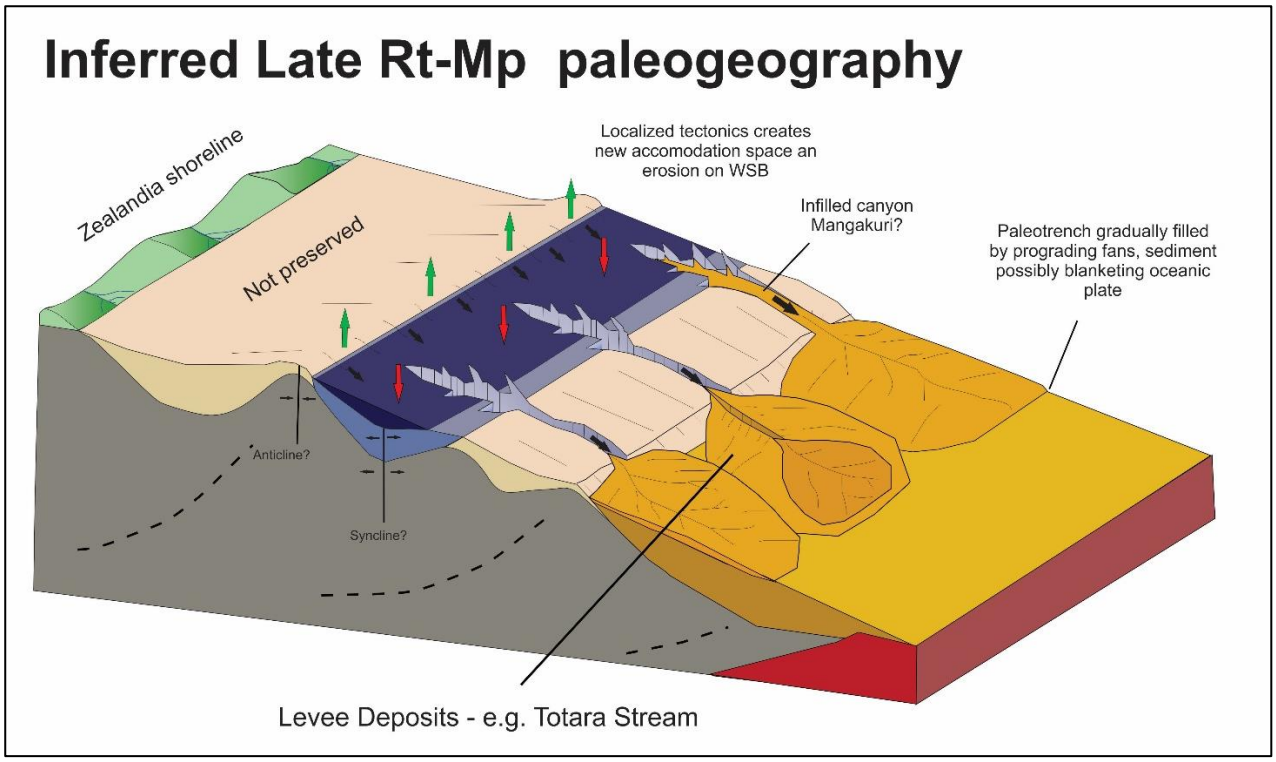

Figure 7.3: Inferred late Teratan to Piripauan (c. 88 Ma to 83.6 Ma) paleogeography.

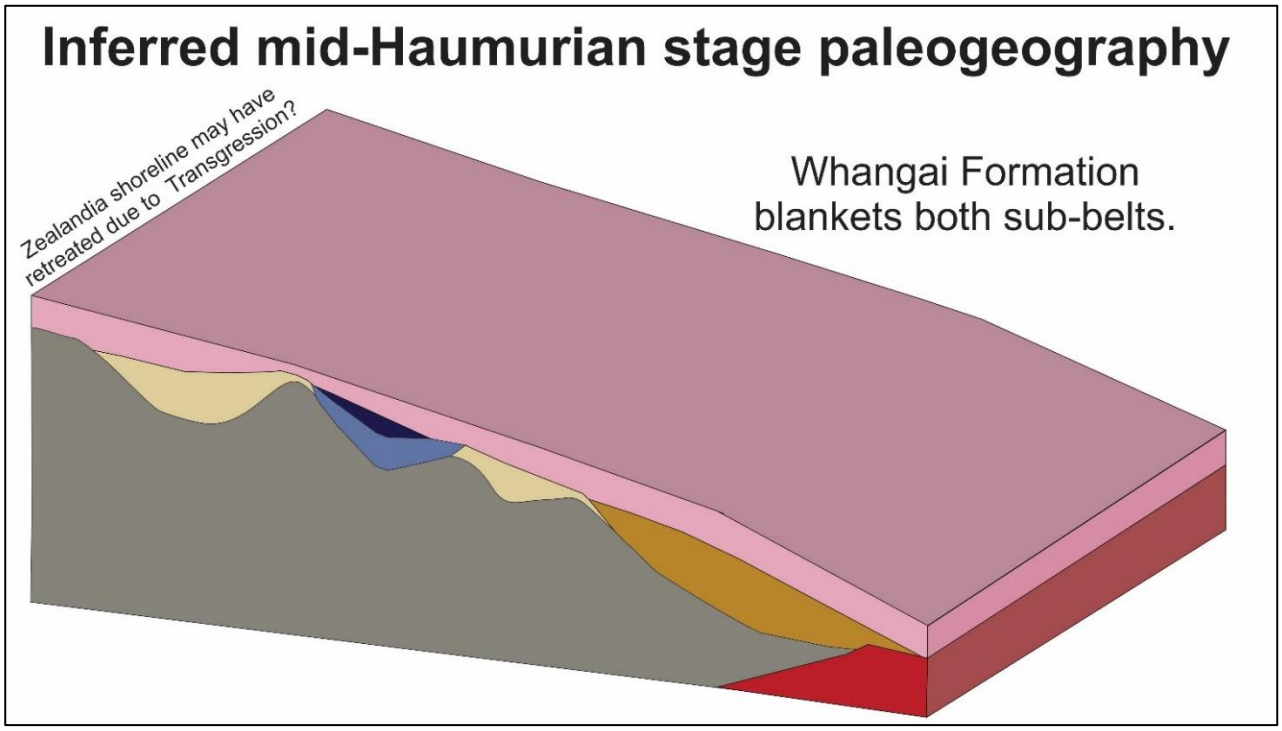

Figure 7.4: Inferred mid-Haumurian (c. 70 Ma) paleogeography.

7.3: Proposed Cretaceous ECB History

The following section proposes a history for the Cretaceous ECB based on available information. This is an interpretation based on the evidence summarised in the previous section.

Pahaoa Group sediment was deposited in a deep marine fan setting during the latest stages of subduction. Barnes and Korsch (1991) provide strong evidence that melanges within the Pahaoa Group were tectonically formed, and were therefore inferred to have been deposited in a trench-slope basin.

A significant tectonic event occurred in the Motuan Stage. This is most likely due to the collision of the Hikurangi Plateau with the Gondwanan plate margin, which occurred near the ECB (Bland et al., 2015). The jamming of the subduction margin caused rapid uplift and tectonic shortening for a short period in the Motuan Stage. This shortening event may have contributed to the intense deformation seen in Pahaoa Group rocks.

Large slumps occurred on the newly steepened, unstable slopes. These events deposited the Gentle Annie Formation. Sheet-like turbidite deposits from the shelf form the basal unit of the Springhill Formation. As the newly steepened slope began to stabilise, these SGF deposits became progressively less frequent in the Springhill Formation, and deposition instead became dominated by dilute turbidites and pelagic sedimentation. The presence of basins on the slope where Mangapurupuru Group sediments were being deposited may have largely choked off sediment supply to the lower slopes, hence the lack of correlative units on the adjacent Eastern Sub-belt. Alternately, correlative strata may exist but are not exposed or preserved.

In the Ngaterian Stage, WSB sediment had largely filled in accommodation space, and locally, sediment began to bypass the WSB trench slope basin (Figure 7.1). In the Glenburn coast area, sediment gravity flows began to deposit clastic material in large basin, inferred here to be the paleotrench. At first, deposits consisted of fine-grained mudflows and occasional thin sandy turbidites, gradually coarsening and thickening into thick-bedded turbidites and channelised debris flow deposits. This sequence is inferred to record the progradation of a canyon fed fan.

By the Mangaotanean Stage, deposition had essentially ceased on the Western Sub-belt, although in places on-going deposition may have been subsequently eroded and removed strata beneath the sub-Tangaruhe Formation unconformity (Section 2.1.3). Several canyons had incised into the slope, delivering coarse sediment through to a number of submarine fans on the ESB (Figure 7.2).

Coarsening and thickening of facies noted in Motuwaireka Stream and Mataikona River show a similar pattern to that observed in Ngaterian-Arowhanan outcrops and represent the growth of the fans and the canyons that fed them. These canyon systems incised into Western Sub-belt deposits, providing the evidence of reworking noted in Crampton (1997) and probably the less-indurated sandstone clasts found in Glenburn Formation conglomerates. This trend continued through until the early Haumurian (Figure 7.3).

The abundance of thin-bedded facies in the Mata Series strata of Totara Stream and Motuwaireka Stream and absence of conglomerates is inferred to be due to the further progradation of the fan system outboard, meaning coarser facies bypassed the sections exposed through large channels. Thin-bedded facies are therefore interpreted as overbank channel-levee deposits. Although this fining of facies could also be interpreted as being due to gradual abandonment of the fan system due to transgression and trapping of sediment in more proximal settings, this would be somewhat in conflict with the observations in the Mataikona River. There, conglomeratic facies first appear in the late Piripauan to early Haumurian overlying inferred lobe deposits, suggesting at least locally a continual progradation of the fan system until the Haumurian.

Tangaruhe Formation on the WSB likely represents a fill sequence in one or more locally formed basins (Figure 7.3). This is probably due to localised tectonic events in the Late Cretaceous. Basal coarser facies are likely due to an initial over-steepening of slopes following said tectonic events, with reworked glaucony from the otherwise sediment starved slopes in a relatively distal environment. These newly formed basins were gradually infilled by sporadic SGF events that became less frequent as the topography became buried, and pelagic sedimentation dominates the upper part of the succession.

Partway through the Haumurian, the rate of SGF events reduced and a transition into the more homogenous Whangai Formation occurred (Figure 7.4). Although occasional sandstone beds occur in the Whangai Formation, the abundance of highly bioturbated mudstone suggests sediment was deposited gradually by pelagic and hemipelagic processes. Some possible explanations include a significant decrease in the production of coarse clastic material onshore, formation of a near-shore basin during transgression that captured the coarse sediment, or the onshore Glenburn Formation sections had “filled” their accommodation space meaning coarse sediment bypassed the system to be deposited further offshore. If the latter case proves true, it may be possible that coarse submarine fan sediments were being deposited further offshore of the Whangai Formation. This study does not further any knowledge regarding this topic.

Chapter 8: Conclusions and summary

8.1: Key Findings

Extensive fieldwork and section logging was undertaken upon the Glenburn Formation. The measured sections presented in appendices D – L detail the various facies observed in the Glenburn Formation by locations and show the marked variability in the nature of the Glenburn Formation both spatially and temporally. Intervals of fine grained massive mudstones through to thick conglomerate dominated sequences are all found within the Glenburn Formation and facies may shift abruptly or gradually. This research provides the most comprehensive and detailed formation-wide record for the Glenburn Formation.

Detailed facies analysis based on these eight measured sections consistently indicates a submarine fan depositional environment for the Glenburn Formation. A number of distinct, canyon fed fans are inferred from paleocurrent directions and conglomerate-clast derived provenance differences. Facies analysis suggests several separate fan depositional environments are present within the Glenburn Formation, including channel-levee complexes, fan-lobes and possibly canyon fill.

A paleogeographic reconstruction of the Late Cretaceous paleogeography of the southern Hawke's Bay and Wairarapa regions suggests the Glenburn Formation was probably deposited in the fossil Gondwanan Trench. Total sediment thickness combined with estimates of paleodepth of the conformably overlying Whangai Formation tentatively suggests a depth of deposition of ~2000-2500 m for lowermost exposed strata, and a depth of deposition of <1000 m for the uppermost strata. Therefore, the Glenburn formation represents the gradual infilling of a relatively shallow trough following the cessation of subduction along the Gondwanan plate margin.

Generally, the Glenburn Formation shows a coarsening and thickening of beds through the Raukumara Series. On the Glenburn coast, this coarsening and thickening occurred in the late parts of Ngaterian Stage through to the early Arowhanan Stage. In the Mataikona River and Motuwaireka Stream, there was coarsening and thickening of strata in the late Mangaotanean to Teratan stages. The simplest explanation for this trend is a prograding fan system. The relatively thinner and finer beds in the late Piripauan in the Totara and Motuwaireka Stream sections are inferred to be levee deposits, consistent with the prograding fan system hypothesis.

8.2: Implications for Offshore Correlatives

Late Cretaceous sediment offshore of the southern Hawke's Bay-Wairarapa regions are likely to be correlative to the Glenburn Formation. However, as shown by the dominantly east-flowing paleocurrents, these sediments would have been deposited in an environment more distal than the exposed onshore equivalents. Because of this, caution is required when comparing offshore sediment of a similar age to onshore Glenburn Formation. For example, in the Teratan Stage, where channel-levee systems dominate onshore outcrops, sediment deposited further offshore would probably be finer-grained lobe systems. Conversely, sediment deposited coevally offshore of the "Totara Stream Lithofacies" may be coarser-grained channel-levee deposits due to progradation of the submarine fan system.

8.3: Suggestions for Future Work

8.3.1: Further Investigation into WSB Formations

As highlighted in chapter two, the depositional environment of formations such as the Springhill and Tangaruhe formations is poorly constrained. Better understanding of the paleogeography of the WSB will help to corroborate the model proposed here.

8.3.2: Correlative Strata on the Raukumara Peninsula

The correlative Tikihore Formation of the ESB on Raukumara Peninsula shares some similarities with the Glenburn Formation, but its depositional environment is poorly constrained. Although facies are similar, SGF-dominated successions can be deposited in several different paleoenvironments, so it would be premature to assume the Tikihore Formation was also deposited in the Gondwanan paleotrench. A similar in-depth facies-based investigation into the Tikihore Formation is needed to determine its depositional environment. If the Tikihore Formation is a horizontal continuation of the Glenburn Formation, the two formations may warrant designation into a stratigraphic group. Alternately, they could be combined to one formation with

several distinct members. Further investigation into the Tikihore Formation would reveal whether this would be appropriate.

8.3.3: Mapping the Lateral Continuity of the "Totara Stream Lithofacies"

As discussed above, the distinct facies exposed in Totara Stream shares some similarities with that found in Motuwaireka Stream and possibly even Huatokitoki Stream. If correlative upper Piripauan Strata in other localities between these sites, this lithofacies might warrant elevation to member status. Mangapiu Stream, tributaries of Kopi Stream, Kaiwhata River tributary immediately south of Totara Stream ("Kowhai Stream" in Moore, 1980), road cuttings on Kaiwhata Road and the headwaters of Arawhata Stream are all potential locations that may show this lithofacies.

8.3.4: Offshore Understanding

Detailed seismic facies analysis could help determine the depositional geometry of inferred Glenburn Formation offshore. Seismic interpretations of elements of the submarine fan system, such as lobes or channel fill successions, can be compared to the onshore correlatives described here to help determine the nature of sediment offshore.

8.3.5: More Detailed Petrography of Sandstones and Conglomerates

A clast count study (Section 5.2) provided some strong evidence regarding the plurality of fan systems in the Glenburn Formation. A more thorough investigation into the petrography of conglomerates in the ECB, including those in formations other than the Glenburn Formation, may help further constrain provenance and paleogeography. Sandstone petrography is another potential avenue for investigation. With more information, questions such as the potential sources of sandstone rafts may be answered.

References

Abbott, D., Drury, R., & Smith, W. H. (1994). Flat to steep transition in subduction style. *Geology, 22(10)*, 937-940.

Adams, A. G. (1985). Late Cretaceous fauna and sediments of southern Hawkes Bay- New Zealand. *Unpublished PhD thesis lodged in the library, University of Auckland*.

Adams, C. J., Campbell, H. J., Mortimer, N., & Griffin, W. L. (2016). Perspectives on Cretaceous Gondwana break-up from detrital zircon provenance of southern Zealandia sandstones. *Geological Magazine, 154(4)*, 661-682.

Adams, C. J., Mortimer, N., Campbell, H. J., & Griffin, W. L. (2013). The mid-Cretaceous transition from basement to cover within sedimentary rocks in eastern New Zealand: evidence from detrital zircon age patterns. *Geological Magazine, 150(3)*, 455-478.

Barnes, N. E., & Normark, W. R. (1985). Diagnostic parameters for comparing modern submarine fans and ancient turbidite systems. *Submarine Fans and Related Turbidite Systems*, Springer-Verlag, New York, N.Y. (1985), pp. 13-14

Barnes, P. M. (1988). Submarine fan sedimentation at a convergent margin: the Cretaceous Mangapokia Formation, New Zealand. *Sedimentary Geology, 59(3-4),* 155-178.

Barnes, P. M., & Korsch, R. J. (1991). Melange and related structures in Torlesse accretionary wedge, Wairarapa, New Zealand. *New Zealand Journal of Geology and Geophysics, 34(4),* 517-532.

Black, R., Brathwaite, R., & Moore, P. (1984). Pillow lava and associated copper minerals at Kairakau Rocks, southern Hawkes Bay*. New Zealand Geological Survey Record, 3,* 92-97.

Bland, K. J., Uruski, C. I., & Isaac, M. J. (2015). Pegasus Basin, eastern New Zealand: A stratigraphic record of subsidence and subduction, ancient and modern. *New Zealand Journal of Geology and Geophysics,* 58(4), 319-343.

Boggs, S.J., 2006, *Principle of Sedimentology and Stratigraphy.* Pearson Education, Upper Saddle River (2006), 662 pp.

Bouma, A. H. (1962). *Sedimentology of some flysch deposits: a graphic approach to facies interpretation.* Elsevier, Amsterdam (1962), p. 168

Brown, D. A. (1943). The geology of the Brocken Range and the Kaiwhata Valley, East Wellington. *Transactions of the Royal Society of New Zealand 72,* 347-352.

Burgreen-Chan, B., Meisling, K. E., & Graham, S. (2016). Basin and petroleum system modelling of the East Coast basin, New Zealand: a test of overpressure scenarios in a convergent margin. *Basin Research, 28(4),* 536-567.

Chen, C., & Hiscott, R. N. (1999). Statistical analysis of turbidite cycles in submarine fan successions: tests for short-term persistence. *Journal of Sedimentary Research, 69(2),* 505-517.

Collier, T. (2015). The geology of Pegasus Basin based on outcrop correlatives in southern Wairarapa and northeastern Marlborough, New Zealand. *Unpublished MSc thesis lodged in the library, Victoria University of Wellington.*

Cooper, R. A., & Agterberg, F. P. (2004). The New Zealand geological timescale (Vol. 22): *Institute of Geological & Nuclear Sciences Monograph 22,* 284 pp.

Crampton, J. (1989). An inferred Motuan sedimentary melange in southern Hawkes Bay. *New Zealand Geological Survey Record, 40,* 3-12.

Crampton, J. S. (1996). Inoceramid bivalves from the late Cretaceous of New Zealand. *Institute of Geological and Nuclear Sciences Monograph 14,* 192p.

Crampton, J. S. (1997). The Cretaceous stratigraphy of the southern Hawke's Bay-Wairarapa region. *Institute of Geological and Nuclear Sciences Report 97(08),* 92.

Crampton, J. S., & Laird, M. G. (1997). Burnt Creek Formation and Late Cretaceous basin development in Marlborough, New Zealand. *New Zealand Journal of Geology and Geophysics, 40(2),* 199-222.

Crampton, J. S., Schiøler, P., & Roncaglia, L. (2006). Detection of Late Cretaceous eustatic signatures using quantitative biostratigraphy. *Geological Society of America Bulletin, 118(7-8),* 975-990.

Davey, F., Hampton, M., Childs, J., Fisher, M., Lewis, K., & Pettinga, J. (1986). Structure of a growing accretionary prism, Hikurangi margin, New Zealand. *Geology, 14(8),* 663-666.

Davis, E., & Hyndman, R. (1989). Accretion and recent deformation of sediments along the northern Cascadia subduction zone. *Geological Society of America Bulletin, 101(11),* 1465-1480.

Davy, B. (2014). Rotation and offset of the Gondwana convergent margin in the New Zealand region following Cretaceous jamming of Hikurangi Plateau large igneous province subduction. *Tectonics, 33(8),* 1577-1595.

Davy, B., Hoernle, K., & Werner, R. (2008). Hikurangi Plateau: Crustal structure, rifted formation, and Gondwana subduction history. *Geochemistry, Geophysics, Geosystems, 9(7).*

de Caen, R. F. B., & Darley, J. H. (1968). Re-examination of the Upper Cretaceous sediment Waimarama coastal section East Coast, North Island. (New Zealand. BP Shell Aquitaine & Todd Petroleum Development Ltd.). *Ministry of Economic Development New Zealand Unpublished Petroleum Report PR381.*

Delteil, J., Morgans, H. E., Raine, J. I., Field, B. D., & Cutten, H. N. (1996). Early Miocene thin-skinned tectonics and wrench faulting in the Pongaroa district, Hikurangi margin, North Island, New Zealand. *New Zealand Journal of Geology and Geophysics, 39(2),* 271-282.

Eade, J. (1966). Stratigraphy and Structure of the Mount Adams Area, Eastern Wairarapa *Transactions of the Royal Society of New Zealand, Geology, 4,* 103-117.

Eyssautier, M., & Faber, J. (1966). Geological notes on the Waimarama, Taingamata and Red Island section, Hawkes Bay (New Zealand Aquitaine Petroleum Ltd.). *Ministry of Economic Development New Zealand Unpublished Petroleum Report PR3484.*

Field B.D., Uruski C.I., Beu A., Browne G., Crampton J., Funnell R., Killops S., Laird M., Mazengarb C., Morgans H., Rait G., Smale D., & Strong P. (1997). Cretaceous-Cenozoic geology and petroleum systems of the East Coast region, New Zealand. *Institute of Geological and Nuclear Sciences Monograph, 19.*

Fisher, N. I. (1995). *Statistical analysis of circular data.* Cambridge University Press, Cambridge, UK, 295 p.

Frances, D. A. (1993a). Report on the geology of the Waimarama-Kidnappers area, Hawke's Bay, adjacent to offshore PPL38321 (Conquest Exploration Ltd.). *Ministry of Economic Development New Zealand Unpublished Petroleum Report PR1926*.

Frances, D. A. (1993b). Report on the geology of the Mahia area, northern Hawkes Bay, adjacent to offshore PPL 38321. (Conquest Exploration Ltd.). *Ministry of Economic Development New Zealand Unpublished Petroleum Report PR1928*.

Gaina, C., Müller, D. R., Royer, J. Y., Stock, J., Hardebeck, J., & Symonds, P. (1998). The tectonic history of the Tasman Sea: a puzzle with 13 pieces. *Journal of Geophysical Research: Solid Earth, 103(B6)*, 12,413-12,433.

Grain, S. (2008). Palaeogeography of a Mid Miocene Turbidite Complex, Moki Formation, Taranaki Basin, New Zealand*. Unpublished MSc thesis lodged in the library, Victoria University of Wellington.*

Haw, D. (1960). Geological report on the eastern Te Aute Subdivision - GR15 (BP Shell Aquitaine & Todd Petreum Development Ltd.). *Ministry of Economic Development New Zealand Unpublished Petroleum Report PR316.*

Higgs, R. (2011). Hummocky cross-stratification-like structures in deep-sea turbidites: Upper Cretaceous Basque basins (Western Pyrenees, France) by Mulder et al., Sedimentology, 56, 997–1015: Discussion*. Sedimentology, 58(2)*, 566-570.

Hines, B.R. (2018). Cretaceous - Paloegene Palinspastic Reconstruction of the East coast Basin, New Zealand. *Unpublished PhD thesis in preparation, Victoria University of Wellington.*

Hollis, C.J. and Manzano-Kareah, K. (compilers) 2005. Source rock potential of the East Coast Basin (central and northern regions). *Institute of Geological and Nuclear Sciences Client Report 2005/118:* 156 pp.

Howard, J. L. (1993). The statistics of counting clasts in rudites: a review, with examples from the upper Palaeogene of southern California, USA. *Sedimentology, 40(2)*, 157-174.

Ingram, R. L. (1954). Terminology for the thickness of stratification and parting units in sedimentary rocks. *Geological Society of America Bulletin, 65(9),* 937-938.

Ito, M., & Saito, T. (2006). Gravel waves in an ancient canyon: analogous features and formative processes of coarse-grained bedforms in a submarine-fan system, the Lower Pleistocene of the Boso Peninsula, Japan. *Journal of Sedimentary Research, 76(12),* 1274-1283.

Johnston, M. R. (1971). Geology of the Tinui District. *Unpublished MSc thesis lodged in the library, Victoria University of Wellington.*

Johnston, M. R. (1975). Sheet N159 and Part Sheet N158, Tinui-Awatoitoi. *Geological map of New Zealand, 1:63,360. Wellington, DSIR.*

Johnston, M. R. (1980). Geology of the Tinui-Awatoitoi district. *New Zealand Geological Survey bulletin 94: 62 p.*

Katz, H. R. (1988). Study into potential occurrence of Cretaceous reservoir rocks, Offshore East Coast North Island, New Zealand with special regard to PL38315. *Ministry of Economic Development New Zealand Unpublished Petroleum Report PR1431.*

Kenny, J. A. (1986). Alternating convergent and non-convergent tectonics, 100 million years to present, Puketoro area, northeastern New Zealand. *Unpublished MSc thesis. Auckland, University of Auckland.*

Killops, S., Hollis, C., Morgans, H., Sutherland, R., Field, B., & Leckie, D. (2000). Paleoceanographic significance of Late Paleocene dysaerobia at the shelf/slope break around New Zealand. *Palaeogeography, palaeoclimatology, palaeoecology, 156(1),* 51-70.

King, P. R., G. H. Browne, M. J. Arnot, and M. P. Crundwell, 2007, A 2-D, oblique-dip outcrop transect through a third-order, progradational, deep-water clastic succession, Urenui–Mount Messenger Formations, New Zealand, *in T.H. Nilsen, R. D. Shew, G. S. Steffens, and J. R. J. Studlick, eds., Atlas of deep-water outcrops: AAPG Studies in Geology 56,* CD-ROM, 42 p.

King, P., Naish, T., Browne, G., Field, B., & Edbrooke, S. (1999). Cretaceous to Recent sedimentary patterns in New Zealand*, Institute of Geological & Nuclear Sciences Folio Series 1,* 1-35

Kingma, J. T. (1971). Geology of Te Aute Subdivision: New Zealand Dept. of Scientific and Industrial Research. *New Zealand Geological Survey Bulletin 70:* 173 p.

Kobe, H. (1976). Petrography and mineralization at Karamea (Red Island) Southern Hawkes Bay. *Tane, 22,* 139-143.

Kobe, H., & Pettinga, J. (1984). Red Island (NZ) and its submarine-exhalative Mn-Fe mineralization. *Syngenesis and Epigenesis in the Formation of Mineral Deposits,* Springer, Berlin (1984), 562-572.

Krause, R. G., & Geijer, T. A. (1987). An improved method for calculating the standard deviation and variance of paleocurrent data. *Journal of Sedimentary Research, 57(4),* 779-780.

Kuenen, P. H., & Migliorini, C. (1950). Turbidity currents as a cause of graded bedding. The *Journal of Geology, 58(2),* 91-127.

Laird, M., Bassett, K., Schiøler, P., Morgans, H., Bradshaw, J., & Weaver, S. (2003). Paleoenvironmental and tectonic changes across the Cretaceous/Tertiary boundary at Tora, southeast Wairarapa, New Zealand: a link between Marlborough and Hawke's Bay. *New Zealand Journal of Geology and Geophysics, 46(2),* 275-293.

Laird, M., & Bradshaw, J. (2004). The break-up of a long-term relationship: the Cretaceous separation of New Zealand from Gondwana. *Gondwana Research, 7(1),* 273-286.

Leckie, D. A., Morgans, H., Wilson, G., & Edwards, A. (1995). Mid-Paleocene dropstones in the Whangai Formation, New Zealand—evidence of mid-Paleocene cold climate? *Sedimentary Geology, 97(3-4),* 119-129.

Lee, J.M., (1995). A Stratigraphic, Biostratigraphic and Structural Analysis of the Geology at Huatokitoki Stream, Glenburn, Southern Wairarapa, New Zealand. *Unpublished MSc thesis lodged in the library, Victoria University of Wellington.*

Lee, J.M., & Begg, J. (2002*). Geology of the Wairarapa area 1: 250 000 Geological Map 11.* Institute of Geological and Nuclear Sciences Limited, Lower Hutt., New Zealand.

Lee J.M., Bland K.J., Townsend D.B., Kamp P.J.J., (2011). *Geology of the Hawkes Bay area. Institute of Geological and Nuclear Sciences 1:250,000 Geological Map 8* Institute of Geological and Nuclear Sciences Limited, Lower Hutt, New Zealand.

Lewis, K. B., Collot, J. Y., & Lallem, S. E. (1998). The dammed Hikurangi Trough: a channel-fed trench blocked by subducting seamounts and their wake avalanches (New Zealand–France GeodyNZ Project). *Basin Research, 10(4),* 441-468.

Lillie, A. R. (1953). The geology of the Dannevirke Subdivision. *New Zealand Geological Survey bulletin 46:* 156 p.

Lowe, D. R. (1982). Sediment gravity flows: II Depositional models with special reference to the deposits of high-density turbidity currents. *Journal of Sedimentary Research, 52,* 279-297.

MacGregor-Fors, I., & Payton, M. E. (2013). Contrasting diversity values: statistical inferences based on overlapping confidence intervals. *PLoS One, 8(2),* e56794.

Martín–Chivelet, J., Fregenal–Martínez, M., & Chacón, B. (2008). Traction structures in contourites. *Developments in Sedimentology, 60,* 157-182.

Marwick, J. (1966). An Aberrant Aucellinoid (Bivalvia, Pteriacea) from Red Island, Hawke's Bay. *New Zealand Journal of Geology and Geophysics, 9(4),* 495-503.

Mayall, M., Jones, E., & Casey, M. (2006). Turbidite channel reservoirs—Key elements in facies prediction and effective development. *Marine and Petroleum Geology, 23(8),* 821-841.

Moernaut, J., Daele, M. V., Heirman, K., Fontijn, K., Strasser, M., Pino, Urrutia, R., & De Batist, M. (2014). Lacustrine turbidites as a tool for quantitative earthquake reconstruction: New evidence for a variable rupture mode in south central Chile. *Journal of Geophysical Research: Solid Earth, 119(3),* 1607-1633.

Moore, P.R (1980). Late Cretaceous-Tertiary stratigraphy, structure, and tectonic history of the area between Whareama and Ngahape, eastern Wairarapa, New Zealand. *New Zealand Journal of Geology and Geophysics, 23(2),* 167-177.

Moore, P. R. (1986). A revised Cretaceous-early Tertiary stratigraphic nomenclature for eastern North Island, New Zealand. *New Zealand Geological Survey report G104:* 31 p.

Moore, P. R. (1988a). Structural divisions of eastern North Island (Vol. 30): *New Zealand Geological Survey record 30*: 24 p.

Moore, P. R. (1988b). Stratigraphy, composition and environment of deposition of the Whangai Formation and associated Late Cretaceous-Paleocene rocks, eastern North Island, New Zealand. *New Zealand Geological Survey bulletin 100:* 82 p.

Moore, P.R, & Speden, I. (1979). Stratigraphy, structure, and inferred environments of deposition of the Early Cretaceous sequence, eastern Wairarapa, New Zealand. *New Zealand Journal of Geology and Geophysics, 22(4),* 417-433.

Moore, P. R., & Speden, I. G. (1984). The Early Cretaceous (Albian) sequence of eastern Wairarapa, *New Zealand. New Zealand Geological Survey bulletin 97:* 98 p.

Moore, P.R., Brathwaite, R., & Roser, B. (1987). Correlation of Early Cretaceous volcanic-sedimentary sequences at Red Island and Hinemahanga Rocks, southern Hawkes Bay. *New Zealand Geological Survey Records, 18,* 27-31.

Mortimer, N., Campbell, H. J., Tulloch, A. J., King, P. R., Stagpoole, V.M., Wood, R. A., Rattenbury, R.A., Sutherland, R., Adams, Collot, J., Seton., M. (2017). Zealandia: Earth's hidden continent. *GSA Today, 27(3),* 27-35.

Mortimer N., Rattenbury M.S., King P.R., Bland K.J., Barrell D.J., A. Bache F., Begg J.G., Campbell H.J., Cox S. C., Crampton J.S., Edbrooke S.W., Forsyth P.J., Johnson M.R., Jongens R., Lee J.M., Leonard G S., Raine J.I., Skinner D.N.B., Timm C., Townsend D.B., Tulloch A.J., Turnbull I.M., & Turnbull R.E., (2014). High-level stratigraphic scheme for New Zealand rocks. *New Zealand Journal of Geology and Geophysics, 57(4),* 402-419.

Mulder, T., & Alexander, J. (2001). The physical character of subaqueous sedimentary density flows and their deposits. *Sedimentology, 48(2),* 269-299.

Mulder, T., Razin, P., & FAUGERES, J. C. (2009). Hummocky cross-stratification-like structures in deep-sea turbidites: Upper Cretaceous Basque basins (Western Pyrenees, France). *Sedimentology, 56(4),* 997-1015.

Mutti, E., Bernoulli, D., Lucchi, F. R., & Tinterri, R. (2009). Turbidites and turbidity currents from Alpine 'flysch'to the exploration of continental margins. *Sedimentology, 56(1),* 267-318.

Mutti, E., & Ricci Lucchi, F. (1978). Turbidites of the northern Apennines: introduction to facies analysis. *International geology review, 20(2),* 125-166.

Mutti, E., Tinterri, R., Benevelli, G., di Biase, D., & Cavanna, G. (2003). Deltaic, mixed and turbidite sedimentation of ancient foreland basins*. Marine and petroleum Geology, 20(6),* 733-755.

Mutti, E., Tinterri, R., Magalhaes, P. M., & Basta, G. (2007). Deep-water turbidites and their equally important shallower water cousins. *Search and Discovery Article, 50057.*

Neef, G. (1992). Geology of the Akitio area (1: 50 000 metric sheet U25BD, east), northeastern Wairarapa, New Zealand. *New Zealand Journal of Geology and Geophysics, 35(4),* 533-548.

Neef, G. (1995). Cretaceous and Cenozoic geology east of the Tinui Fault Complex in northeastern Wairarapa, New Zealand*. New Zealand Journal of Geology and Geophysics, 38(3),* 375-394.

Nicol, A., Mazengarb, C., Chanier, F., Rait, G., Uruski, C., & Wallace, L. (2007). Tectonic evolution of the active Hikurangi subduction margin, New Zealand, since the Oligocene. *Tectonics, 26(4).*

Payton, M. E., Miller, A. E., & Raun, W. R. (2000). Testing statistical hypotheses using standard error bars and confidence intervals. *Communications in Soil Science & Plant Analysis, 31(5-6),* 547-551.

Pettinga, J. R. (1980). Geology and landslides of the eastern Te Aute district, southern Hawkes Bay. *Unpublished PhD thesis lodged in the library, University of Auckland.*

Pettinga, J. R. (1982). Upper Cenozoic structural history, coastal southern Hawke's Bay, New Zealand. *New Zealand Journal of Geology and Geophysics, 25(2),* 149-191.

Pickering, K. T., & Corregidor, J. (2005). Mass transport complexes and tectonic control on confined basin-floor submarine fans, Middle Eocene, south Spanish Pyrenees. *Geological Society, London, Special Publications, 244(1),* 51-74.

Pickering, K. T., & Hiscott, R. N. (2015). *Deep Marine Systems: Processes, Deposits, Environments, Tectonic and Sedimentation.* American Geophysical Union, John Wiley & Sons (2015), 1393 p.

Pickering, K. T., Hiscott, R. N., & Hein, F. J. (1989). *Deep-marine environments: Clastic sedimentation and tectonics:* Unwin Hyman, London (1989), 416 pp.

Raine, J.I., Beu, A.G., Boyes, A.F., Campbell, H.J., Cooper, R.A., Crampton, J.S., Crundwell, M.P., Hollis, C.J., Morgans, H.E.G., Mortimer, N. (2015). New Zealand geological timescale NZGT 2015/1. *New Zealand Journal of Geology and Geophysics, 58(4),* 398-403.

Rebesco, M., Hernández-Molina, F. J., Van Rooij, D., & Wåhlin, A. (2014). Contourites and associated sediments controlled by deep-water circulation processes: state-of-the-art and future considerations. *Marine Geology, 352,* 111-154.

Ridd, M. F. (1964). The geology of northern Wairarapa, NI, New Zealand, GR28 (BP Shell & Todd Petreum Development Ltd.). *Ministry of Economic Development New Zealand Unpublished Petroleum Report PR329.*

Rumeau, J. L. (1966). The Cretaceous of the northern part of the East Coast, NI. (New Zealand Aquitaine Petroleum Ltd.). *Ministry of Economic Development New Zealand Unpublished Petroleum Report PR477.*

Schiøler, P., & Crampton, J. S. (2014). Dinoflagellate biostratigraphy of the Arowhanan Stage (upper Cenomanian–lower Turonian) in the East Coast Basin, New Zealand. *Cretaceous research, 48,* 205-224.

Shanmugam, G. (1997). The Bouma sequence and the turbidite mind set. *Earth-Science Reviews, 42(4),* 201-229.

Shanmugam, G. (2000). 50 years of the turbidite paradigm (1950s—1990s): deep-water processes and facies models—a critical perspective. *Marine and petroleum Geology,* 17(2), 285-342.

Shanmugam, G. (2008). Deep-water bottom currents and their deposits. *Developments in Sedimentology,* 60, 59-81.

Shanmugam, G. (2016). Submarine fans: a critical retrospective (1950–2015). *Journal of Palaeogeography,* 5(2), 110-184.

Shanmugam, G., Spalding, T., & Rofheart, D. (1993). Process sedimentology and reservoir quality of deep-marine bottom-current reworked sands (sandy contourites): an example from the Gulf of Mexico. *AAPG Bulletin, 77(7),* 1241-1259.

Simpson, J., & Jarvis, J. (1993). Technical review of the East Coast Basin (Petrocorp Exploration Ltd.). *Ministry of Economic Development New Zealand Unpublished Petroleum Report PR1972.*

Speden, I. G. (1976). Geology of Mt Taitai, Tapuaeroa Valley, Raukumara Peninsula. *New Zealand Journal of Geology and Geophysics 19(1),* 71-119.

Stow, D. A., & Mayall, M. (2000). Deep-water sedimentary systems: new models for the 21st century. *Marine and petroleum Geology, 17(2),* 125-135.

Surlyk, F. (1984*).* Fan-delta to submarine fan conglomerates of the Volgian-Valanginian Wollaston forland group, east Greenland*. Sedimentology of Gravels and Conglomerates: Can. Soc. Petroleum Geologists Mem. 10,* p. 359-382.

Tucker, R. S. (1992). Evaluation of Reservoir Rock Quality from Outcrop Samples, Upper Cretaceous-Pliocene Sandstone, East Coast Basin, New Zealand (Amoco NZ Exploration Co Ltd.). *Ministry of Economic Development New Zealand Unpublished Petroleum Report PR2143.*

Underwood, M. Moore, G.F. (1995). Trenches and trench-slope basins. *Tectonics of sedimentary basins, Blackwell Science Ltd.,* Oxford (1995), 179-219.

Underwood MB, Orr R, Pickering K, Taira A (1993). Provenance and dispersal patterns of sediments in the turbidite wedge of Nankai Trough. *Proc Ocean Drilling Program, Sci Results 131,* 15–33

Van den Heuvel, H. (1959). The geology of the Te Wharau Flat Point area, eastern Wairarapa. *Unpublished MSc thesis lodged in the library, Victoria University of Wellington.*

Van den Heuvel, H. (1960). The geology of the Flat Point area, eastern Wairarapa. *New Zealand Journal of Geology and Geophysics, 3(2),* 309-320.

Walker, R. G. (1978). Deep-water sandstone facies and ancient submarine fans: models for exploration for stratigraphic traps*. AAPG Bulletin, 62(6),* 932-966.

Walpole, L.W. (1940). Geological reconnaissance report on central Hawke's Bay, North Island, New Zealand (New Zealand Oil Exploration Ltd*.). Ministry of Economic Development New Zealand Unpublished Petroleum Report PR3.*

Walpole, L. W., & Burr, I. L. (1939). Report on Cretaceous Section exposed in the Mataikona River, Southern Hawkes Bay. *Ministry of Economic Development New Zealand Unpublished Petroleum Report PR8.*

Weimer, P., & Link, M. H. (1991). Global petroleum occurrences in submarine fans and turbidite systems. *Seismic facies and sedimentary processes of submarine fans and turbidite systems* Springer, New York (1991), 9-67.

Wellman, P. (1970). Geology of the Ngahape area, eastern Wairarapa. *Transactions of the Royal Society of New Zealand, earth sciences 8 (11),* 157-171.

Westech Energy Ltd. (2001). Hukarere-1 Well Completion Report (Westech Energy New Zealand Ltd). *Ministry of Economic Development New Zealand Unpublished Petroleum Report PR2656.*

Appendices

Appendix A: Paleocurrents. Averages calculated as per Fisher (1993).

Glenburn Coast

Location	Age	Current direction	Feature examined	Source
BQ35 382 209	Ra	105	Flute	This study
BQ35 410 282	Cn	90	Flute	Van den Heuval (1959)
BQ35 409 282	Cn	90	Cross-lamination	"
BQ35 430 323	Cn	100	Flute+Cross-lamination	"
BQ35 427 322	Ra-Rm?	85	Flute	"
BQ35 430 317	Ra-Rm?	95	Flute	"
BQ35 427 322	Ra-Rm?	90	Cross-lamination	"
BQ35 446 332	Ra-Rm?	80	Cross-lamination	"
BQ35 449 329	Rm-Rt?	55	Cross-lamination	"
BQ35 438 375	Rm-Rt?	90	Cross-lamination	"
BQ35 448 330	Rm-Rt?	50	Flute	"
BQ35 424 333	Rm-Rt?	140	Flute	"
BQ35 423 322	Rm-Rt?	90	Flute	"
BQ35 426 297	Rm-Rt?	105	Drag fold	"
BQ35 437 303	Mp	70	Cross-lamination	"
BQ35 411 341	Mp	260*	Flute	"
BQ35 332 335	Mp	65	Flute	"
BQ35 355 322	Mp	245*	Flute	"

*Possibly offset by 180°?

Glenburn Coast Circular Statistical averages:

Age:	Average
Ngaterian	93
Raukumara Series	88
Piripauan	68

Motuwaireka Stream

Location	Age	Current direction	Feature examined	Source
BP35 513 516	Mp	107°	Flute	This study
BP35 516 510	Rt-Mp	90°	Flute	"
BP35 516 510	Rt-Mp	95°	Flute	"
Average		97°	Flutes	

Mataikona River

Location	Age	Current direction	Feature examined	Source
BN36 739 860	Rm	116°	Flute	This study
BN36 736 868	Rt	94°	Flute	This study
Calc. Average	Rm-Mp	70°	Combined	Crampton (1997), Figure A1b
Calc. Average	Mh	110°	Combined	Crampton (1997), Figure A1a

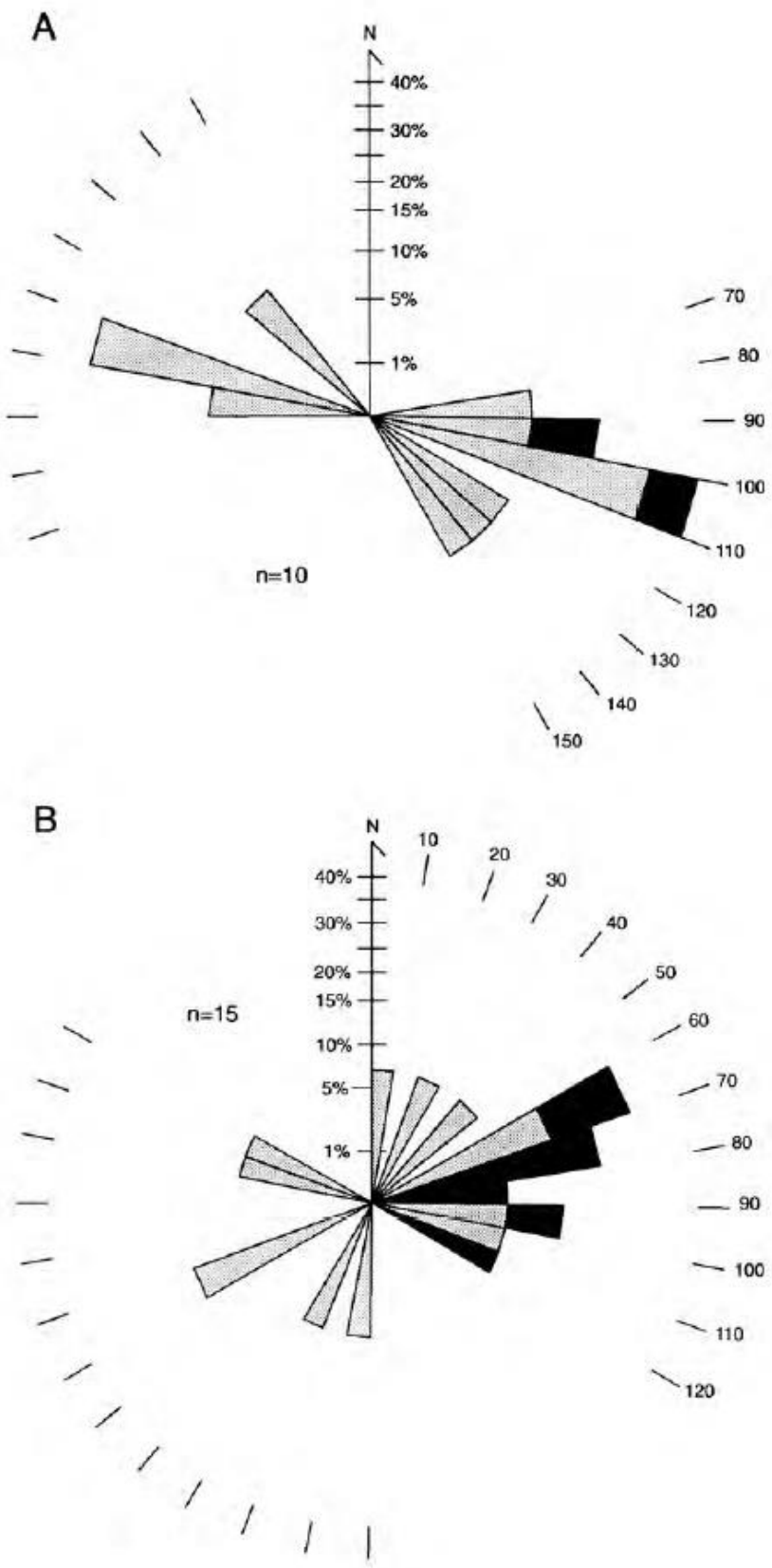

7

Figure A.0.1: Crampton (1997) Mataikona River paleocurrent rose diagrams. A = Haumurian, B = Mangaotanean to Piripauan. His Figure 10.

Waimata River

Location	Age	Current direction	Feature examined	Source
BN37 949 096	Rt	73°	Flute	This study
BN37 951 089	Rt	66°	Flute	This study
BN37 951 089	Rt	74°	Cross-beds	This study
Average		71°		

Additional paleocurrents:

Totara Stream: "North-south" – Moore (1980).

Johnston (1971) – Southeast" – 135?

Waimarama Beach: Pettinga (1980), see figure A.2.

"Te Ahau Member" = 97°

"Te Puku Member" = 172.5°

"Te Wainohu Member" #1 = 98.4°

"Te Wainohu Member" #2 = 139.6°

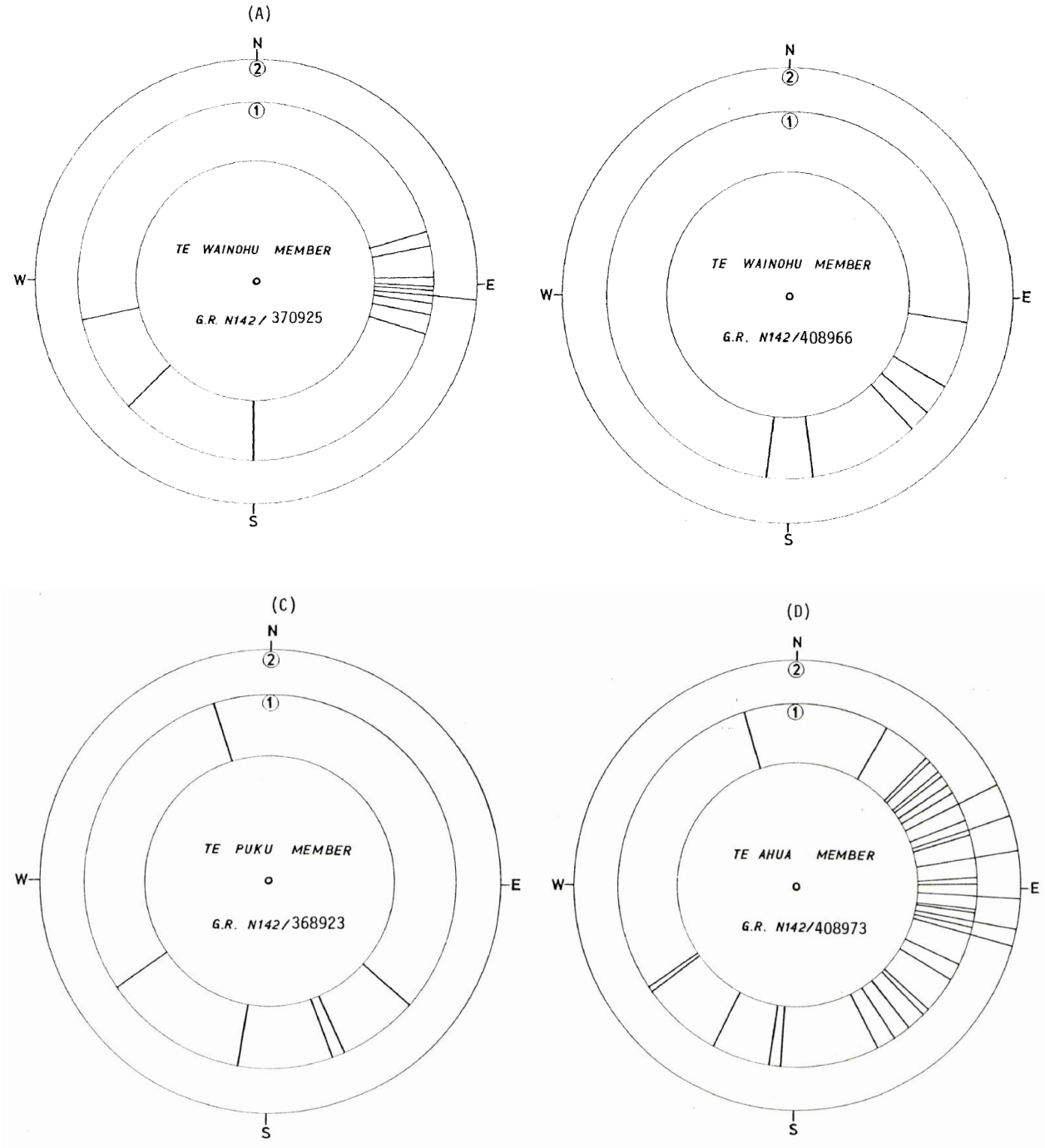

Figure A.2: Pettinga (1980) rose diagrams. His Figure 10.3.

Appendix B: Index of fossils

All fossils identified in this study by either J. McClintock using descriptions from Crampton (1996) or J. Crampton.

Honeycomb Light

Name/FR #	Species	Age	Grid Ref
HCL 1	*I. fyfei*	Ngaterian	BQ35 370 190
HCL 2	*M. rangatira ?haroldi*	Arowhanan	BQ35 369 188

Horewai Point

Name/FR #	Species	Age	Grid Ref
HP1	*I. fyfei*	Ngaterian	BQ35 380 208
HP2	*I. fyfei*	Ngaterian	BQ35 380 208
T27/f0353	*M. rangatira haroldi*	Arowhanan	BQ35 381 208
HP2	*M. rangatira ?haroldi*	Arowhanan	BQ35 381 208
T27/f0361	*M. rangatira rangarira*	Arowhanan	BQ35 381 208

Totara Stream

Name/FR #	Species	Age	Grid Ref
TS 1	*C. bicorrugatus ?bicorrugatus*	Mangaotanean	BP35 460 423
TS 2	*I. ?opetius*	Tertatan	BP35 457 424
T27/f0329	*I. opetius*	Teratan	BP35 456 424
T27/f0331	*I. ?pacificus*	Piripauan	BP35 453 424

Motuwaireka Stream

Name/FR #	Species	Age	Grid Ref
T26/f9531*	*C. Bicorrugatus?*	Rm	BP36 524 498
MW1	*I. spedeni*	Rm-Rt	BP36 521 502
T26/f0437	*I. opetius*	Teratan	BP35 518 506
MW2	*I. australis*	Piripauan	BP35 513 515

*Fossil was found below bottom of measured section

Mataikona River

Name/FR #	Species	Age	Grid Ref
MT1	*C. bicorrugatus ?bicorrugatus*	Mangaotanean	BN36 745 859
U25/f0236	*C. bicorrugatus bicorrugatus*	Mangaotanean	BN36 740 859
U25/f0239	*I. opetius, I. ?madagascariensis*	Teratan	BN36 739 859
U25/f0238	*I. ?madagascariensis*	Teratan	BN36 736 860
MT2*	*I. pacificus*	Piripauan	BN36 729 856

*Field record from Crampton (1997)

U25/f6584

Waimata River

Name/FR #	Species	Age	Grid Ref
WT1	*I. opetius*	Teratan	BN37 949 095
WT2	*I. madagascariensis*	Teratan	BN37 942 104
U24/f9505*	*I. pacificus*	Piripauan	BN37 948 097

*Outcrop currently obscured, but demonstrates Piripauan sediment is present in the area.

Mangakuri Beach

Name/FR #	Species	Age	Grid Ref
V23/f6494	*I. pacificus*	Piripauan	BL39 324 636
MK1	*I. pacificus*	Piripauan	BL39 333 649
V23/f0078	*I. opetius*	Teratan	BL39 336 657
V23/f6550	*I. pacificus*	Piripauan	BL39 336 661
MK2	*I. ?australis*	Piripauan	BL39 337 662
MK3	*I. madagascariensis*	Teratan	BL39 353 693

Waimarama

Name/FR #	Species	Age	Grid Ref
WM1	*I. opetius*	Teratan	BL39 402 791
W22/f8610	*C. ?bicorrugatus*	Mangaotanean?	BL39 405 798
WM2	*I. madagascariensis*	Teratan	BL39 411 807
WM3	*I. opetius*	Teratan	BL39 426 826

Appendix C: Legend for Measured Sections

Lithology

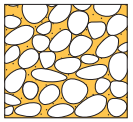
Conglomerate or pebbly sandstone

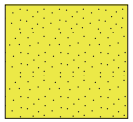
Sandstone

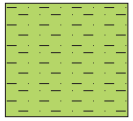
Sandy silt or thin sand-mud couplets

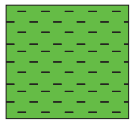
Mudstone

Volcanic rocks

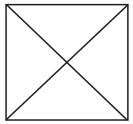
Missing outcrop

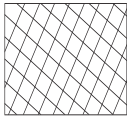
Missing outcrop - distance unknown

Additional symbols

Bedded, thickness indicated

Non-bedded (massive)

Cross-laminated

Parallel-laminated

Wavy-laminated

Convolute-laminated

Normally graded

Inversely graded

Slump structures

Conglomerate band/lens

Thin sandstoneband

Channelised

Fossil locality (this study)

Fossil locality (FRED)

Concretion

Concretionary layers

Clast imbrication

Rafted sandstone clasts

Rip-up clast

Intact shells

Shell fragments

Bioturbation

Burrows

Carbonaceous material

( ) Indicates minor occurance

P Pyrite

Scale break

F. 1.1a Figure, number indicated

Appendix D: Honeycomb Light Measured Section

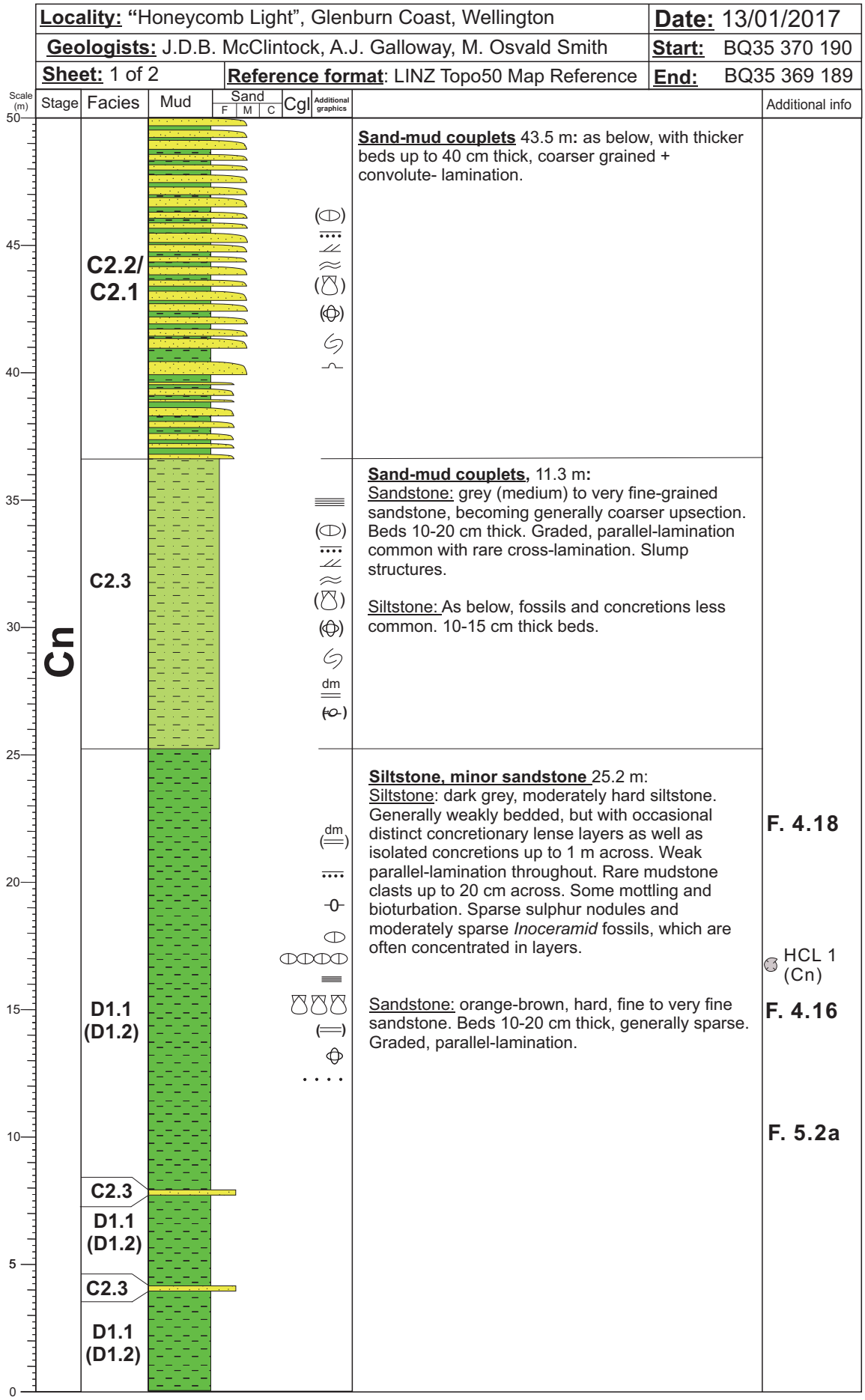

S

S , min M , con

C2

Sheet:

HCL 2M

C2

C2

5560657075808590951005 0Sand/mud couplets, continued from page 1. Bed thickness and coarseness of sandstone highly variable. Coarse, up to 1 m thick sandsto

m)

C2

Scale

Appendix E: Measured Section of Horewai Point

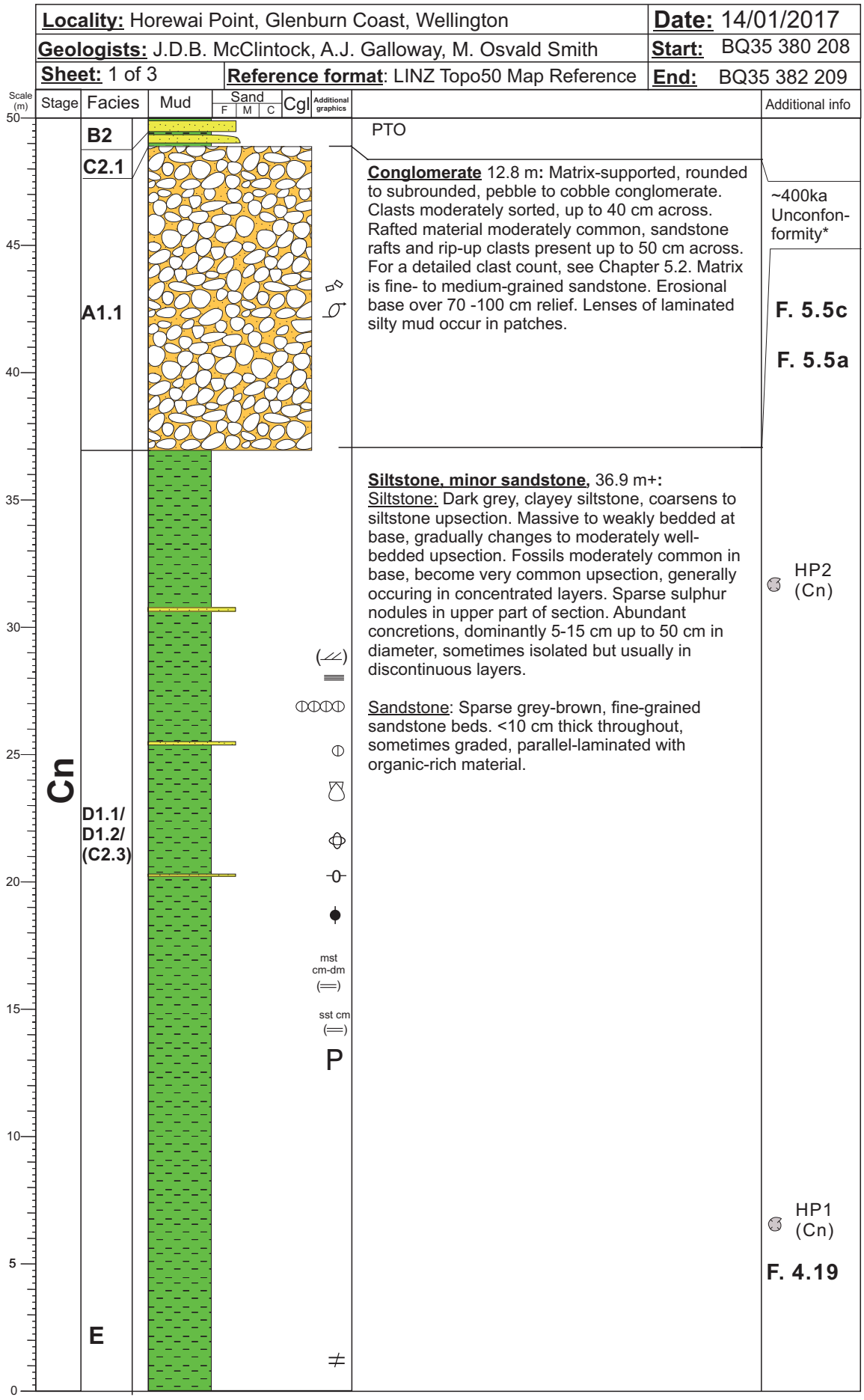

Locality: Horewai Point, Glenburn Coast, Wellington | **Date:** 14/01/2017

Geologists: J.D.B. McClintock, A.J. Galloway, M. Osvald Smith | **Start:** BQ35 380 208

Sheet: 2 of 3 | **Reference format**: LINZ Topo50 Map Reference | **End:** BQ35 382 209

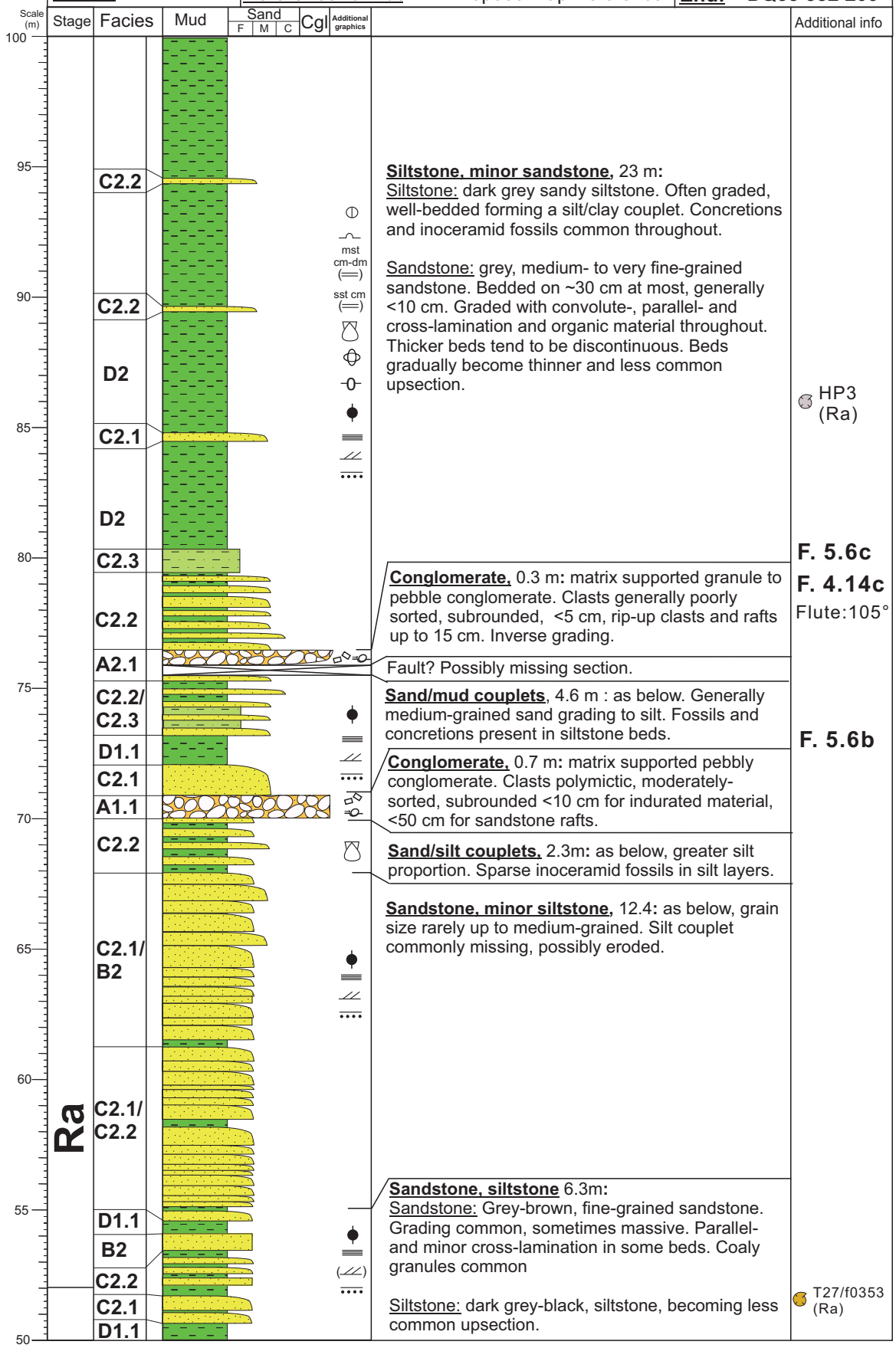

Locality: Horewai Point, Glenburn Coast, Wellington | **Date:** 14/01/2017

Geologists: J.D.B. McClintock, A.J. Galloway, M. Osvald Smith | **Start:** BQ35 380 208

Sheet: 3 of 3 | **Reference format**: LINZ Topo50 Map Reference | **End:** BQ35 382 209

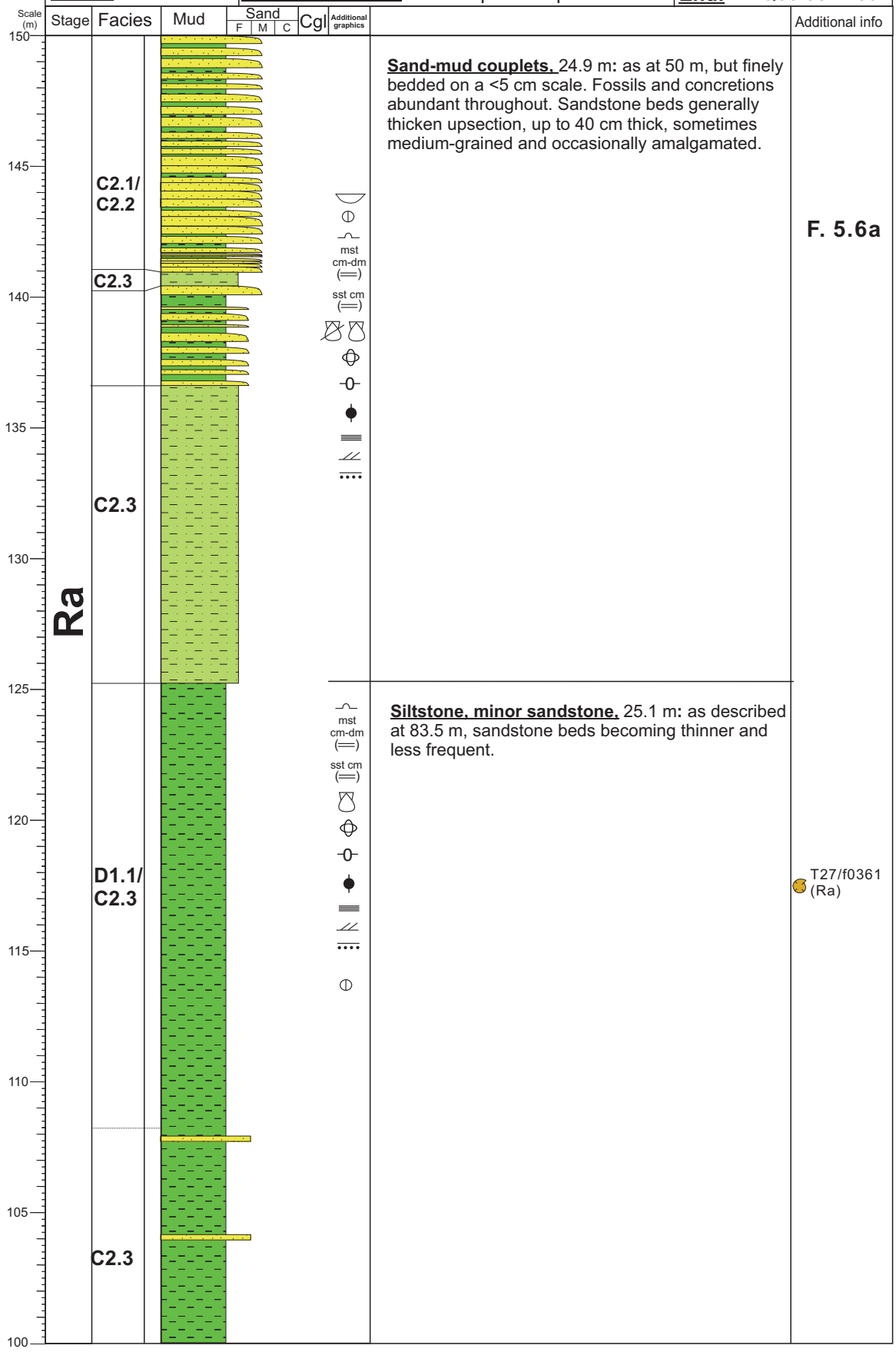

Appendix F: Measured Section of Totara Stream

Locality: Totara Stream, Ngahape, Wellington | **Date:** 16/04/2017

Geologists: J.D.B. McClintock, A.J. Galloway, M. Osvald Smith | **Start:** BP35 460 423

Sheet: 1 of 9 | **Reference format**: LINZ Topo50 Map Reference | **End:** BP35 448 428

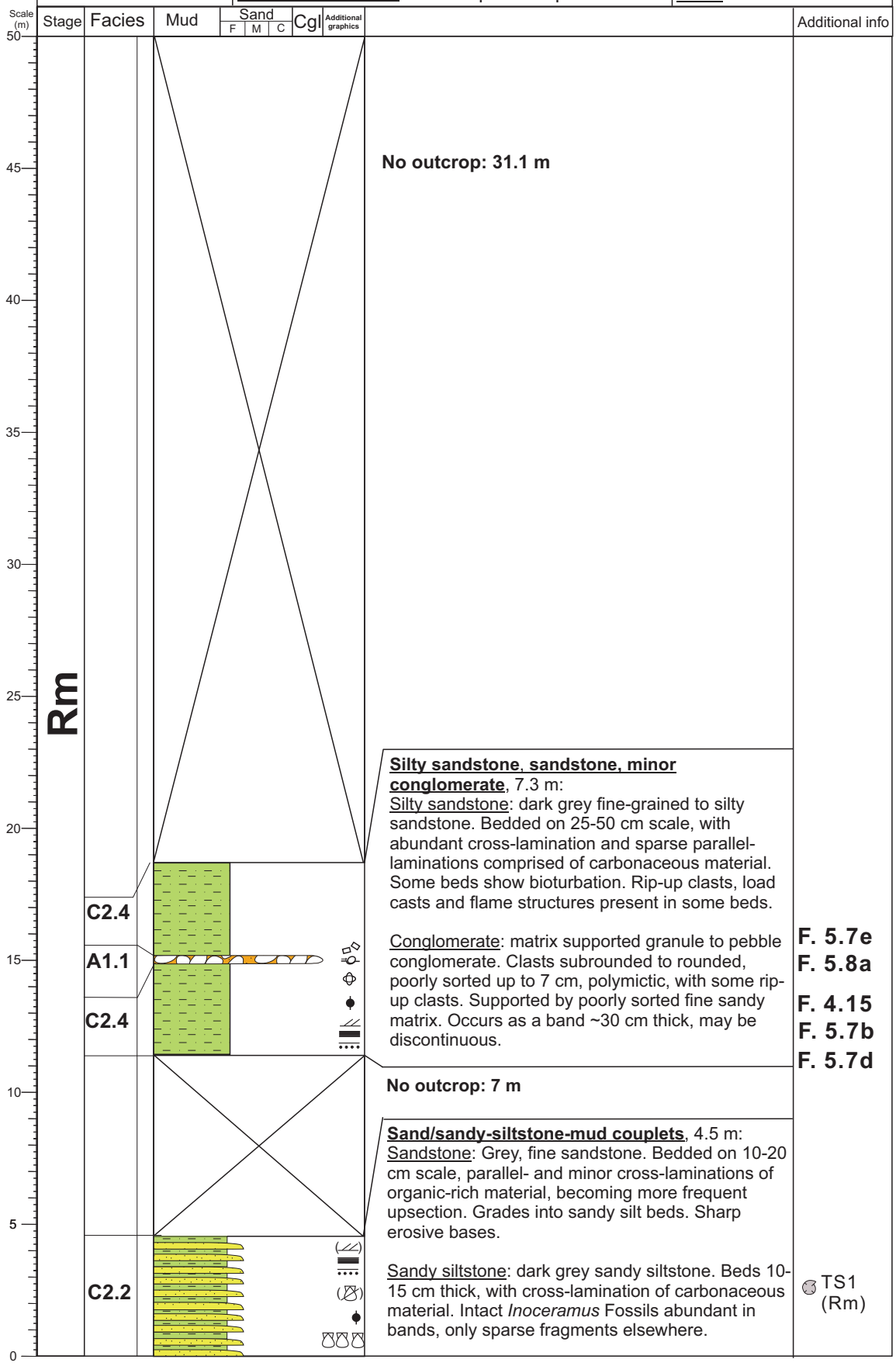

Locality: Totara Stream, Ngahape, Wellington | **Date:** 16/04/2017

Geologists: J.D.B. McClintock, A.J. Galloway, M. Osvald Smith | **Start:** BP35 460 423

Sheet: 2 of 9 | **Reference format**: LINZ Topo50 Map Reference | **End:** BP35 448 428

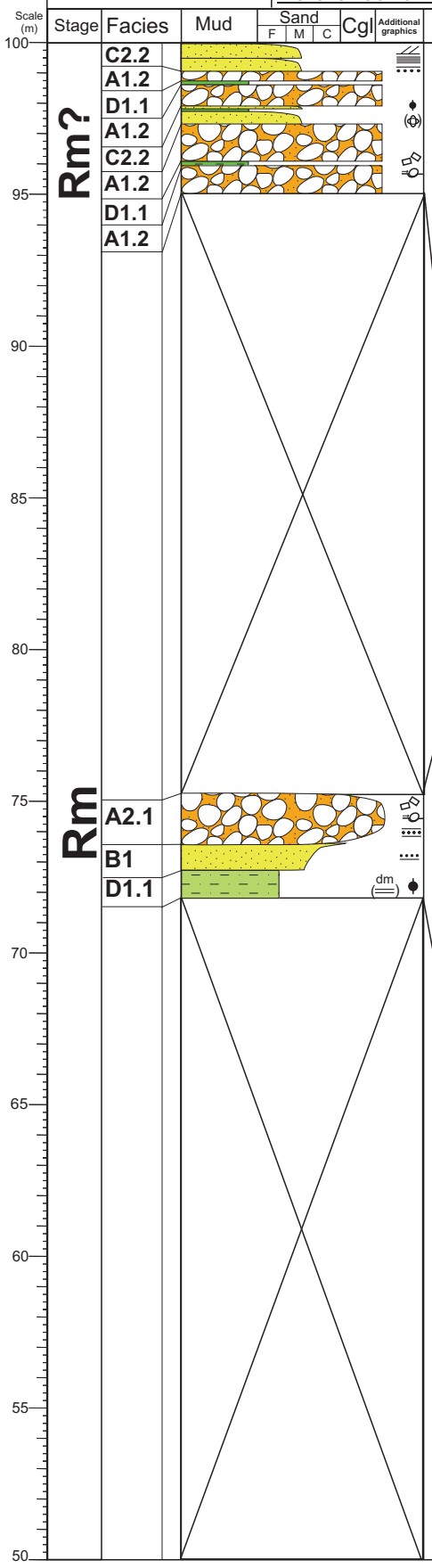

Conglomerate, sandstone, minor siltstone, 5 m:
Conglomerate: Matrix supported, granule to sparse cobble conglomerate. Clasts polymictic, moderately sorted, mostly 1-3 cm but occasional <25 cm cobbles. Rip-up clasts abundant. Supported by muddy matrix.

Pebbly mudstone (from 97.8-98.6 m): Very poorly sorted pebbly mud. Muddy matrix supported, sparse 5-10cm clasts but mostly 2-4cm granules.

Sandstone: Orange-brown to grey medium to fine-grained moderately-sorted sandstone. Normally graded, amalgamated. Parallel- and cross-lamination common. Beds 20-30cm thick.

Siltstone: Dark grey siltstone. Heavily weathered, minor bioturbation.

No outcrop, 19.2 m

Conglomerate, sandstone, siltstone, 3.2 m:
Conglomerate: clast- to matrix-supported, pebble to cobble conglomerate. Clasts polymictic, poorly sorted, subrounded to subangular, mostly between 2-20 cm in diameter, some up to 30 cm. Matrix of poorly sorted sand. Inverse grading over lower 30 cm, possible minor normal grading in top ~50 cm.

Sandstone: Light grey, fine-grained, well-sorted sandstone. Sharp lower contact with siltstone. No obvious bedding, occasional 2-5 cm clast in upper part as it grades into the overlying conglomerate.

Siltstone: Dark grey, sandy siltstone. Heavily weathered, weakly bedded on dm scale.

No outcrop, 22.6 m

Additional info

F. 4.8a

Locality: Totara Stream, Ngahape, Wellington | **Date:** 16/04/2017

Geologists: J.D.B. McClintock, A.J. Galloway, M. Osvald Smith | **Start:** BP35 460 423

Sheet: 3 of 9 | **Reference format**: LINZ Topo50 Map Reference | **End:** BP35 448 428

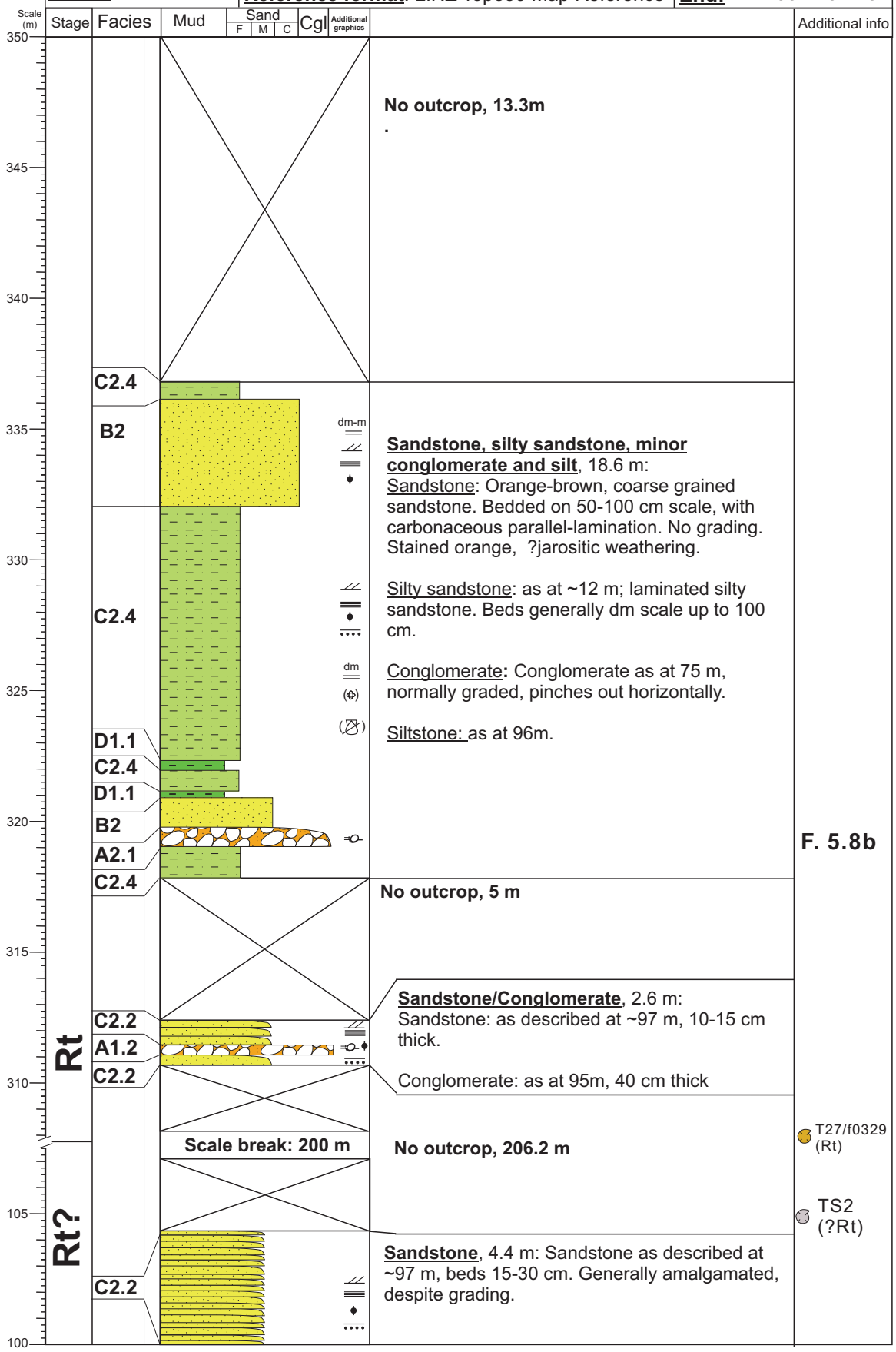

Locality: Totara Stream, Ngahape, Wellington | **Date:** 16/04/2017

Geologists: J.D.B. McClintock, A.J. Galloway, M. Osvald Smith | **Start:** BP35 460 423

Sheet: 4 of 9 | **Reference format**: LINZ Topo50 Map Reference | **End:** BP35 448 428

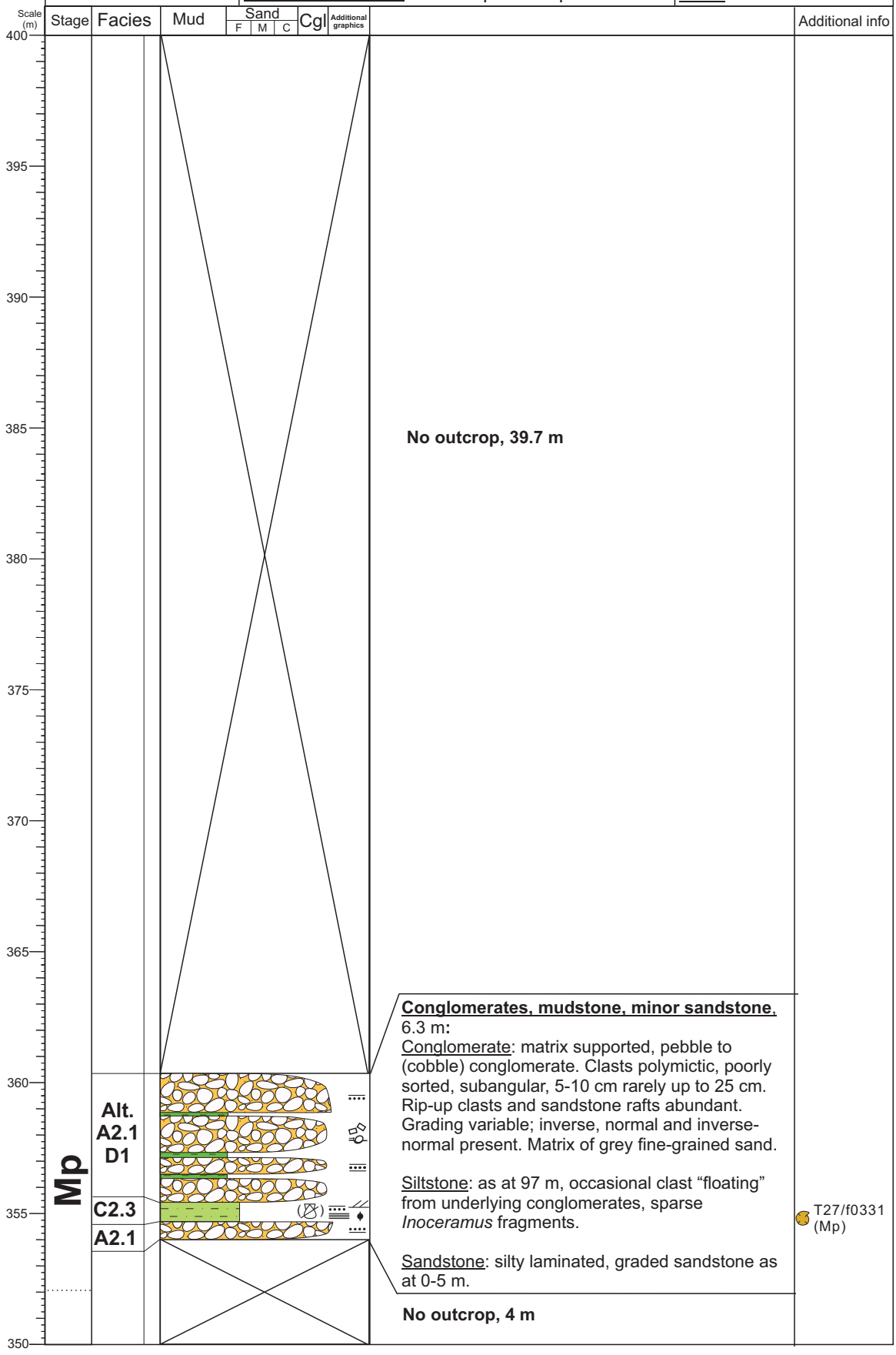

Locality: Totara Stream, Ngahape, Wellington | **Date:** 16/04/2017

Geologists: J.D.B. McClintock, A.J. Galloway, M. Osvald Smith | **Start:** BP35 460 423

Sheet: 5 of 9 | **Reference format**: LINZ Topo50 Map Reference | **End:** BP35 448 428

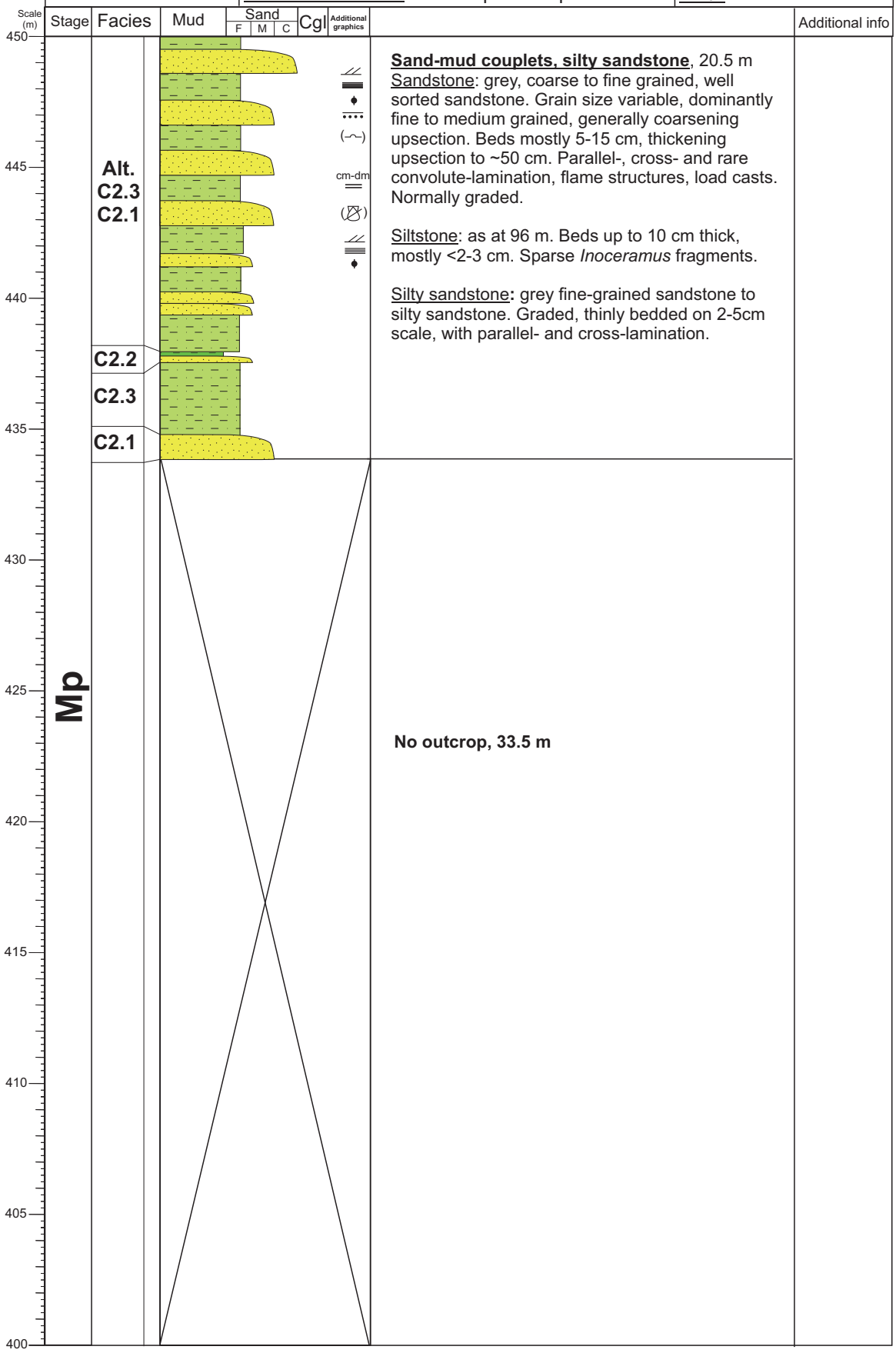

Locality: Totara Stream, Ngahape, Wellington | **Date:** 16/04/2017

Geologists: J.D.B. McClintock, A.J. Galloway, M. Osvald Smith | **Start:** BP35 460 423

Sheet: 6 of 9 | **Reference format**: LINZ Topo50 Map Reference | **End:** BP35 448 428

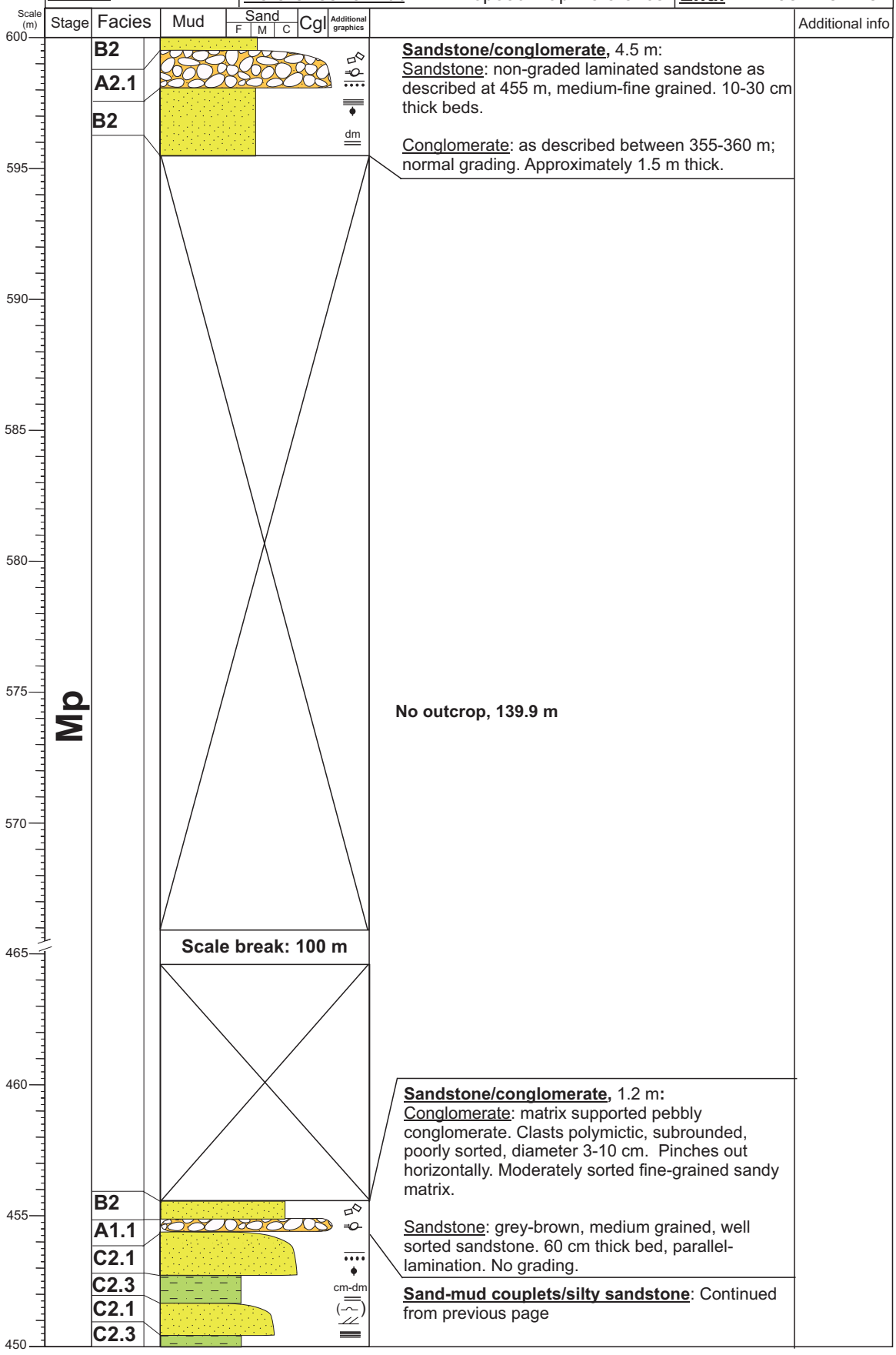

Locality: Totara Stream, Ngahape, Wellington | **Date:** 16/04/2017

Geologists: J.D.B. McClintock, A.J. Galloway, M. Osvald Smith | **Start:** BP35 460 423

Sheet: 7 of 9 | **Reference format**: LINZ Topo50 Map Reference | **End:** BP35 448 428

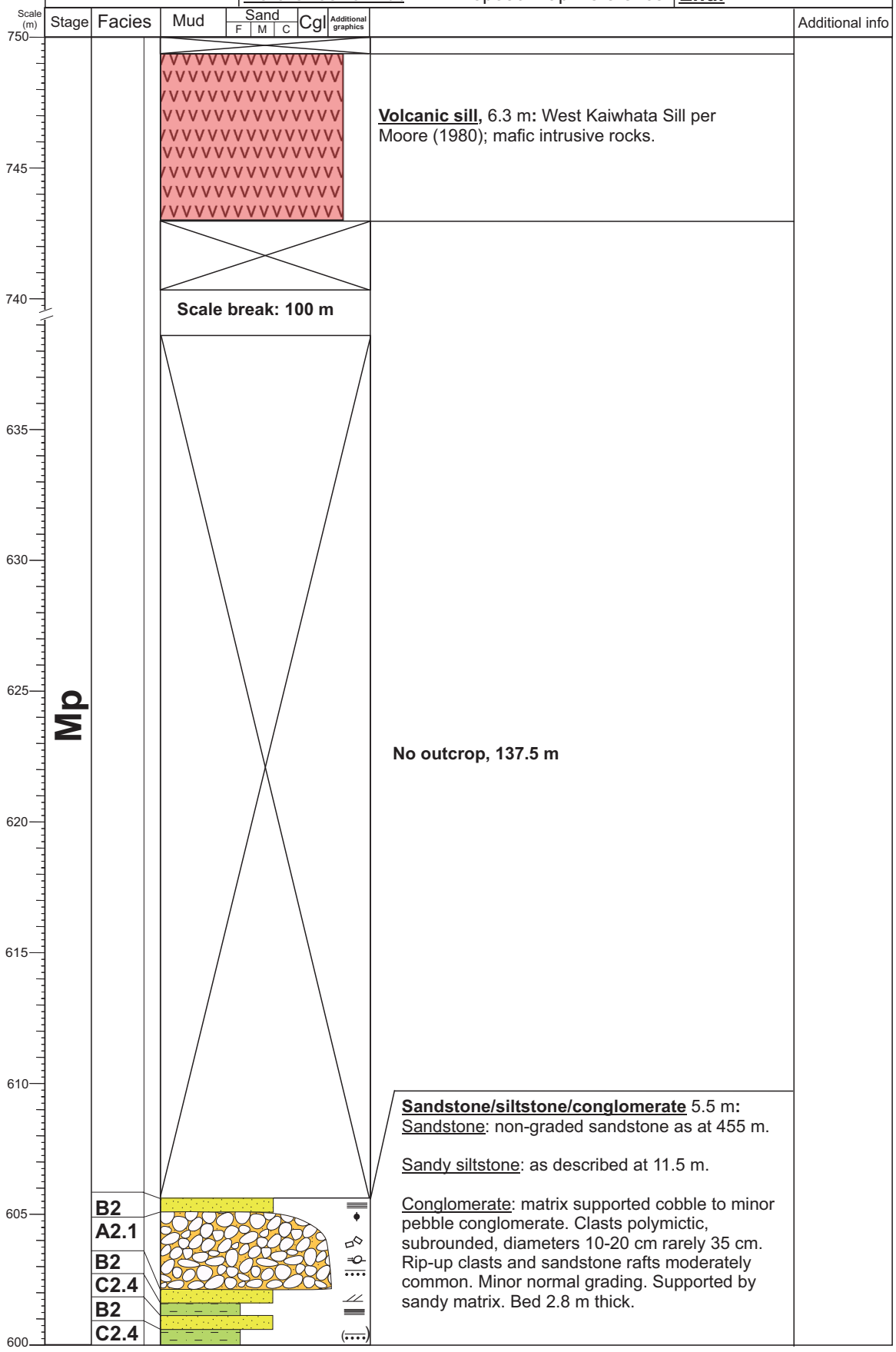

Locality: Totara Stream, Ngahape, Wellington | **Date:** 16/04/2017

Geologists: J.D.B. McClintock, A.J. Galloway, M. Osvald Smith | **Start:** BP35 460 423

Sheet: 8 of 9 | **Reference format**: LINZ Topo50 Map Reference | **End:** BP35 448 428

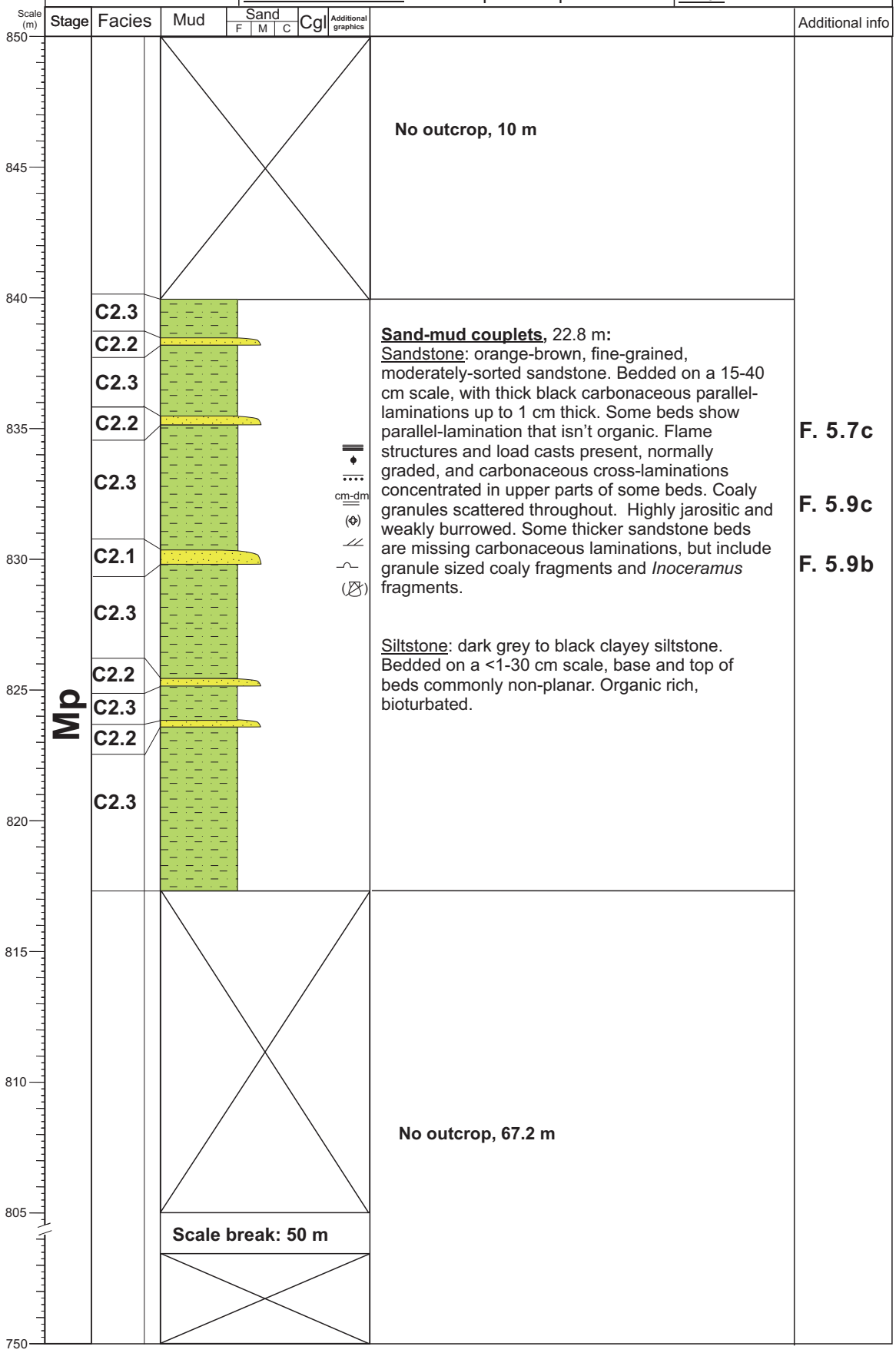

Locality: Totara Stream, Ngahape, Wellington | **Date:** 16/04/2017

Geologists: J.D.B. McClintock, A.J. Galloway, M. Osvald Smith | **Start:** BP35 460 423

Sheet: 9 of 9 | **Reference format**: LINZ Topo50 Map Reference | **End:** BP35 448 428

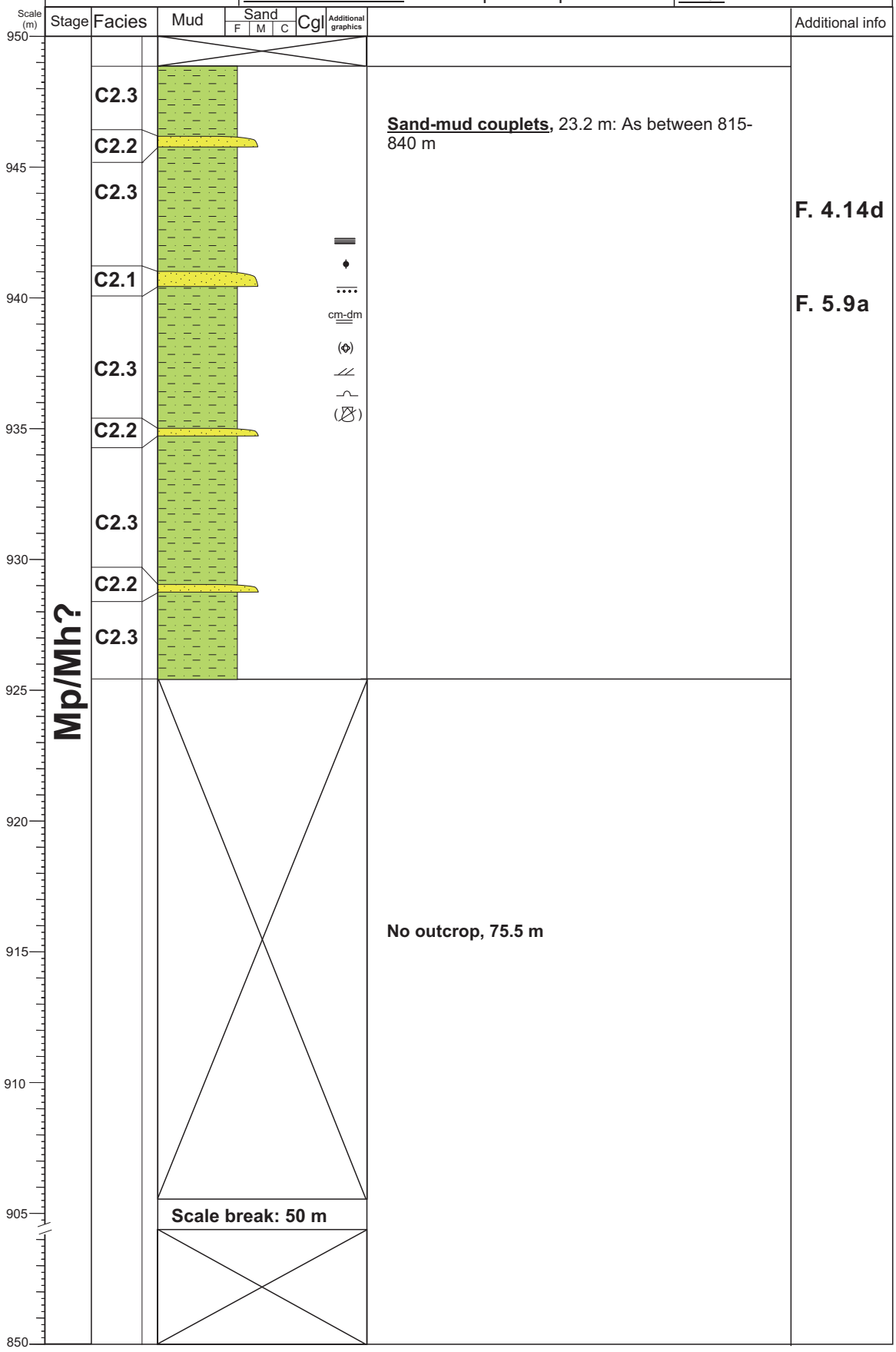

Appendix G: Motuwaireka Stream Measured Section

Locality: Motuwaireka Stream, Riversdale, Wellington | **Date:** 23/04/2017

Geologists: J.D.B. McClintock, A.J. Galloway, M. Osvald Smith | **Start:** BP36 522 499

Sheet: 1 of 13 | **Reference format**: LINZ Topo50 Map Reference | **End:** BP35 513 515

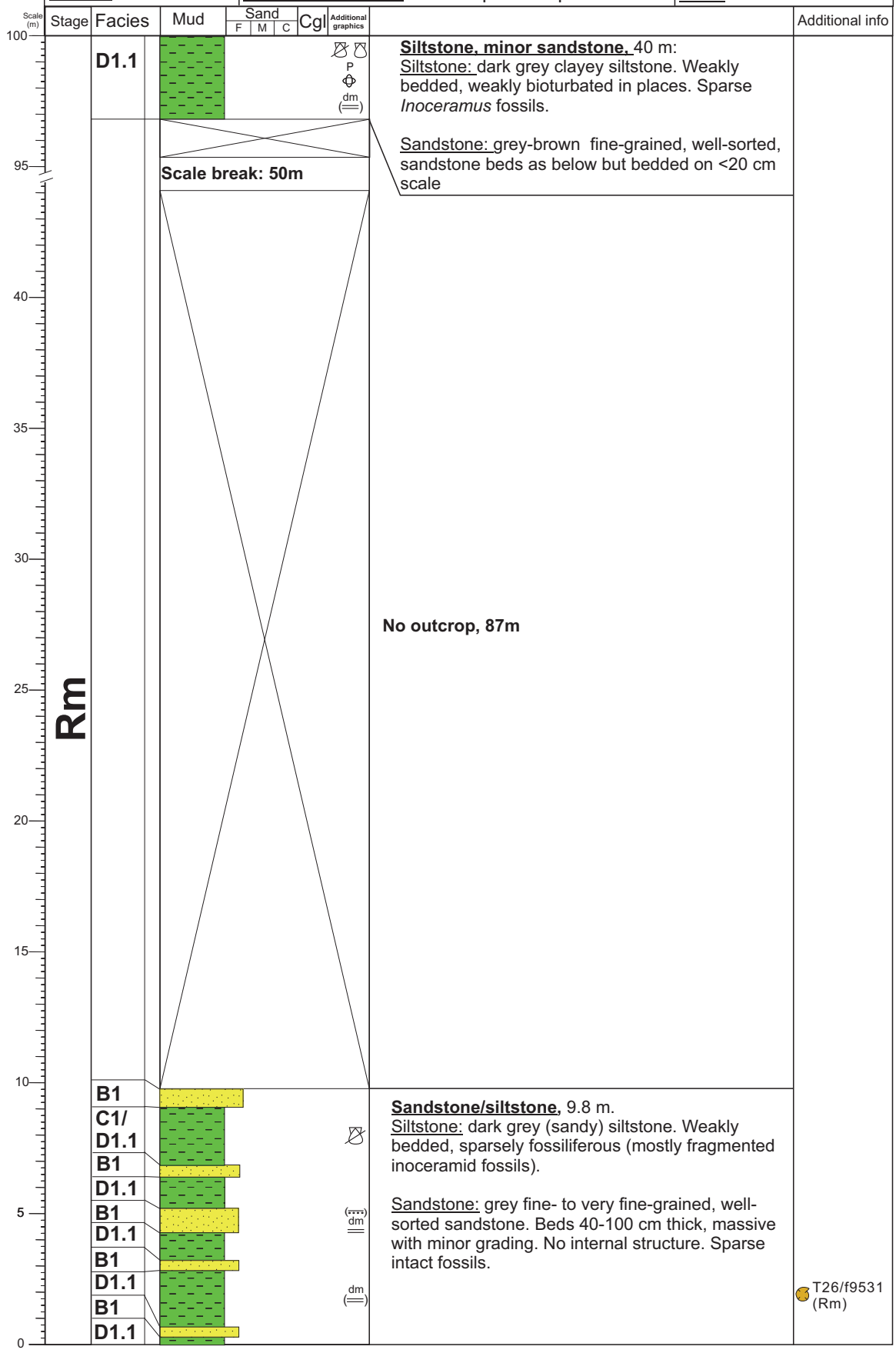

Locality: Motuwaireka Stream, Riversdale, Wellington | **Date:** 23/04/2017

Geologists: J.D.B. McClintock, A.J. Galloway, M. Osvald Smith | **Start:** BP36 522 499

Sheet: 2 of 13 | **Reference format**: LINZ Topo50 Map Reference | **End:** BP35 513 515

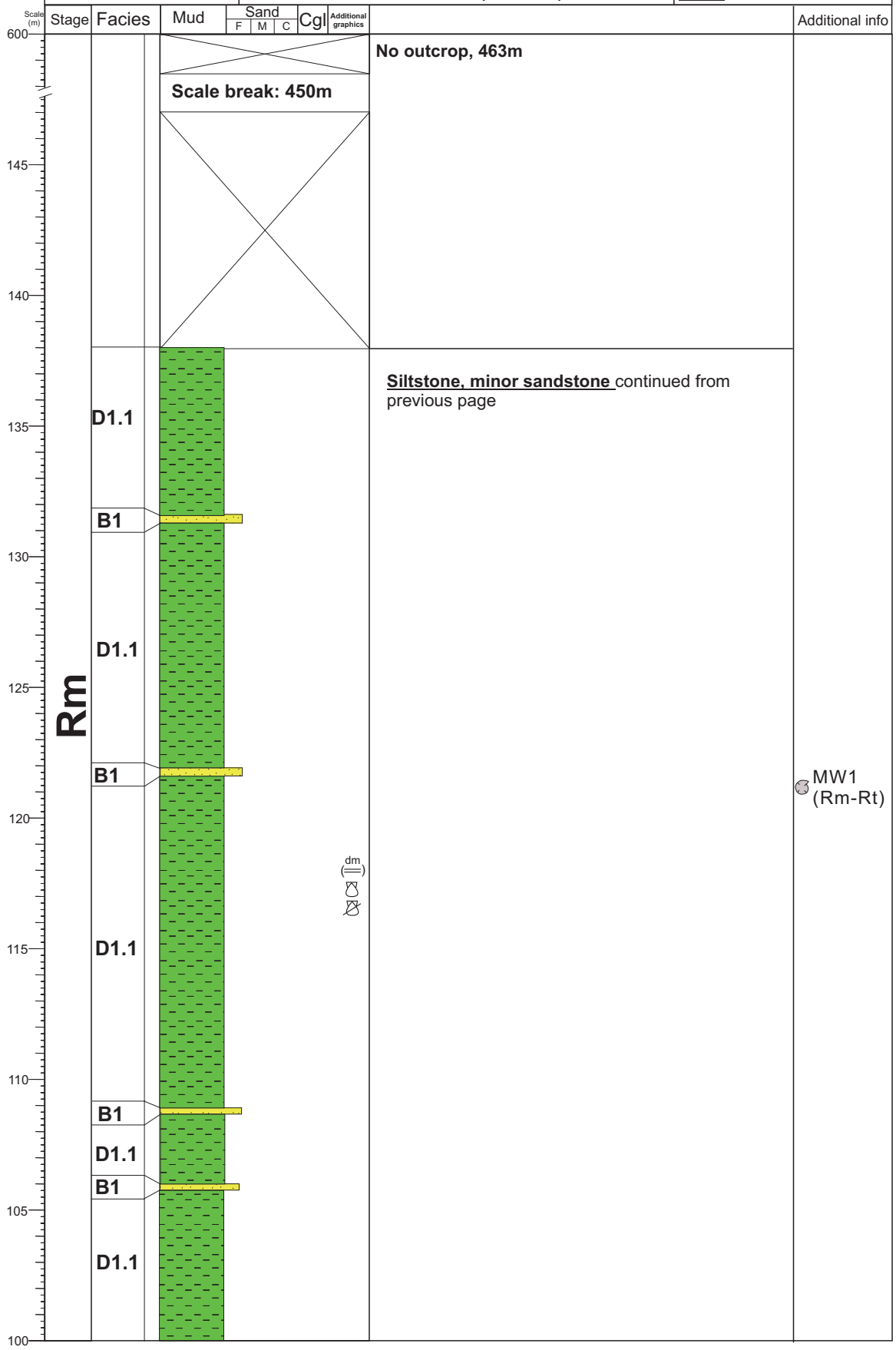

Locality: Motuwaireka Stream, Riversdale, Wellington | **Date:** 23/04/2017

Geologists: J.D.B. McClintock, A.J. Galloway, M. Osvald Smith | **Start:** BP36 522 499

Sheet: 3 of 13 | **Reference format**: LINZ Topo50 Map Reference | **End:** BP35 513 515

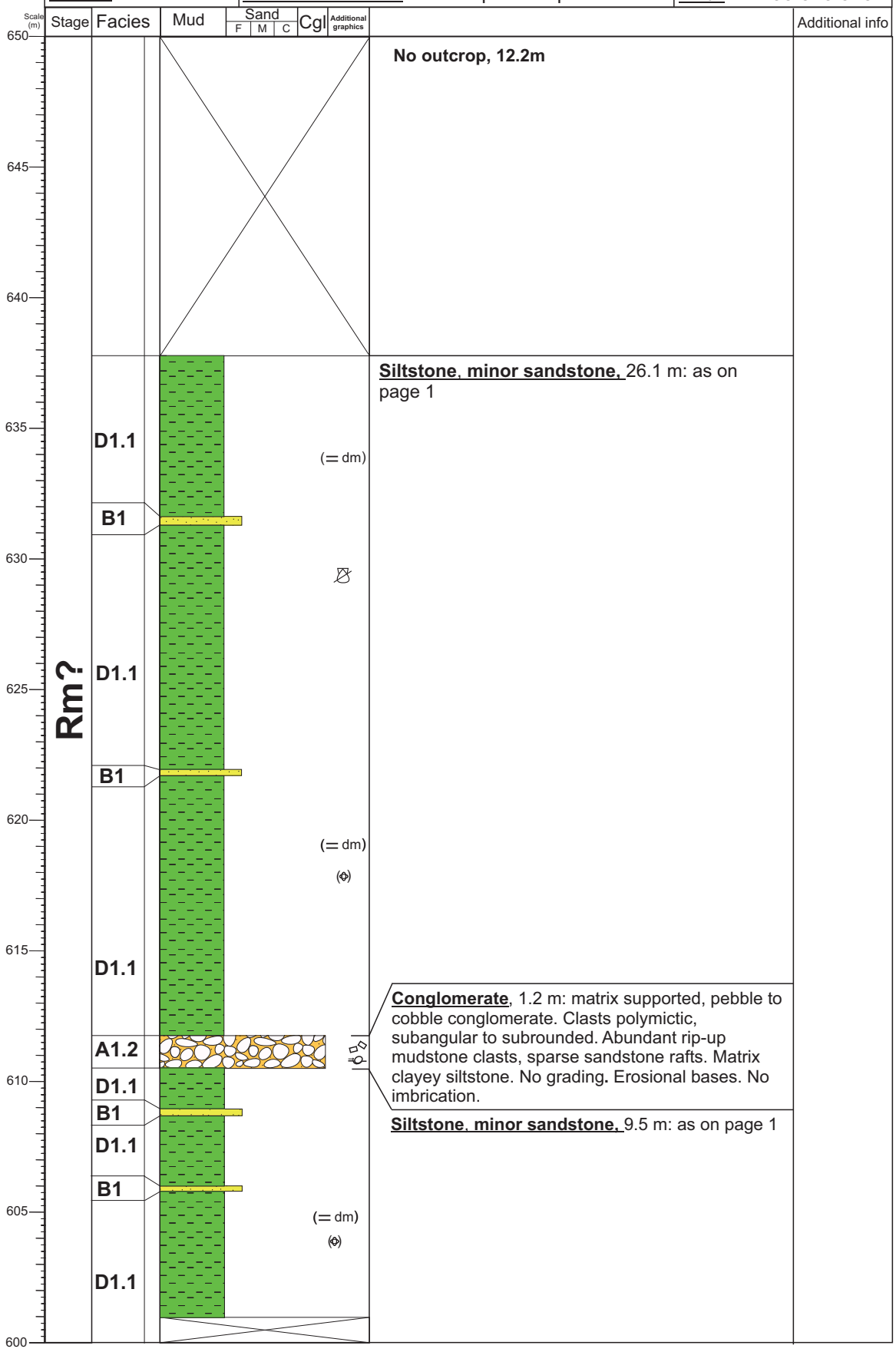

Locality: Motuwaireka Stream, Riversdale, Wellington | **Date:** 23/04/2017

Geologists: J.D.B. McClintock, A.J. Galloway, M. Osvald Smith | **Start:** BP36 522 499

Sheet: 4 of 13 | **Reference format**: LINZ Topo50 Map Reference | **End:** BP35 513 515

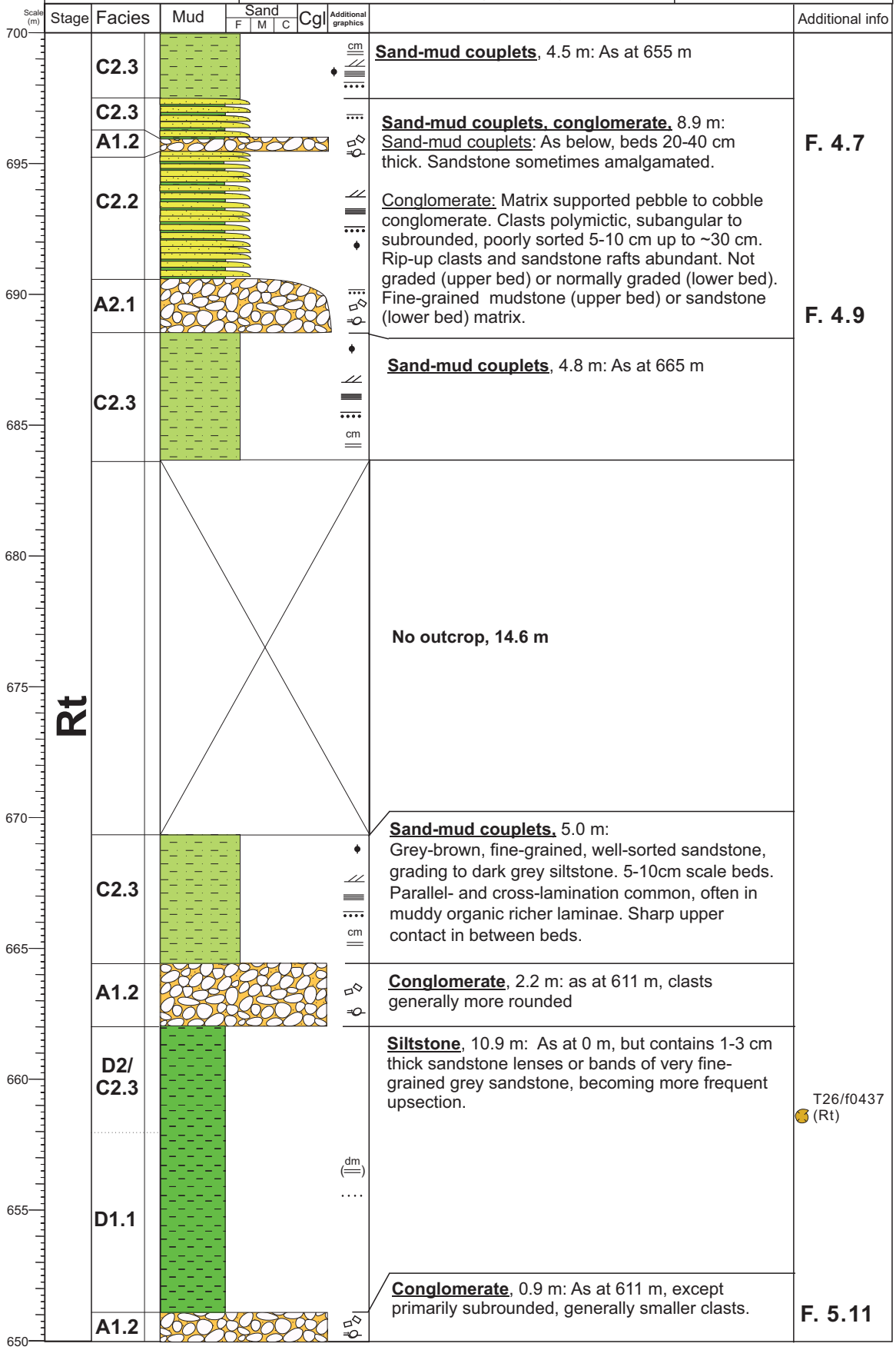

Locality: Motuwaireka Stream, Riversdale, Wellington | **Date:** 23/04/2017

Geologists: J.D.B. McClintock, A.J. Galloway, M. Osvald Smith | **Start:** BP36 522 499

Sheet: 5 of 13 | **Reference format**: LINZ Topo50 Map Reference | **End:** BP35 513 515

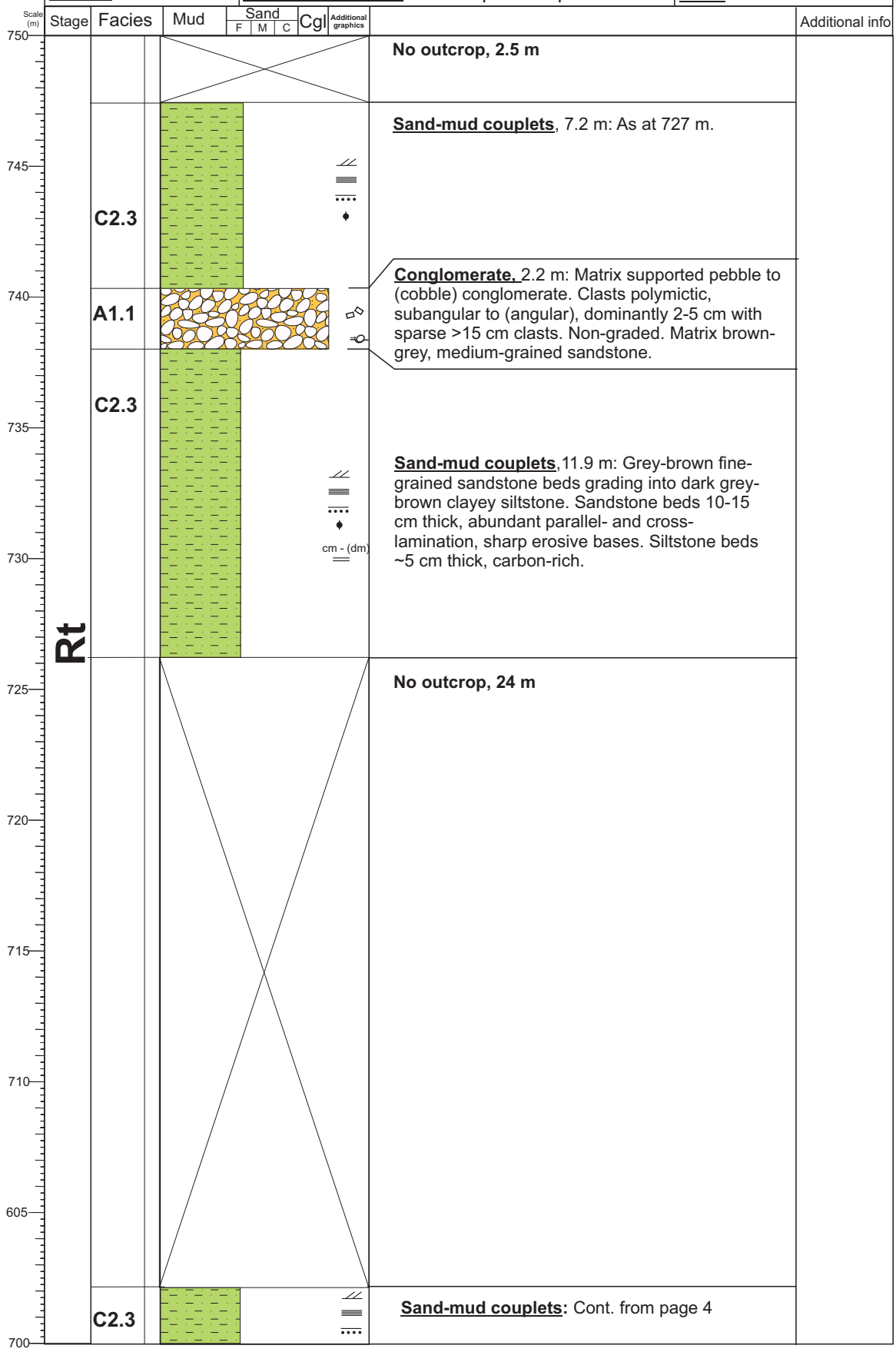

Locality: Motuwaireka Stream, Riversdale, Wellington | **Date:** 23/04/2017

Geologists: J.D.B. McClintock, A.J. Galloway, M. Osvald Smith | **Start:** BP36 522 499

Sheet: 6 of 13 | **Reference format**: LINZ Topo50 Map Reference | **End:** BP35 513 515

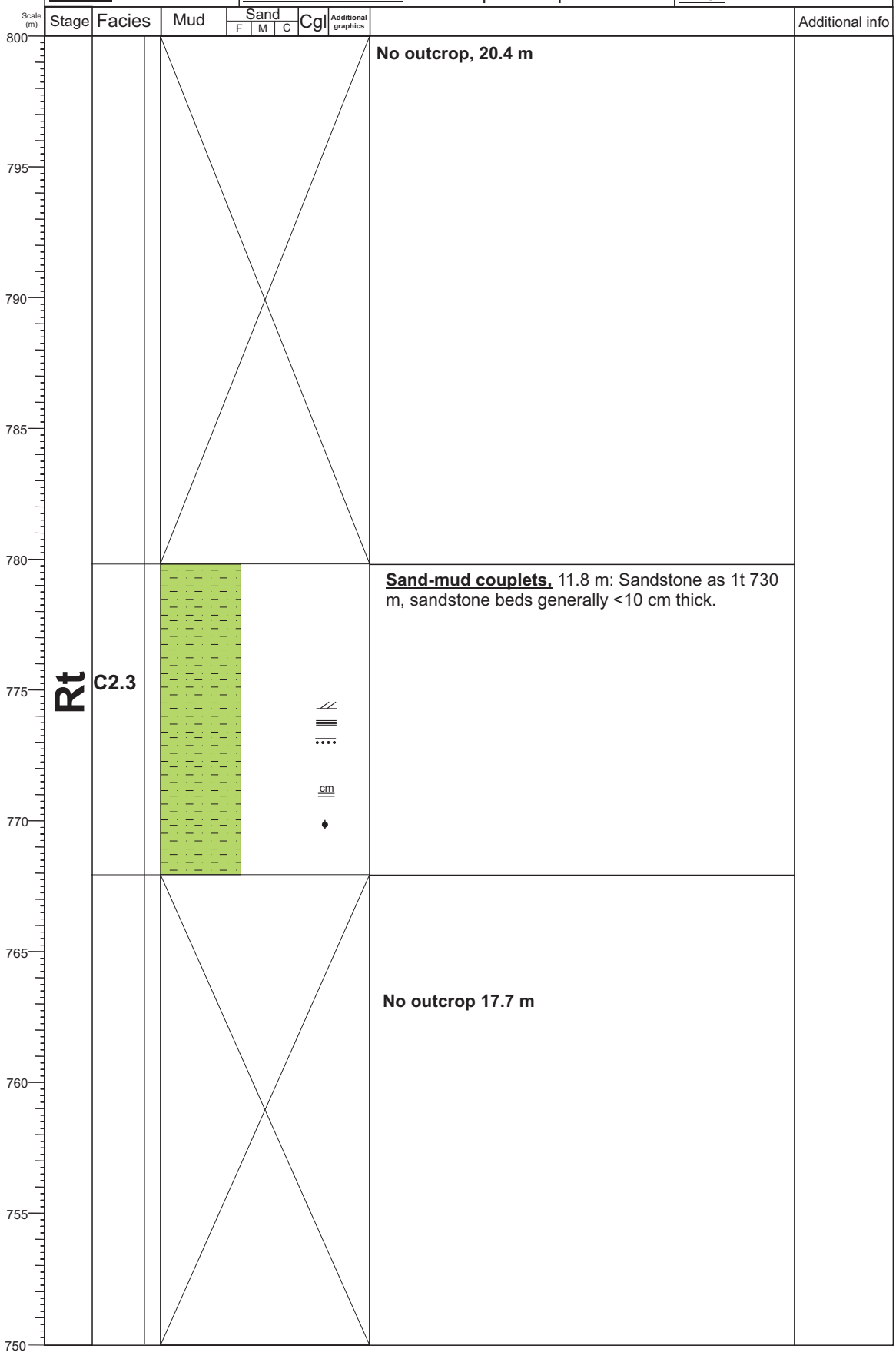

Locality: Motuwaireka Stream, Riversdale, Wellington | **Date:** 23/04/2017

Geologists: J.D.B. McClintock, A.J. Galloway, M. Osvald Smith | **Start:** BP36 522 499

Sheet: 7 of 13 | **Reference format**: LINZ Topo50 Map Reference | **End:** BP35 513 515

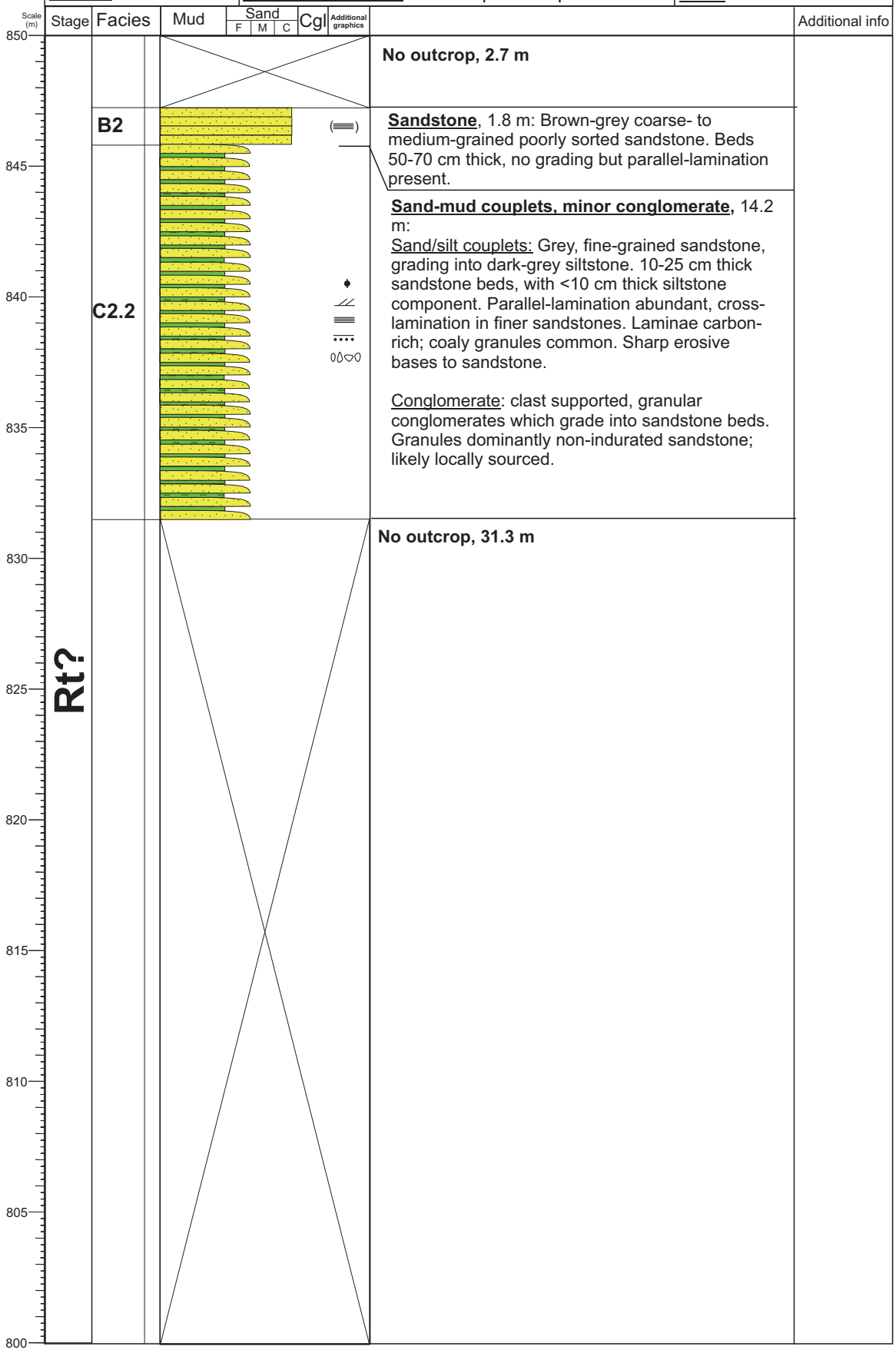

Locality: Motuwaireka Stream, Riversdale, Wellington | **Date:** 23/04/2017

Geologists: J.D.B. McClintock, A.J. Galloway, M. Osvald Smith | **Start:** BP36 522 499

Sheet: 8 of 13 | **Reference format**: LINZ Topo50 Map Reference | **End:** BP35 513 515

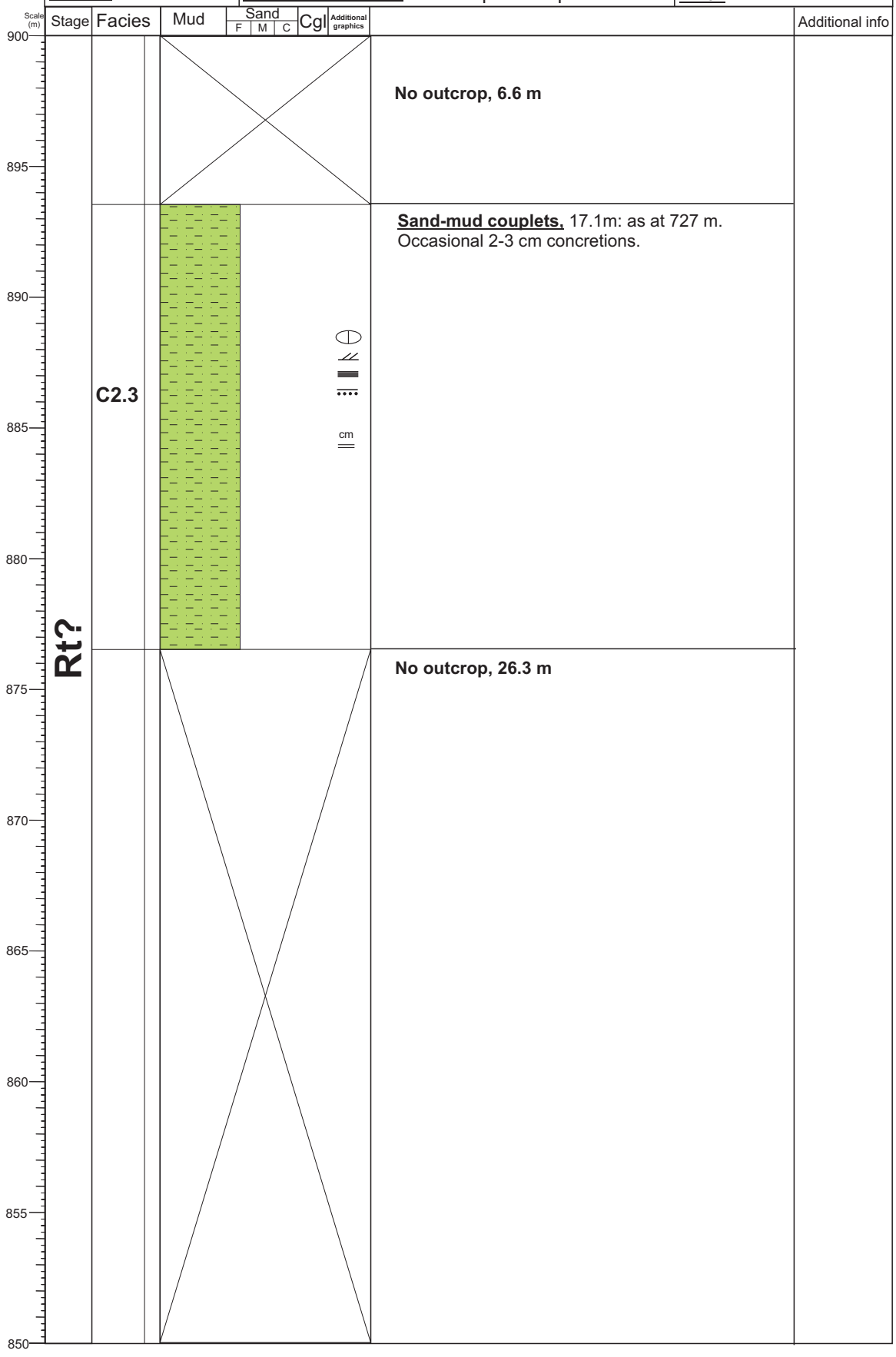

Locality: Motuwaireka Stream, Riversdale, Wellington | **Date:** 23/04/2017

Geologists: J.D.B. McClintock, A.J. Galloway, M. Osvald Smith | **Start:** BP36 522 499

Sheet: 9 of 13 | **Reference format**: LINZ Topo50 Map Reference | **End:** BP35 513 515

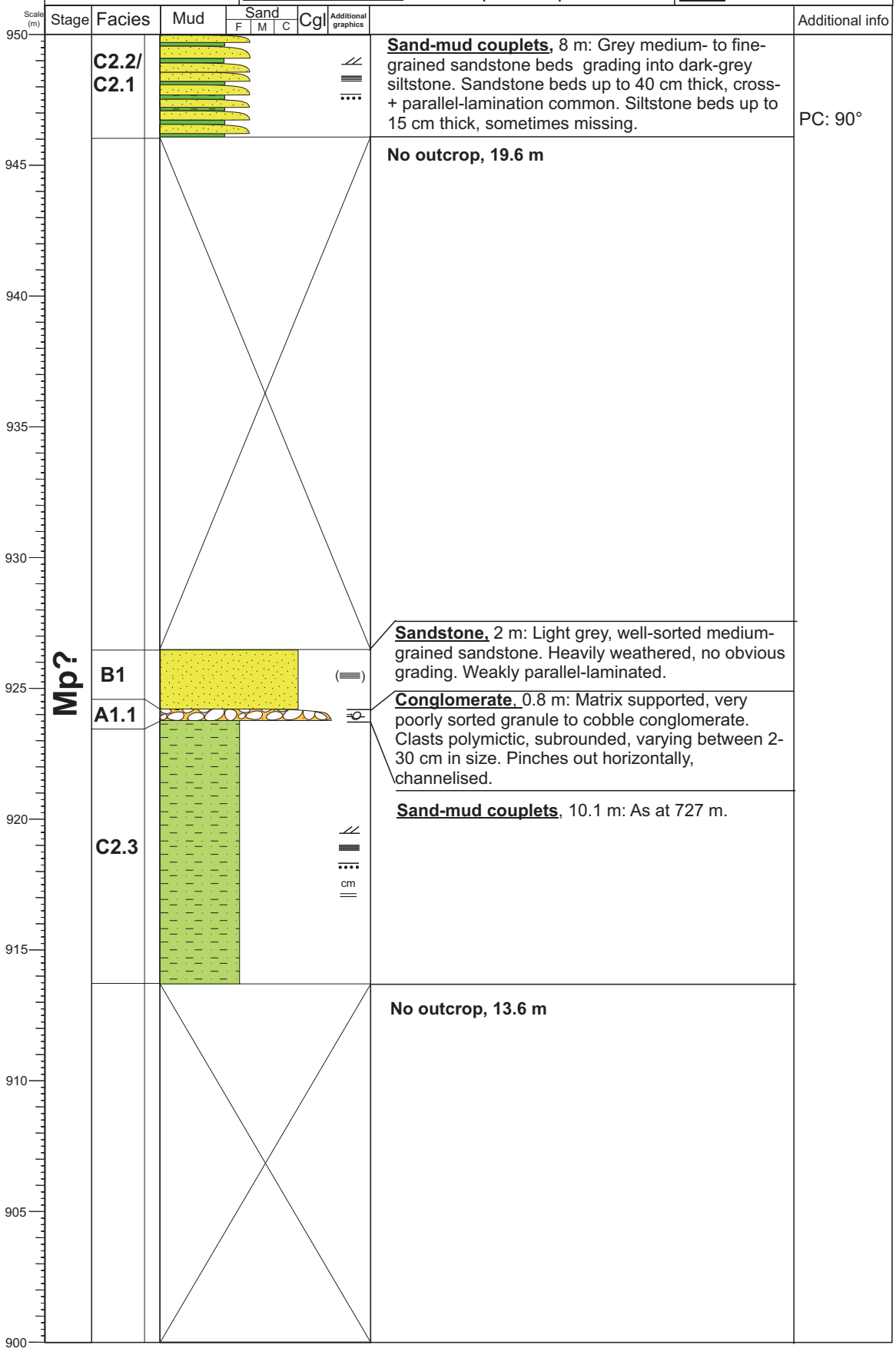

Locality: Motuwaireka Stream, Riversdale, Wellington | **Date:** 23/04/2017

Geologists: J.D.B. McClintock, A.J. Galloway, M. Osvald Smith | **Start:** BP36 522 499

Sheet: 10 of 13 | **Reference format**: LINZ Topo50 Map Reference | **End:** BP35 513 515

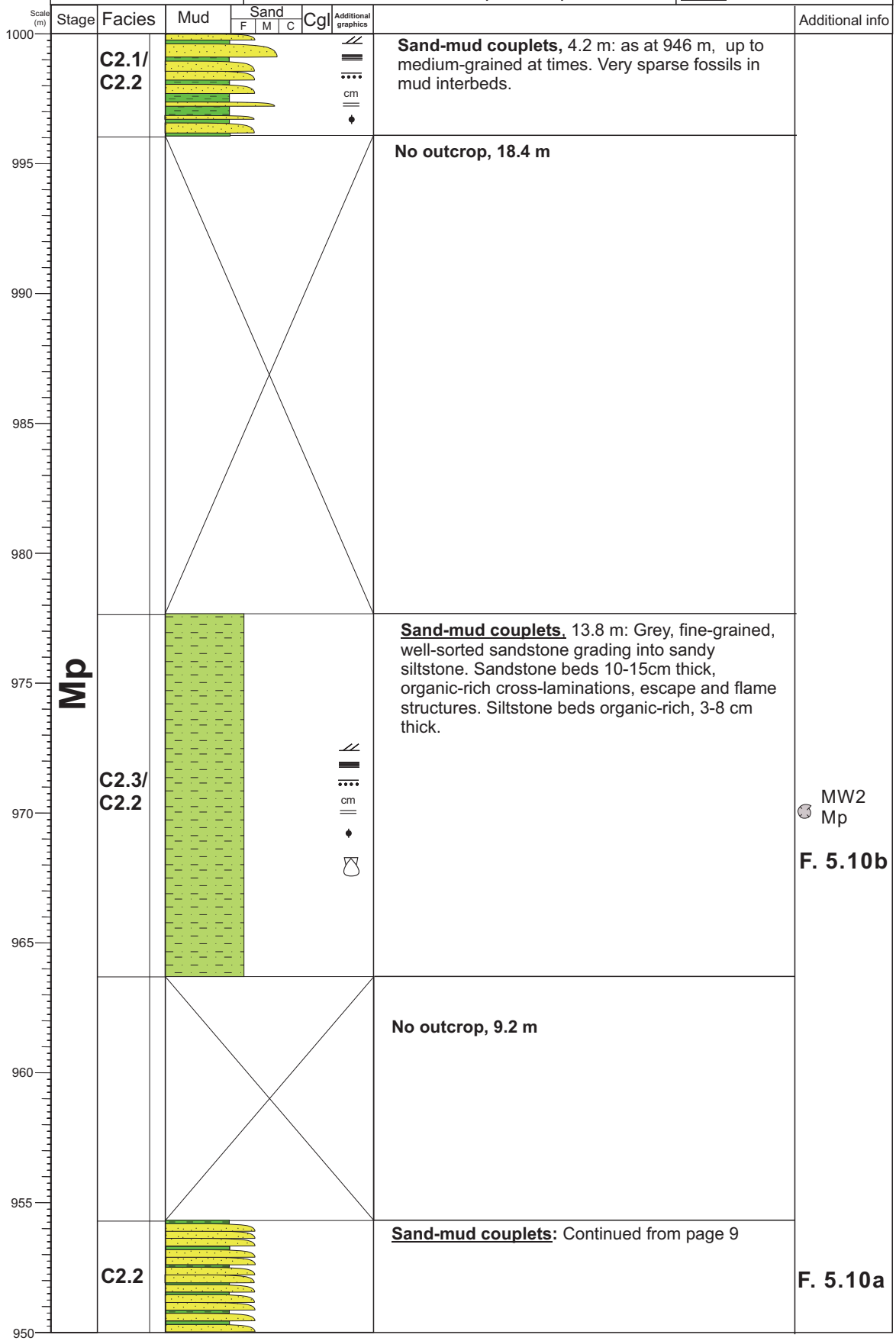

Locality: Motuwaireka Stream, Riversdale, Wellington | **Date:** 23/04/2017

Geologists: J.D.B. McClintock, A.J. Galloway, M. Osvald Smith | **Start:** BP36 522 499

Sheet: 11 of 13 | **Reference format**: LINZ Topo50 Map Reference | **End:** BP35 513 515

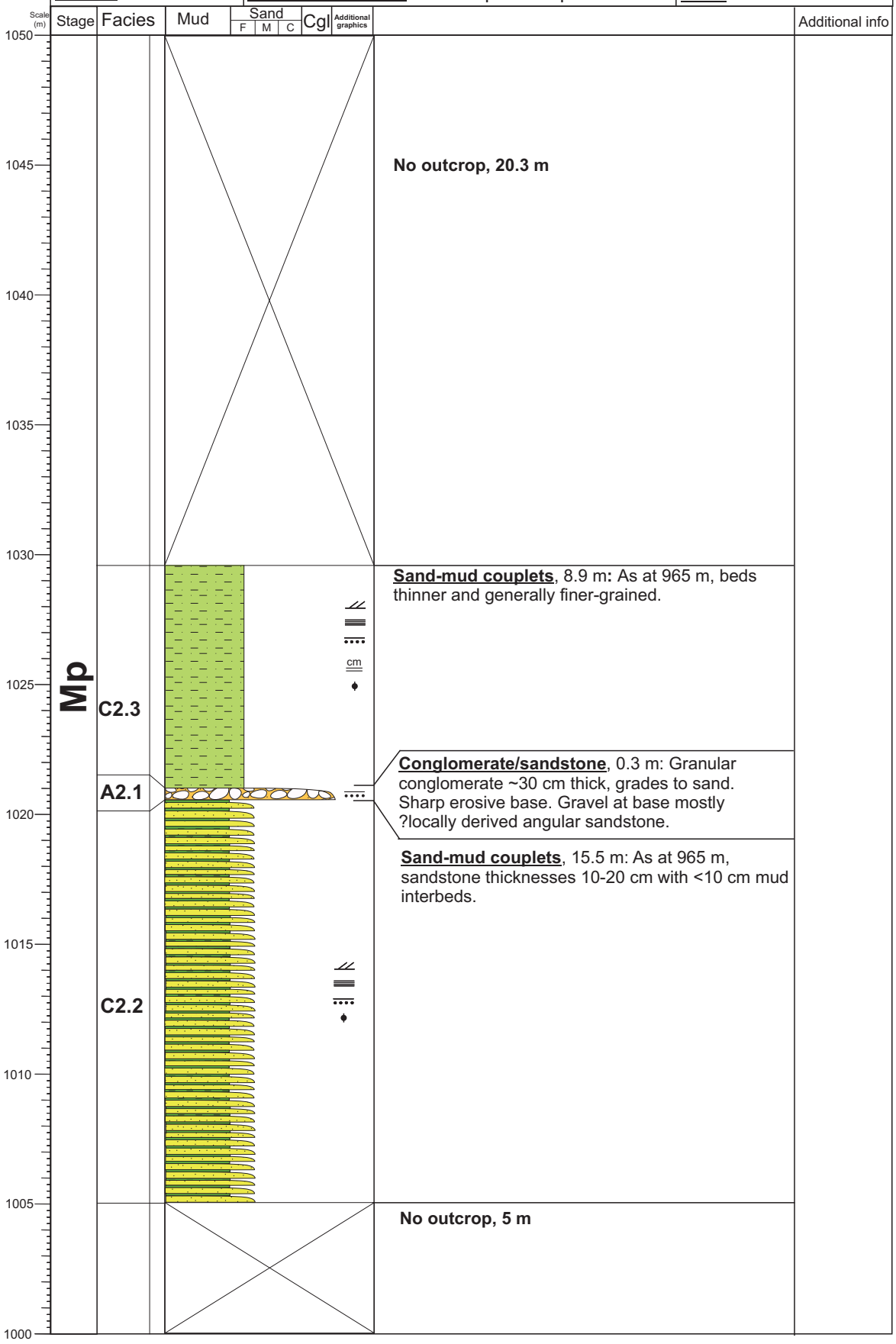

Locality: Motuwaireka Stream, Riversdale, Wellington | **Date:** 23/04/2017

Geologists: J.D.B. McClintock, A.J. Galloway, M. Osvald Smith | **Start:** BP36 522 499

Sheet: 12 of 13 | **Reference format**: LINZ Topo50 Map Reference | **End:** BP35 513 515

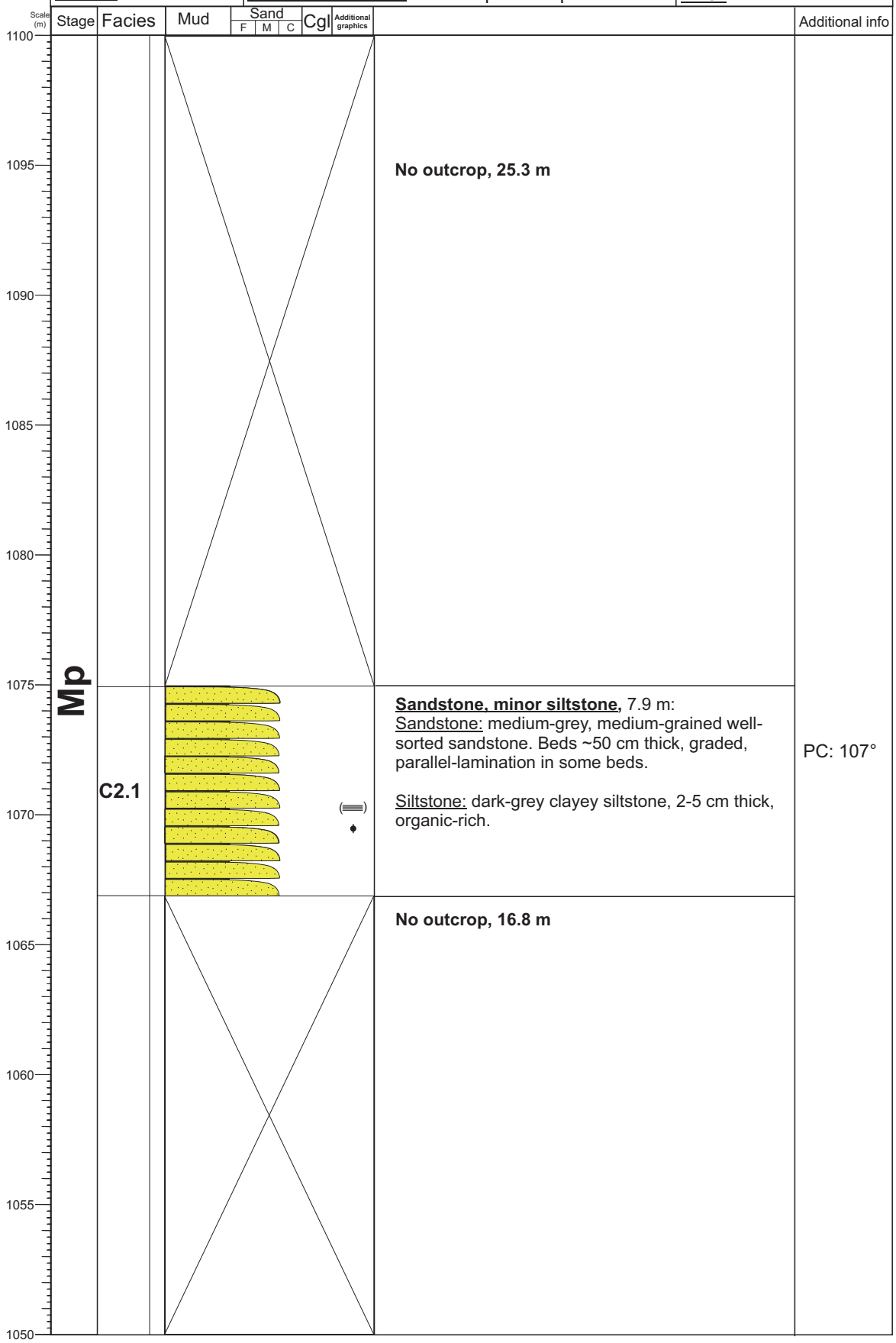

Locality: Motuwaireka Stream, Riversdale, Wellington | **Date:** 23/04/2017

Geologists: J.D.B. McClintock, A.J. Galloway, M. Osvald Smith | **Start:** BP36 522 499

Sheet: 13 of 13 | **Reference format**: LINZ Topo50 Map Reference | **End:** BP35 513 515

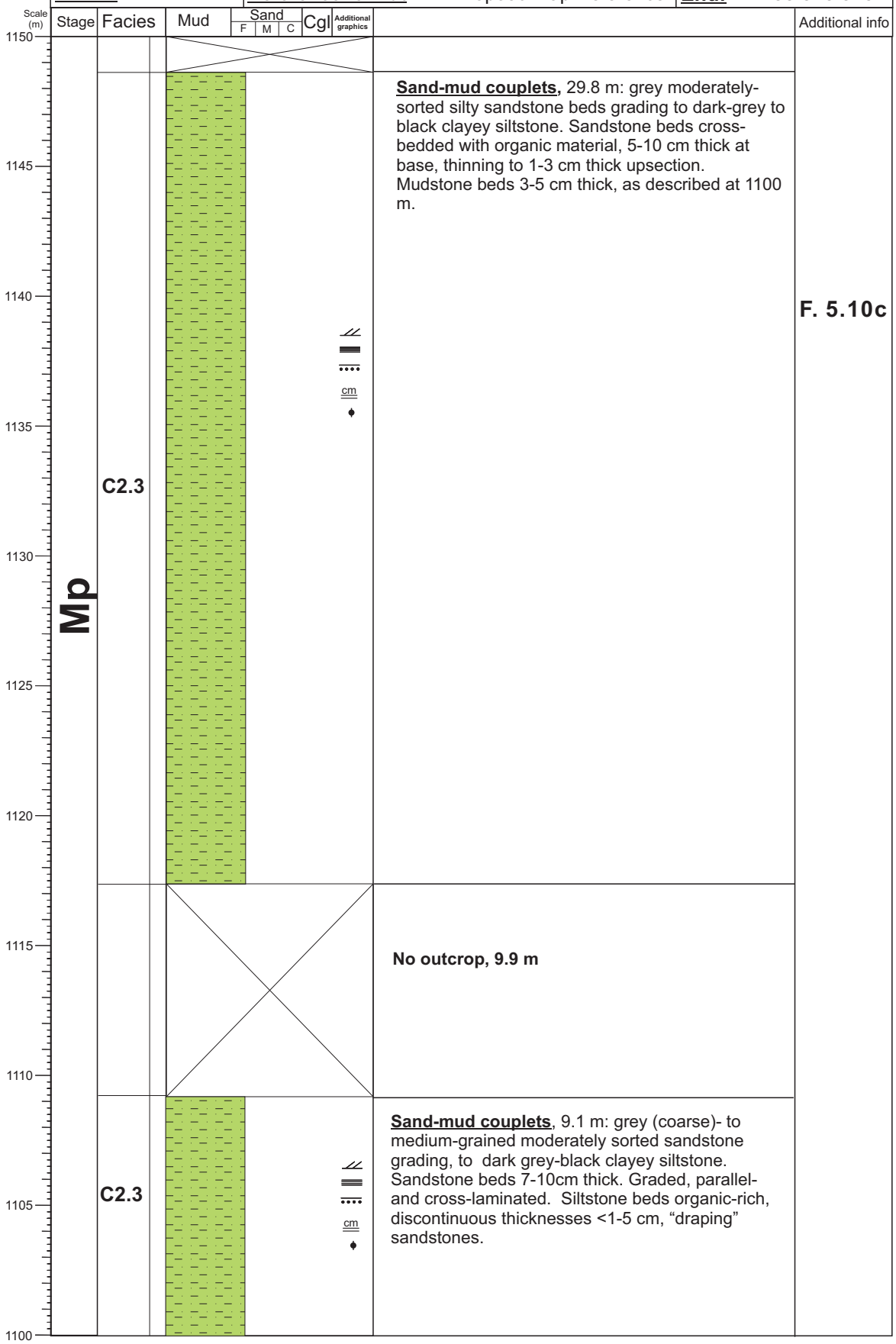

Appendix H: Measured Section of Mataikona River

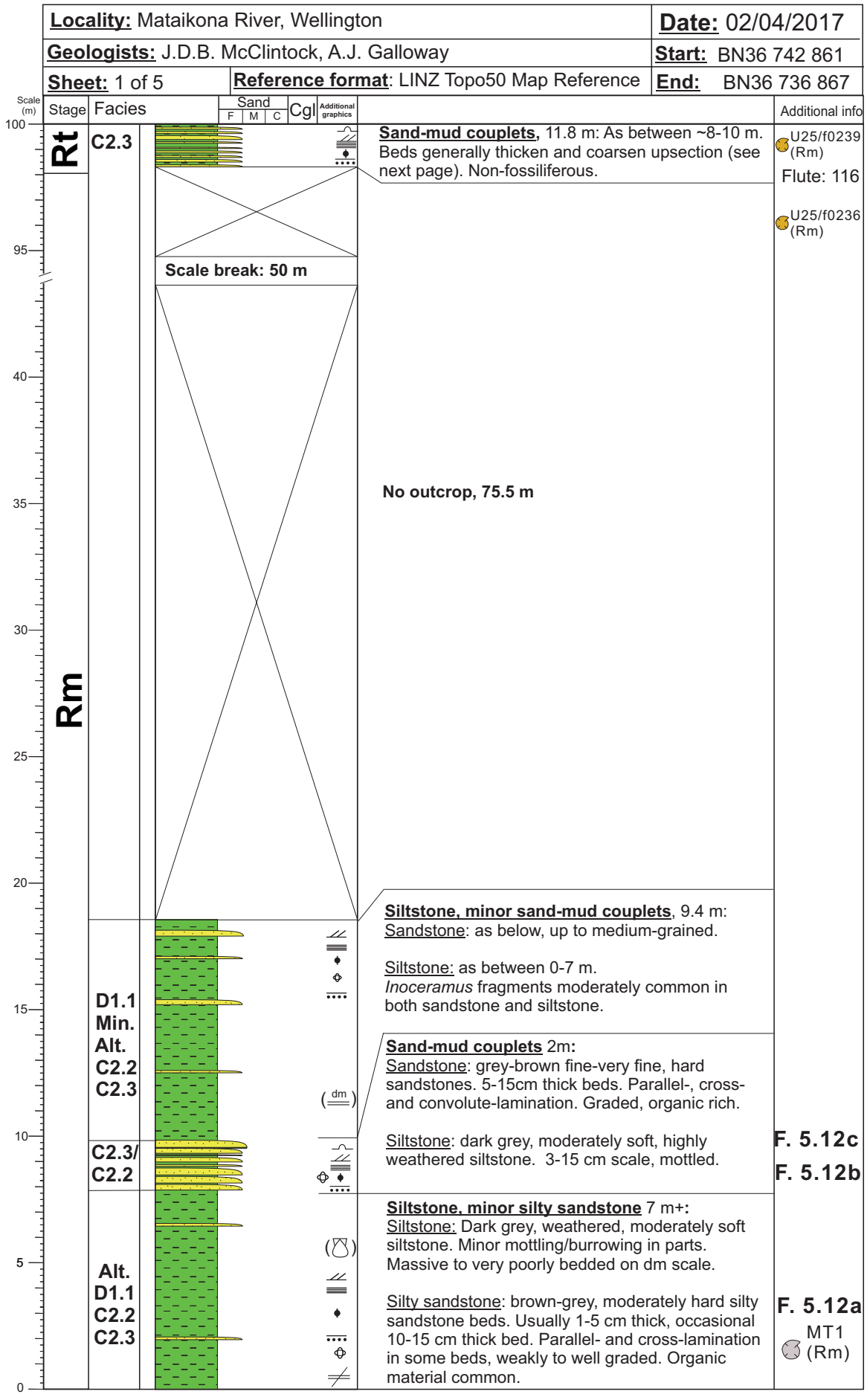

Locality: Mataikona River, Wellington | **Date:** 02/04/2017

Geologists: J.D.B. McClintock, A.J. Galloway | **Start:** BN36 742 861

Sheet: 2 of 5 | **Reference format**: LINZ Topo50 Map Reference | **End:** BN36 736 867

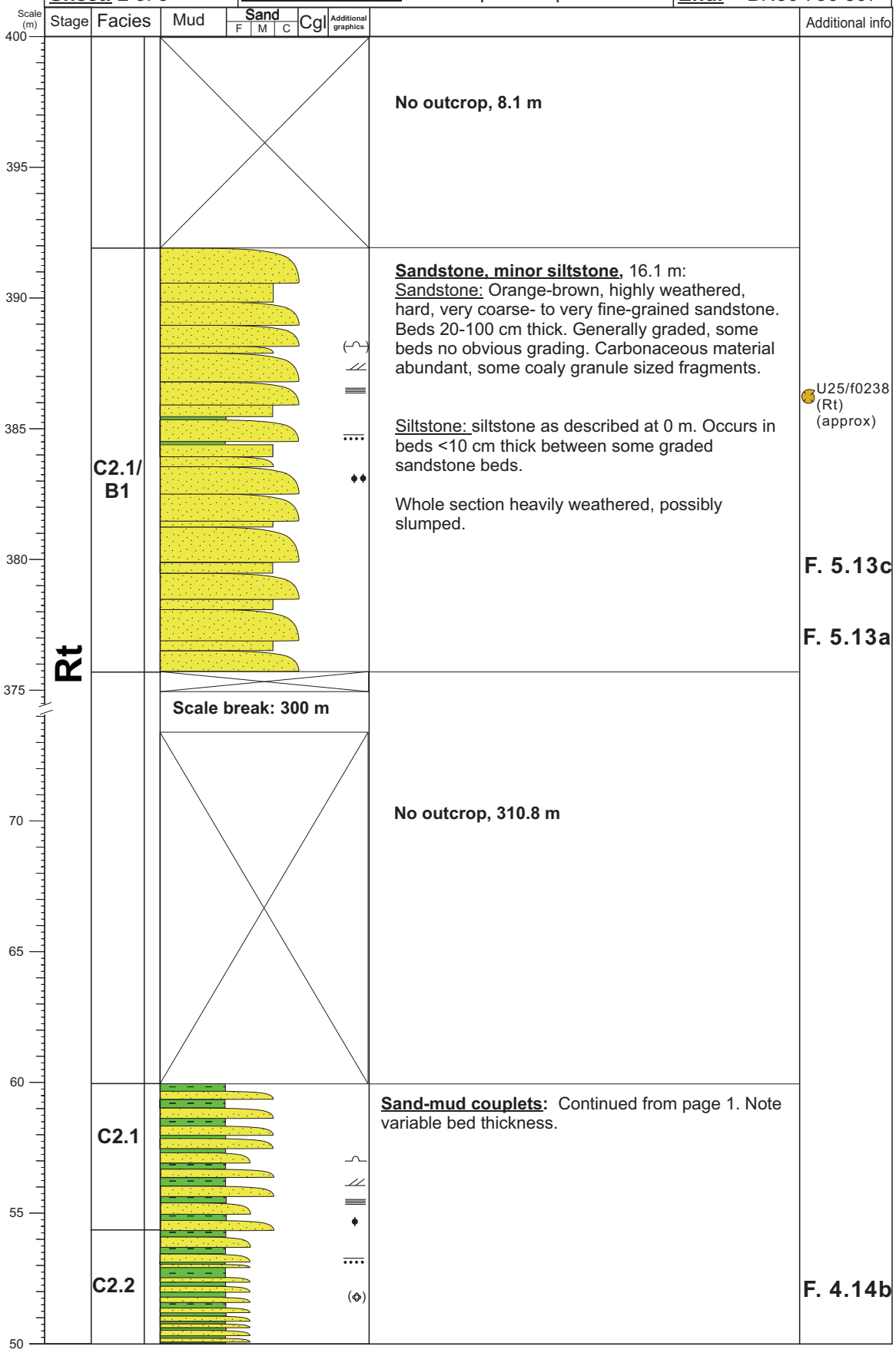

Locality: Mataikona River, Wellington | **Date:** 02/04/2017

Geologists: J.D.B. McClintock, A.J. Galloway | **Start:** BN36 742 861

Sheet: 3 of 5 | **Reference format**: LINZ Topo50 Map Reference | **End:** BN36 736 867

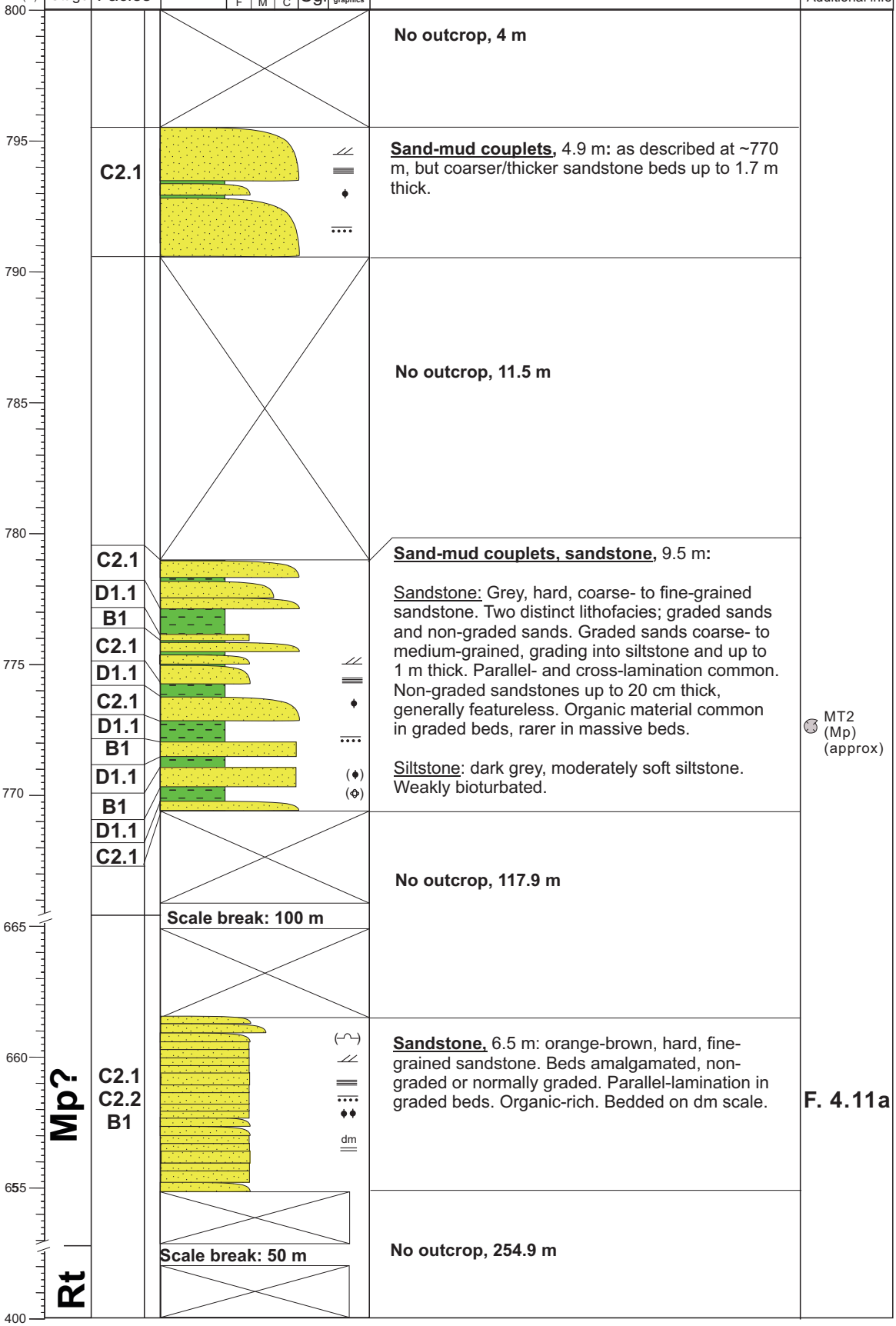

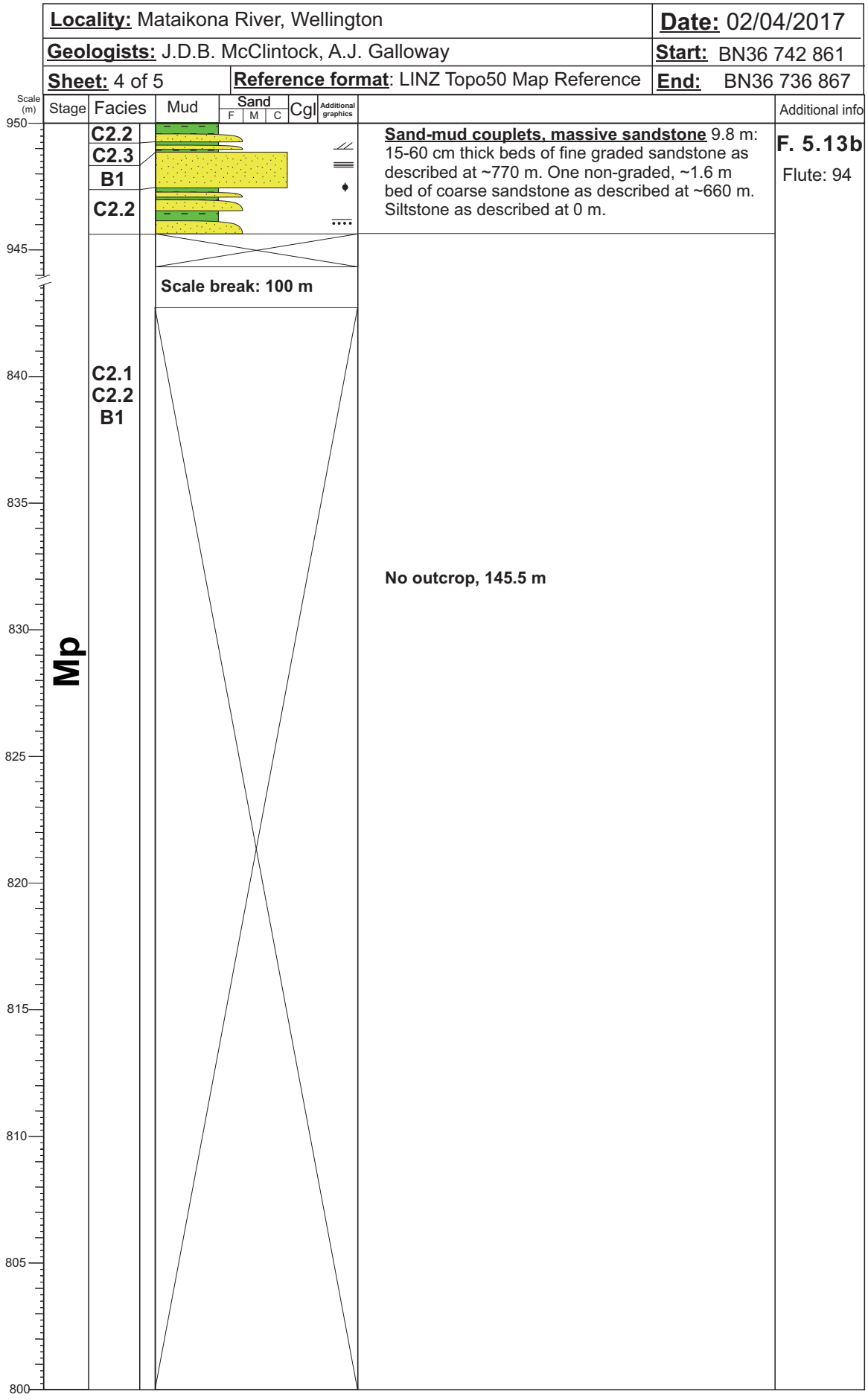
Locality: Mataikona River, Wellington
Date: 02/04/2017
Geologists: J.D.B. McClintock, A.J. Galloway
Start: BN36 742 861
Sheet: 4 of 5
Reference format: LINZ Topo50 Map Reference
End: BN36 736 867
Scale (m)
Stage
Facies
Mud
Sand
F
M
C
Cgl
Additional graphics
Additional info
950
945
840
835
830
825
820
815
810
805
800
Mp
C2.2
C2.3
B1
C2.2
C2.1
C2.2
B1
Sand-mud couplets, massive sandstone 9.8 m: 15-60 cm thick beds of fine graded sandstone as described at ~770 m. One non-graded, ~1.6 m bed of coarse sandstone as described at ~660 m. Siltstone as described at 0 m.
Scale break: 100 m
No outcrop, 145.5 m
F. 5.13b
Flute: 94

Locality: Mataikona River, Wellington | **Date:** 02/04/2017

Geologists: J.D.B. McClintock, A.J. Galloway | **Start:** BN36 742 861

Sheet: 5 of 5 | **Reference format**: LINZ Topo50 Map Reference | **End:** BN36 736 867

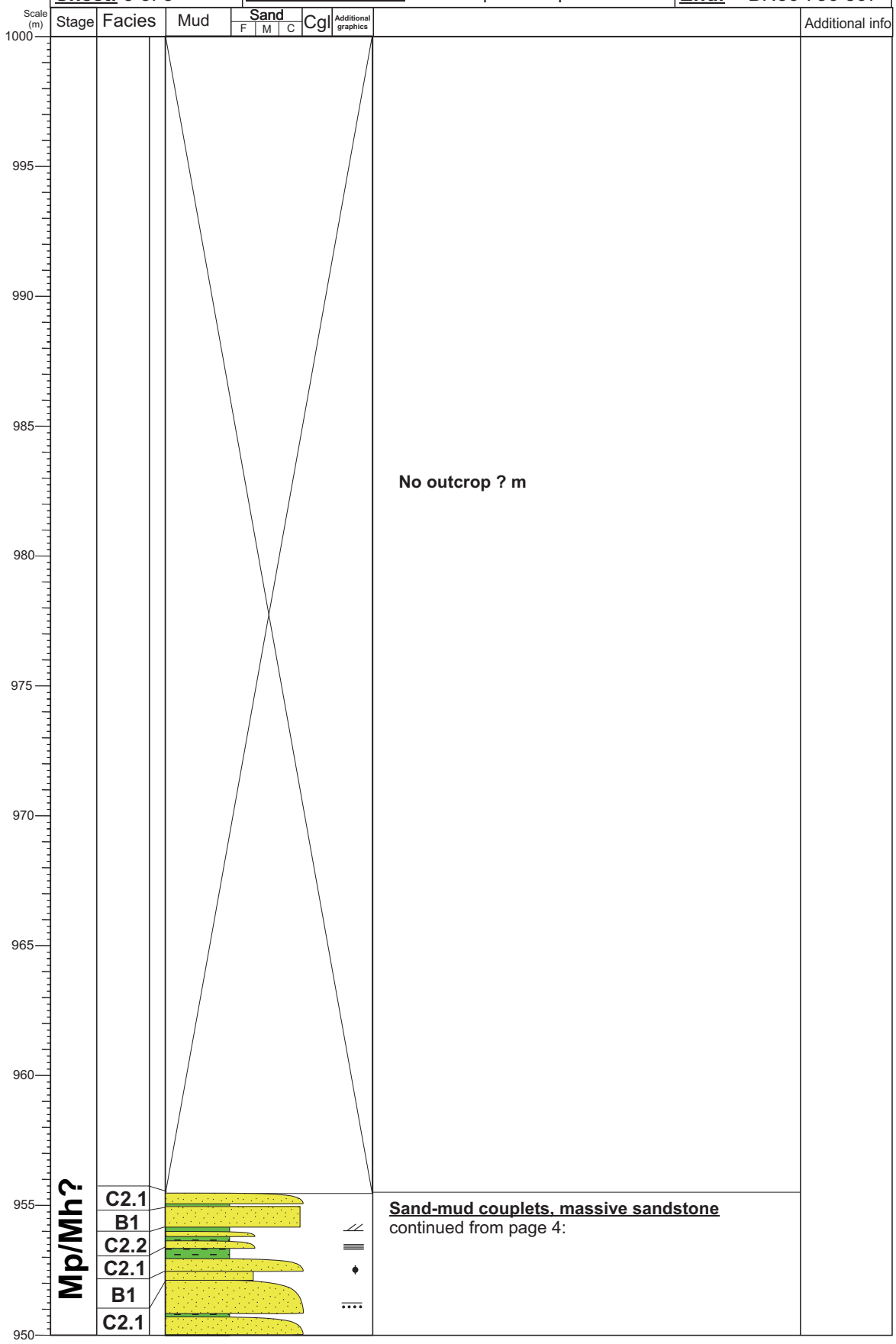

Appendix I: Composite Measured Section of Waimata River

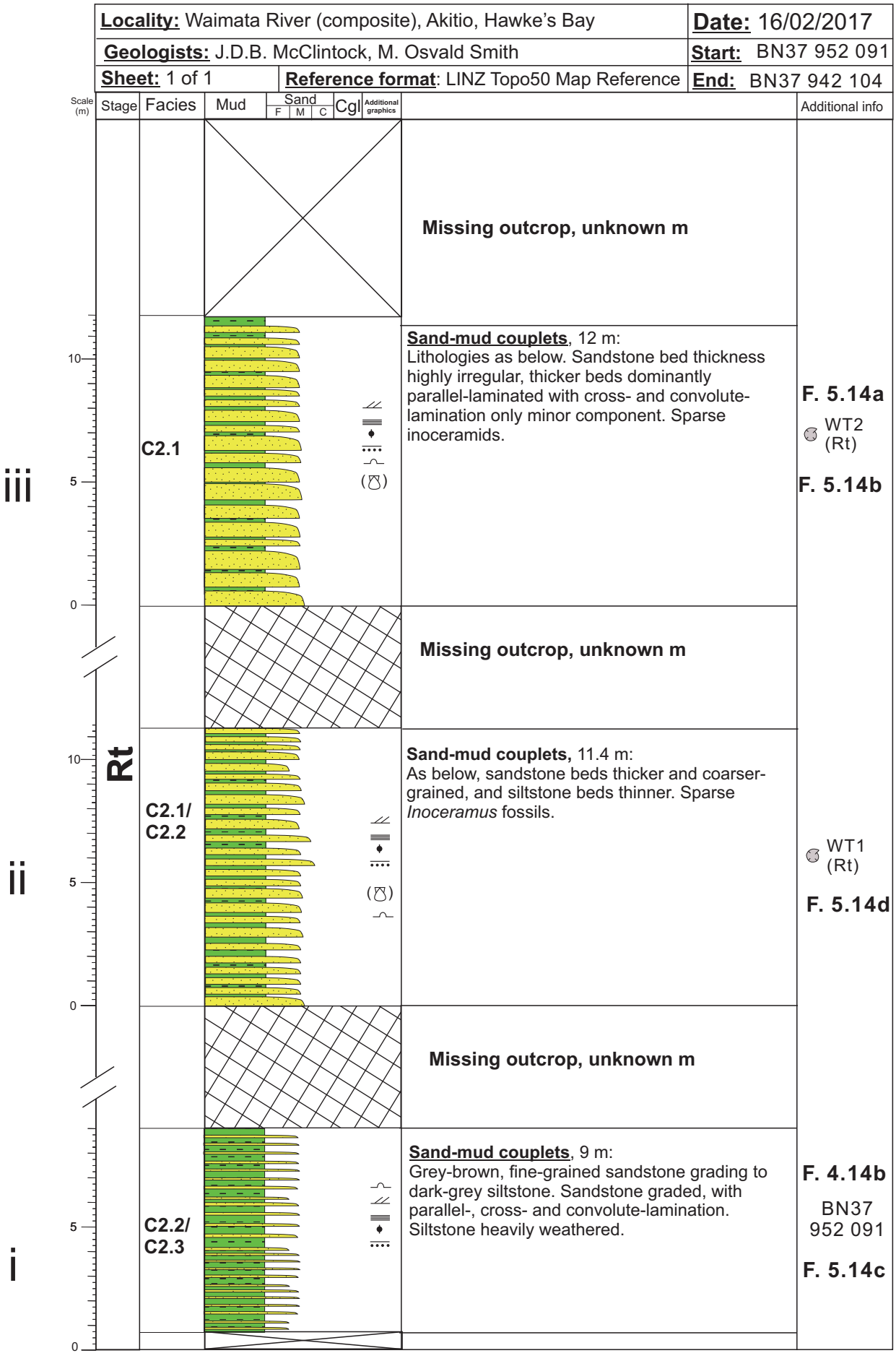

Appendix J: Composite Measured Section of Mangakuri Beach

Locality: Mangakuri Beach (composite), Hawke's Bay | **Date:** 12/06/2017

Geologists: J.D.B. McClintock, M. Osvald Smith, A.J. Galloway | **Start:** BL39 327 637

Sheet: 1 of 2 | **Reference format**: LINZ Topo50 Map Reference | **End:** BL39 338 670

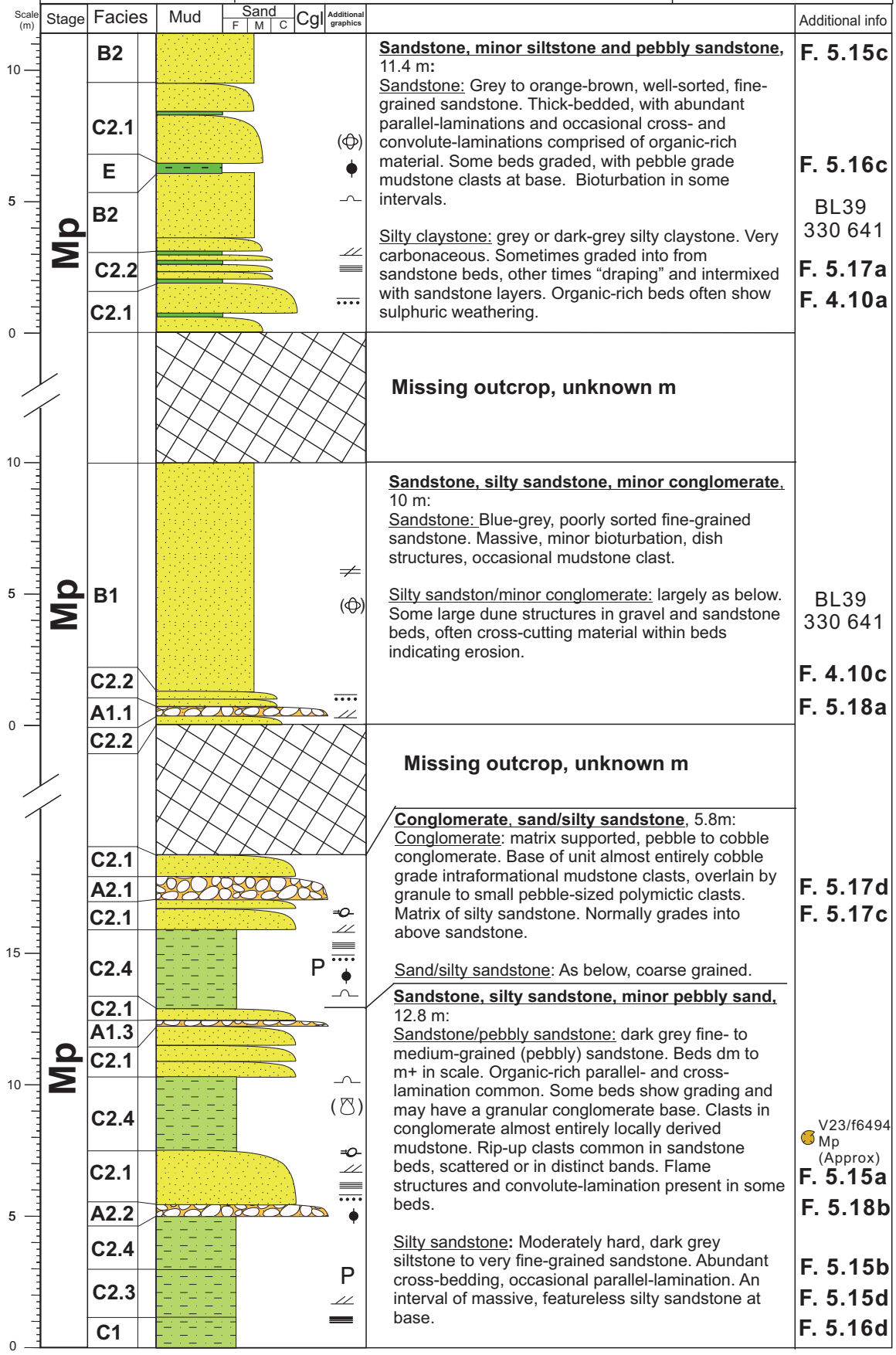

Sandstone, minor siltstone and pebbly sandstone, 11.4 m**:**
Sandstone: Grey to orange-brown, well-sorted, fine-grained sandstone. Thick-bedded, with abundant parallel-laminations and occasional cross- and convolute-laminations comprised of organic-rich material. Some beds graded, with pebble grade mudstone clasts at base. Bioturbation in some intervals.

Silty claystone: grey or dark-grey silty claystone. Very carbonaceous. Sometimes graded into from sandstone beds, other times "draping" and intermixed with sandstone layers. Organic-rich beds often show sulphuric weathering.

Missing outcrop, unknown m

Sandstone, silty sandstone, minor conglomerate, 10 m:
Sandstone: Blue-grey, poorly sorted fine-grained sandstone. Massive, minor bioturbation, dish structures, occasional mudstone clast.

Silty sandston/minor conglomerate: largely as below. Some large dune structures in gravel and sandstone beds, often cross-cutting material within beds indicating erosion.

Missing outcrop, unknown m

Conglomerate, sand/silty sandstone, 5.8m:
Conglomerate: matrix supported, pebble to cobble conglomerate. Base of unit almost entirely cobble grade intraformational mudstone clasts, overlain by granule to small pebble-sized polymictic clasts. Matrix of silty sandstone. Normally grades into above sandstone.

Sand/silty sandstone: As below, coarse grained.

Sandstone, silty sandstone, minor pebbly sand, 12.8 m:
Sandstone/pebbly sandstone: dark grey fine- to medium-grained (pebbly) sandstone. Beds dm to m+ in scale. Organic-rich parallel- and cross-lamination common. Some beds show grading and may have a granular conglomerate base. Clasts in conglomerate almost entirely locally derived mudstone. Rip-up clasts common in sandstone beds, scattered or in distinct bands. Flame structures and convolute-lamination present in some beds.

Silty sandstone**:** Moderately hard, dark grey siltstone to very fine-grained sandstone. Abundant cross-bedding, occasional parallel-lamination. An interval of massive, featureless silty sandstone at base.

Additional info
F. 5.15c
F. 5.16c
BL39 330 641
F. 5.17a
F. 4.10a
BL39 330 641
F. 4.10c
F. 5.18a
F. 5.17d
F. 5.17c
V23/f6494 Mp (Approx)
F. 5.15a
F. 5.18b
F. 5.15b
F. 5.15d
F. 5.16d

Locality: Mangakuri Beach (composite), Hawke's Bay | **Date:** 12/06/2017

Geologists: J.D.B. McClintock, M. Osvald Smith, A.J. Galloway | **Start:** BL39 327 637

Sheet: 2 of 2 | **Reference format**: LINZ Topo50 Map Reference | **End:** BL39 338 670

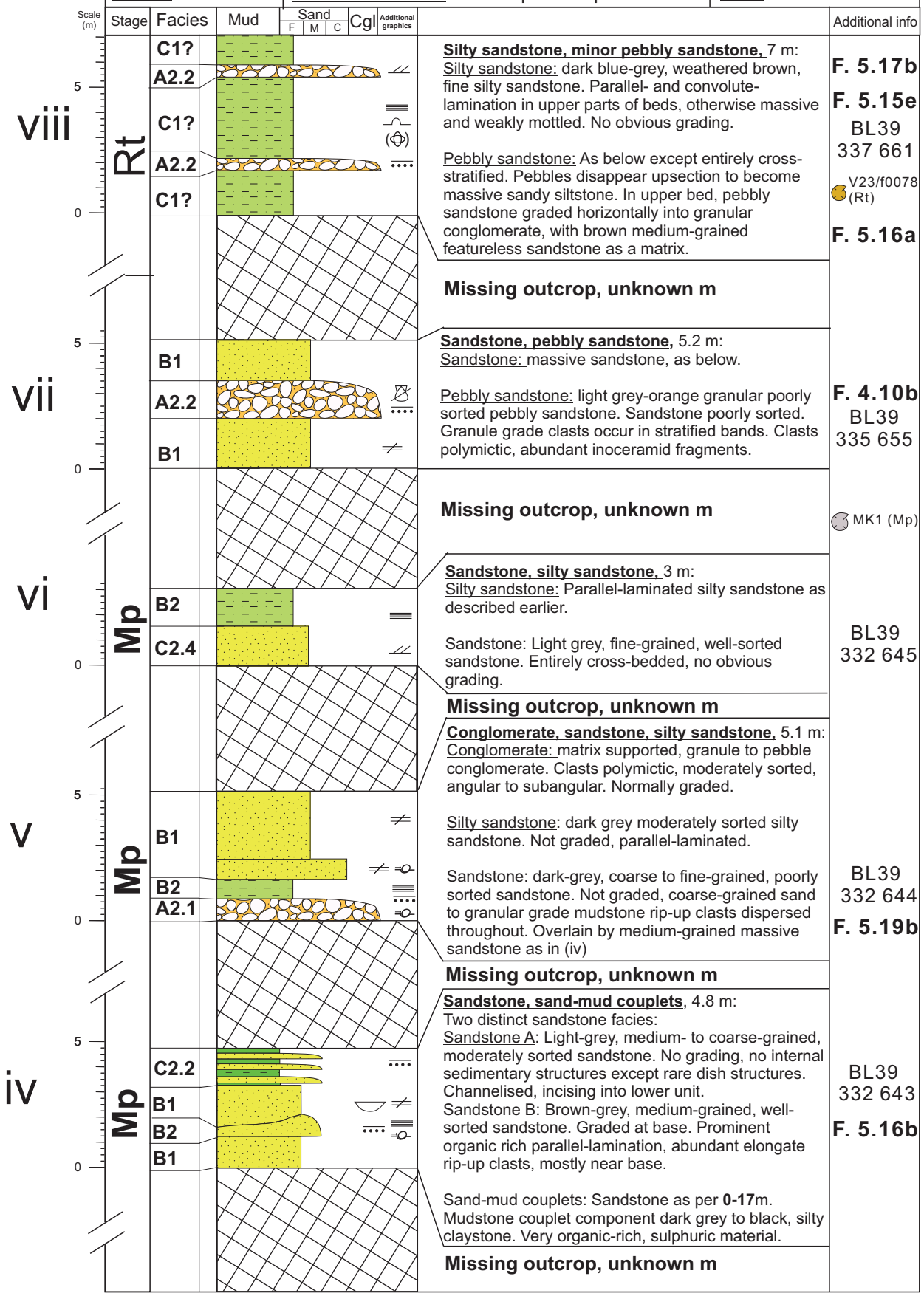

Appendix K: Crampton (1997) North Mangakuri Beach Measured Seciton

MEASURED SECTION DETAIL SHEET

REGION: _____ SCALE: 1 cm : 1 m (1:100) 1 cm : 10 m (1 : 1000) 1 cm : 50 m (1 : 5000)

LOCALITY: Mangakuri - Kairakau

GEOLOGIST(S): _____

V22 (NZMS 260 sheet) | C 1 (serial number) | – (horizon) | _____ (remeasurement?)

DATE OF MEASUREMENT: ___ (day) ___ (month) 19 (year)

GRID REFERENCES: (metric) 19 (map date) * _____ (easting) _____ (northing) BASE OF SECTION * _____ (easting) _____ (northing) TOP OF SECTION *

DRILLHOLES: Has thickness been corrected for dip? YES , NO

METHOD OF MEASUREMENT: _____

Elevation of drillhole collar _____ metres a.s.l.

Stage	Formation	Samples taken and results: Petrological data	Paleontological data	'f' number	Disturbance	Scale (metres)	GRAPHIC LOG	Additional graphic	Description: Name of rock; hardness and cementation; colour; weathering and sedimentary structures (including biogenic); fossils; texture (grain size, sorting, shape, round ness); accessory minerals; preliminary assessment of environment of deposition	Structural data (N)
Rt	Glenburn Formation					260 250 240 230 220		dm-m bdd; lam; gm-dm; dm; cc	Sandstone / minor siltstone / minor conglomerate. 69m. Dm - m bdd, as described below (0-116m). Carbonaceous material locally abundant	70

PAGE 2 OF 2

START PLOTTING AND NUMBERING SAMPLES AT THE BOTTOM OF THE SHEET. EXACT LOCATION OF THIS MEASURED SECTION TO BE SHOWN ON MAP ON BACK OF THIS SHEET.

Appendix L: Composite Measured Section of Waimarama

Locality: Waimarama Beach, Hawke's Bay | **Date:** 13/06/2017

Geologists: J.D.B. McClintock, M. Osvald Smith, A.J. Galloway | **Start:** BP35 460 423

Sheet: 1 of 2 | **Reference format**: LINZ Topo50 Map Reference | **End:** BP35 448 428

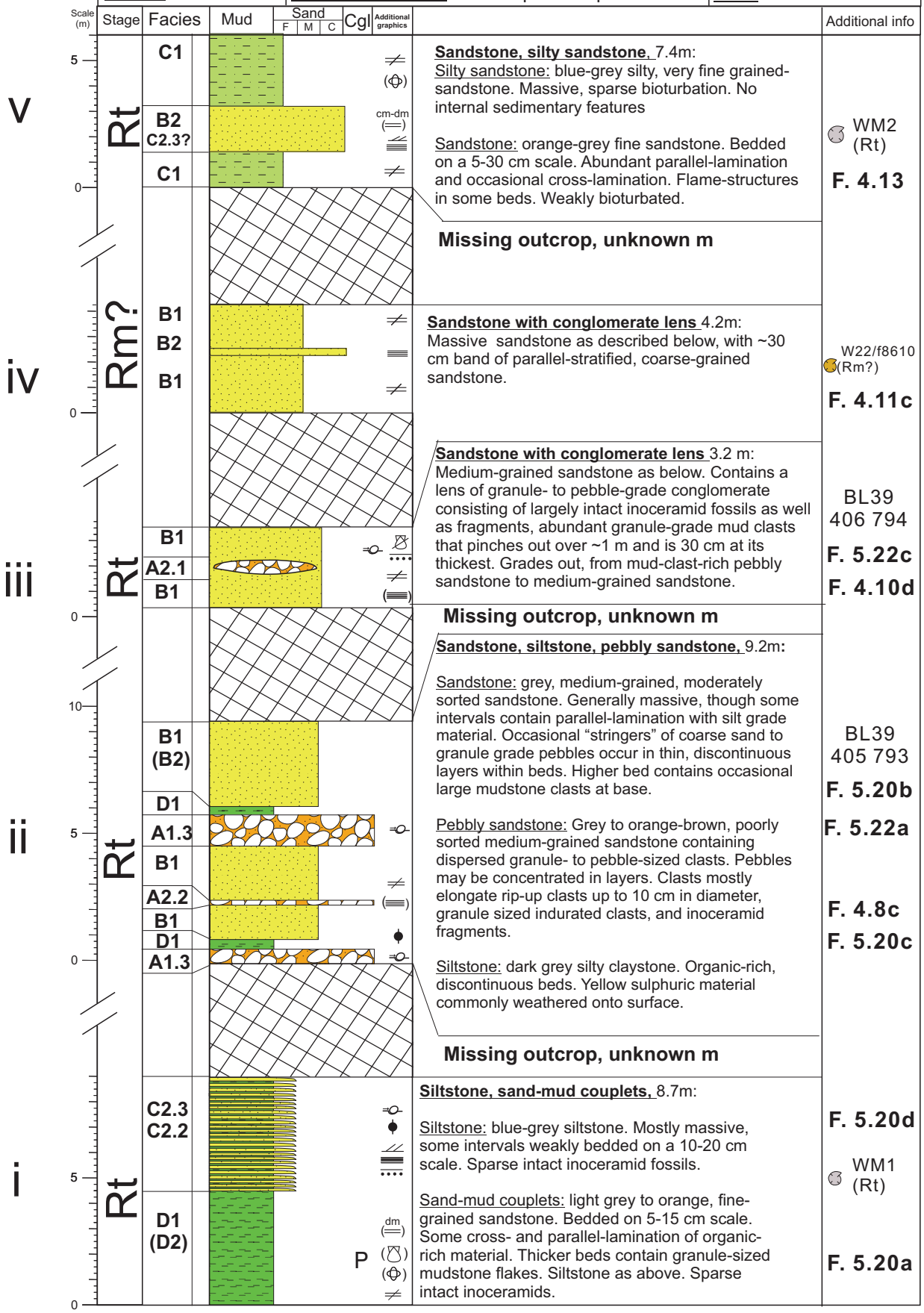

Locality: Waimarama Beach, Hawke's Bay | **Date:** 13/06/2017

Geologists: J.D.B. McClintock, M. Osvald Smith | **Start:** BP35 460 423
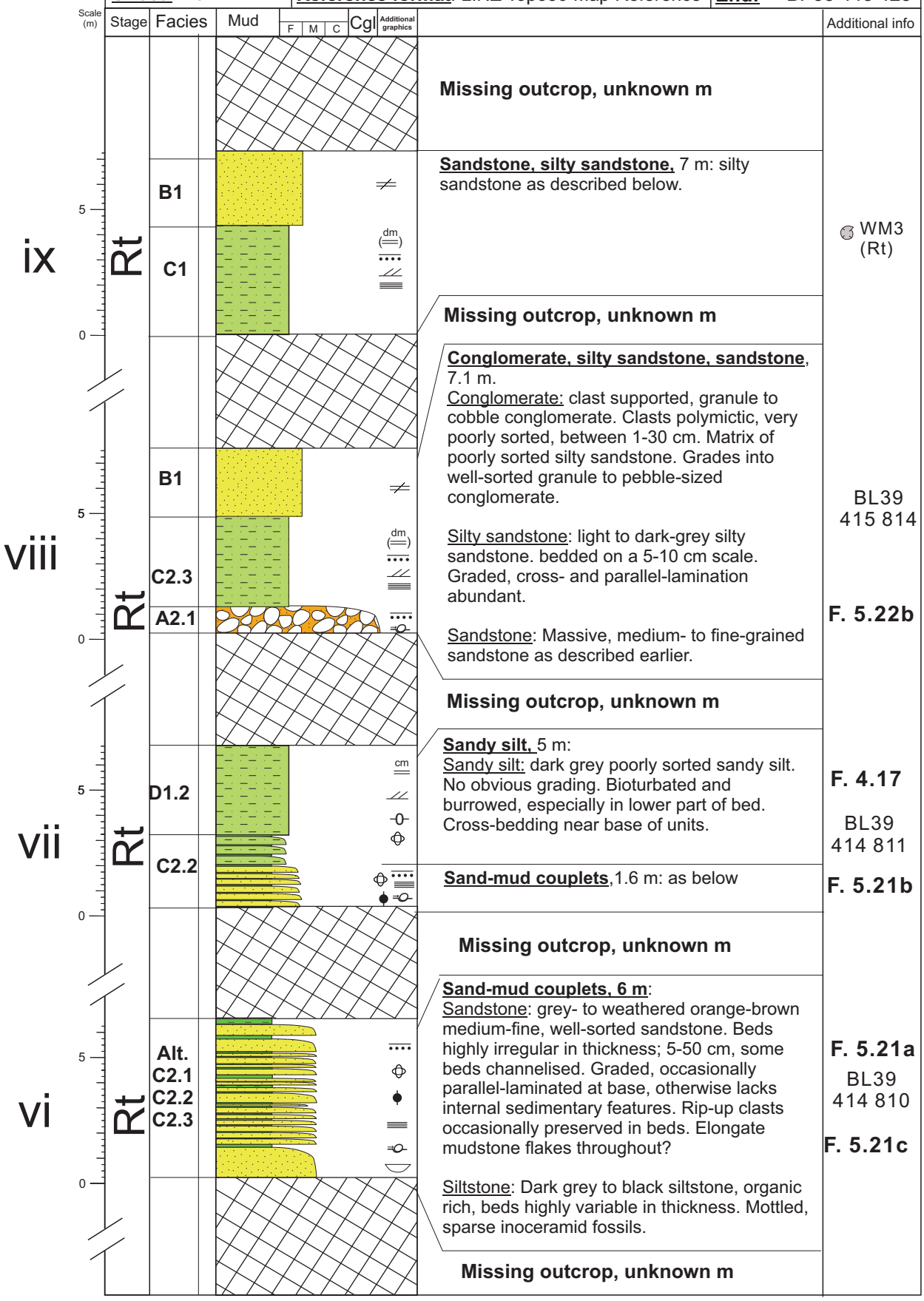
Sheet: 2 of 2 | **Reference format**: LINZ Topo50 Map Reference | **End:** BP35 448 428